Functional ultrasound (fUS) imaging of brain functional connectivity alterations in a mouse model of neuropathic pain : impact of nociceptive symptoms and associated comorbidities

Silvia Cazzanelli

PSL UNIVERSITÉ PARIS

THÈSE DE DOCTORAT
DE L'UNIVERSITÉ PSL

Préparée à Ecole Supérieure de Physique et de Chimie Industrielles de la ville de Paris (ESPCI Paris) en collaboration avec Iconeus.

Functional ultrasound (fUS) imaging of brain functional connectivity alterations in a mouse model of neuropathic pain: impact of nociceptive symptoms and associated comorbidities

Etude des altérations de la connectivité fonctionnelle cérébrale par imagerie fonctionnelle ultrasonore (fUS) dans un modèle murin de douleur neuropathique : impacts des symptômes nociceptifs et comorbidités associées

Soutenue par
Silvia CAZZANELLI
Le 21/06/2024

Ecole doctorale n° 158
Cerveau, cognition, comportement (ED3C)

Spécialité
Neurosciences et Sciences Cognitives

Composition du jury :

Cécile VIOLLET Directrice de recherche ESPCI – Paris Science et Lettres	*Président du jury*
Fabien MARCHAND Maître de conférences INSERM	*Rapporteur*
Franziska DENK Professeure King's College London	*Rapportrice*
Ipek YALCIN Directrice de recherche CNRS Strasbourg	*Examinatrice*
Sophie PEZET Maître de conférences ESPCI – Paris Science et Lettres	*Directrice de thèse*
Jeremy FERRIER PhD, Iconeus	*Co-encadrant*

ESPCI PARIS | PSL

Laboratoire UMR 8063 PHYSMED

Remerciements

First of all, I would like to thank the members of the jury for accepting to read and evaluate my work.

I would like to thank Ipek Yalcin for being part of my thesis committee every year and also for collaborating with us and helping us develop the sciatic nerve cuff model in our laboratory.

Un très grand merci à **Sophie,** pour ta passion et ton énergie débordante, pour ton envie inépuisable de tout faire, pour tout le monde, et de le faire toujours de la meilleure manière. Merci d'avoir toujours été présente, une porte ouverte où frapper et trouver un goûter avec thé et gâteau. Merci de m'avoir toujours comprise sans que j'aie à trop expliquer. Tu as toujours su m'aider, m'encourager et me motiver, mais aussi me dire "tu dois partir en vacances et te reposer !" Travailler à tes côtés a été tellement stimulant, tu m'as permis d'apprendre énormément. Merci d'avoir fait partie d'une équipe, ou plutôt d'un binôme si bien assorti avec Jérémy. Vous avez été l'équilibre parfait et l'exemple à suivre. Merci **Jérémy** pour ton calme zen et ta patience, pour tes conseils ponctuels et précis. C'était vraiment un plaisir de travailler avec toi. Tu as su me guider en me comprenant et en me laissant suivre mon propre rythme de maturation.
Bruno, merci de m'avoir donné une chance chez Iconeus, d'avoir cru en ce projet et de m'avoir donné une opportunité. Merci pour tous tes conseils et tes attentions. Merci **Ludovic** pour m'avoir accueillie dans cette belle famille qu'est Iconeus.
Merci aussi à **Mickaël et Mathieu** de m'avoir donné la possibilité de faire partie de cet incroyable laboratoire, et pour avoir contribué à créer, au fil des années, un ambience de pure collaboration et de passion pour ce que nous faisons. J'ai eu une chance immense d'avoir rencontré Sophie et d'avoir pu faire partie de ce laboratoire.
Merci à **Luc et Thibaud** : la task force d'IcoLab ! Merci pour votre réactivité et votre disponibilité, pour avoir toujours répondu à mes messages sur Slack avec des solutions et des stratégies, et pour avoir recompilé des versions à 19h d'un vendredi soir. C'était un plaisir de travailler avec vous !
Merci à toute la bande d'**Iconeus**, aux applications spécialistes avec qui on a partagé tous nos problèmes, et merci aussi à tous les autres, anciens et nouveaux. Même si je n'étais jamais sur place, vous m'avez toujours fait sentir partie de la famille.

Merci aussi à tous mes collègues de **Physmed**, cette grande famille avec qui j'ai grandi pendant ces quatre dernières années. L'ambiance que j'ai retrouvée dans ce labo est incroyable, tout le monde travaille et aide tout le monde, c'est tellement beau. J'ai appris beaucoup grâce à vous tous.
Manon, merci pour les croissants du samedi, **Maxime** pour tes skills en hydroponie, **Solène** pour ta spontanéité, **Alex et Anatole** pour le jogging du midi (enfin, Anatole, c'était plutôt les dix premières minutes). Merci **Henry** pour tes blagues nulles ahaha et les courses de vélo le matin, **Flora** merci d'être toujours la meilleure coloc de chambre. **Clara** pour le dej-cifre-rooftop. **Felipe**, merci d'être toujours très zen, parler avec toi c'est comme faire de la méditation. **Mathis**, merci pour cette dynamique très école maternelle qu'on a réussi à créer entre nous deux, j'adore ! **Touka**, merci pour les conseils de style et **Janie** pour les sushi rooftop, toujours présente ;), **Fred** pour les séances d'escalade. Merci aux nouveaux de l'équipe gestion, **David et Claire**. Merci à **Patricia** pour toujours trouver ce dont on a besoin, merci **Mai** pour tout ce que tu fais pour nous; cet échange de courriels est déjà entré dans l'histoire ! Merci aux anciens aussi : **Marta** pour ta rigueur scientifique, tous les conseils de chirurgie et les Eduard-cookies ! **Lauriane**, pour toujours voir le côté positif et logique des choses, j'ai beaucoup appris grâce à toi, merci. **JB**, grazie per avermi fatto compagnia dall'altra parte del vetro, nei miei lunghi giorni di manip.
Nathalie, merci pour tout ! Pour ta gentillesse avant tout, pour toutes les rigolades pendant les journées de chirurgie ! Merci pour tous tes conseils, astuces et stratégies pour améliorer mes manips, on était une équipe incroyable ! Je vais bientôt revenir à l'animalerie pour te faire compagnie. **Lanto**, merci pour ta bonne humeur et ton rire tellement contagieux ! Tu as amené de la couleur à l'animalerie. **Salima**, merci

pour ton cœur si grand ! Pour avoir été la maman et la star du labo. Ça me manque de te voir rentrer dans le bureau avec ton micro en chantant. Tous les jours c'était un spectacle de stand-up comedy avec toi. Merci pour les meilleurs bricks au thon du monde et à bientôt pour un couscous ;) ! **Hinde**, tu as laissé un gros vide au labo, dans nos oreilles et au-dessous de nos souris. **Hicham**, merci pour les chocolats, les gâteaux et tout ce que tu m'as donné à manger pendant mes longues journées de manip ! Merci d'avoir toujours été si disponible pour aider n'importe quand et n'importe comment. Tu m'as même aidée à construire une arène en bois, c'était trop marrant !
Rami, tu étais un super collègue et un super pote. Tu m'as aidée énormément, toujours. Sans toi, je n'aurais pas pu ni commencer, ni avancer et ni arriver à la fin de tout ça. Depuis notre première manip ensemble (je pense ma première semaine au labo), j'avais déjà compris qu'on aurait très bien travaille ensemble ! Merci pour tout ton soutien. Tu as toujours compris à l'instant quand j'avais besoin d'un petit (très gros parfois) discours de motivation, même quand tu n'étais plus au labo. Merci aussi pour ta playlist des soirées et tes supers skills pour la jouer à n'importe quelles conditions. **Youenn**, tu as ramené le bonheur et la musique en salle de manip. Depuis que tu es arrivé, passer les journées en manip dans le noir était devenu même agréable et marrant, sauf pour la musique ahaha. On était sur la même longueur d'onde très vite au boulot et même en dehors du taff. Tu étais toujours là pour me motiver, me booster et aussi pour me dire de me reposer et de prendre des vacances, ou me convaincre à venir en manif avec toi. Merci pour tout vraiment. **Sam**, merci pour ta passion contagieuse et ton : "oui t'inquiètes je te fais ça en deux secondes" avec le bruit de fond de tes doigts qui tapent très rapidement sur ton clavier. Merci de m'avoir toujours aidée à n'importe quelles conditions. Sans ton aide je n'aurais pas pu arriver là.
Un grand merci à mes **co-bureau**, aux nouveaux qui m'ont soutenue très chaleureusement pendant toute la période de la rédaction ! Merci de m'avoir fliquée sur mes horaires et merci d'avoir été si mignons en me ramenant le petit déj, des gâteaux et même un kit de survie pour les moments les plus durs ! Vous m'avez réchauffé le cœur ! Merci **Nico**, toujours attentif aux autres et avec tes questions existentielles qui démarrent des discussions profondes qui durent des heures. **Victor**, le gendarme le plus strict, qui devient un petit loup quand il met sa musique et il chante en playback ou il siffle. C'est très marrant de t'avoir à côté au quotidien, c'est comme bizuter un petit frère. **Juliette**, la petite sœur passive-agressive du bureau. Il y a une connexion entre nous que j'adore et ça ne s'explique pas trop avec les mots mais plutôt avec des bruits chelous. Merci pour les gâteaux du vendredi et pour ne jamais m'entendre quand je te parle ! **Bénoît**, bah voilà la blague est déjà là, je peux m'arrêter ici. Non en vrai, t'es trop cool (ahah j'adore les remerciements les plus nuls ! Je sais que ça va te faire marrer). **Bella**, that postponed her flight back to the US just to be there for my defense, so cute ! **Elias** qui va bientôt payer des bières ! Ou peut-être Nicolas en fait. Merci également aux anciens co-bureau **Stéphanie**, tu nous manques trop avec ta bonne humeur contagieuse et tes reportages photo qui arrivent à capter toujours le moment parfait. **Oscar**, merci d'avoir été si gentil au début quand j'étais perdue et je ne parlais pas encore français. Après, une très belle amitié a commencé, depuis que t'es parti, tu as laissé un petit vide dans le bureau et dans mes pauses merenda ;). **Benoît**, merci pour toutes les canelles que tu m'as fait bouffer. **Haritha**, thank you for being there at the beginning and mentoring me.
Merci à l'ancienne bande des sportifs infatigables. **Hugues**, toujours zen et imperturbable. **Sofiane**, merci pour ta bonne humeur et ta spontanéité adorable. **Nono**, merci pour toutes les randos, les discours de motivation. Merci pour tes plans à la dernière minute, j'adore comment tu arrives toujours à trouver la place pour me caser quelque part, même quand t'as 20 minutes d'attente à la gare de Lyon. Merci d'avoir toujours pensé à moi, avant et maintenant aussi même si t'es loin. **Papi Flo**, merci de m'avoir montré 1001 manières de se bloquer le dos ! C'est un talent au final ! **Toto**, merci d'être toujours toi-même, déjà ça, ça met de bonne humeur. Merci pour tous les sketchs dans le couloir, y en a des ratés mais y a eu de bonnes choses aussi ! Merci d'être toujours si attentif et gentil même si tu le fais passer tout le temps pour une blague.

Olivier et Cyp, grazie belli !!! Tout a commencé avec un petit sticker et là les albums sont devenus cinq. Grazie pour toutes les merende ensemble, les verres à trois dehors les bars parce qu'ils étaient déjà fermés depuis longtemps. Merci pour m'avoir toujours remonté le moral avec vos conneries et avoir toujours dit "DAIDAI", sans trop réfléchir, à mes propositions. Je pense qu'il aurait fallu réfléchir à certaines occasions :). **Olivier**, merci pour tous les trottoirs qu'on a faits ensemble, souvent avec une bière à la main mais de temps en temps avec ton vélo par terre ! Merci pour ta motivation constante et contagieuse et grazie pour croire en moi plus que moi-même et de me pousser toujours à dépasser mes limites (autrement appelé, dans certains cas, avant dernière prise ;)). Heureusement j'ai appris le français sinon on serait passé à côté d'une si belle amitié. **Cyp**, merci d'être toujours en désaccord (et en accord) avec moi. Merci pour me comprendre si bien, même quand je prononce mal les UUU ! Grazie pour tout le support (oui, ça je n'ai pas corrigé) de cette dernière période, pour les pauses déj/dîner/goûter de deux heures qui se transformaient très vite en sessions de psy, consultations ophtalmo, leçons de botanique, étude des nuages, italian splaining, revival année 2000, ... la liste est longue. Tout ça pour dire merci d'avoir été toujours là, et 'toujours là' ce n'est pas une expression dans ce cas, ahahah dai scherzo ! Je suis très contente d'avoir partagé ce moment avec toi. Mais en vrai de vrai, merci surtout pour m'avoir appris l'art de la vectorisation et, j'écris en petit, avoir sauvé ma plante.

Un grazie gigante a tutti gli amici di qui e di là.

Grazie ai **Monteras** a quella casa rifugio, cucina stellata, hotel per genitori e amici, casa dei trapani e delle smerigliatrici, casa delle piante, dei pomodori e delle pizze, degli stromboli party, casa delle poltrone più brutte della storia delle poltrone, casa delle ciabatte tirolesi, del cucito e dei flauti traversi ma soprattutto casa piena di amore e di momenti felici di noi attorno a una tavolo a mangiare e bere e chiacchierare di tutto, seduti o sdraiati un po' ovunque ma sempre e comunque qualcuno sul davanzale. **Lollo**, grazie per le tante bevute e le tante chiacchiere, per le serate senza piani ma che comunque in ogni caso dovevo portare il tabacco. **Chiara**, grazie per i saluti volanti dalla finestra, per tutti i pacchi che riesci sempre a farti perdonare non si sa come e per il tuo essere sbadato attento (la finisco qua perché so bene che manco la volevi sta riga di ringraziamenti, ti daro una pacca sulla spalla che la gestisci meglio e la finiamo qui). **Matti** grazie per la tua passione nel fare qualsiasi cosa e soprattutto nel fare la pizza perfetta. Bon e inutile che ci giro intorno, grazie per la bici! mi hai salvata! **Francesco** detto Cecco Beppi detto il Nocciolina. Prima di tutto come potrei non ringraziarti per tutte le noccioline. E poi grazie per essere sempre presente, attento e puntuale nel stare vicino alle persone. Grazie per 'SSSSIIIII vorrei rubarla' e per tutti i pranzi e le cene con cui ci sai coccolare solo tu. **Francis**, déjà je t'entend te plaindre en disant pourquoi je suis en dernier, et bah voilà pour ça. Sérieusement, merci pour ta sassyness infatigable! Merci d'être toujours là avec tes blagues de cabaret et tes bières blanches à l'apéro! Et merci pour tes remarques un peu méchantes :) quand j'en avais besoin (but that's your style I know!).

Grazie a quei pazzi amici di Rotterdam, che anche oggi sono qui a sostenermi e aspettarmi per fare festa! Grazie a tutti e tre, dopo anni siamo ancora uniti ed è bellissimo! Grazie **Cami** per aver smesso di odiarmi ahaha e per aver iniziato questa bellissima tradizione dei cazzanatali e i cazza qualsiasi altra cosa insieme. Grazie **Fra** per la tua spontaneità romana e il tuo enorme cuore che ha sempre posto per me, pure col fuso orario, e pure se si tratta di spostare voli intercontinentali per non perderti questo giorno. Grazie **Lore** per essere il folle amico con cui poter fare e parlare di qualsiasi cosa, mi hai sempre capito al volo senza bisogno di parlare troppo (noi gente di lago e montagna non abbiamo bisogno di parlare).

Grazie ai Gingini di Padova, ragazzi sono passati anni e siete ancora qui, non potete capire quanto mi rende felice. **Giuli** la tua spontaneità e buonumore mi hanno sempre tenuta legata a te, ogni volta che arrivavo con un problema lo scioglievi in un attimo. **Beppe** sempre pronto per fare qualsiasi cosa e ovunque, non

ti ferma nulla solo a volte dei pantaloni troppi stretti o dei calzini un po troppo usati. Ma la cosa più importante: grazie ancora per i tuoi appunti!

Marti che ti devo dire, non avevo dubbi che saresti stata qui anche oggi, non siamo più vicine fisicamente ma è come se non ci fossimo allontanate mai, tutto e ancora cosi quotidiano. Grazie per esserti presa cura di me per tutti questi anni nel modo speciale che sai fare solo tu, sempre attento e puntuale ma caciarone quanto bisogna relativizzare.

Franca sorelle da genitori diversi anche se ormai i nostri genitori ci fanno da genitori a vicenda. (Poi mi rubi le cose proprio come vere sorelle). Inseparabili da più di quindici anni, non è mai cambiato nulla dal liceo anche adesso quando siamo insieme facciamo sempre le stesse cazzate. Grazie per esserci sempre stata e per non farmi dubitare un secondo che sempre ci sarai.

Arj compagna di tutto, da sempre, abbiamo condiviso tutto dai banchi del liceo fino ad una stanza senza porta. Grazie per esserti sempre presa cura di me con i tuoi wurstel al formaggio. Quando torno da te a Padova e come tornare a casa e anche se gli anni passano, casa resta.

Anna e Lorenzo troppi anni e troppe cose da ricordare, sarebbe impossibile ringraziarvi per tutte. Siamo cresciuti insieme un po' come fratelli e cosi stiamo continuando a fare, ci vedo gia a 50 anni a scherzare e litigare sempre per le stesse cose, non vedo l'ora.

Un grazie speciale a tutta la mia famiglia, a tutti gli zii e cugini. Ai nonni e alla nonna Carmen, da sempre il mio fan club numero uno, non importa cosa io stia facendo, l'importante é farlo a pancia piena.

Grazie **mamma e papà** per il vostro supporto costante e silenzioso. Grazie per aver sempre capito senza fare troppe domande o pretendere risposte. Grazie per avermi sempre seguita con il vostro furgoncino ovunque io fossi, sempre carico di grappa e vino. Ora quel furgone è diventato un treno merci pieni di cibo per tutti.

Il ringraziamento più importante va a **Gabriele**, grazie di tutto! ciao!

Ahahah sarebbe stato bello finire così, come i messaggi di mio papà. Dai seriamente grazie per credere in me sempre. Grazie per essere il mio motivational coach, badante, cuoco, preparatore atletico, psicologo, signore delle pulizie. Grazie per i tuoi discorsi motivazionali che sanno sempre arrivare al punto. E grazie per esserti trasformato in party planner, il tuo incubo peggiore, solo per farmi stare tranquilla e concentrata. Senza di te non sarei mai arrivata fino a qui.

TABLE OF CONTENTS

ABSTRACT

Neuropathic pain is an abnormal pain sensation that persists longer than the temporal course of natural healing. It interferes with the patient's quality of life and leads to several comorbidities, such as anxiety and depression. It has been suggested that chronic pain may result from abnormal and maladaptive neuronal plasticity in the structures known to be involved in pain perception (Bliss et al. 2016). This means that nerve injury would trigger long-term potentiation of synaptic transmission in pain-related areas (Zhuo, 2014). Since these regions are also involved in the emotional aspects of pain, our hypothesis is that the aforementioned maladaptive plasticity in these brain areas could constitute a key mechanism for the development of comorbidities such as anxiety and depression.

My PhD aimed at testing this working hypothesis, through the study of brain resting state functional connectivity (FC) using functional ultrasound imaging (fUS) in a mouse model of neuropathic pain. FUS is a relatively recent neuroimaging technique that enabled numerous advances in neuroscience, thanks to its high spatio-temporal resolution, its sensitivity, but also its adaptability, allowing studies in anesthetized or awake animals.

In a first study, I developed an experimental protocol allowing the brains of awake mice to be imaged in a reproducible manner and with minimal stress and movement artifacts and was also involved in the development of a new algorithm for the analysis of the signals generated by these acquisitions. As this first approach was carried out with a moving linear probe which does not allow the entire brain to be visualized, in a second study, I participated in the development of a new compiled and motorized probe technology.

Building on these technological developments, I then used these new approaches to test my neurobiological hypothesis. I undertook two parallel studies in animals anesthetized for one and awake for the second, in which we studied the temporal link between alterations in cerebral FC and the development of neuropathic pain and/or associated comorbidities. To do this, we measured the resting-state functional connectivity (FC) in anesthetized and in awake head-fixed mice, at three time points: I) 2 weeks after induction of neuropathic pain (cuff around the sciatic nerve), II) at 8 weeks post-induction during the emergence of anxiety (8W) and III) at 12 weeks post-induction during the emergence of depression. This longitudinal follow-up has been conducted concurrently on a control group.

Our results show significant changes in FC in major pain-related brain regions in accordance with the development of neuropathic pain symptoms. These findings suggest that the pain network undergoes maladaptive plasticity following nerve injury which could contribute to pain chronification. Moreover, the

time course of these connectivity alterations between regions of the pain network could be correlated with the subsequent apparition of associated comorbidities.

RESUME

La douleur neuropathique est une sensation de douleur anormale qui persiste au-delà du cours temporel de la guérison naturelle. Elle interfère avec la qualité de vie du patient et est associée à plusieurs comorbidités telles que l'anxiété et la dépression. Des études antérieures ont suggéré que la douleur chronique pourrait résulter d'une plasticité neuronale anormale et inadaptée dans les structures connues pour être impliquées dans la perception de la douleur (Bliss et al. 2016). Cela signifie qu'une lésion nerveuse déclencherait une potentialisation à long terme de la transmission synaptique dans les aires cérébrales liées à la douleur (Zhuo et al. 2014). Comme ces régions sont également impliquées dans les aspects émotionnels de la douleur, notre hypothèse est que la plasticité inadaptée susmentionnée dans ces zones cérébrales pourrait constituer un mécanisme clé pour le développement de comorbidités, telles que l'anxiété et la dépression.

Au cours de ma thèse, nous avons choisi de tester cette hypothèse de travail par l'étude des altérations de la connectivité fonctionnelle (CF) intrinsèque des réseaux cérébraux par imagerie fonctionnelle ultrasonore (fUS) dans un modèle murin de douleur neuropathique. Cette technique de neuro-imagerie relativement récente a permis de nombreuses avancées en neurosciences, grâce à sa haute résolution spatio-temporelle, à sa sensibilité, mais aussi son adaptabilité, permettant des études chez l'animal anesthésié ou éveillé.

Dans une première étude, j'ai mis au point un protocole expérimental permettant d'imager le cerveau des souris éveillées de façon reproductible et avec un minimum de stress et d artefacts de mouvements et ai également été impliquée dans le développement d'un nouvel algorithme d'analyse des signaux générées par ces acquisitions. Cette première approche étant réalisée avec une sonde linéaire en mouvement qui ne permet pas de visualiser l'entièreté du cerveau, dans une seconde étude, j'ai participe au développement d'une nouvelle technologie de sonde compilées et motorisée.

Fort de ces développements technologiques, j'ai alors utilisé ces nouvelles approches pour tester mon hypothèse neurobiologique. J'ai entrepris deux études en parallèle chez des animaux anesthésiés pour l'une et éveillés pour la seconde, chez lesquelles nous avons étudié le lien temporel entre les altérations de la CF cérébrale et le développement de la douleur neuropathique et/ou des comorbidités associées. Pour cela, nous avons mesuré la CF (en période de repos) chez des souris atteintes de douleur neuropathique, à trois moments différents : I) 2 semaines après l'induction de la douleur neuropathique (manchon autour du nerf sciatique) II) à 8 semaines post-induction, lorsque l'anxiété émerge et III) à 12

semaines post-induction, lorsque la dépression apparait (12W). Ce suivi longitudinal a également été réalisé en parallèle sur un groupe d'animaux contrôles.

Nos résultats indiquent des changements significatifs de la CF dans les principales régions cérébrales impliquées dans la transmission ou la modulation de la sensibilité ou de la douleur, suggérant la mise en place d'une plasticité inadaptée du réseau de la douleur, suite à la lésion nerveuse. De plus, nous observons une évolution temporelle de ces altérations, potentiellement corrélée à l'apparition des comorbidités associées. Ainsi, ces mécanismes pourraient participer à la chronicisation de la douleur.

CHAPTER 1

INTRODUCTION

1 PAIN DEFINITION

Pain is officially defined by the International Association for the Study of Pain (IASP), as an unpleasant sensory and emotional experience associated with actual or potential tissue damage.
The English word, **pain** come from the old French *peine*, which traces back to the Latin *poena*, meaning punishment or penalty, and the Greek *poine*, price paid, penalty, punishment.
While commonly associated with conscious sensations linked to bodily harm or illness, the word 'pain' and its synonyms are also used to describe discomfort related to other unpleasant feelings (Perl 2007).

As can be inferred from this first analysis, pain was not exactly considered to be a specific sensory modality but rather an affliction of the soul, something considered beyond the experience of classic sensory system (Kandel et al. 2014 5th edition). Indeed, while most sensory and somatosensory modalities are fundamentally informative, pain has also a protective role.

What sets pain apart from the classical senses like hearing, smell, taste, touch, and vision is its dual nature. In their early description, Melzack and collaborators (1968) supported the idea that pain has a unique, distinctly unpleasant, affective quality that differentiates it from the other sensory experiences. It becomes overwhelming, demands immediate attention, and disrupts ongoing behavior and thought. It motivates or drives the organism into activity aimed at stopping the pain as quickly as possible. They describe pain sensation as a **multidimensional integration of sensory discriminative, cognitive, and affective-motivational axes**. In essence, pain is both a discriminative sensation and a graded emotional experience associated with actual or potential tissue damage.
Pain usually serves an adaptive role by protecting and alerting the body as a warning signal of tissue inflammation and damage, and inducing behavioral changes that facilitate wound healing and recuperation.
Prinking, burning, aching, stinging and soreness are the most common of all the sensory modalities associated with pain. Yet, pain is not the direct encoding process of a sensory event; it is rather the product of elaborate processing by the brain of a variety of neural signals (Kandel et al. 2014 5th edition). Instead, the direct neural process of encoding noxious stimulus is called **nociception**. Pain and nociception are two distinct phenomena. Pain is considered a personal experience influenced by varying degrees by biological, psychological, and social factors and it can't be inferred solely from activity in sensory neurons as nociception. There are two layers of elaboration of a noxious stimulus: the direct encoding of the sensory

stimulus, nociception, and then the cortical elaboration and perception which is the actual pain perception (Figure 1).

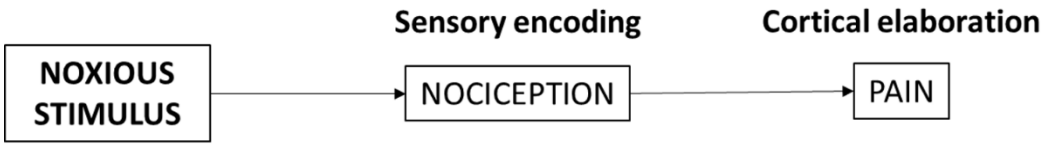

Figure 1: Elaboration of the noxious stimulus. Schematic representation of the noxious stimulus processing, involving at first the sensory signal encoding (nociception) followed by the cortical integration of the stimulus, resulting in the perception of pain.

2 NOCICEPTIVE PATHWAYS

Sometimes sensory stimuli can be dangerous for the body because they could cause tissue damage. These types of stimuli are called noxious stimuli, and they need to be perceived and elaborated to avoid tissue damage.

A sensory stimulus is processed by the somatosensory system. The stimulus activates a chain of neurons starting at the periphery with the peripheral first-order afferent and ending in the cerebral cortex.

The sensory pathway can be divided into three different consecutive processes: transduction, transmission, and perception (Figure 2). The pathway begins with the **transduction** of the sensory stimulus in electrical activity by the activation of sensory receptors located in the primary afferent sensory neurons endings. The receptors activation generates an action potential in the nerve ending which is propagated from the periphery to the second-order neurons located in the dorsal horn of the spinal cord (**transmission**). Neurons in the spinal cord, either directly or through interneurons, convey information to various areas of the nervous system that provide for the elaboration of the sensory information and organization of the responsive behaviors (**perception**).

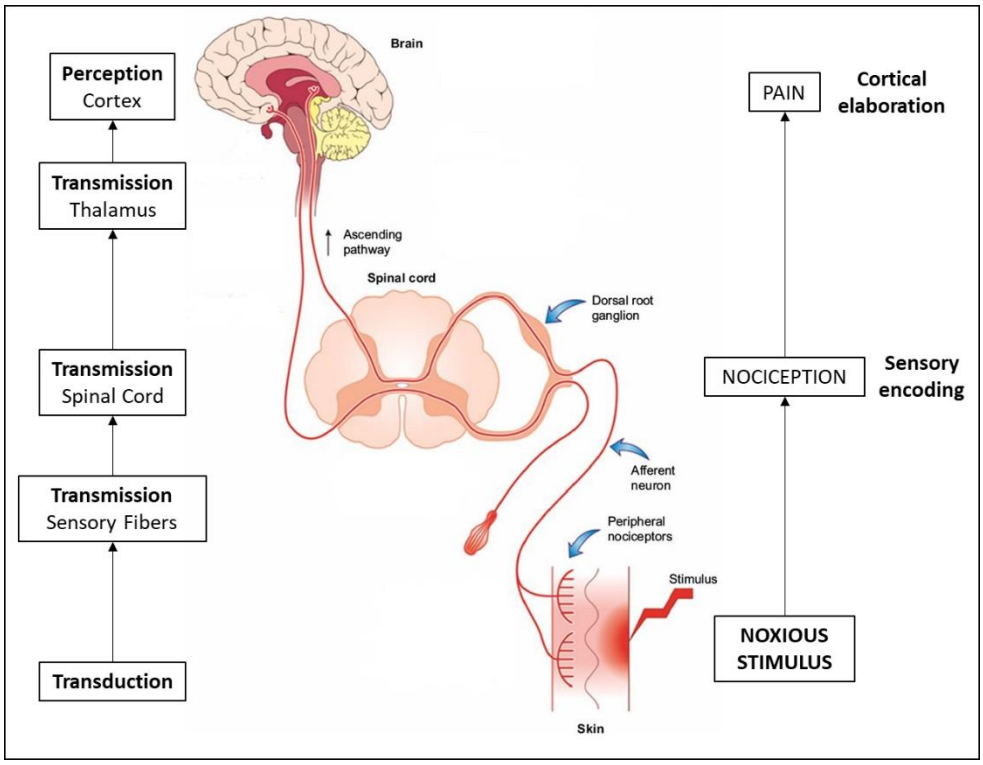

Figure 2: Nociceptive pathways. The sensory pathway is divided into three different consecutive processes. The transduction takes place in the nociceptors, followed by the transmission of the electrical

signal across the sensory fibers in the spinal cord. Finally, the signal ascends through the thalamus to the cortex, where perception and elaboration of the sensory signal occur.

2.1 TRANSDUCTION

Nociceptors are a subset of primary sensory neurons, activated by noxious stimuli and convey nociceptive information to the spinal cord dorsal horn.

The membrane of the nerve terminal of the nociceptor contains **receptors and ion channels** that detect stimuli that have potential to cause damage. These receptors convert the thermal, mechanical, or chemical energy of noxious stimuli into a depolarizing electrical potential (Figure 3).

Some of these channels are listed below:

- Transient Receptor Potential (TRP) ion channel family, nonselective cation channels (Kandel et al. 5th edition):
    - TRPV1: is expressed selectively by nociceptive neurons and mediates the pain-producing actions of capsaicin. This channel is also activated by noxious thermal stimuli, which suggests that it normally transduces the sensation of painful heat.
    - TRPV2: is activated by very high temperature.
    - TRPM8: is activated by low temperature and by chemicals such menthol.
- Acid-Sensing Ion Channels (ASIC) are voltage-independent, proton gated cation channels. They detect a broad range of physiological pH changes.
- Piezo family of ion channels. They are non-selective cation channels permeable to Ca^{2+}. They are activated by mechanical noxious stimulus.

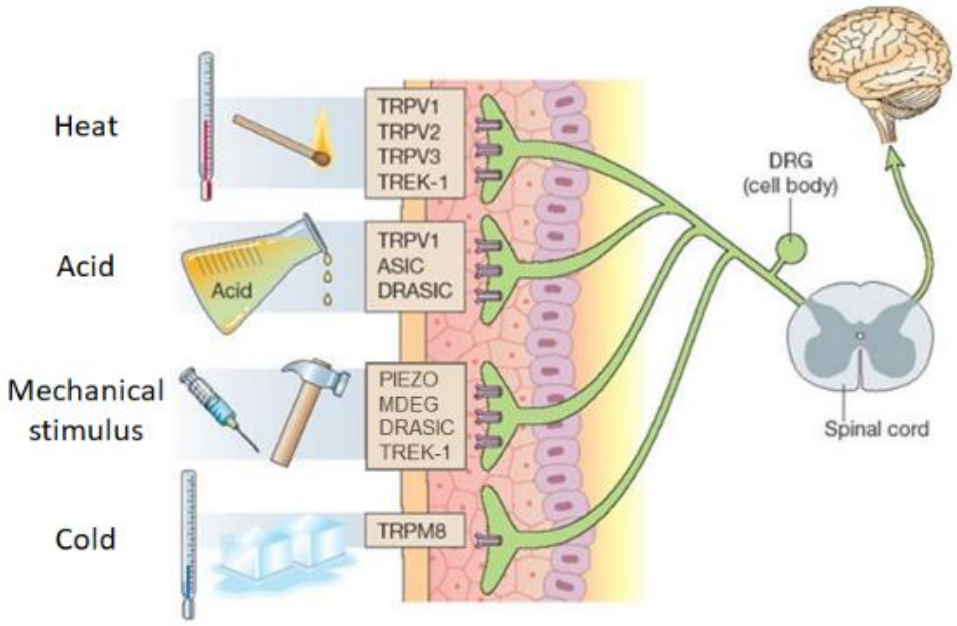

Figure 3: Transducers. Schematic representation of nociceptor's axon terminals in which the noxious stimuli transducers are located. They detect different kinds of stimulus including heat, acid, mechanical and cold.

2.2 TRANSMISSION

2.2.1 Nociceptors

The activation of those different receptors and ion channels by the noxious stimulus generates an action potential which is transmitted from the periphery to the Central Nervous System (CNS) by the nociceptive fibers.

Nociceptors are free endings nerve located in the skin, muscle, joints, bone, and viscera. Nociceptors, like other primary somatosensory neurons, are pseudounipolar (Figure 4): a single process emanates from the cell body in the dorsal root ganglion (DRG) or trigeminal ganglion (TG) and bifurcates, sending a **peripheral axon** to innervate the skin and a **central axon** to synapse on second-order neurons in the dorsal horn of the spinal cord or the trigeminal subnucleus caudalis, respectively (Dubin and Patapoutian 2010).

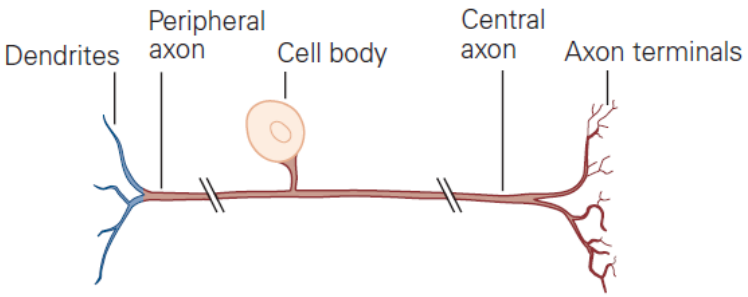

Figure 4: Pseudounipolar structure of nociceptive fibers (Kandel et al. 2014 5th edition).

Anatomical and in vivo/in vitro electrophysiological studies have shown that there are two major types of nociceptive fibers: myelinated Aδ-fibers and unmyelinated C-fibers; different subsets of which are sensitive to a different range of stimuli, most being polymodal, but others responding to a narrower range of stimuli (J. Brooks and Tracey 2005) (Figure 5A-B).

C-fibers: unmyelinated fibers defined as polymodal nociceptors because they respond mainly to noxious heat but also to high-intensity mechanical and chemical stimuli. Since they are unmyelinated fibers, they conduct the action potential at a speed of 1 m/s. Their peripheral afferent innervates the skin (dermis and/or epidermis) and central axon projects to superficial laminae I and II of the dorsal horn (Figure 5C).

A-fibers: myelinated fibers with a conduction velocity in the Aδ range of 5 to 30 m/s. They respond predominantly to heat or mechanical stimuli; however, sensitivity to noxious cold is also observed. Their central processes project to superficial laminae I and V. (Dubin and Patapoutian 2010) (Figure 5D).

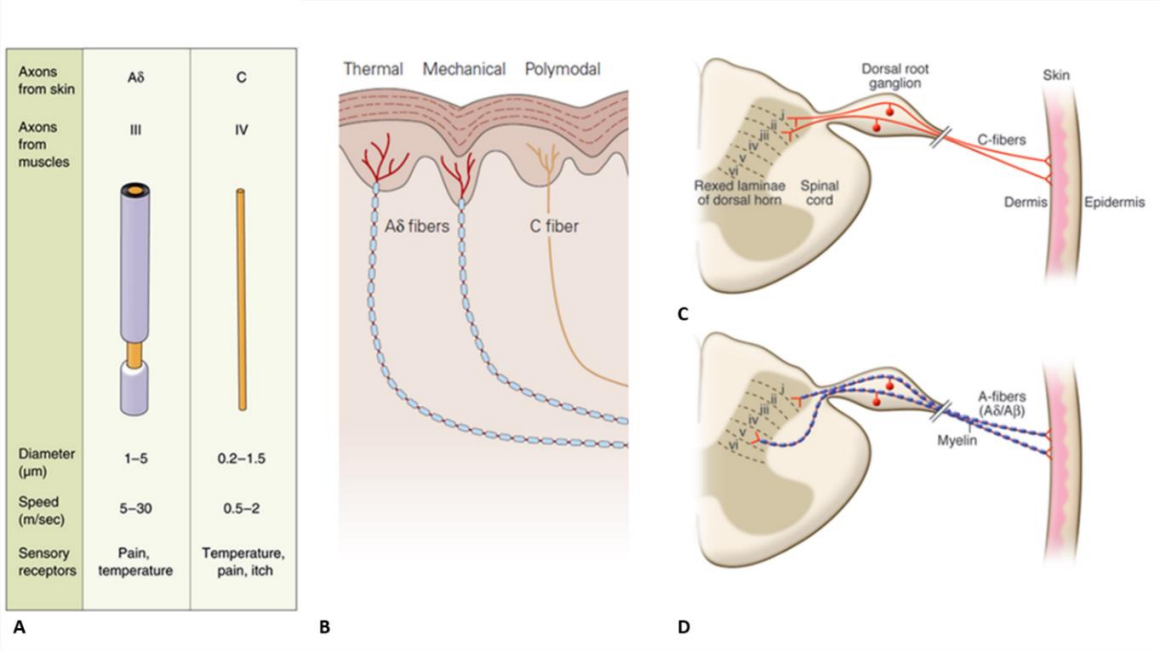

Figure 5: **Classification of nociceptive fibers**. (A) Characteristics of classification between A-fibers and C-fibers. (B) schematic distinction between myelinated and non-myelinated fibers. C-fibers polymodal. (C) C-fibers project to laminae I and II of the dorsal horn. (D) A-fibers project to superficial laminae I and V of the dorsal horn. (Adapted from Kandel et al. 2014 5th edition).

2.2.1.1 Spinal cord dorsal horn organization

Within the general organization of the somatosensory system, primary afferent neurons project to second order neurons located in the spinal cord dorsal horn. The spinal gray matter is subdivided into 10 laminae (or layers), numbered I to X from dorsal to ventral, based on differences in cell and fiber composition. There is a tight link between the anatomical organization of the dorsal horn neurons and their functions in sensory processing (Figure 6) (Kandel et al. 2014 5th edition).

Lamina I:

- A set of neurons, called *nociceptive-specific neurons*, located in Lamina I ,respond to noxious stimuli conveyed by Aδ and C-fibers. This set of neurons project to higher brain centers, notably the thalamus.
- A second class of Lamina I neurons receive inputs from C-fibers selectively activated by noxious cold stimuli.
- There is a third class of Lamina I neurons, called *wide-dynamic-range neurons*, they respond to both innocuous and noxious mechanical stimuli.

Lamina II is a densely packed layer that contains many different classes of local interneurons, some excitatory and others inhibitory. Some of these interneurons respond selectively to nociceptive inputs (from both Aδ and C-fibers), whereas others also respond to innocuous stimuli.

Laminae III and IV contain a mixture of local interneurons and supraspinal projection neurons. Many of these neurons receive inputs from Aβ afferent fibers that respond to innocuous cutaneous stimuli.

Lamina V contains neurons that respond to a wide variety of noxious stimuli and project to the brain stem and thalamus. These neurons receive direct inputs from Aβ and Aδ fibers and because their dendrites extend into lamina II, are also innervated by C fiber nociceptors. Neurons in lamina V also receive inputs from nociceptors in visceral tissues. The convergence of somatic and visceral nociceptive inputs onto individual lamina V neurons provides one explanation for a phenomenon called "referred pain," a condition in which pain arising from injury to a visceral tissue is perceived as originating from another region of the body surface. Patients with myocardial infarction, for example, frequently report pain from the left arm as well as the chest.

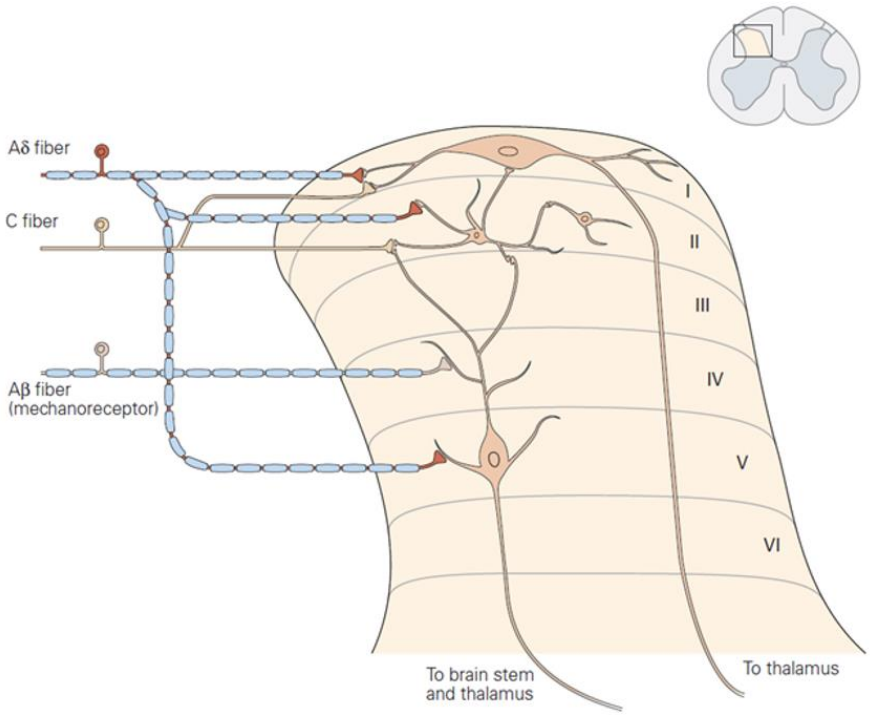

Figure 6: Spinal cord dorsal horn organization. Neurons in lamina I of the dorsal horn receive direct input from myelinated (Aδ) nociceptive fibers and both direct and indirect input from unmyelinated (C) nociceptive fibers via interneurons in lamina II. Lamina V neurons receive low threshold inputs from large-diameter myelinated fibers (Aβ) of mechanoreceptors as well as inputs from nociceptive afferent fibers (Aδ and C fibers). Lamina V neurons send dendrites to lamina IV, where they are contacted by the

terminals of Aβ primary afferents. Dendrites in lamina III arising from cells in lamina V are contacted by the axon terminals of lamina II interneurons (Kandel et al. 2014 5th edition).

Neurons in lamina VI receive inputs from large diameter fibers that innervate muscles and joints. These neurons are activated by innocuous joint movement and do not contribute to the transmission of nociceptive information. In contrast, many neurons located in laminae VII and VIII, the intermediate and ventral regions of the spinal cord, do respond to noxious stimuli.

2.2.1.2 Double pain sensation

C and Aδ fibers are often coactivated by noxious stimuli and the action potential is respectively propagated at different speeds in the two types of fibers (Perl 2007) (Figure 7A). This explains the two sequential pain sensations in short time intervals experienced after a painful stimulation (Figure 7B). The initial sensation, occurring immediately after the injury, is characterized by a sharp pain (first pain). Subsequently, several seconds later, a more sustained and occasionally burning pain arises (second pain). The distinct temporal gap between these two sensations is attributed to the rapid transmission of information by Aδ fibers, responsible for the first pain, followed by a delayed transmission of pain information carried by C-fibers. This phenomenon is known as the "double pain sensation."

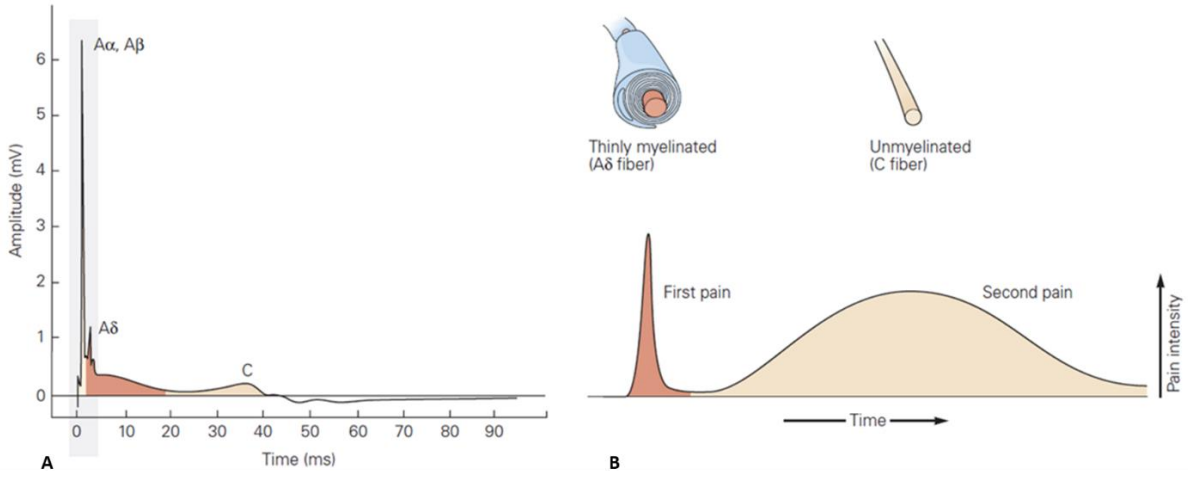

Figure 7: Propagation of action potentials in different classes of nociceptive fibers. (A) The speed at which action potentials are conducted is a function of each fiber's cross-sectional diameter. The first peak and its subdivisions are the summed electrical activity of myelinated A fibers. A delayed (slowly conducting) detection represents the summed action potentials of unmyelinated C fibers. (B) First and second pain are carried by two different primary afferent fibers (Adapted from Kandel et al. 2014 5th edition).

2.2.2 Five Major Ascending Pathways

The nociceptive information is transmitted from the second order-neurons located in the spinal cord to the Central Nervous System (CNS) by several ascending pathways (Kandel et al. 2014 5th edition).
Five main ascending pathways: the spinothalamic, spinoreticular, spinomesencephalic, cervicothalamic, and spinohypothalamic tracts contribute to the central processing of nociceptive information (Figure 8).

- **The spinothalamic tract** has the most important role in the transmission of nociceptive information since it represents the most prominent ascending nociceptive pathway in the spinal cord. It consists of axons of nociception-specific, thermosensitive, and wide-dynamic-range second-order neurons located in Lamina I and V through VII on the dorsal horn. From their segment of origin, they immediately decussate in the spinal cord, reaching the contralateral part. Then, these axons ascend the anterolateral white matter tract until they reach the thalamic nuclei (Figure 8A).
- **The spinoreticular tract** consists of axons of second-order neurons located in Laminae VII and VIII. These axons decussate and reach the contralateral part of the spinal cord in the anterolateral quadrant. They then project to the medullary-pontine reticular formation, and from there, other neurons project to the thalamus (Figure 8B).
- **The spinomesencephalic (or spinoparabrachial) tract** has an important role in the **emotional component of pain.** This tract contains axons of neurons located in Laminae I and V. Some of these axons cross and project in the anterolateral quadrant of the spinal cord, terminating in the mesencephalic reticular formation and periaqueductal gray matter. Some other axons of this pathway travel up the spinal cord via the dorsal part of the lateral funiculus, terminating in the parabrachial nucleus. Neurons of the parabrachial nucleus project to the amygdala, a key nucleus of the limbic system that regulates emotional states (Figure 8C).
- **The cervicothalamic tract** consists of axons of the lateral cervical neurons which receive inputs from neurons in lamina III and IV. These axons are located in the lateral white matter of the upper two cervical segments of the spinal cord.

  Some axons decussate and ascend in the medial lemniscus of the brain stem, until the midbrain nuclei and in the ventroposterior lateral and posteromedial nuclei of the thalamus. Some other axons project directly into the dorsal columns and terminate in the cuneate and gracile nuclei of the medulla.
- **The spinohypothalamic tract** contains axons of neurons located in Laminae I, V, and VIII. These axons project to hypothalamic nuclei which function as autonomic control centers responsible for regulating the neuroendocrine and cardiovascular responses associated with pain syndromes.

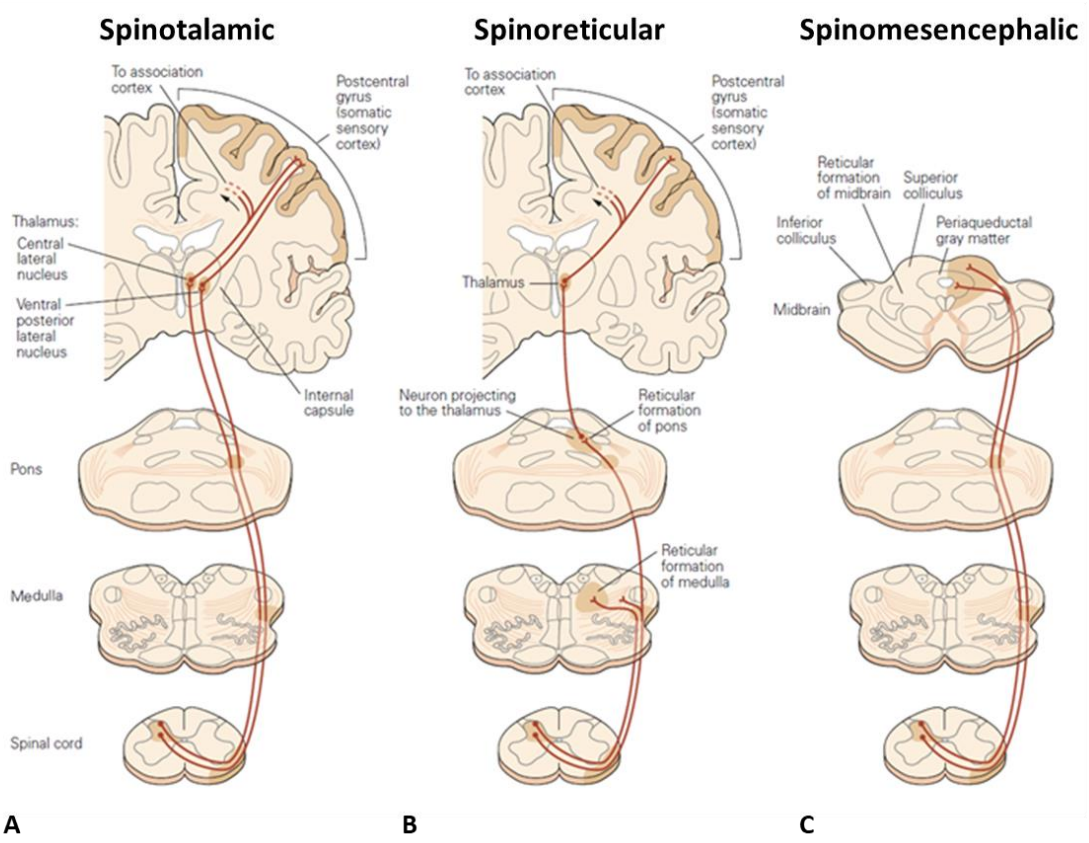

Figure 8: Ascending pathways. Three of the five ascending pathways that transit nociceptive information from the spinal cord to higher centers (Kandel et al. 2014 5th edition).

2.3 PERCEPTION

As previously mentioned, the nociceptive inputs are transduced via the nociceptors to the spinal cord dorsal horn, and finally, after modulation and integration, this information is relayed to central areas of the nervous system (Figure 2). The cortical elaboration of the nociceptive stimulus manifests in actual **pain perception**, which is characterized by the integration of sensory-discriminative, cognitive, and affective modalities.

2.3.1 Thalamus

Nociceptive information enters the brain primarily through projections to the thalamus (Figure 9A). This brain structure is positioned in the dorsal part of the diencephalon, and it is considered a key structure for the processing of sensory information. The thalamus represents the essential link between the sensory

receptors and the Cerebral Cortex. It is not just a relay of information, but it acts by blocking or enhancing the passage of specific information.

The thalamus is subdivided into 50 nuclei (Figure 9B), that are clustered into four groups: anterior, medial, ventrolateral, and posterior. Two of the most important regions for the nociceptive pathways are the lateral and medial nuclear groups (Craig et al 2003). Numerous groups of researchers identify several nuclei in **the lateral thalamus** (VPL, VPM, VPI, VMpo) and in the **medial thalamus** (CL, MDvc, Pf). From these two groups of thalamic nuclei, third-order neurons project to cortical areas like the primary somatosensory cortex (S1), secondary somatosensory cortex (S2), insula, anterior cingulate cortex (ACC) and prefrontal cortex (PFC) (Treede et al. 1999).

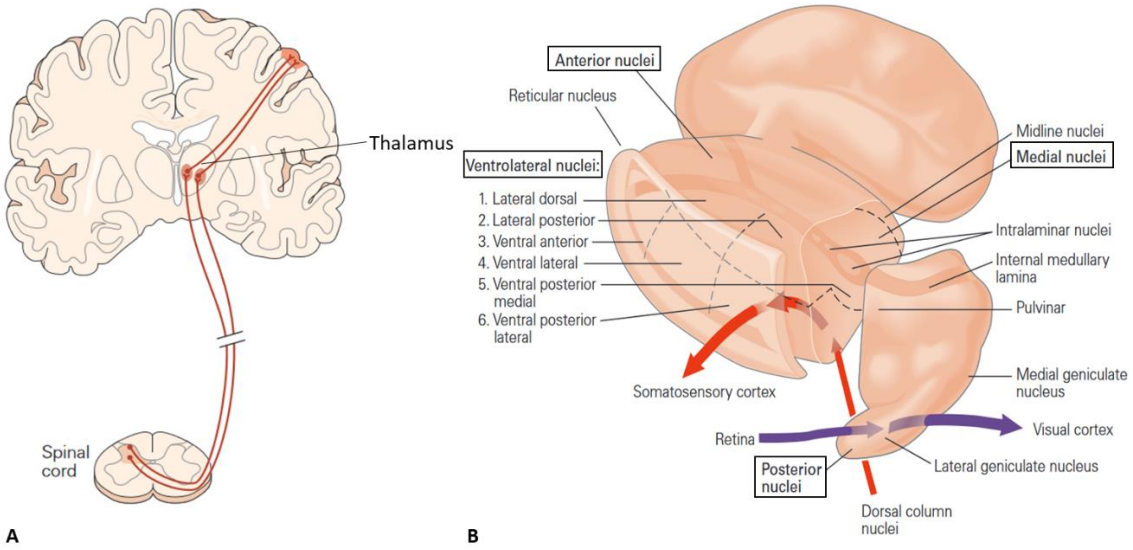

Figure 9: The major subdivisions of the Thalamus. (A) Spinotalamic pathway. (B) The thalamus is the critical relay for the flow of sensory information from peripheral receptors to the neocortex. Somatosensory information is conveyed from dorsal root ganglia to the ventral posterior lateral nucleus and, from there, to the primary somatosensory cortex. Likewise, visual information from the retina reaches the lateral geniculate nucleus, which conveys it to the primary visual cortex in the occipital lobe. Each of the sensory systems, except olfaction, has a similar processing step within a distinct region of the thalamus (adapted from Kandel et al. 2014 5th edition).

2.3.2 Cortical regions

Up until the end of the 20th century, the involvement of the cerebral cortex in pain perception was a controversial issue, and most of the evidence at that time supported the idea that pain was perceived only as a result of thalamic processing (Head and Holmes 1911). Then, with the advent of functional **brain**

imaging techniques, such as PET (Positron Emission Tomography) and fMRI (functional Magnetic Resonance Imaging) it has been shown that painful stimuli in fact activate multiple cortical areas (Treede et al. 1999).

The first three human brain imaging studies of pain were published in the early 1990s by Talbot and colleagues (Talbot et al. 1991) and Jones and collaborators , using PET, followed by Apkarian and colleagues (A. V. Apkarian et al. 1992), using SPECT (Single-Photon Emission Computed Tomography). All three studies used noxious heat stimulation, and although they brought forward different results, together they showed that multiple cortical and sub-cortical regions are activated by noxious stimulations (A. V. Apkarian et al. 2005a). Following these first studies, many other imaging experiments have been conducted since and have confirmed that noxious stimulation results in the activation of a distributed set of cortical and subcortical regions.

2.3.2.1 The concept of Pain Matrix, different theories

Such studies make it clear that processing of information within the neural systems linked to nociception and pain partly occurs across several brain regions operating simultaneously (Perl 2007). Structures such as the primary (S1) and secondary (S2) somatosensory cortices, the insula and the anterior cingulate cortex (ACC), have been consistently shown to respond to nociceptive stimulation using either fMRI, positron emission tomography (PET), electroencephalographic (EEG) or magnetoencephalography (MEG) (Iannetti and Mouraux 2010).
Different interpretations were employed to describe the functional significance of the various cortical and subcortical regions that were activated by a noxious stimulus.

2.3.2.1.1 Neuromatrix

In 1989, Ronald Melzack proposed the concept of **Neuromatrix** to describe the complexity of cortical perception and elaboration. He stated: “the Neuromatrix, distributed throughout many areas of the brain, comprises a widespread network of neurons that processes information that flows through it and produces the pattern that is felt as a whole body possessing a sense of self” (Melzack 2005). In essence the Neuromatrix was described as a widespread ensemble of neurons comprised of sensory (S), affective (A), and cognitive (C) neuromodules (Figure 10). The Neuromatrix receives various sources of input from three different macro-categories: sensory, cognitive-relative and emotional-relative. The inputs are

processed at the cortical level by different brain regions integrating simultaneously and this would generate the output sense of body-self. The outputs from the Neuromatrix are classified in pain perception and behavioral response, like action-motor programs and stress-regulation programs.

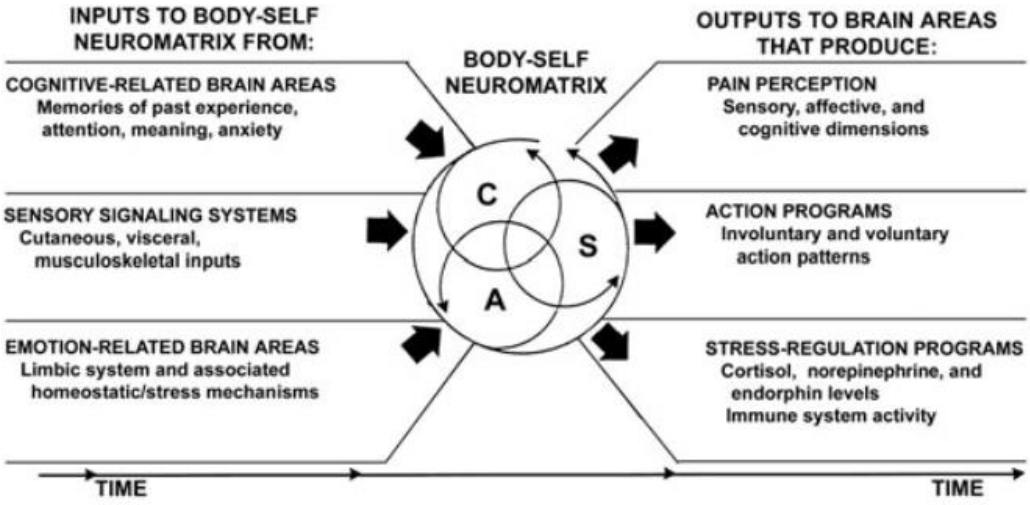

Figure 10: Body-self Neuromatrix. Factors that contribute to the patterns of activity generated by the body-self neuromatrix, which is comprised of sensory (S), affective (A), and cognitive (C) neuromodules. The output patterns from the neuromatrix produce the multiple dimensions of pain experience, as well as concurrent homeostatic and behavioral responses (Melzack 2005).

In several studies this definition has been revised, restricted, and focused on the interpretation of pain perception, which originally was considered to be only one of the many possible perceptual outputs of the Neuromatrix. From there, the concept of the Pain Matrix began to take shape.

2.3.2.1.2 Medial and lateral pain system

In Figure 11, Treede and collaborators (1999) proposed a simplified organization based on the projection sites from lateral or medial thalamic nuclei to the cortex and proposed a distinction between **medial and lateral pain system**, with the primary and secondary somatosensory cortices (S1 and S2) belonging to the lateral system and the anterior cingulate cortex (ACC) to the medial system. The insula occupies an intermediate position since it receives its main inputs from the lateral system, but itself projects to the limbic system.

The lateral pain system is primarily thought to play a role in the sensory discrimination of the location and intensity of painful stimuli (M. C. Bushnell et al. 1999; Kanda et al. 2000), whereas **the medial pain system** (Rainville et al. 1997; Vogt, Berger, and Derbyshire 2003) is involved in the affective (cognitive-evaluative) component of pain. The insula, however, encodes both the intensity (Coghill et al. 1999; Craig et al. 2000) and the laterality (J. C. W. Brooks et al. 2002; Bingel et al. 2003) of painful and non-painful thermal stimuli, but may also have a role in affective pain processing ((Bud) Craig 2003; Critchley et al. 2004; Seymour et al. 2004; Singer et al. 2004). Thus, as Peyron and collaborators demonstrated in 2002, the insula probably occupies a space between the medial and lateral systems, facilitating integration of information from both (R. Peyron, Laurent, and García-Larrea 2000; J. Brooks and Tracey 2005).

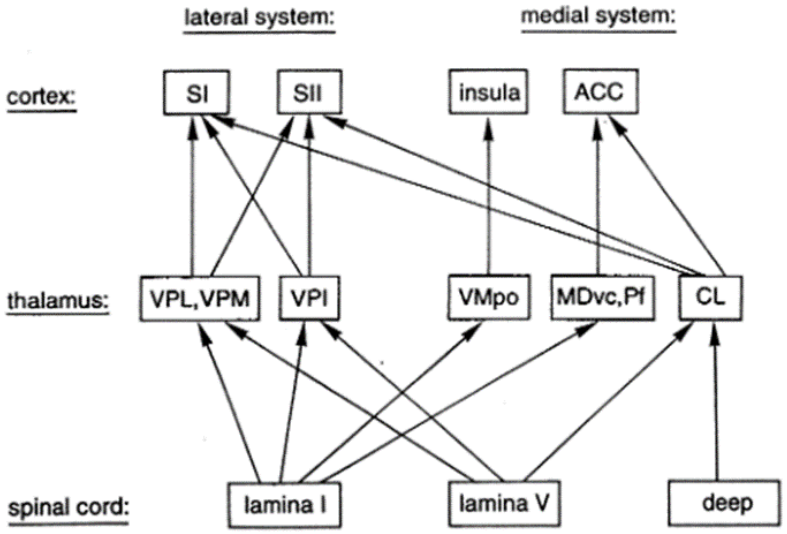

Figure 11: Medial and lateral pain system. Schematic representations of main spinothalamic and thalamocortical projections. Cortico-cortical connections are not shown. ACC, anterior cingulate cortex; CL, centrolateral nucleus; MDvc, ventrocaudal part of medial dorsal nucleus; Pf, parafascicular nucleus; SI, primary somatosensory cortex; SII, secondary somatosensory cortex; VMpo, posterior part of ventromedial nucleus; VPI, ventral posterior inferior nucleus; VPL, ventral posterior lateral nucleus; VPM, ventral posterior medial nucleus. (Note that the insula is now considered to lie between the lateral and medial systems, since it has both a sensory-discriminative and a cognitive-evaluative role in pain sensation) (J. Brooks and Tracey 2005).

2.3.2.1.3 The Pain Matrix

The **pain matrix (PM)** is usually defined as a group of brain structures jointly activated by painful stimuli (Garcia-Larrea and Peyron 2013). This concept was initially proposed based on neuroimaging studies that identified consistent patterns of brain regions activation in response to painful stimuli. As explained at the beginning of the section, several experiments were performed by applying noxious stimuli to healthy

volunteers while measuring brain activity using different functional neuroimaging techniques (EEG, MEG, fMRI, PET).

The structures most commonly identified to be part of the pain matrix were (Figure 12):

1. Primary (S1) and secondary (S2) somatosensory cortices
2. Insular cortices
3. Anterior cingulate cortex (ACC)
4. Prefrontal cortex.

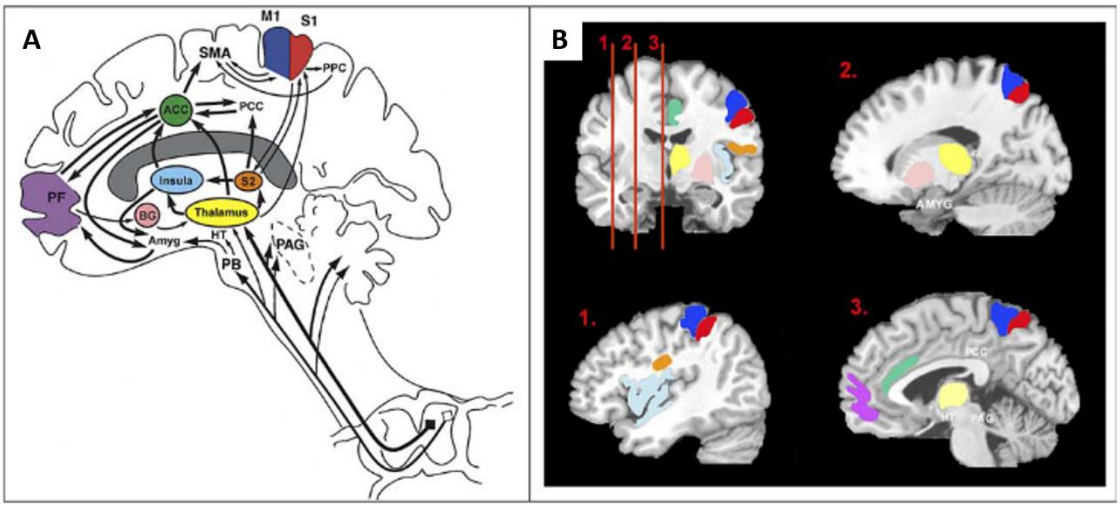

Figure 12: Cortical and sub-cortical regions involved in pain perception, their inter-connectivity and ascending pathways. The locations of brain regions involved in pain perception are color-coded in a schematic drawing and in an example MRI. (A) Schematic shows the regions, their inter-connectivity and afferent pathways. (B) The areas corresponding to those shown in the schematic are shown in an anatomical MRI, on a coronal slice and three sagittal slices as indicated on the coronal slice. The six areas are primary and secondary somatosensory cortices (S1, S2, red and orange), anterior cingulate (ACC, green), insula (blue), thalamus (yellow), and prefrontal cortex (PF, purple), primary and supplementary motor cortices (M1 and SMA), posterior parietal cortex (PPC), posterior cingulate (PCC), basal ganglia (BG, pink), hypothalamus (HT), amygdala (AMYG), parabrachial nuclei (PB), and periaqueductal gray (PAG). (Apkarian et al. 2005).

The conceptual consequence of this evidence would be to consider these regions as a part of a network specifically activated by noxious stimuli. However, some regions such as the anterior cingulate cortex, the anterior insula and the prefrontal areas showed enhanced activity also in a wide range of non-painful experiences. Hence, these regions do not appear to be exclusively activated in painful contexts (Roland Peyron et al. 1999; Sawamoto et al. 2000; Garcia-Larrea and Peyron 2013).

After accumulating evidence, researchers began to debate the idea that the Pain Matrix was a specific network responsible solely for pain processing. While there is a widespread agreement that the Pain Matrix is partially specific for pain processing, there is no universal consensus on its exact definition.
Some authors considered the Pain Matrix a unique cerebral signature for pain perception, while other investigators argued for its specificity as a pain-related network.
Indeed, some believed that it is the activation pattern within the various structures of the Pain Matrix, taken together, may constitute the neural substrate of pain perception. According to this view, the emergence of pain would not stem from the activation of one or more specific brain areas but would arise "from the flow and integration of information" among these areas (J. Brooks and Tracey 2005).

Following this concept and extending it further, Garcia-Larrea and Peyron in 2013 proposed a three-order level interpretation of the Pain Matrix.
They postulated that the multidimensionality of pain (sensory, affective, and cognitive) are different features managed by different networks. They conceptualized the Pain Matrix as a fluid system composed of three networks and the resulting pain experience would be the combination and integration of these three-order brain processing of progressive complexity.

1) The nociceptive matrix: the first-order network.

The nociceptive information is conducted by spinothalamic projections and guarantees the bodily specificity of pain and is the only one whose destruction employs selective pain deficits.
The cortical targets of spinothalamic tract are the posterior insula, the medial parietal operculum and the mid-cingulate cortex. These receiving regions are the source of the earliest responses to noxious stimuli recorded in the human brain (Maud Frot et al. 1999; 2013; Lenz, Rios, Chau, et al. 1998; Lenz, Rios, Zirh, et al. 1998) and contain a nociceptive matrix specific for spinothalamic projections. Lenz and associates (1995) reported “full pain experiences” when stimulating thalamic regions projecting to the posterior insula and operculum.

2) The second-order perceptual matrix, from nociception to pain:

Transition from cortical nociception to conscious pain relies on a second-order network, including: mid and anterior insulae; the anterior cingulate, prefrontal, and posterior parietal areas; and, with less consistency, the striatum, supplementary motor area, hippocampus, cerebellum, and temporoparietal junction. None of these regions is a direct target of the spinothalamic system, their direct stimulation does not evoke pain sensation, their selective destruction does not induce analgesia, they are also activated in

contexts not involving pain, and their contribution to the Pain Matrix depends upon the context in which noxious stimuli are applied.

3) The third-order network: from perception to pain memory:

Pain experience can still be elaborated as a function of beliefs, emotions, and expectations through activity of third-order areas, such as the perigenual cingulate, the orbitofrontal cortex, the temporal pole, and the anterolateral prefrontal areas. Activity in such third-order networks can therefore modify the immediate percepts driven by the nociceptive and second-order pain matrices.

In their interpretation of the Pain Matrix, Garcia-Larrea and collaborators considered the pain-related emotional and cognitive phenomena as a component of pain, rather than a reaction to it. In summary, the resulting pain experience arises from the coordinated and integrated activity of these three networks, which comprehend several brain regions. Their theory is schematized in Figure 13.

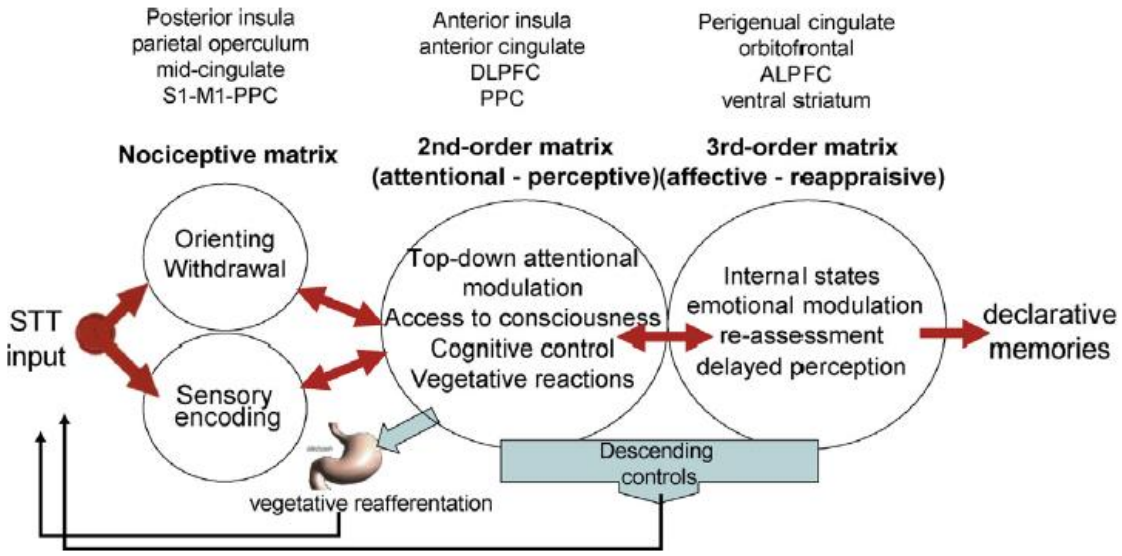

Figure 13: Schematic representation of the three order level pain matrices. The nociceptive matrix includes posterior insula, parietal operculum, mid-cingulate S1, M1, PPC. The second-order matrix includes anterior insula and anterior cingulate cortices, DLPFC, PPC. The three-order matrix includes pregenual cingulate, orbitofrontal cortex, ALPFC, ventral striatum (Garcia-Larrea and Peyron, 2013).

Figure 13 highlight the fact that the regions receiving spinothalamic inputs ensure the somatic-specific (corporal) quality of the sensation; they trigger activity in parietal, frontal and anterior insular circuits, supporting conscious perception, vegetative reactions and their modulation by attention and vigilance.

The immediate perception issued from these activities can itself be modulated by higher-order networks driven by emotional contexts and internal states.

2.3.2.1.4 Pain network

Iannetti and collaborators put forward a different interpretation, by arguing that the Pain Matrix was often considered as a unique cerebral signature for pain perception. In their paper in 2010, they focused on three different evidences against the concept of the pain matrix as a “brain pain center”:

- **No spatially segregated cortical area for nociception**

  It has been shown that neurons responding to different submodality of somatosensation, for example light touch or deep pressure, are organized in segregated cortical columns. This is not the case for nociceptive-specific neurons, they are mostly sparsely distributed, instead of organized in columns. Furthermore, not all the neurons identified as responding to nociceptive stimuli are nociceptive-specific. There is a sub-category of neurons defined as polymodal neurons, which means they also respond to stimuli belonging to other sensory modalities.

  In summary, the current lack of evidence for nociceptive cortical columns implies a different cortical organization compared to similar sensory modalities. Together with the small number and the sparse distribution of nociceptive-specific neurons in most of the cortical regions constituting the Pain Matrix, this theory suggests that, at the cortical level, nociception may not be represented as a distinct sensory modality or even as a distinct submodality of somatosensation (Andersson and Rydenhag 1985).

- **Activation of the pain matrix by non-nociceptive sensory input**

  Several studies have shown that brain regions activated by a noxious stimulus can also be activated by other non-nociceptive stimuli. Therefore, those regions mostly contain multimodal neurons, meaning that they respond to a range of stimuli, regardless of their sensory modality. As mentioned before, Melzack initially proposed that the experience of pain could emerge from the transient binding of a widespread network of neurons (Melzack 1989; 2005) and not solely from the activity of a spatially segregated cortical area containing nociceptive-specific neurons that exclusively ‘‘encode’’ pain in the brain.

- **Disruption of the correlation between intensity of pain and magnitude of the pain matrix response**

Functional neuroimaging studies using fMRI or PET have shown that the magnitude of the responses in the Pain Matrix can predict the amount of pain perceived by a human subject (Derbyshire et al. 1997; Porro et al. 1998; Coghill et al. 1999; Bornhövd et al. 2002; Büchel et al. 2002; Tolle et al. 1999). However, recent studies using EEG have shown that, in a number of circumstances, the magnitude of the elicited brain responses can be clearly dissociated from both the intensity of the nociceptive stimulus and the reported pain level (Chapman et al. 1981; Dillmann, Miltner, and Weiss 2000; A. Mouraux, Guérit, and Plaghki 2004; A. Mouraux and Plaghki 2007; Clark et al. 2008; Iannetti et al. 2008; Lee, Mouraux, and Iannetti 2009). All these observations constitute strong evidence against the functions of the Pain Matrix to encode the intensity of pain perceived (Rainville 2002; Porro 2003).

To conclude, based on these arguments, Iannetti and collaborators debate the concept that regions within the pain matrix are exclusively activated for pain processing, unlike other sensory modalities such as vision or audition. In their interpretation, they suggest that the regions being activated after a noxious stimulus do not exclusively reflect nociceptive-specific brain activities but instead brain activities equally involved in processing nociceptive and non-nociceptive sensory inputs. They infer that the nociceptive stimulus, due to its noxious nature, has intrinsically high saliency content so they hypothesized that at least a part of the responses is involved in the detection of salient sensory events, regardless of whether these sensory events are conveyed by nociceptive pathways and also regardless of whether they are perceived as painful. They consider the Pain Matrix as a multimodal network as originally proposed by Melzack in the Neuromatrix theory which, originally, was not pain specific.

Pain perception at cortical level is rather the result of the integration, at a network level, of several brain regions that process different features of the diverse attributes of pain. Pain is the conjunction of several attributes, such as the threatening association with bodily damage and the intrinsic unpleasantness of the experience. It is usually triggered by sensory inputs but can potentially be generated independently of them.

More recently, it was also shown that a virtually identical ‘pain matrix’ response can be observed in patients with congenital insensitivity to pain (Salomons et al. 2016), thus providing further evidence that these brain responses are largely non-specific to pain. This statement does not imply that neural activities specific for pain do not exist. Instead, it implies that the neural activities captured by current EEG or imaging techniques like fMRI, which reflect synchronous activity within large populations of neurons, are unspecific for pain (André Mouraux and Iannetti 2018).

While the concept of the pain matrix has been influential, ongoing research is exploring more nuanced and comprehensive models that consider the multifaceted nature of pain perception. Many researchers

now refrain from using the term ‘pain matrix’ and opt instead for terms like ‘pain network’, ‘pain signature’ or ‘neural circuits’ (Tracey and Mantyh 2007; Lelic et al. 2012; Longo et al. 2012; De Simone et al. 2013; Wager et al. 2013).

3 NOCICEPTIVE PAIN

Up to this point, we have described the pathways that a noxious stimulus follows to the brain, where the sensory stimulus is perceived and processed as pain sensation (Figure 1). In this case, we referred to an acute pain sensation, also called nociceptive pain, which is the physiologic response to nociception.

It alerts and protects the body from potential tissue damage. It occurs in response to external or internal noxious stimuli and continues only in the maintained presence of the harmful stimulus (Costigan, Scholz, and Woolf 2009). As schematized in Figure 14, it is a stimulus-dependent pain and the stimulus is physiological, and it follows the nociceptive pathway we described previously. The intensity and the duration of the nociceptive response depends on the intensity and the duration of the harmful stimulus.

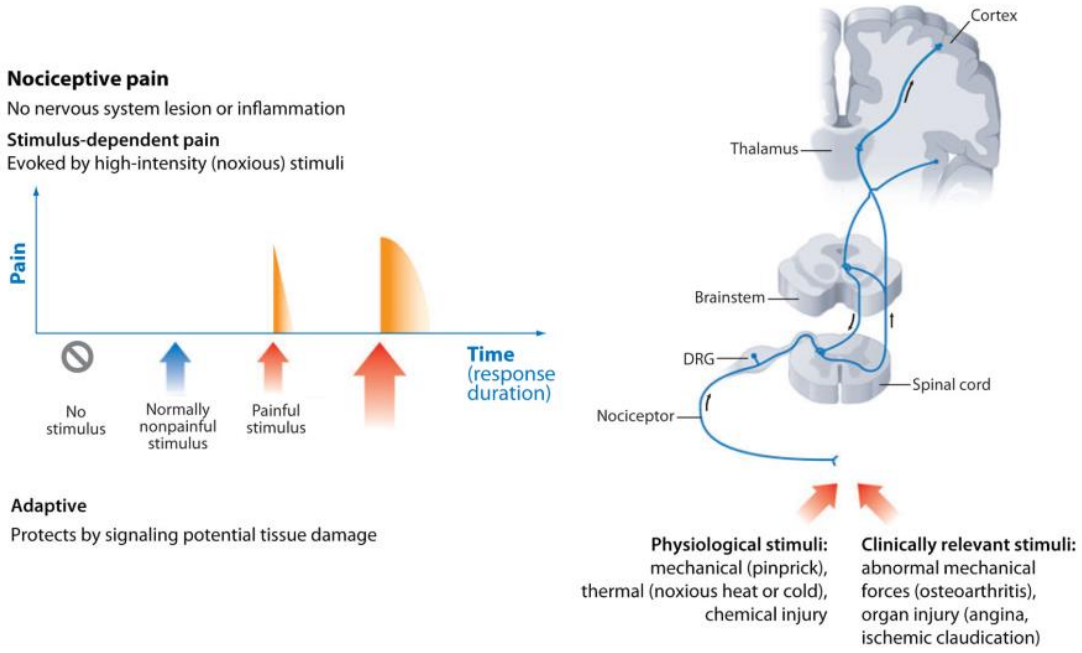

Figure 14: **Nociceptive pain.** Schematic of characteristic features of nociceptive pain. It is a stimulus-dependent pain evoked by a high-intensity noxious stimulus. Representation of the ascending pathway. (Costigan, Scholz, and Woolf 2009).

An ongoing exposure to a noxious stimulus can lead to tissue damage. In this case, the injury promotes a breakdown of the plasma membrane and the initiation of the inflammatory cascade. It involves the release of various chemical mediators, such as histamine, prostaglandins, and cytokines, which cause the activation of nociceptors, and the consequent release of substance P which activate immune cells (mast

cells, macrophage, and neutrophil granulocyte) and provokes vasodilatation and vascular leakage (Figure 15).

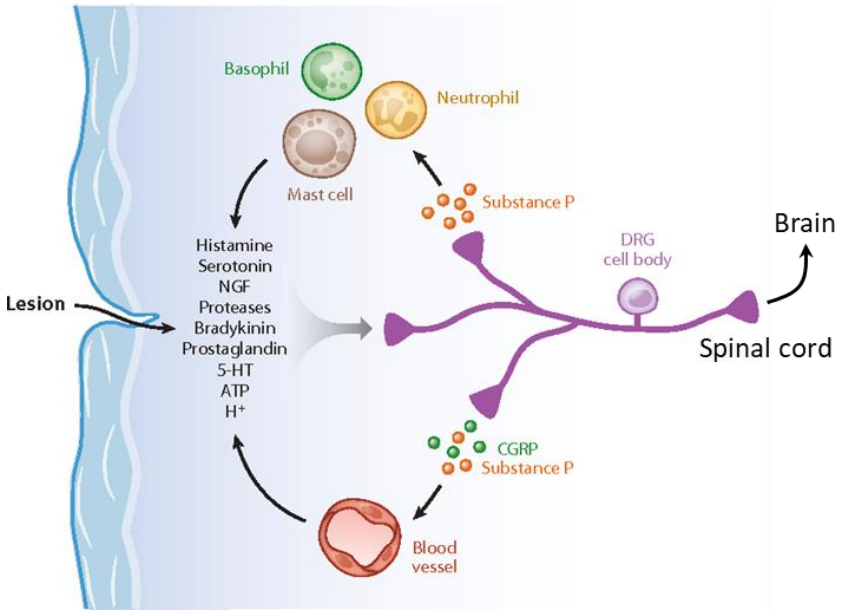

Figure 15: Inflammatory cascade. The tissue lesion triggers the release of chemical mediators that activate the nociceptors. Activation of nociceptors leads to the release of substance P and CGRP. Substance P acts on mast cells, neutrophil and basophil in the vicinity of sensory endings to evoke degranulation and the release of histamine, which directly excites nociceptors. Substance P produces plasma extravasation, and CGRP produces dilation of peripheral blood vessels.

To aid healing and repair of the injured body part, the sensory nervous system undergoes a profound change in its responsiveness, called **pain sensitization** (Figure 16). During active inflammation, normally innocuous stimuli induce a pain perception (allodynia) and responses to noxious stimuli are both exaggerated and prolonged (hyperalgesia, (Costigan, Scholz, and Woolf 2009)).

Typically, inflammatory pain disappears after resolution of the initial tissue injury.

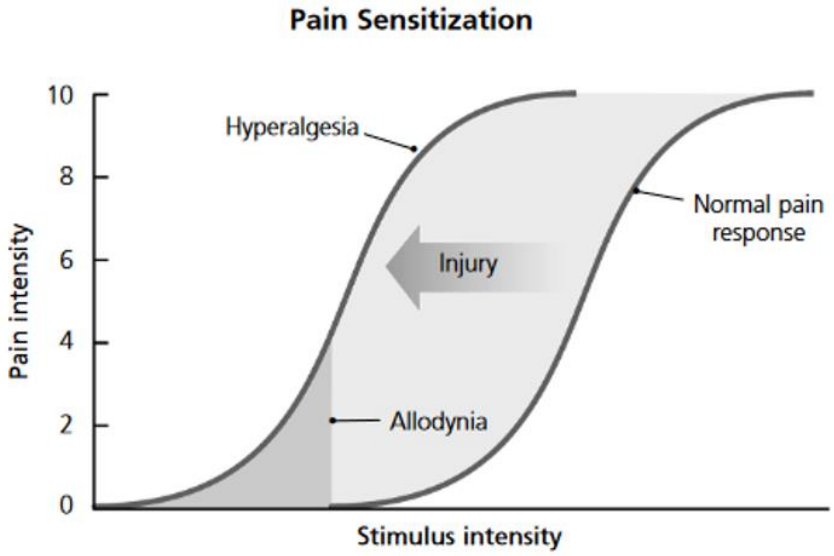

Figure 16: **Pain sensitization**. Noxious stimuli can sensitize the nervous system response to subsequent stimuli. The normal pain response as a function of stimulus intensity is depicted by the curve at the right, where even strong stimuli are not experienced as pain. However, a traumatic injury can shift the curve to the left. Then, noxious stimuli become more painful (hyperalgesia) and typically painless stimuli are experienced as pain (allodynia) (Gottschalk and Smith 2001).

4 CHRONIC PAIN

What we have described so far is a short-lasting pain, a physiologic pain sensation consequent to a noxious stimulus that, in many cases, can cause tissue damage. This pain sensation lasts for the temporal course of natural healing. In some circumstances, it may occur that the pain sensation lasts longer than the normal healing time, more than several months, which is often beyond the expected recovery time. We are describing here a pathological state called **chronic or persistent pain**.

Chronic pain is caused by some maladaptive plasticity within the nociceptive pathway following an injury. It is a distinct and well-recognized condition experienced by around 25% of the European adult population (De Courcy et al. 2016). It can be categorized in two different types depending on his causes:

1) **Chronic inflammatory pain** arises from peripheral **tissue injury** and inflammation. It is characterized by spontaneous pain and hypersensitivity to painful stimuli (hyperalgesia) and to normally nonpainful stimuli (allodynia). The mechanisms involved in the chronification of the inflammatory pain include peripheral sensitization, which causes increased excitability of nociceptive dorsal root ganglion (DRG) neurons innervating the inflamed tissue, and central sensitization (Weng et al. 2012). It is typically associated with rheumatoid arthritis and autoimmune diseases.
2) **Neuropathic pain** results after a peripheral or central **nerve injury** which leads to damage or dysfunction of the nervous system.

4.1 NEUROPATHIC PAIN

As we introduced in the previous paragraph neuropathic pain is caused by a nerve injury which leads to damage or abnormal function of the somatosensory system. It can be classified in Peripheral or Central neuropathic pain based on the anatomic location of the lesion.

- **Peripheral** neuropathic pain results from lesions of the peripheral nervous system (PNS) caused by mechanical trauma, metabolic diseases, neurotoxic chemicals, infection, or tumor invasion and involves multiple pathophysiological changes both within the PNS and in the CNS (Dworkin et al. 2003; Woolf and Mannion 1999).

- **Central** neuropathic pain is due to a lesion or disease of the spinal cord and/or the brain. Cerebrovascular disease affecting the central somatosensory pathways (post-stroke pain) and neurodegenerative diseases (notably Parkinson disease) are brain disorders that often cause central neuropathic pain. Spinal cord lesions or diseases that cause neuropathic pain include spinal cord injury, syringomyelia and demyelinating diseases, such as multiple sclerosis, transverse myelitis and neuromyelitis optica (Colloca et al. 2017).

The conventional approach to neuropathic pain has been to classify it and treat it based on the underlying disease (Dworkin et al. 2007). However, such an etiological approach does not capture the essential features of neuropathic pain. The primary disease and the neural damage that it causes are only the initiators of a cascade of changes that lead to and sustain neuropathic pain.

Furthermore, data clearly indicate that not one, but several mechanisms can lead to neuropathic pain. Importantly, many of these mechanisms do not depend on the cause of the disease: the same mechanism can be found in different diseases (Baron, Binder, and Wasner 2010).

4.1.1 Epidemiology

Neuropathic pain is a major health issue all over the world since it affects 7–10% of the general population. It is more frequent in women (8% versus 5.7% in men) and in patients over 50 years old (8.9% versus 5.6% in those under 50 years old) (Colloca et al. 2017).

As explained in the previous paragraph, neuropathic pain is caused by a nerve lesion under different disease conditions. The most common conditions for peripheral neuropathic pain include trigeminal neuralgia, traumatic peripheral nerve injury, painful polyneuropathy, postherpetic neuralgia and painful radiculopathy. For central neuropathic pain, the most common etiologies are: chronic central neuropathic pain associated with spinal cord injury or with brain injury, chronic central post-stroke pain and chronic central neuropathic pain associated with multiple sclerosis (Scholz et al. 2019) (Figure 17).

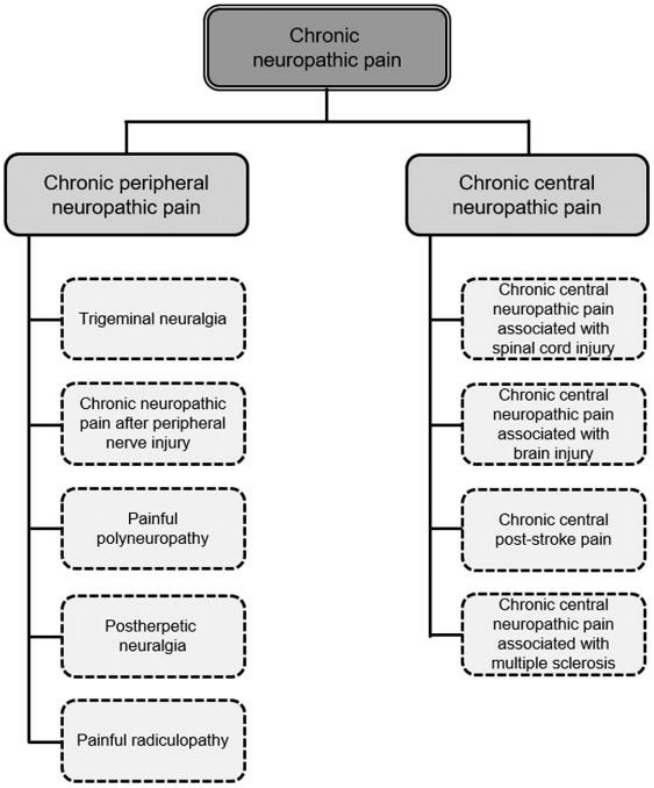

Figure 17: Classification of chronic neuropathic pain (Adapted from Scholtz et al. 2019).

Among the pain syndromes, neuropathic pain is one of the most difficult to treat (Radat, Margot-Duclot, and Attal 2013). The conventional approach has been to classify and treat neuropathic pain on the basis of the underlying disease (Dworkin et al. 2007). However, such an etiological approach does not capture the essential features of neuropathic pain, which is the manifestation of maladaptive plasticity in the nervous system leading to an abnormal function of the somatosensory system (Costigan, Scholz, and Woolf 2009).

Patients typically experience a distinct set of symptoms correlated with the altered transmission of sensory signals, such as burning and electrical-like sensations, and pain resulting from non-painful stimulations (such as light touch). Symptoms persist and have a tendency to become chronic and resistant to conventional pain medications (Colloca et al. 2017). The two most common symptoms are allodynia (nociceptive response to a normally non-nociceptive stimulus) and hyperalgesia (exaggerated response to a noxious stimulus) (Zhuo 2008).

4.1.1.1 Comorbidities

The term comorbidity refers to the presence of two or more medical conditions simultaneously within a single individual. That is the case for patients suffering from neuropathic pain: besides the sensory symptoms, they frequently manifest mood disorders such as anxiety, depression and poor sleep. As previously mentioned, neuropathic pain is extremely difficult to treat and there is growing evidence that it may be partly because of psychological factors rarely taken into account in therapeutic management. Such comorbidities may have a significant impact on quality of life (Von Korff et al. 2005) and are often associated with a poorer response to therapy (Edwards et al. 2010).

On this idea it has been proposed that neuropathic pain and its comorbid conditions represent negatively reinforcing pathologies. Thus, it is usually necessary to treat comorbid conditions as well as pain itself (Nicholson and Verma 2004).

The most common comorbidities associated with neuropathic pain are:

- **Sleep disturbance**. Several surveys of chronic pain of various etiologies have shown significant interference with sleep. Most patients reported that their difficulties with sleep started after they began experiencing chronic pain (Smith et al., 2000). Most studies show a positive correlation between pain intensity and degree of sleep disturbance (Nicholson and Verma 2004).
- **Anxiety and depression**. Many studies and reviews have documented the high degree of comorbidity between depression and chronic pain disorders (Magni et al. 1990), and some evidences show that the incidence of depression among persons with chronic pain is higher than for other chronic medical illnesses (Banks et al 1996). Moreover, patients with higher self-rated pain experience a greater degree of tension/anxiety (Nicholson and Verma 2004) (Atkinson et al 1988).

4.1.2 Pathophysiology of neuropathic pain

Lesion of the somatosensory system results in the alteration of the electrical properties of the sensory nerves, which in turn leads to imbalances between central excitatory and inhibitory signaling. Indeed, preclinical studies have revealed several anatomical, molecular, and electrophysiological changes from the periphery to the central nervous system (CNS) that produce a gain of function, which results from a gain of excitation and facilitation and a loss of inhibition. Overall, these multiple alterations distributed widely across the nervous system led to the neuropathic pain phenotype by shifting the sensory pathways to a state of hyperexcitability (Colloca et al. 2017). These alterations involve modifications in the periphery at the level of primary and secondary sensory neurons and at the central level.

4.1.2.1 Primary sensory neurons: Ectopic neuronal activity

Patients suffering from neuropathic pain experience ongoing spontaneous pain, numbness, and evoked pain. **Spontaneous pain** arises as a result of ectopic (ongoing) action potential generation within the nociceptive pathways following a nerve lesion and does not originate in response to a stimulus (Costigan, Scholz, and Woolf 2009).

As shown in Figure 18, following peripheral nerve damage, spontaneous activity is generated at multiple sites, including in the neuroma (the site of injury with aborted axon growth), in the cell body of injured dorsal root ganglia (DRG) neurons (Figure 18A) (Amir, Kocsis, and Devor 2005), and in neighboring intact afferents (Figure 18B) (Wu et al. 2002).

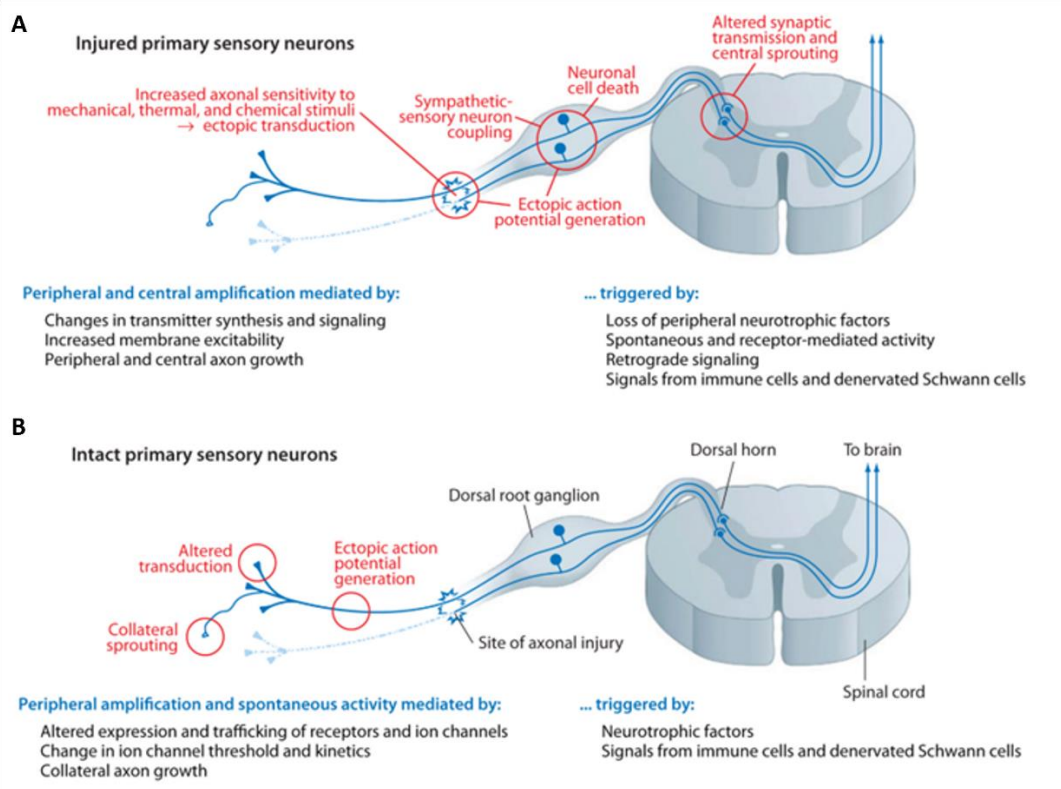

Figure 18: Primary sensory neurons. Schematic representation of the major mechanisms underlying peripheral neuropathic pain, their location, and the triggers responsible for their activation. (A) Mechanism involved when injured primary sensory neurons. (B) Mechanism involved when the primary sensory neurons are intact (adapted from Costigan, Scholz, and Woolf 2009).

The ectopic activity is caused by an increased expression of voltage-gated sodium channel in both injured and neighboring uninjured nociceptive afferents, leading to an increased excitability, signal transduction and neurotransmitter release (Baron et al. 2010 and Colloca et al 2017). In addition to voltage-gated sodium channels, several other ion channels such as voltage-gated potassium channels, probably undergo alterations after a nerve lesion which might also contribute to changes in membrane excitability of nociceptive nerves (Baron et al 2010). The changes in ion channel expression can be explained by the fact that following the injury, the neuron undergo various molecular and cellular changes to adapt to the new physiological state. Retrograde signal mediated by RasGTPase induces consequent transcriptional changes in the soma of the injured neurons leading to the production of new proteins or the suppression of existing ones (Yudin et al 2008).

4.1.2.2 Second-order sensory neurons: Synaptic potentiation and central sensitization

Central sensitization might develop as a consequence of ectopic activity in primary nociceptive afferent fibers (Figure 19). Ongoing discharges of peripheral afferent fibers that release excitatory amino acids and neuropeptides within the dorsal horn of the spinal cord leading to **postsynaptic changes of second-order nociceptive neurons,** such as phosphorylation of NMDA and AMPA receptors or expression of voltage-gated sodium channels. Those mechanisms are similar to those underlying the Long-Term Potentiation (LTP) of synaptic responses already studied in many circuits in the brain. These changes induce neuronal hyperexcitability that enables low-threshold mechanosensitive Aβ and Aδ afferent fibers to activate second-order nociceptive neurons and expands their receptive fields, so a given stimulus excites more second-order nociceptive neurons, generating the so-called central sensitization (Baron, Binder, and Wasner 2010).

These second-order changes could explain physical allodynia and are reflected by enhanced sensory thalamic neuronal activity, as supported by data from animal (Patel and Dickenson 2016) and human studies (Peyron et al 2016).

Hyperexcitability can also be caused by a loss of GABA-releasing inhibitory interneurons that can also switch to exert consequently excitatory actions at spinal levels. In addition, there are less well-understood functional changes in non-neuronal cells within the spinal cord, such as microglia and astrocytes, which contribute to the development of hypersensitivity (Colloca et al. 2017).

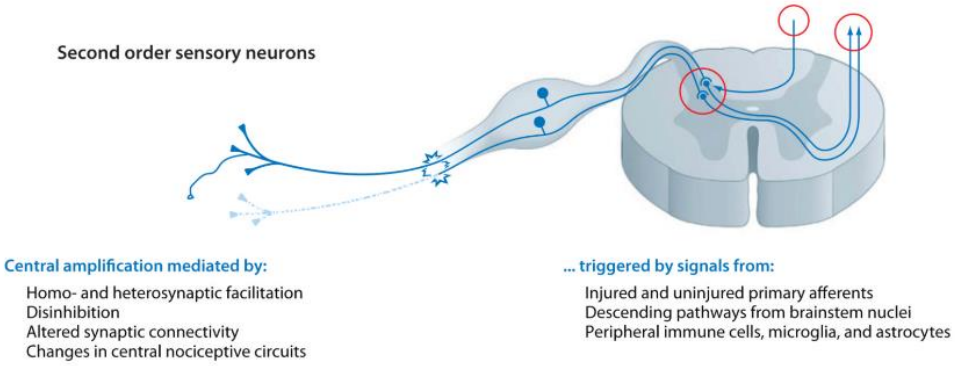

Figure 19: Second-order sensory neurons (adapted from Costigan et al. 2009).

4.1.2.3 Maladaptive brain plasticity

Several preclinical and clinical studies have shown that chronic pain is not just associated with molecular or structural changes in peripheral afferents and spinal cord circuitry. Indeed, brain-imaging studies have shown that patients suffering from neuropathic pain present morphological and functional reorganization in cortical and subcortical areas compared to healthy controls (Bliss et al. 2016; Huang et al. 2019).
To really comprehend the transitions from acute to chronic pain, the traditional understanding of central sensitization, primarily thought as a peripherally triggered process, needs to be expanded to include the role of supraspinal mechanisms. Brain reorganization is necessary for maintaining the central sensitization over the long term (Farmer, Baliki, and Apkarian 2012).
Acute and chronic pain states share similar neural pathways. A major challenge is to uncover the networks, cellular and molecular mechanisms that differentiate chronic from acute pain (Bliss et al. 2016).

One key hypothesis is the long-term potentiation (LTP) in the cortical synapses. Such potentiation or excitation persists for a long period of time, and consequently might generate abnormal neuronal spike activity in the brain without obvious peripheral sensory stimulation (Zhuo 2008).
Long-term potentiation (LTP) and long-term depression (LTD) are forms of synaptic plasticity that have been widely studied in the context of learning and memory. Chronic pain can be thought of as a type of persistent sensory memory, and increasing evidence suggests that LTP and LTD in the dorsal horn of the spinal cord and cortical areas, are causally related to chronic pain (Bliss et al. 2016).
Synaptic plasticity has been reported in many of the structures that are known to be involved in the processing of pain including the dorsal horn of the spinal cord (Ruscheweyh et al. 2011; Sandkühler and

Liu 1998) and numerous cortical structures. Among these higher centers, synaptic plasticity has been reported in the thalamus (Guilbaud et al. 1990; Zhao, Waxman, and Hains 2006), amygdala (Ikeda et al. 2007), insular cortex (Liu et al. 2013), prefrontal cortex (Metz et al. 2009), anterior cingulate cortex (Zhuo, 2004), and somatosensory cortices (Eto et al. 2011). Genetic, pharmacological, and electrophysiological approaches have been used to investigate the basic mechanisms for LTP, mostly in ACC synapses.

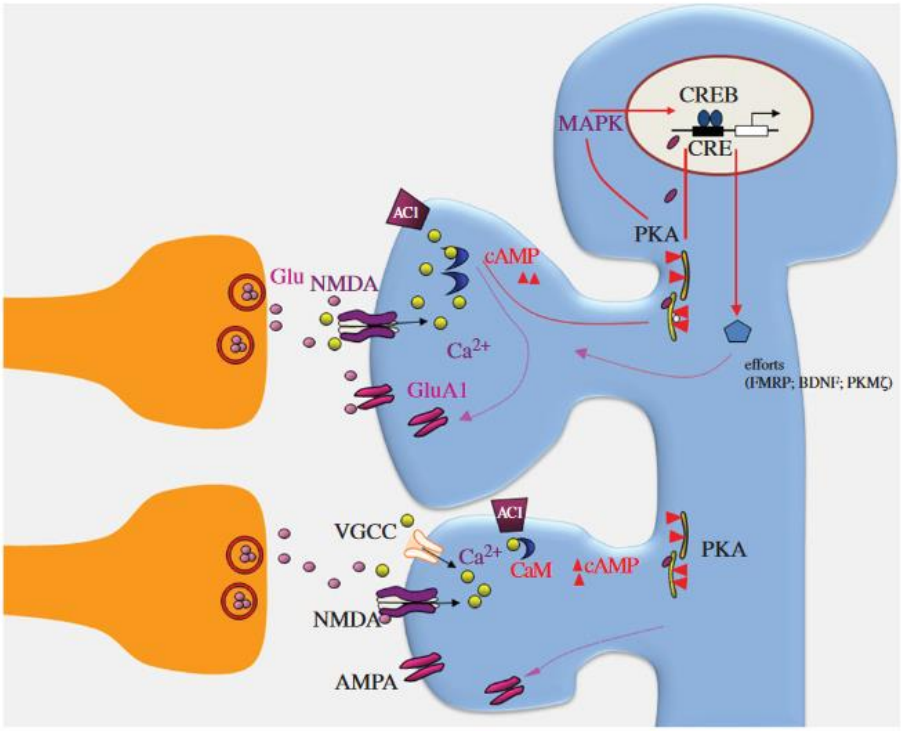

Figure 20: Synaptic model for LTP in the ACC. Activation of glutamate NMDA receptors leads to an increase in postsynaptic Ca^{2+} in dendritic spines. Both NMDA receptor containing GluN2B (NR2B) and GluN2A (NR2A) subunits are important for NMDA receptor functions in the ACC neurons. Ca^{2+} serves as an important intracellular signal for triggering a series of biochemical events that contribute to the expression of LTP. Ca^{2+} binds to calmodulin (CaM) and leads to activation of Ca^{2+}-stimulated adenylyl cyclases (Acs), mainly AC1 and Ca^{2+}/CaM-dependent protein kinases. The trafficking of postsynaptic GluA1 containing AMPA receptor contributes to enhanced synaptic responses. An NMDA receptor independent form of LTP can be also induced. Activation of L-type voltage-gated calcium channels (L-VGCCs) is important. It is likely similar calcium-dependent downstream signaling pathways are involved. In addition, activation of AC1 leads to activation of PKA-CREB, including MAP kinase (MAPK). Several candidate gene products may contribute to L-LTP, such as FMRP, BDNF and PKMζ. (Zhuo et al. 2014).

As summarized in Figure 20, the release of neurotransmitters in the synaptic cleft activates the glutamate NMDA receptors that leads to an increase in postsynaptic Ca^{2+} influx within the dendritic spines. Ca^{2+} serves as an important intracellular signal for triggering a series of biochemical events that contribute to

the expression of LTP (Zhuo et al 2014). Four different biochemical events triggered by the increase of postsynaptic Ca^{2+} which might contribute to the expression of LTP have been identified (Zhuo et al 2008):

- postsynaptic enhancement of glutamate AMPA receptor-mediated responses
- recruitment of previously 'silent' synapses or synaptic trafficking or insertion of AMPA receptors
- structural changes in synapses
- presynaptic enhancement of the release of glutamate

LTP is just one among the several mechanisms known to contribute to cortical sensitization.

In his study from 2008, Zhuo summarized in his "**cortical model for chronic pain**" the cellular and synaptic mechanisms for chronic pain in the cortex (Figure 21). This model contains three different phases:

I. **Early phase**: after the injury it follows a potentiation of the synaptic transmission, LTP, which can last for hours to days. Then, changes in presynaptic releases and postsynaptic receptors will follow. Moreover, possible changes in local inhibitory transmission may occur.

II. **Late phase**: in this phase, prolonged structural changes are taking place, such as increased synthesis of key synaptic signaling proteins such as NMDA-NR2B receptors and novel signaling messengers. Trophic factors and other growth-related molecules might be involved in cortical reorganization. Some of these signaling proteins and receptors might even form positive feedback loops and induce prolonged excitation of cortical circuits.

III. **Enduring phase/brain reorganization**: to maintain central sensitization over the long-term, reorganization of the cortical networks is needed, which can take years to occur. It consists in the formation of new structural connections within cortical areas. Such plastic changes are not limited to pain-related areas. Potential neuronal cell loss (including inhibitory neurons) might occur among certain populations of cells.

The three proposed phases are mutually exclusive; early phase will likely interfere or set up events that are critical for the next phase.

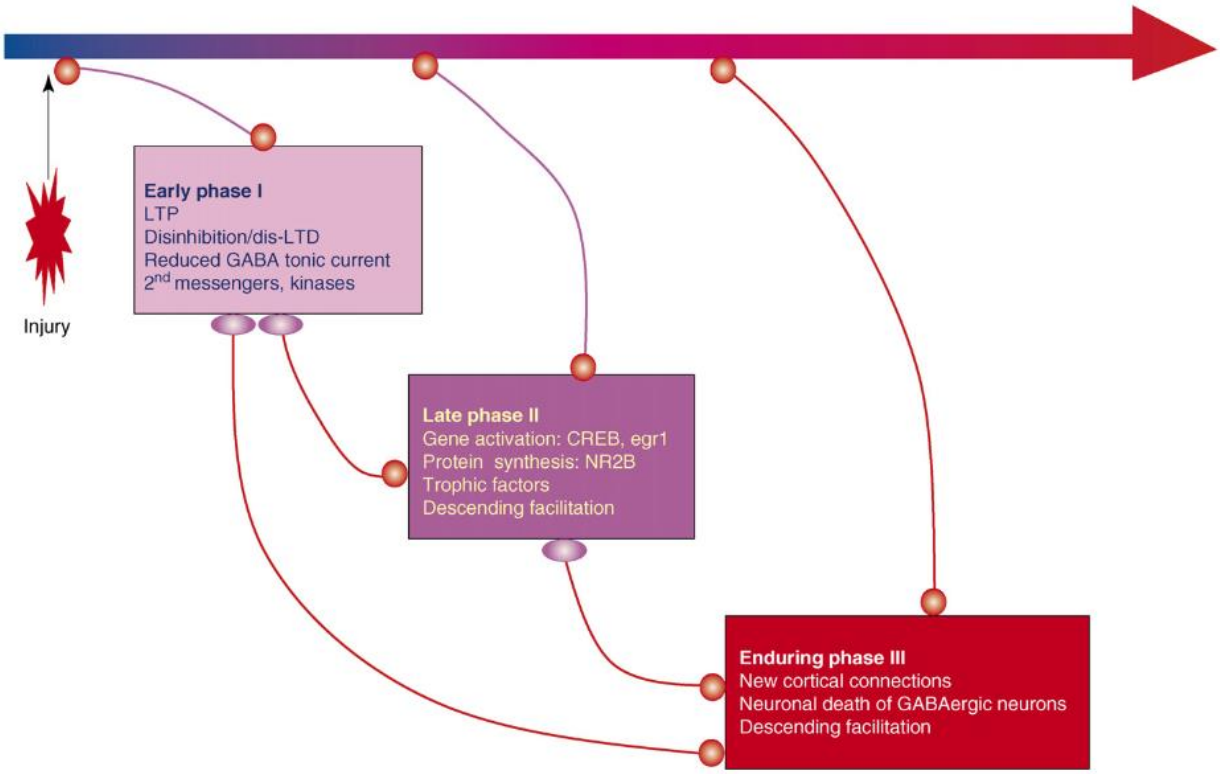

Figure 21: Cortical model for chronic pain. Cortical plasticity and reorganization in chronic pain (Zhuo et al. 2008).

Brain reorganization during chronic pain has been investigated by several groups using different techniques. These will be detailed later in paragraph 5.

4.1.3 Treatments

Neuropathic pain, due to the diversity in etiology, clinical manifestations and comorbidity, is extremely difficult to treat. Generally, the management of neuropathic pain focuses on treating symptoms because the cause of the pain can be rarely treated.

Due to the complexity in finding a standardized treatment approach, researchers in the field have proposed guidelines, evidence-based recommendations and best practices for the diagnosis, assessment, and management of neuropathic pain (Finnerup et al. 2015) , in order to guide healthcare professionals and improve treatment outcomes. The guidelines approach proposed is to initiate the treatment with conservative pharmacological and complementary therapies before interventional strategies, such as nerve blocks and neuromodulation (Colloca et al. 2017).

Concerning the pharmacological therapy, there are different levels of intervention.

- First-line treatments: antidepressant and antiepileptics have been the most studied drugs and confirmed their efficacy in various neuropathic pain conditions. Drugs like pregabalin, gabapentin, duloxetine and various tricyclic antidepressants.
- Second-line treatments: high concentration capsaicin patches, lidocaine patches and tramadol.
- Third-line treatments: Strong opioids and botulinum toxin A.

If the pharmacological therapy is ineffective, the treatment will then proceed with an interventional therapy, such as nerve blocks or surgical procedures that deliver drugs to targeted areas, or modulation of specific neural structures.

Few examples are:

- Neural blockade and steroid injections. For trauma-related and compression-related peripheral neuropathic pain, perineural injection of steroids can provide transient relief from 1 to 3 months (Bhatia, Flamer, and Shah 2015).
- Spinal cord stimulation. Application of low-intensity electrical stimulation of large myelinated Aβ fibers based on the gate control theory as a strategy to modulate the pain signals transmitted by the unmyelinated C fibers (Figure 22A) (Melzack and Wall 1965). The most commonly used and studied neuromodulation strategy is the spinal cord stimulation with a monophasic square-wave pulse (frequency ranging 30–100 Hz), resulting in paresthesia in the painful region (Yearwood et al 2010).
- Dorsal root ganglion, peripheral nerve and peripheral nerve field stimulation. Neurostimulation of afferent fibers outside the spinal cord and subcutaneous peripheral nerve field stimulation have been reported to provide pain relief in various chronic neuropathic pain states (Krames 2014; Petersen and Slavin 2014).
- Epidural and transcranial cortical neurostimulation. Epidural motor cortex stimulation (ECMS), repetitive transcranial magnetic stimulation (rTMS) and trans- cranial direct current stimulation (tDCS) of the pre- central motor cortex at levels below the motor threshold have been proposed as treatment options for patients with refractory chronic neuropathic pain (Figure 22B) (Sukul and Slavin 2014).
- Deep brain stimulation. The use of long-term intracranial stimulation for neuropathic pain remains controversial. The UK National Institute for Health and Care Excellence (NICE) guidelines recognize that the procedure can be beneficial in some patients who are refractory to other forms of pain control, but current evidence on the safety of deep brain stimulation shows significant potential risks, such as intra-operative seizure, lead fractures and wound infections (Tan et al. 2010) (Figure

22C).Intrathecal therapies. Intrathecal therapies have been developed to deliver drugs to targeted nerves through an implanted and refillable pump in patients with severe and chronic pain that is refractory to conservative treatments (Figure 22D) (Deer et al. 2012; Colloca et al. 2017).

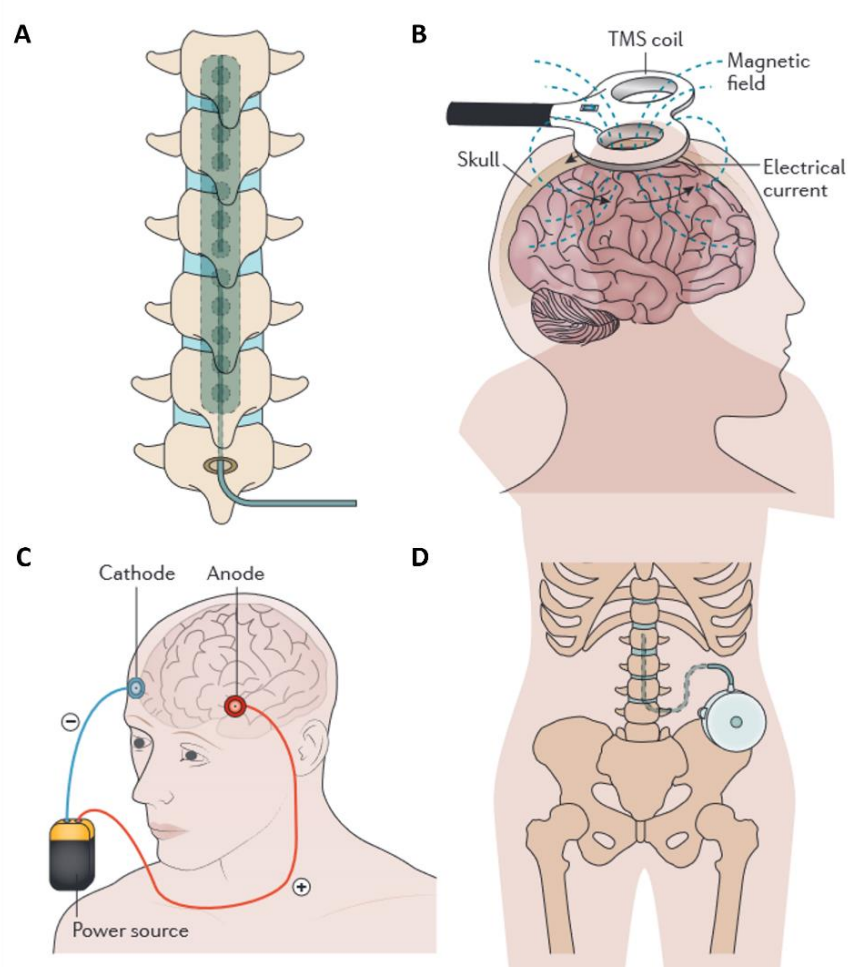

Figure 22: Examples of interventional treatments for neuropathic pain. (A) Spinal cord stimulation traditionally applies a monophasic square-wave pulse (at a frequency in the 30–100 Hz range) that results in paraesthesia in the painful region. (B) Cortical stimulation involves the stimulation of the pre-central motor cortex below the motor threshold, using either invasive epidural or transcranial non-invasive techniques (such as repetitive transcranial magnetic stimulation (TMS) and transcranial direct current stimulation). (C) Deep brain stimulation uses high-frequency chronic intracranial stimulation of the internal capsule, various nuclei in the sensory thalamus, periaqueductal and periventricular grey, motor cortex, septum, nucleus accumbens, posterior hypothalamus and anterior cingulate cortex as potential brain targets for pain control. (D) Intrathecal treatments provide a targeted drug delivery option in patients with severe and otherwise refractory chronic pain. The pumps can be refilled through an opening at the skin surface (Colloca et al. 2017).

As an alternative or complement approaches to the traditional pharmacological and interventional therapies, several non-pharmacological strategies have been investigated. Among such, physical therapies and exercise can help to reduce pain and prevent further deterioration. Acupuncture may help alleviate neuropathic pain by stimulating nerves and releasing endorphins. Music therapy, mindful and meditation therapies may help distract from pain, reduce anxiety and improve mood. Heat and cold therapy consisting in applying heat or cold to the affected area can help alleviate neuropathic pain by modulating pain signals and reducing inflammation.

4.1.4 Rodent models of NP

Due to the limited efficacy of the drugs, the aging population, polymedication in elderly patients and numerous drugs-related adverse effects (for example for opioids, antidepressant and antiepileptics), as we explained in the previous paragraph, finding an appropriate treatment for neuropathic pain is very complicated. Clinical studies are lacking to help and guide physicians in finding the optimal therapy for each patient. Hence, there is still much to understand about the basic mechanisms that lead to neuropathic pain in order to find better treatments. Therefore, various animal models have been developed, especially in rodents. They have been designed to study different aspects of pain: some mimic human diseases and others explore the basic pathophysiological mechanisms in the nervous system. Collectively, these models have great utility in exploring the maladaptive plasticity induced by neural damage (Costigan, Scholz, and Woolf 2009).

In order to mimic the diverse etiology and consequently the diverse manifestations of neuropathy, different types of animal models have been developed:

- Peripheral nerve injury models
- Central pain models
- Drug-induced neuropathy models
- Disease-induced neuropathy models

This paragraph will describe mostly models of peripheral nerve injury. Most of them focus on the lesion of the sciatic nerve. The ideal models should result in reproducible sensory deficits such as allodynia, hyperalgesia and spontaneous pain over a sustained period.

These models depend on compression and/or section of the sciatic nerve.

Some of the most common are (Figure 23):

1. **Chronic Constriction Injury (CCI)**: this model has been developed by Bennett and Xie in 1988. It consists of some ligatures (3 to 4) placed around the sciatic nerve (Figure 23A). It leads to nerve injury and subsequent neuropathic pain symptoms. The behavioral changes include mechanical and thermal hyperalgesia, chemical hypersensitivity and cold allodynia. These symptoms have been evidenced to develop within a week with maximal pain-related behaviors and postural asymmetries during the second week after the surgery (Bennett and Xie 1988; Jaggi, Jain, and Singh 2011).
2. **Spared Nerve Injury (SNI)**: this model has been developed by Decosterd and Woolf in 2000. This model involves selective ligation and transection of some branches of the sciatic nerve, leaving others intact. As shown in Figure 23B, the sciatic nerve has three terminal branches: the sural, the common peroneal, and the tibial nerves. In this model the sural nerve is spared and the other two nerves, tibial and common peroneal, are axotomized. Two variants of SNI have also been developed using the same surgical techniques, but with different combinations of nerve transections (Jaggi, Jain, and Singh 2011). Mechanical and thermal hyperalgesia and allodynia have been noted to occur within 4 days of injury and persist for several weeks (up to 6 months) postinjury (Bourquin et al. 2006).
3. **Partial Sciatic Nerve Ligation (PSNL)**: this model has been developed by Seltzer and collaborators in 1990. PSNL involves the tight ligation of a portion of the sciatic nerve, resulting in partial nerve injury and neuropathic pain symptoms (Figure 23D). The behavioral alterations like cold allodynia, chemical hyper-reactivity, and mechanical hyperalgesia have been noted to occur within 1 week after the surgery and most of the changes persist for 6 weeks (Jaggi, Jain, and Singh 2011).
4. **Spinal Nerve Ligation (SNL)**: this model has been developed by Kim and Chung in 1992. This model consists in ligaturing the spinal nerves L5 and L6 (Figure 23D). Behavioral alterations such as mechanical allodynia, cold allodynia, thermal hyperalgesia, and spontaneous pain have been noted to develop within 24-48 h and persist for approximately 10-16 weeks (Jaggi, Jain, and Singh 2011).

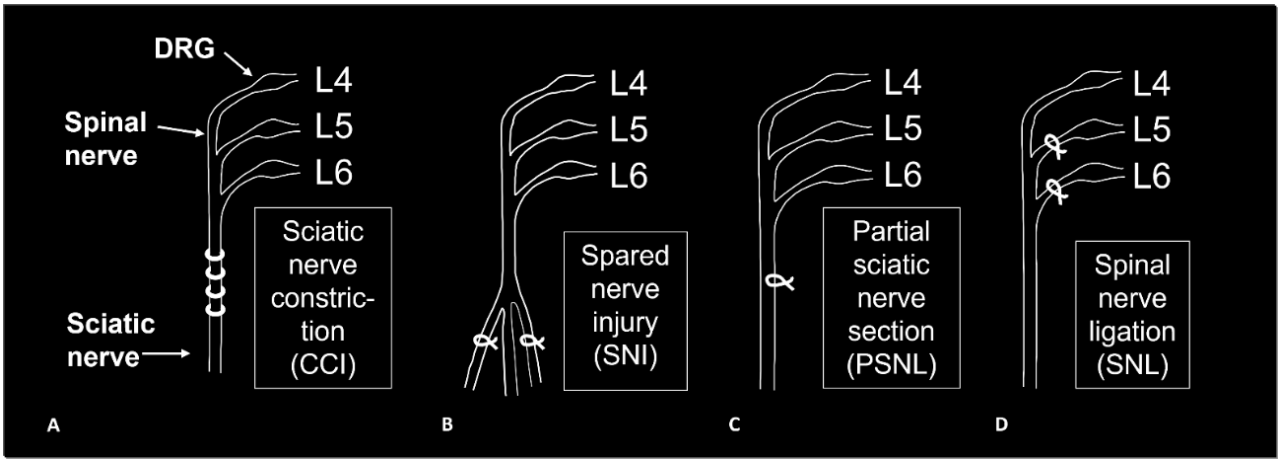

Figure 23: Most common peripheral nerve injury rodents' models. (A) Chronic Constriction Injury (CCI), (B) Spared Nerve Injury (SNI), (C) Partial Sciatic Nerve Ligation (PSNL), (D) Spinal Nerve Ligation (SNL).

4.1.4.1 The sciatic nerve cuffing model

4.1.4.1.1 Sciatic nerve cuffing model in mice

In 1996, Mosconi and Kruger developed a model of peripheral neuropathic pain in which short cuffs (2 mm in length, inner diameter 0.7 mm) of polyethylene tubing were surgically implanted around the main branch of the sciatic nerve in rats. With an ultrastructural morphometric analysis of axonal alterations, they showed that cuff-implantation minimizes the variability in the degree of nerve constriction (Benbouzid et al. 2008). This model has been well described in rats by several research groups (Mosconi and Kruger 1996; Pitcher, Ritchie, and Henry 1999; Coull et al. 2003). Recently has also been developed in mice (C57Bl/6J) by Benbouzid and collaborators in 2008.

4.1.4.1.2 Surgical procedures

The surgical procedures developed by Benbouzid and collaborators consist in exposing the main branch of the right sciatic nerve and implanting around it a cuff of PE-20 polyethylene tubing of standardized length (2 mm, ID = 0.38 mm, ED = 1.09 mm; PE-20, Harvard Apparatus, Les Ulis, France) (Figure 24). The shaved skin layer is then closed and sutured (Benbouzid et al. 2008).

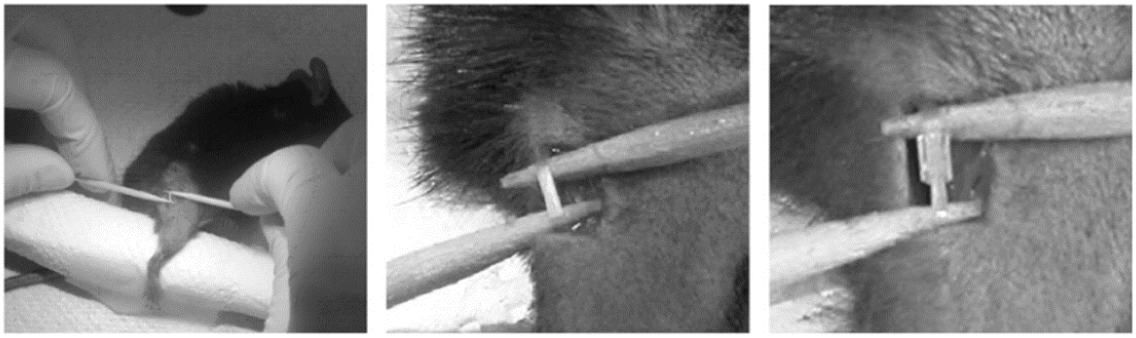

Figure 24: Cuff-implantation. The common branch of the right sciatic nerve was isolated and a 2 mm section of split PE-20 polyethylene tubing was placed around it (Benbouzid et al. 2008).

4.1.4.1.3 Behavioral characterization

In 2008, Benbouzid and collaborators studied the behavioral consequences of this model in mice. They evaluated nociceptive parameters by using the von Frey hairs and the Plantar test to respectively assess mechanical and thermal nociceptive sensitivities. Then, they evaluated the alteration of some aspects of spontaneous behavior and assessed the emotional consequences of the model.

Thermal sensitivity was assessed using the Hargreaves's method, showing a development of heat hyperalgesia. As shown in Figure 25, the cuff-implanted group presents a significant ipsilateral decrease in the latency for paw withdrawal as compared to the control group. The hyperalgesia to a hot stimulus disappeared by 3 weeks post-surgery (Figure 25A). They evaluated the mechanical sensitivity by using Von Frey filaments, cuff-implanted mice showed mechanical allodynia which persisted for at least 60 days after the surgery (Figure 25B).

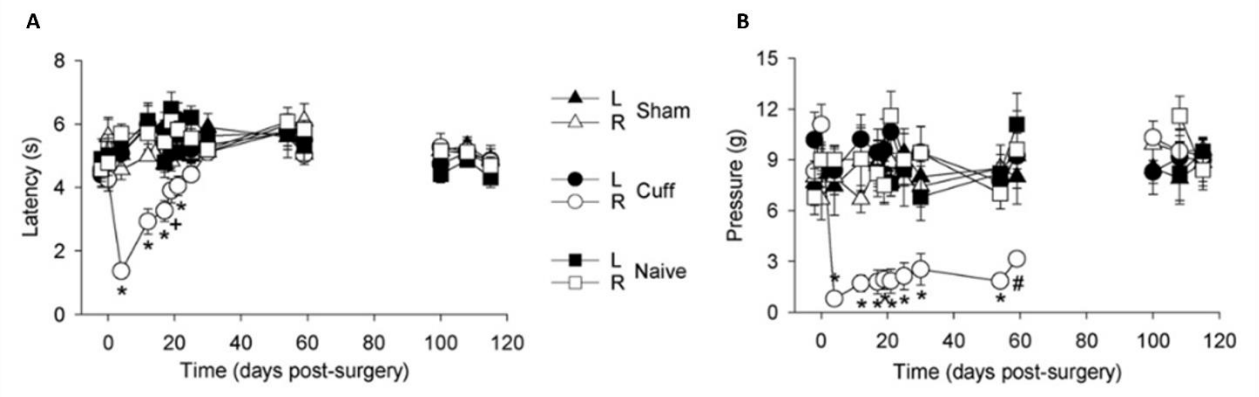

Figure 25: Thermal and mechanical responses after cuff implantation. (A) The cuff implantation induced an ipsilateral thermal hyperalgesia that disappeared around 3 weeks post-surgery and (B) the cuff

implantation induced an ipsilateral mechanical allodynia that persisted at least 2 months (Benbouzid et al. 2008).

Moreover, they assessed the emotional consequences of this model by testing the anxiety-like behavior with the elevated plus-maze and the marble burying test. They found that the cuff-implanted mice developed an anxiety-like phenotype. It was evidenced by the reduction of time spent in the open-arms of an elevated plus-maze (Figure 26A) and by the increased number of buried marbles in the marble burying test (Figure 26B).

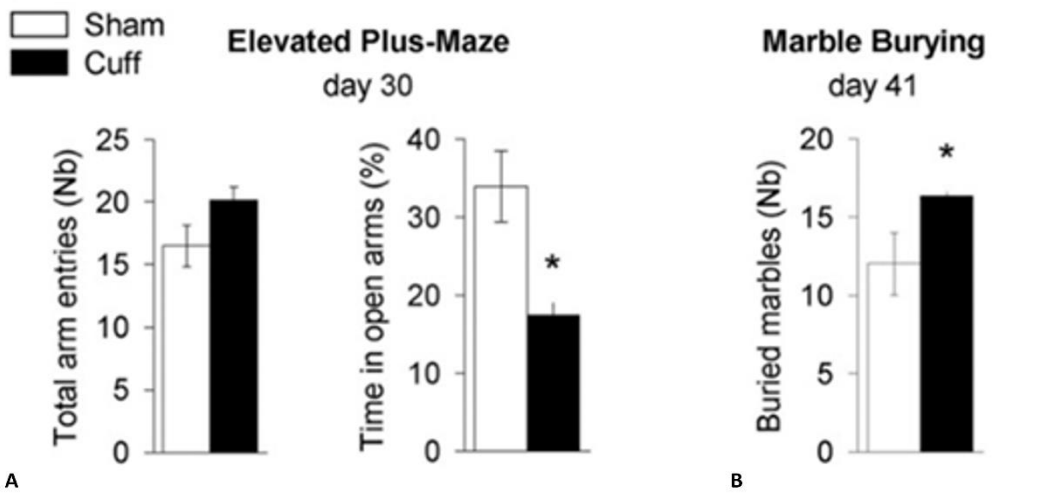

Figure 26: Anxiety-like behavior after cuff implantation. (A) In the elevated plus-maze, the number of arm entries was not different between Cuff and Sham animals, but cuff implantation induced a decrease in the time spent in the open arms (Benbouzid et al. 2008).

These results show that the sciatic nerve cuffing model induces nociceptive symptoms, such as ipsilateral thermal hyperalgesia and ipsilateral mechanical allodynia. Moreover, they show that the cuff implantation has minor consequences on the spontaneous behavior of the animals but induces an anxiogenic state from 4 to 6 weeks post-surgery. They characterized this model as a good and ethically acceptable animal model for the study of sustained neuropathic pain (Benbouzid et al. 2008).

Other groups have further characterized the neuropathic behavior of this model. Especially, Yalcin and collaborators in 2011, and then Barthas and collaborators in 2015, highlighted the importance of the time factor in the development of the symptoms and especially in the arising of comorbidity. They showed that neuropathic pain induced anxiety and depression-related behaviors in a precise chronology. Indeed,

neuropathic mice developed anxiety-related behavior from 4 weeks after the surgery, whereas depression-related behavior was only observed after 6 weeks following the induction of the model.

In 2014, Dimitrov and colleagues showed that depressive-like behaviors are still present 2 weeks after recovery from mechanical hypersensitivity, raising the question of whether these consequences of chronic pain might be maintained in the long-term, independently from sensory aspects.

5 FUNCTIONAL CONNECTIVITY

5.1 STRUCTURAL AND FUNCTIONAL CONNECTOMES

The organization of the brain has been extensively studied by the neuroscience community because it is crucial for a better understanding of sensory perception, cognition and behavior.

The brain organization has been investigated at different levels, from the microscopic organization by studying neurons and the synapses connections. The microscopic characteristics of neurons guide to a macroscopic anatomical segregation based on cyto-, myelo- and/or receptor architecture resulting in the characterization of brain regions detailing the structural heterogeneity of the cerebral cortex (Eickhoff and Müller 2015). This represents the concept of **functional segregation**, or to rephrase it, it refers to the fact that the brain, particularly the cerebral cortex, can be subdivided into regionally distinct modules that differ from each other in terms of microanatomy and response characteristics. Those modules are physically connected to each other by fiber tracts containing multiple individual axons. Such structural connections are a prerequisite for any interaction between different parts of the brain. And this explains the dynamic interplay and exchange of information between different brain regions. Several studies have demonstrated that, to perform cognitive tasks, the interconnection and the integration of different brain regions is needed; no brain region by itself is sufficient to perform a particular cognitive, sensory or motor process. This represents the principles of **functional integration**.

The brain is organized along these two fundamental principles, which are not necessarily in contrast, but rather complement each other; functional integration represents the interaction between specialized regions, each performing a distinct computational subprocess (Eickhoff and Müller 2015).

By this principle, we are identifying the brain as a complex network of local circuits and long-range fiber pathways. This complex network forms the structural substrate for distributed interactions among specialized brain systems (Hagmann et al. 2008). Thus, the brain's organization can be modelled as a connectivity matrix, called 'connectome'. Several studies have established two types of connectivity in the brain: the **structural** and the **functional** (Figure 27) (Cabral, Kringelbach, and Deco, 2017).

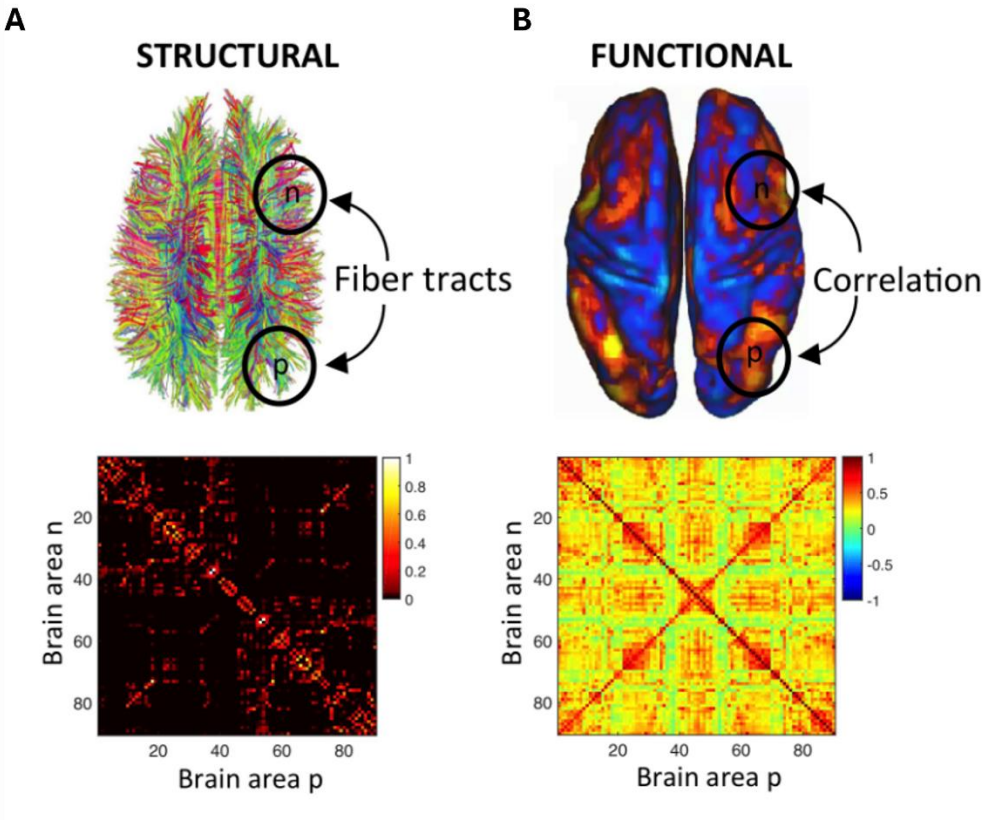

Figure 27: Structural and Functional connectivity. (A) Advanced tractography algorithms allow reconstructing the white matter fiber tracts from Diffusion-MRI. The structural connectivity matrix SC (n,p) is estimated in proportion to the number of fiber tracts detected between any two brain areas n and p. (B) On the other hand, the functional connectivity matrix FC (n,p) is computed as the correlation between the brain activity (e.g. BOLD signal) estimated in areas n and p over the whole recording time. Here, the areas refer to 90 non-cerebellar brain areas from the AAL template (Cabral, Kringelbach, and Deco, 2017).

Structural (or anatomical) connectivity (SC) corresponds to the anatomical white-matter fibers connecting brain areas, representing the scaffold on which any transfer of information may take place. It represents the wiring diagram of the entire brain.

Given the massive range of connectivity in the mammalian brain, it can be studied and described at multiple levels: macro-, meso- and microscale.

At the macroscale level, long-range, region-to-region connections can be inferred from imaging white matter fiber tracts through diffusion tensor imaging (DTI) in the living brain (Van Essen et al. 2013).

At the microscale level, connectivity is described at the level of individual synapses, for example, through electron microscopic reconstruction at the nanometer scale (Bock et al. 2011).

At the mesoscale level, both long-range and local connections can be described using a sampling approach with various neuroanatomical tracers that enable whole-brain mapping across many animals. An example of a mesoscale connectome of the adult mouse brain is shown in Figure 28, with a specific focus on the structural cortico-striatal (Figure 28C) and cortico-thalamic projections (Figure 28D).

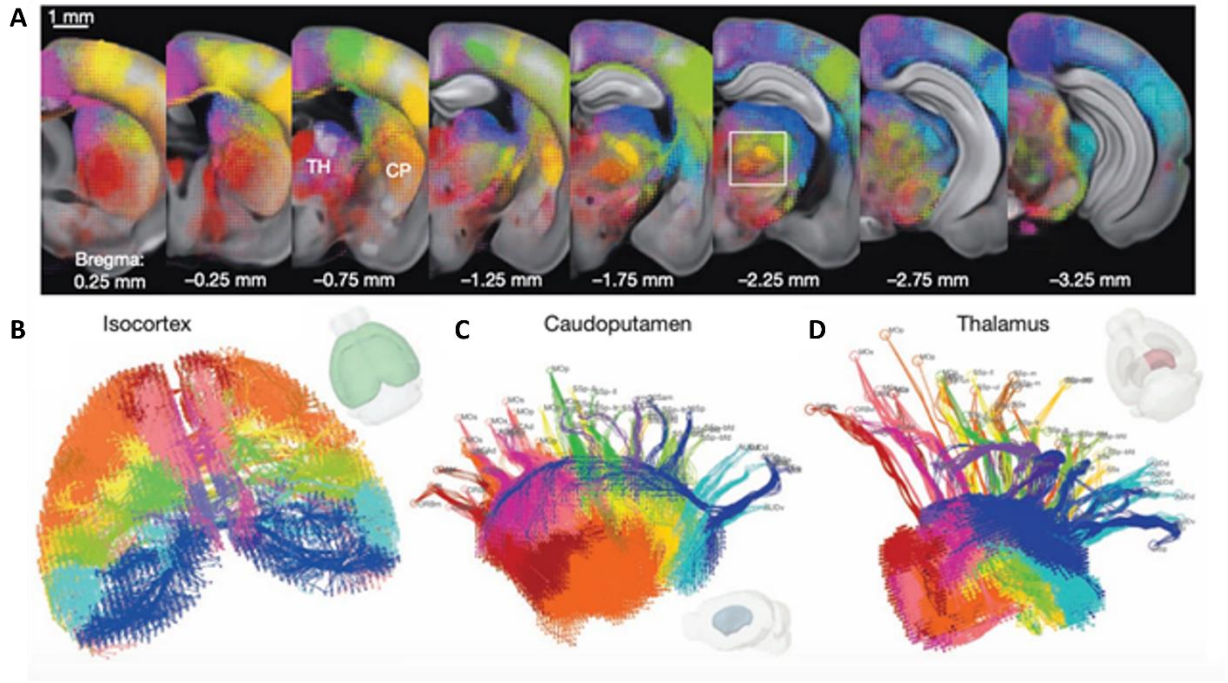

Figure 28 Structural (or anatomical) connectivity (SC) of the mouse brain. Axonal projections from regions throughout the brain are mapped into a common 3D space using a standardized platform to generate a comprehensive and quantitative database of inter-areal and cell-type-specific projections. 3D tractography path in the (B) isocortex, (C) caudoputamen, (C) thalamus (Oh et al. 2014).

Functional connectivity represents the coupling and the dynamic interaction between different parts of the brain, it denotes the interactions between regional activity and hence the dynamic within the respective networks (Eickhoff and Müller 2015). It represents different neural activation patterns that spontaneously emerge from a single structural, anatomical network.

While structural connectivity describes the physical wiring of the brain, functional connectivity examines how these regions work together and communicate during different tasks or states, even if they are not directly anatomically connected. However, structural and functional connectivities are not in contrast, but rather share similarities in the brain networks they respectively define (Cabral, Kringelbach, and Deco, 2017). In 2008, Hagmann and collaborators, using diffusion imaging techniques (DTI), constructed a

connection map covering the entire cortical surface. They found that regions of the cortex that are highly connected and highly central form a structural core. Key components of this core are portions of the posterior medial cortex that are known to be highly activated at rest when the brain is not engaged in a cognitively demanding task. They found that structural connection patterns and functional interactions between regions of the cortex were significantly correlated. Their interpretation suggests that the structural core of the brain may have a central role in integrating information across functionally segregated brain regions (Hagmann et al. 2008). With this work and several others, it was demonstrated that neuroanatomical network structure can shape spontaneous brain activity on a very slow timescale, giving rise to consistent patterns of functional connectivity (Cabral, Kringelbach, and Deco, 2017).
Integrating both structural and functional connectivity data is crucial for gaining a comprehensive understanding of brain organization and function.

5.2 Resting State Functional Connectivity

5.2.1 Discovery of the resting state functional connectivity

Analyzing functional connectivity (FC) can provide insights into how different brain regions are coordinated and communicate with each other to support various cognitive functions.
For example, analysis of the FC can be conducted during the performance of a task in order to detect all those brain regions that are activated by the stimulus and the circuits they form. Through functional studies, neuroimaging has brought forward invaluable information to the field of neuroscience. These studies investigated the changes in blood oxygen level dependent (BOLD) signal during a task (eyes open in the example given in Figure 29) and compared to the signal during the baseline period (eyes closed), giving rise to maps of significant changed during the task (Figure 29) (Fox and Raichle 2007). These maps represent the brain regions being activated by the experimental paradigm.

Note that the nature of BOLD signal will be detailed in paragraph 6.

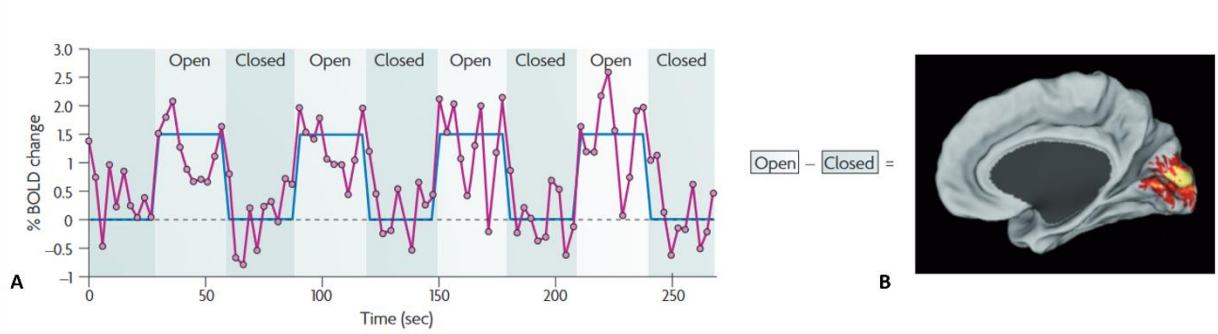

Figure 29: Task-based FC. (A) Unaveraged blood oxygen level dependent (BOLD) time course (magenta) from a region in the primary visual cortex during a simple task paradigm that requires subjects to open and close their eyes. The paradigm is shown in blue (delayed to account for the haemodynamic response). (B) subtraction of the eyes-closed condition from the eyes-open condition identifies a BOLD signal intensity difference in the primary visual cortex (Fox and Raichle 2007).

However, looking at the BOLD time-series in Figure 29, aside from the pattern of activity, the BOLD signal fluctuates during the baseline. Initially, these spontaneous fluctuations were considered as "noise" in task-response studies. Nevertheless, several researchers have focused their efforts on measuring and interpreting these signals. In particular, Biswal and collaborators in 1995 recorded the BOLD signal in subjects that were not subjected to any stimulus. They extracted the time course of the BOLD signal from a seed region, the left somatomotor cortex, and studied the temporal correlations between this signal and those of all other brain voxels (Fox et al. 2005; Hampson et al. 2002; Gillebert and Mantini 2013). They observed that a large number of bilateral structures fluctuate coherently. Also, each type of synchronization was specific to a precise network. Importantly, the networks defined by their coherent fluctuations were functionally altered in neurological disorders, where these pathways are altered, such as in Alzheimer's disease. These findings were soon confirmed in animal models.

Therefore, spontaneous BOLD signal in the human brain at rest is not random, but is specifically organized, allowing the study of functional connectivity at rest. Such measure opens new avenues in the neuroimaging field, as it allows the individual mapping of the brain functional organization in the absence of task or external input (Fox and Raichle 2007). This approach permits to study the neuronal **baseline activity of the brain** and identify functionally relevant resting-state networks (Damoiseaux et al. 2006; Gillebert and Mantini 2013).

The study from Biswal and colleagues has revealed the first Resting State Network (RSN) reported in the literature. Since then, many other RSNs have been reported. These include the visual (Damoiseaux et al.

2006; Mantini et al. 2007), auditory (Damoiseaux et al. 2006; Mantini et al. 2007), default (Damoiseaux et al. 2006; Fox et al. 2005; Greicius et al. 2003; Mantini et al. 2007), self-referential (Mantini et al. 2007), core (Dosenbach et al. 2007), dorsal and ventral attention (Fox et al. 2006), frontoparietal control (Vincent et al. 2008), and language networks (Hampson et al. 2002; Gillebert and Mantini 2013) (Figure 30).

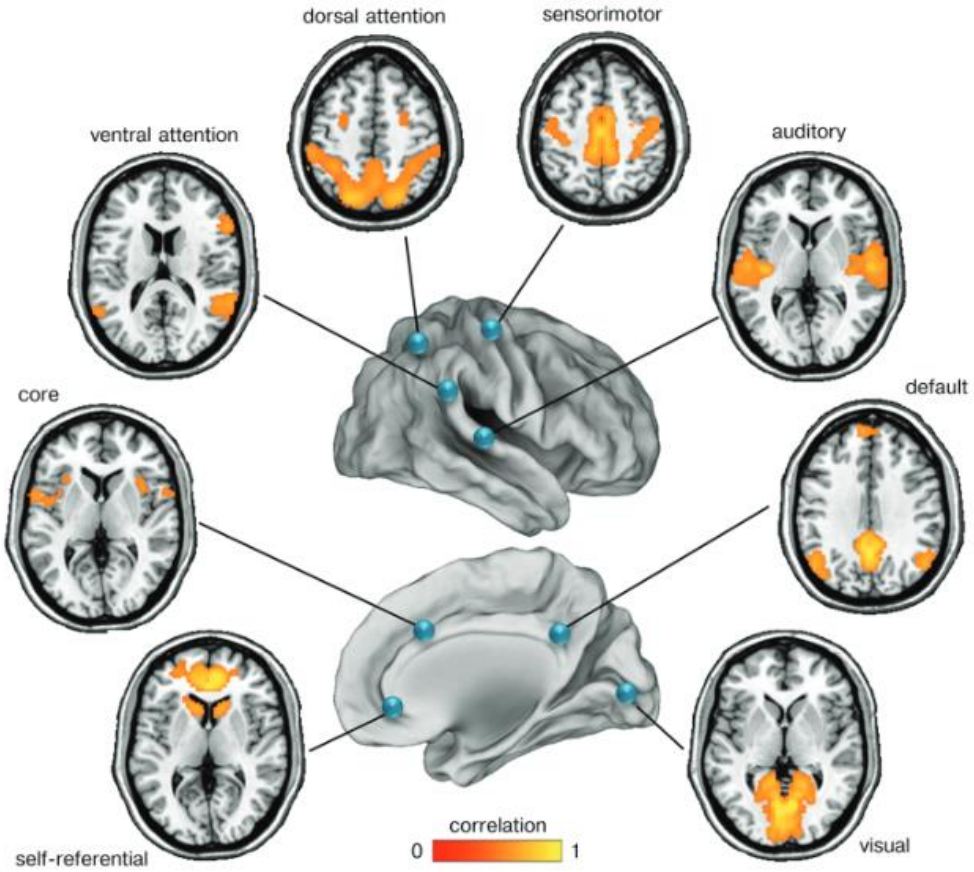

Figure 30: Resting State Networks (RSN). Networks of functionally related brain regions revealed by seed-based connectivity. By comparing the blood oxygen level–dependent (BOLD) signal between a seed region (each blue sphere) and the rest of the brain, it is possible to generate a correlation map that reveals the whole network of regions with brain activity similar to that of the seed. In the figure, the spatial maps of eight main resting state networks are shown: visual, sensorimotor, auditory, default, dorsal attention, ventral attention, core, and self-referential. The color code indicates the correlation strength (Gillebert and Mantini 2013).

5.2.2 Approaches to study the functional connectivity

The notion behind the **connectivity** approach is that areas presumed to be coupled or being part of the same functional network, exhibits coherent spontaneous fluctuations. The strength of connection

between them is measured by the force of these correlations. To rephrase, two regions are functionally connected if the increased activity in one region is correlated with the increased activity in another (Eickhoff and Müller 2015). FC can be recorded and evaluated using different techniques that are able to record neuronal activity, either directly or indirectly. The most used are:

1. Electroencephalography (EEG), records electrical activity generated by groups of neurons in the brain, using electrodes placed on the scalp. Functional connectivity can be inferred from EEG data by analyzing the synchrony or coherence of neural oscillations between different brain regions.
2. Magnetoencephalography (MEG): Similar to EEG, MEG measures the magnetic fields produced by neuronal activity in the brain. Functional connectivity can be assessed using MEG by analyzing the synchronization of neural oscillations across brain regions.
3. Functional Magnetic Resonance Imaging (fMRI): is the leading technique for the study of FC. With this technique, the functional connectivity is estimated by the study of low-frequency (<0.1 Hz) spontaneous fluctuations in the blood oxygen level–dependent (BOLD) signal. The signal is compared between multiple brain regions, and the linear correlation coefficients between regionally-averaged BOLD time-series is estimated (Eickhoff and Müller 2015). Then, the selective correlations are used to map the organization of brain systems (networks) (Fox and Raichle 2007; Gillebert and Mantini 2013).

5.2.3 Analysis of the functional connectivity

5.2.3.1 Seed-based analysis

There are different approaches to study FC. In the studies delineated up to this point, the functional connectivity (FC) analysis was performed using a **seed-based correlation approach**. These analyses are performed on one *a priori* defined region of interest (seed region), whose activity pattern is then cross-correlated with every identified voxel of the brain.. Functional connectivity between the seed and the rest of the brain may then be quantified and statistically tested by using different approaches, in particular linear correlation coefficients, which in most cases are subsequently transformed into Fisher Z-scores for standardization (Eickhoff and Müller 2015). An example of the result is shown in Figure 31.

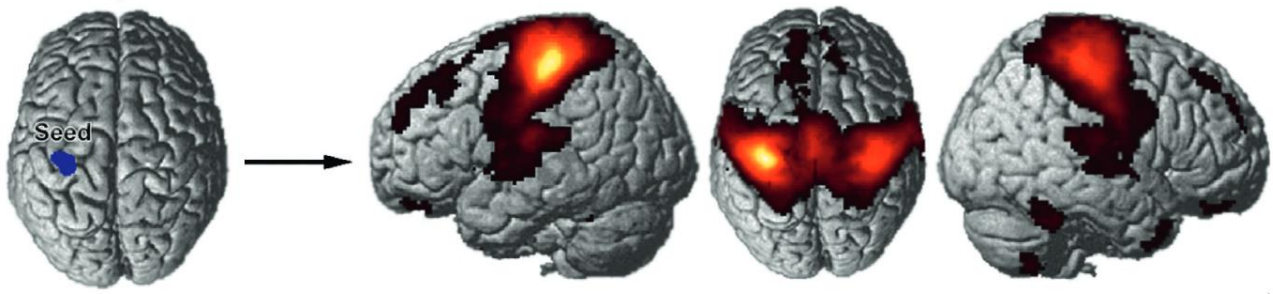

Figure 31: Example of seed-based functional connectivity analyses. Based on a functionally defined seed in the hand area of the left primary motor cortex (blue), functional connectivity was delineated by resting-state functional connectivity analyses (adapted from Eickhoff and Müller 2015).

This approach is broadly used due to its simplicity, sensitivity and ease of interpretation. However, it has some disadvantages. The results are dependent on the a priori definition of the seed region and multiple systems cannot be studied simultaneously.

In response to these limitations, other approaches have been proposed (Fox and Raichle 2007).

5.2.3.2 Static and Dynamic functional connectivity

5.2.3.2.1 Static functional connectivity

In order to study the connectivity between many regions simultaneously, a global parcellation of the brain based on anatomical atlases is required. The time courses from all identified regions are obtained and a correlation matrix is constructed (Figure 32B). A clustering algorithm is then used to determine which regions are most closely correlated and which regions are more distantly correlated (Fox and Raichle 2007). An example of FC analysis covering the entire brain is shown in Figure 32, where functional connectivity is represented as a matrix with rows and columns representing nodes (seed regions) and each element of the matrix representing the edge strength or functional connection between the corresponding nodes (Figure 32B) (Menon and Krishnamurthy 2019).

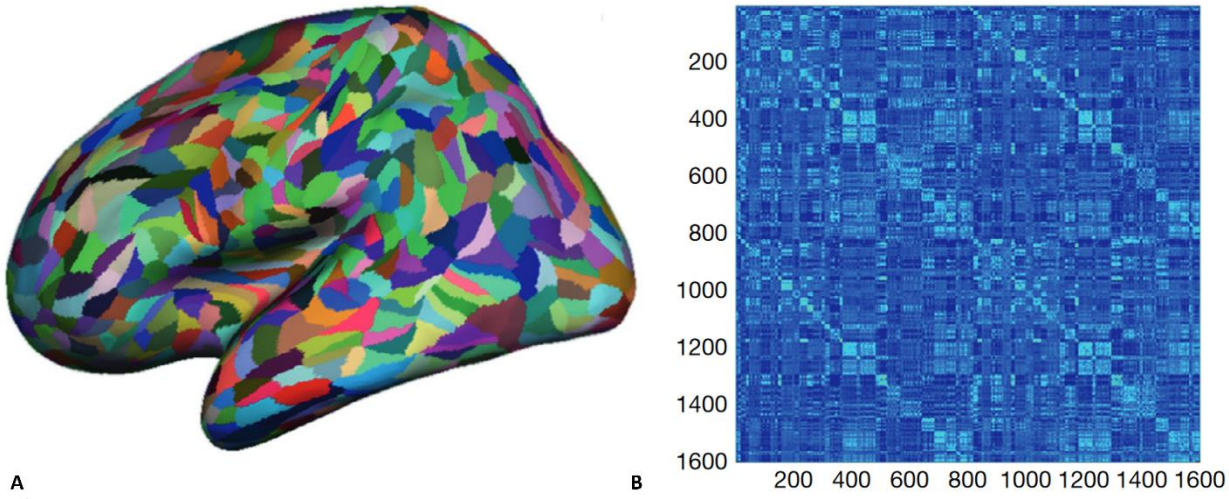

Figure 32: Example of a static functional connectivity analysis covering the entire brain. (A) The whole brain was subdivided into 1600 equally sized regions of interests. (B) Resting-state functional connectivity was then determined by correlating all 1600 nodes with each other resulting in a full connectivity matrix for the entire brain (Eickhoff and Müller 2015).

The correlation matrix shown in Figure 32 is obtained with a static approach to the analysis of the FC. This approach considers the connectivity patterns between regions as time-invariant, meaning they do not change over the data acquisition period. As shown in panel B (Figure 32) the static approach considers the data as stationary by cross-correlating the time-series extracted over the complete acquisition. The result consists in a correlation matrix showing the strength of connections between different regions but does not capture potential temporal fluctuation in the connectivity.

5.2.3.2.2 Dynamic functional connectivity

Several researchers questioned the assumption that resting-state functional connectivity patterns are not changing overtime (C. Chang and Glover 2010) and proposed a different approach, illustrated in panel C and D in Figure 33. They considered that brain regions might exhibit different patterns of communication over time (White and Calhoun 2019). By considering the temporal variations in functional connectivity over the course of the acquisition, we are able to reveal the dynamics of the connectivity patterns. The dynamic FC analysis consists in cross-correlating the time-series over a shorter sliding time windows (Figure 33C). Then, by applying a K-means clustering algorithm, recurring connectivity patterns are identified and grouped as different functional brain states occurring during the data acquisition period

(Figure 33D). The dynamic approach enables to capture changes in the network's interaction providing insight into the dynamic organization of brain regions connections and flexibility.

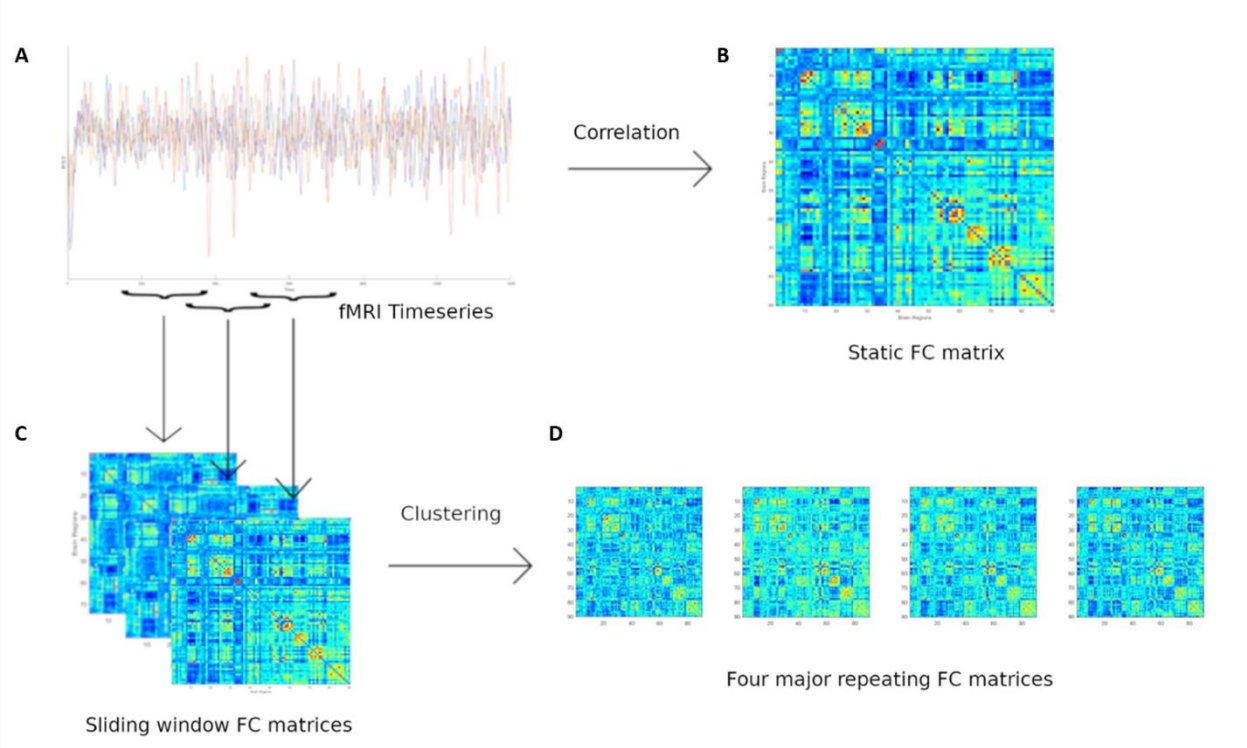

Figure 33: Static and dynamic FC. Matrices derived from fMRI time series. Static FC was calculated using Pearson correlation coefficients of the entire time series; however, dynamic FC was calculated considering a moving window of the time series and finding the major repeating FC matrices using a clustering algorithm (Menon and Krishnamurthy 2019).

To conclude, static and dynamic FC approaches have their advantages and limitations. Static FC provides the overall connectivity patterns but may overlook transient changes in connectivity. Dynamic FC, on the other hand, captures temporal dynamics and offers insights into network flexibility but requires additional computational methods and may be more sensitive to noise.

Overall, integrating static and dynamic FC analyses can provide a more comprehensive understanding of brain function and connectivity, allowing to explore both stable network configurations and transient fluctuations in neural interactions.

5.3 INVESTIGATING THE MALADAPTIVE BRAIN PLASTICITY IN NEUROPATHIC PAIN USING MEASUREMENTS OF FUNCTIONAL CONNECTIVITY

As introduced in paragraph 4 section 4.1.2.3, it has been documented that persistent pain is also correlated with brain reorganizations and consequently FC patterns disruption.

Several studies have shown that patients suffering from chronic pain present **morphological** and **functional** reorganization in cortical and subcortical areas compared to healthy controls (Bliss et al. 2016; Huang et al. 2019). Morphological changes refer to alterations in the physical structure of the brain, such as alterations in grey-matter volume, in glial activity, in structural integrity and connectivity of white matter. Functional reorganization, on the other hand, pertains to changes in how different brain regions communicate and process information. For example, altered resting-state and pain-evoked functional connectivity, expansion and shifts of cortical representations and impaired descending inhibitory control (Figure 34).

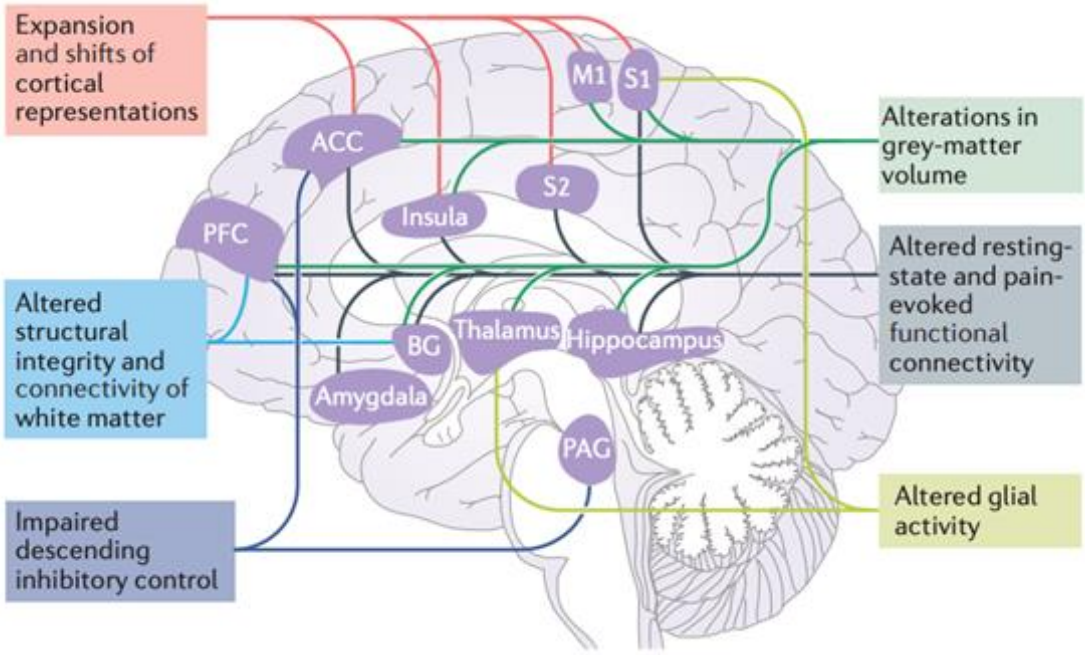

Figure 34: Structural and functional changes in the human brain in chronic pain (Kuner and Flor 2017).

5.3.1 Structural plasticity

In 2004, Apkarian and collaborators conducted the first study that revealed brain morphological abnormalities in chronic pain patients. They demonstrated morphological reorganization in the neocortex of patients suffering from chronic back pain (CBP). Using structural magnetic resonance imaging (MRI), they found evidences for a decrease in grey matter density, indicative of brain atrophy, in CBP patients compared to controls (Figure 35, (A. V. Apkarian et al. 2004; A. V. Apkarian, Baliki, and Geha 2009a).

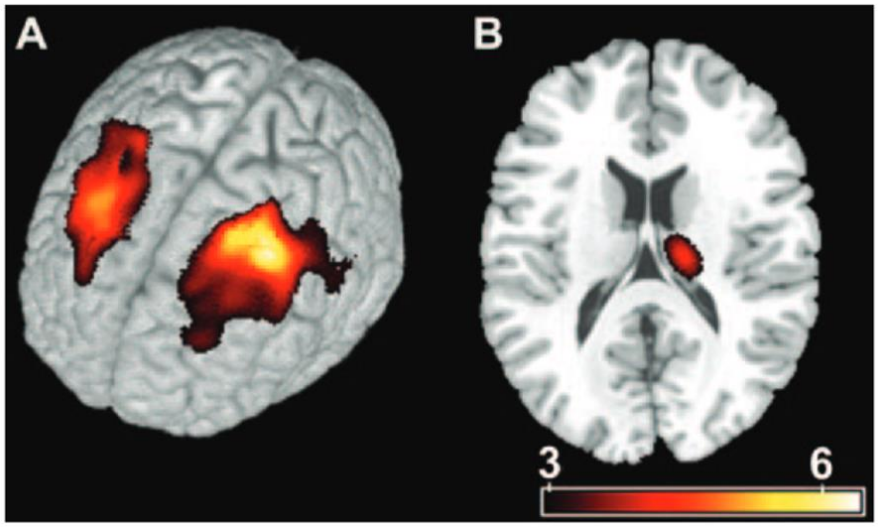

Figure 35: Regional gray matter density decreases in CBP subjects. (A) bilateral decrease in grey matter density in the dorso-lateral prefrontal cortex (DLPFC), and in panel B, in the right anterior thalamus (A. V. Apkarian et al. 2004; A. V. Apkarian, Baliki, and Geha 2009a).

With this study, Apkarian and collaborators demonstrated that, during chronic pain, the brain undergoes structural reorganization, with grey matter density appearing to decrease locally in pathological conditions.

In their study published in 2013, Farmer and collaborators developed the idea that chronic pain *re-shapes* the brain. They revised several studies conducted in different pain conditions and, across all these studies, most of them show **grey matter alterations** (that could be increased or decreased) in chronic pain patients. Many studies have identified alterations, especially located in brain regions associated with pain processing (A. V. Apkarian, Baliki, and Geha 2009a; V. A. Apkarian, Hashmi, and Baliki 2011; A. V. Apkarian et al. 2004; M. N. Baliki, Baria, and Apkarian 2011; M. N. Baliki et al. 2008; Marwan N. Baliki et al. 2011). Data also suggests that different pain conditions exhibit distinct alterations patterns, reflecting not only

pain, but also the clinical manifestations associated with the disease (Marwan N. Baliki et al. 2011), as shown in Figure 36. Patterns of grey matter changes distinguish chronic back pain (CBP), osteoarthritis (OA), and complex regional pain syndrome (CRPS) from healthy individuals. This study demonstrated that structural reorganization follows distinct trajectories for different types of chronic pain (Marwan N. Baliki et al. 2011).

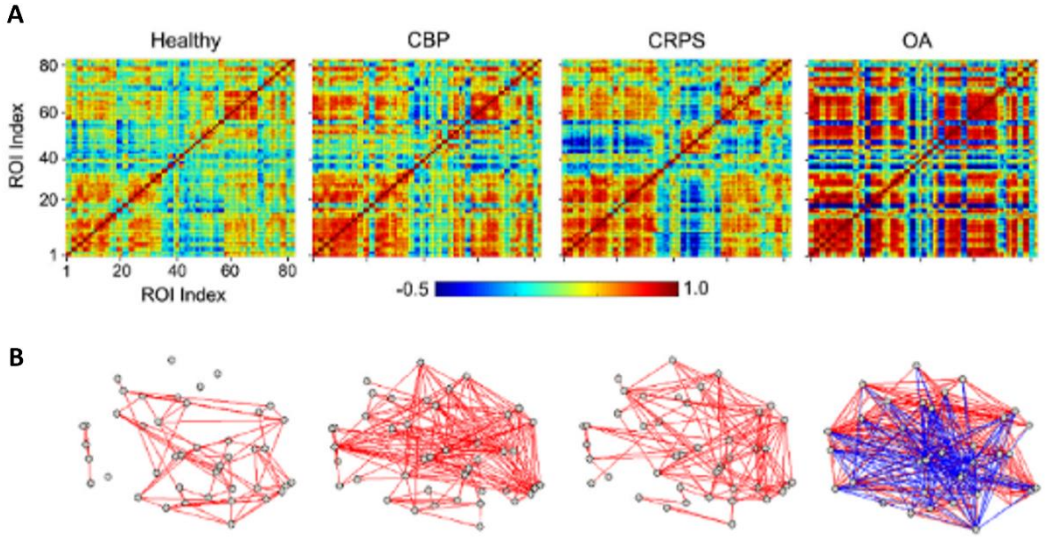

Figure 36: Cortical grey matter interrelationships (structural covariance) are specific for different chronic pain groups. (A) The relationships between grey matter regions were studied by calculating pair-wise correlations of grey matter density between the 82 Brodmann Area-defined regions (left panel) across subjects, separately for healthy controls, CBP, CRPS, and OA. The resulting correlation matrices show widespread increases in correlation strength in all three patient groups, compared to controls. (B) Graph representation of the data in (A) showing the association between the pairs of regions. Red and blue lines represent positive and negative correlations (links), grey date are the pairs of regions (nodes) (adapted from (Farmer, Baliki, and Apkarian 2012).

These results suggest a long-term change in brain architecture, although the precise mechanisms of this restructuring have not been yet fully characterized. Besides, a large spectrum of studies of chronic pain populations have shown reductions in grey matter that are not found in healthy cohorts, and a successful treatment for chronic back pain appears to partially reverse grey matter atrophy (Seminowicz et al. 2011). Collectively, these evidence reinforce the notion that the brain's structure dynamically reflects the clinical pain state (Farmer, Baliki, and Apkarian 2012).

Moreover, several groups among which Cauda and collaborators (2014) applied a network approach to study the gray matter alterations and found that chronic pain alters brain dynamics beyond pain perception, by indeed distorting spatial and temporal properties of large-scale brain networks (Farmer, Baliki, and Apkarian 2012).

In their study, they have identified three regional clusters of shrinkage and two of gray matter expansion. Increased gray matter volume were observed not only in the somatosensory and somatomotor areas, as previously reported (P. Schweinhardt et al. 2008), but also in the operculo-insular cortex.

Decreases were observed in the fronto-parietal regions, temporal and pontine regions and in the anterior insula.

The increase and the decrease occur within distinct neural networks. As already suggested by previous studies on chronic pain, it is highly likely that differential networks respond to noxious and painful stimuli in a different manner and with different temporal envelopes (Cauda et al. 2014; Mayhew et al. 2013; Moulton et al. 2012).

5.3.2 Alterations of brain functional response in chronic pain diseases

In this paragraph we will describe some examples of studies of alteration in the functional response to nociception in chronic pain patients.

In 2006, Baliki and Apkarian conducted one of the earliest studies demonstrating alterations in functional response in chronic pain. By investigating the specific condition of spontaneous pain in patients suffering from CBP, they identified increased activity in the medial prefrontal cortex (mPFC), which might be linked to spontaneous pain sensation. Their functional study suggests that, when spontaneous pain of CBP is high and sustained, it engages brain areas involved in emotion, cognition, and motivation (M. N. Baliki et al. 2006; Davidson 2002; Dolan 2002; Phelps et al., 2004), and these changes are associated with the intensity of chronic back pain experienced by the patients (M. N. Baliki et al. 2006).

Consequently, a large number of studies have investigated the changes in cerebral blood volume or local neuronal activity in several chronic pain conditions and have shown increased or decreased responses in different brain areas classically activated by noxious stimulations, or not (see for reviews Moisset and Bouhassira 2007; Lin 2014; R. Peyron, Laurent, and García-Larrea 2000; A. V. Apkarian et al. 2005b).

In CBP patients, there is a dissociation in the coding of pain intensity between the brain regions involved in the sensory (insula) and in the emotional aspects of pain (medial prefrontal cortex) (Marwan N Baliki et

al. 2006). Also, Hasmi et al. showed in a longitudinal study that in healthy/acute/subacute and chronic back pain patients, brain activity for back pain in the early, acute/subacute back pain group was limited to regions involved in acute pain, whereas in the chronic back pain group, activity is confined to emotion-related circuitry (Hashmi et al. 2013a). The results demonstrate that brain representation for back pain can undergo large-scale shifts in brain activity with the transition to chronic pain (Hashmi et al. 2013a).

Furthermore, PET studies showed, using a radiotracer of dopaminergic neurotransmission that the dopaminergic neurotransmission was altered in the ventral striatum of chronic non-neuropathic back pain patients (Martikainen et al. 2015). Interestingly, an fMRI study showed that VTA (Ventral Tegmental Area) activity during pain and anticipation of both pain and relief periods was dramatically reduced or abolished in fibromyalgia patients (Loggia et al. 2014). As the VTA is a source for reward-linked dopaminergic/GABAergic neurotransmission in the brain, this observation agrees with reports of altered dopaminergic/GABAergic neurotransmission in fibromyalgia. These results highlight the existence of an alteration in the mesolimbic dopaminergic reward circuit in chronic pain conditions.

5.3.3 Alterations of the functional connectivity in chronic pain diseases

FC alterations in chronic pain involved changes in the communication and coordination of activity between different brain regions. While specific alterations may vary depending on factors, such as the etiology of neuropathic pain and individual differences, several brain regions commonly exhibit FC alterations in patients with neuropathic pain.

Below, are presented some of key regions involved in the impaired functional brain reorganization.

5.3.3.1 Functional connectivity alteration in the Default Mode Network (DMN)

The default mode network (DMN) was shown to be altered in several neurological conditions, such as Schizophrenia and Alzheimer's disease. Disturbances in the correlation structure of spontaneous activity were reported in several pathological states (see Whitfield-Gabrieli and Ford 2012; Fox and Greicius 2010for review), including Alzheimer's disease (Greicius et al. 2004), multiple sclerosis (Lowe et al. 2002), depression (Greicius et al. 2007), schizophrenia (Salvador et al. 2007). They are related to the severity of the disease (He et al. 2007; Greicius et al. 2007) and recovery from functional deficits (He et al. 2007), and

have shown good segregation between healthy and patient populations (Greicius et al. 2004), suggesting that intrinsic activity may hold valuable diagnostic and prognostic information.

Interestingly, Apkarian and collaborators compared the changes in three chronic pain pathologies (Chronic back pain, CRPS and osteoarthritis) and showed that in all three chronic pain conditions, the DMN was altered with some common features, such as a decreased connectivity of medial prefrontal cortex (mPFC) to the posterior constituents of the DMN, and increased connectivity to the insular cortex in proportion to the intensity of pain. However, as already suggested by the same team in a previous review, each pathology displayed a particular 'signature' of these alterations (Marwan N Baliki et al. 2014; 2011; A. V. Apkarian, Baliki, and Geha 2009a). Therefore, chronic pain seems to reorganize the dynamics of the DMN, and this is maybe one of the underlying mechanisms of the maladaptive physiology of different types of chronic pain.

Importantly, many of these alterations were observed in brain areas of the emotional and reward circuitries, providing a possible explanation for high incidence of comorbid affective disorders in chronic pain patients.

5.3.3.2 Functional connectivity alterations in the Sensory Motor Network (SMN)

The SMN encompasses brain regions involved in the processing of sensory information and motor control, including primary somatosensory cortex (S1), primary motor cortex (M1), supplementary motor area (SMA), and premotor cortex (PMC). For example, Hotta and colleagues, in their study (2023) on CRPS patients revealed multiple alterations in FC of the primary sensorimotor cortex. They found a decrease in the interhemispheric FC between primary sensorimotor cortex (SM1) areas and a strengthened FC between SM1 and the right anterior insula (AI) and periaqueductal grey matter (PAG). Specifically, their results suggest that chronic pain reshapes the cortical SMN, with somatotopic emphasis (Hotta et al. 2023). Changes in FC within the SMN may reflect disruptions in sensorimotor integration, motor planning, and execution processes in individuals with neuropathic pain.

5.3.3.3 Prefrontal cortex

The medial part of the PFC (mPFC) is involved in emotional and cognitive processing in chronic pain (Kang et al. 2019). The prelimbic and infralimbic mPFCs receive inputs from brain regions including the basolateral amygdala (BLA), hippocampus, thalamus, and contralateral mPFC and send excitatory

projections to the amygdala (J. M. Thompson and Neugebauer 2019). Chronic pain is considered to develop as a result of the persistence of pain memory and inability to erase pain memory after injury (A. V. Apkarian, Baliki, and Geha 2009b). Moreover, preclinical evidence suggests that mPFC function is associated with pain states, based on electrophysiological studies in anesthetized rats showing a reduction in evoked and background activity in the mPFC in acute arthritis pain (Ji and Neugebauer 2014; Ji et al. 2010).

5.3.3.4 Anterior Cingulate Cortex

The ACC is associated with affective and motivational aspects of pain (L. Becerra et al. 2013; Navratilova, Atcherley, and Porreca 2015; Neugebauer et al. 2009; Neugebauer 2015). Nociceptive inputs are sent from the medial thalamus to ACC and combined with motivation and affective information received from other areas of the brain, such as the insular cortex, mPFC, and BLA (M. Catherine Bushnell, Čeko, and Low 2013; Navratilova, Atcherley, and Porreca 2015; J. M. Thompson and Neugebauer 2017; Williams, Crossman, and Slater 1977; Marwan N. Baliki and Apkarian 2015). The ACC then generates affective and motivational pain responses through its projections to the amygdala, NAc, and mPFC (Navratilova, Atcherley, and Porreca 2015; J. M. Thompson and Neugebauer 2017; Williams, Crossman, and Slater 1977; Marwan N. Baliki and Apkarian 2015; Marwan N Baliki et al. 2006). FC alterations within the ACC and its connections with other brain regions may contribute to the affective and motivational aspects of neuropathic pain.

5.3.3.5 Insular cortex

The insular cortex is divided based on his cytoarchitecture into posterior and anterior. The posterior IC (PI) participates in the somatosensory features of pain, while the anterior portion (AI) preferably mediates its affective aspects (Craig et al. 2000).

Posterior insula is part of the pain-related cortical networks with a preference for the sensory aspect, due to its connections with the primary and secondary motor and somatosensory cortices (M. Frot 2003; Maud Frot et al. 2013). The connectivity profile between the IC and the cingulate cortex further demonstrates that the PI plays a role in the sensory dimension of pain (Luppino et al. 1993).

Unlike the PI, of which the main connections are confined to thalamic nuclei and somatosensory areas, most connections of the AI are with multiple sites involved in the affective aspects of pain for example

with amygdala (Moraga-Amaro and Stehberg 2012), nucleus accumbens (Jasmin, Granato, and Ohara 2004), anterior cingulate and medial prefrontal cortex (Fox et al. 2005).

Several studies confirmed that insula is involved in the sensory-discriminative and affective-motivational aspects of pain processing (C. Lu et al. 2016). Accumulating clinical evidence shows that chronic pain can lead to anatomical and functional alterations in the Insular cortex (IC) which are correlated with cognitive and affective disorders (Moriarty, McGuire, and Finn 2011). More precisely, some studies have shown that the functional connectivity of the nucleus accumbens, core to the IC, and the primary and secondary somatosensory cortex (S1/S2) is significantly decreased in depressive rats, in parallel with its functional connectivity to the insula and the S1/S2 cortices in neuropathic pain model. In fact, the process of pain chronification is associated with a shift of brain activation from sensory to affective-emotional circuitry and the insular cortex might have a key role in this mechanism (Hashmi et al. 2013b).

5.3.3.6 Amygdala

The amygdala receives cortical and thalamic inputs, and the lateral/basolateral (LA/BLA) complex of the amygdala adds emotional and affective context to sensory information (Neugebauer 2015; Neugebauer et al. 2009; J. M. Thompson and Neugebauer 2017).

Studies have reported activation of the amygdala in pain states, suggesting that the amygdala plays an important role in emotional affective aspects of pain (Vachon-Presseau et al. 2016; Neugebauer 2015; Neugebauer et al. 2009; J. M. Thompson and Neugebauer 2017; Simons et al. 2014).

Altered functional connectivity involving the amygdala reflects disruptions in the integration of sensory, affective, and cognitive aspects of pain processing.

5.3.3.7 Nucleus Accumbens (NAc)

The NAc is a forebrain structure that integrates cortical and affective information and assigns motivation and value for the selection of appropriate behavioral responses (A. V. Apkarian, Baliki, and Geha 2009b; Marwan N. Baliki and Apkarian 2015; M. N. Baliki et al. 2006; Floresco 2015; Ito and Hayen 2011; Salgado and Kaplitt 2015). The NAc participates in emotional learning, evaluation of reward signals, and encoding of salience for pain (P.-C. Chang et al. 2014). Changes in NAc circuitry and connectivity are risk factors for pain chronification. A brain-imaging study reported that changes in NAc circuitry were predictive of the

transition to chronicity in patients with back pain (A. V. Apkarian, Baliki, and Farmer 2013; Vachon-Presseau et al. 2016).

5.3.4 Functional connectivity studies in rodents

Up to this point, we have described FC studies in chronic pain patients. Imaging human patients was the first approach employed to reveal dysfunctional brain reorganization, these studies have been critical for identifying the brain circuitry involved in pain processing and modulation, and for understanding the disruption of those circuitry in chronic pain. Despite the important information provided by imaging human subjects, there are many limitations. Conversely, animal models, especially rodents imaging studies, can overcome many of these limitations and provide a mechanism for back-translation of findings from humans to rodent models. In animal models more detailed analyses can be performed (such as *ex vivo* analysis). In addition, animal models are absolutely necessary for the early phase of drugs development, (such as new analgesic treatments); these being tested in animals before their further tests in clinical phase II and III in human.

Moreover, longitudinal imaging studies in patients are difficult, and since neuropathic pain - and more generally other diseases - can be modelled in rodents and since their life spans are short, longitudinal brain imaging studies are much more feasible in rodent subjects (S. J. Thompson and Bushnell 2012).

5.3.4.1 Functional definition of the pain network in rodents

Regarding pain imaging research, pilot experiments were conducted to demonstrate the similarities between the nociceptive pathway between rodents and humans. Thompson and Bushnell, in their review published in 2012, collected several studies of pain-evoked activation patterns in rodents. Despite variations in stimuli, anesthetics or restraining methods, scanning tools or analytical procedures, a consistent pattern of nociception-evoked activations emerges. The most consistently observed responses include the primary somatosensory cortex (S1), cingulate cortex (CC), and thalamus, all regions known in humans to receive afferent nociceptive information. Other regions known to be involved in pain processing and/or pain modulation that were frequently activated include the frontal cortex, caudate-putamen, periaqueductal grey matter (PAG), hippocampus, hypothalamus and insular cortex (IC).

A study involving the application of painful stimuli in awake restrained animals with fMRI BOLD have been conducted by Borsook and collaborators (Borsook and Becerra 2011) (Figure 37). The activated areas

included regions known to be involved in pain processing and modulation that are also activated in human studies as explained before. However, other regions, such as the visual and auditory cortices have been found consistently activated in this study, usually they are infrequently activated in human studies and are unlikely to be directly involved in pain (S. J. Thompson and Bushnell 2012).

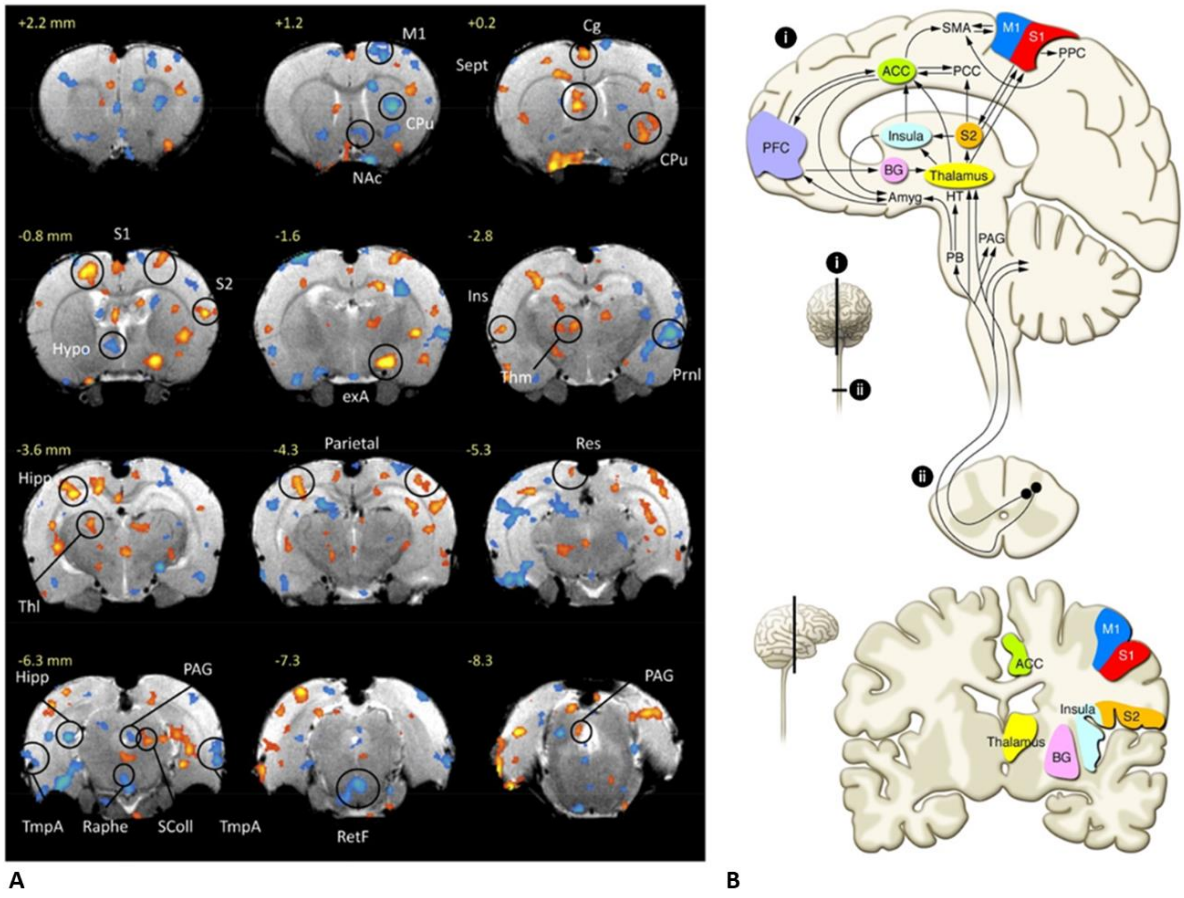

Figure 37: Functional definition of the pain matrix in rodents. (A) Increases (orange) and decreases (blue) in the BOLD signal in response to 50°C thermal stimuli applied to the hindpaw in awake restrained rats. More than 70 significant changes were observed in response to the painful stimulus. Regions activated included those typically activated in similar human pain imaging studies, but many additional regions were altered (Borsook and Becerra 2011). (B) Graphic depiction of brain regions receiving nociceptive input in humans and activated in MRI studies (S. J. Thompson and Bushnell 2012; Petra Schweinhardt and Bushnell 2010).

Several imaging studies in the literature have demonstrated that the study of FC in rodents with imaging techniques is feasible and shows appropriate parallels with human imaging studies. Moreover, pain imaging studies have focused, initially, on characterizing the brain regions related to acute nociceptive processing. Studies have demonstrated that the network of regions activated after a nociceptive stimulus in the rodent brain is similar to the network found in humans. However, little was known about resting-state fMRI in animal models of persistent pain.

5.3.4.2 Alterations of the functional connectivity in animal models of persistent pain

5.3.4.2.1 Feasibility in studying functional connectivity in animal models

Pilot experiments were conducted to demonstrate the feasibility of studying FC in rodents, by showing the presence of intrinsic network using resting state fMRI technique. It has been demonstrated that similar RSNs, such as the bilateral connectivity in sensory and motor networks, can be consistently identified in the anesthetized rat (Majeed, Magnuson, and Keilholz 2009; Pawela et al. 2008), awake rat (Lino Becerra et al. 2011; Liang, King, and Zhang 2012; Upadhyay et al. 2011), and, more recently, anesthetized mouse (Grandjean et al. 2014; Chuang and Nasrallah 2017; Sforazzini et al. 2014). In particular, Lu and colleagues (2012) (H. Lu et al. 2012a) demonstrated that, despite the distinct evolutionary paths between rodents and primates, rats possess a well-organized, intrinsically coherent DMN, which is broadly similar to the DMNs of nonhuman primates and humans (Figure 38).

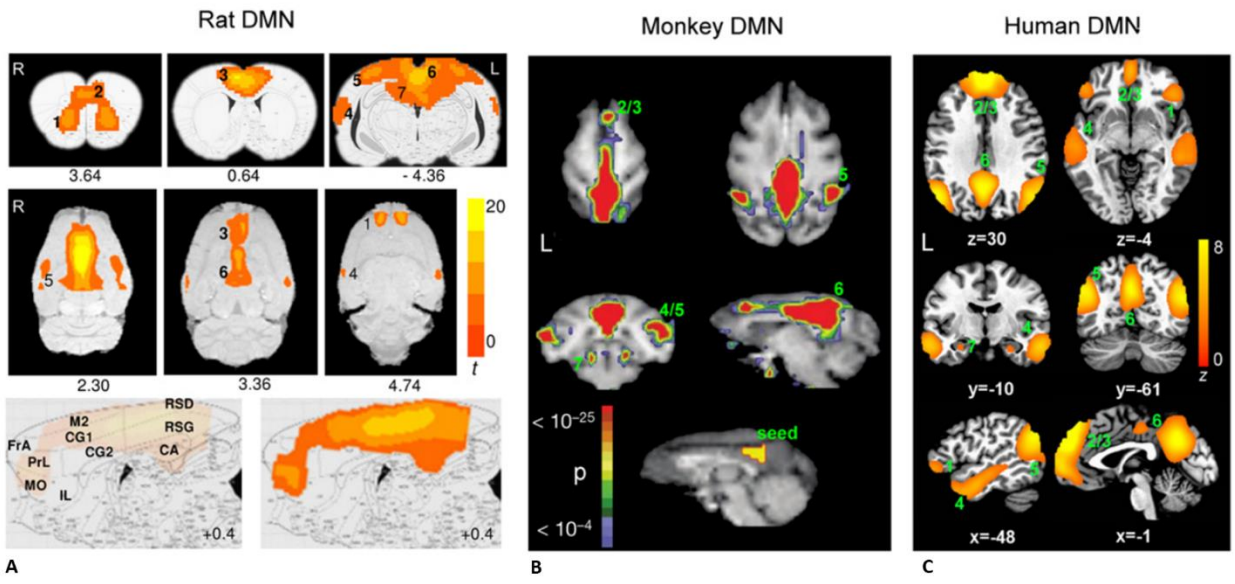

Figure 38: DMN in animal models. Differences in the morphological organization of the DMN between rat (A), monkeys (B) and human (C) In rats and monkeys, the DMN includes the entire medial bridge, which can be best visualized in the sagittal and coronal planes. In the human brain, it remains more focal (H. Lu et al. 2012b).

5.3.4.2.2 Alterations of functional connectivity in the limbic system

In 2014, Baliki and colleagues aimed to image and characterize brain reorganization following induction of neuropathic pain in a rodent model. Their study demonstrates that functional reorganization in neuropathic pain followed the time course of the disease. As mentioned at the beginning of this section, imaging studies in rodents have advantages in longitudinal studies. Due to their short lifespan, it is easier to follow the course of the disease. By imaging a rodent model of neuropathic pain at two different stages of the disease, 5 and 28 day post-injury, they found that intrinsic network showed minimal disruption at day 5 and more extensive reorganization at day 28.

This study relied on the use of rsfMRI to examine the intrinsic reorganization of rat brain functional connectivity following spared nerve injury (SNI). They compared longitudinal changes in topology and functional connectivity of resting-state neural networks between SNI and sham animals following peripheral injury (Figure 39).

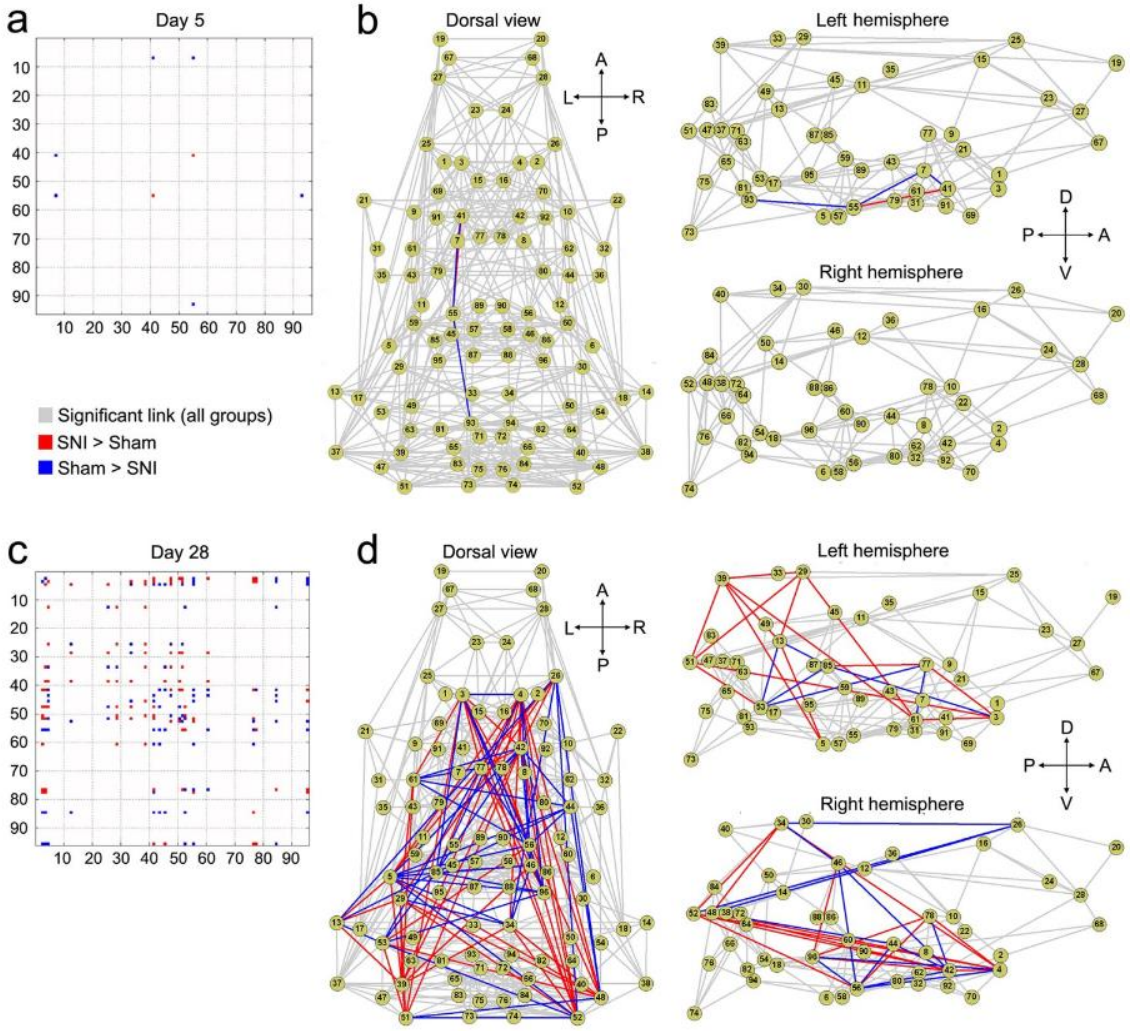

Figure 39: SNI is associated with late brain functional connectivity reorganization. (a-b) five days post-injury, SNI animals exhibited minimal changes in functional connectivity compared to sham. (c-d) In contrast, day 28 SNI animals showed a significant number of functional connectivity changes, both increases and decreases. In their analysis they focus the investigation on two systems of interest, the nociceptive and the limbic system (M. N. Baliki et al. 2014).

The results show that SNI was associated with increased connectivity within the striatum, hippocampus, and amygdala (Figure 40b). Specifically, the striatum showed increased connectivity to the thalamus, amygdala, and parts of the hippocampus, as well as to itself. Furthermore, the amygdala showed increased connectivity to sensorimotor areas. These increases in functional connectivity were coupled with decreases in hippocampal connectivity to thalamic and sensorimotor regions (Figure 40c). Collectively, these results indicate that most functional changes (both increases and decreases) in 28-day SNI animals were either limbic-limbic or limbic-nociceptive in nature (M. N. Baliki et al. 2014).

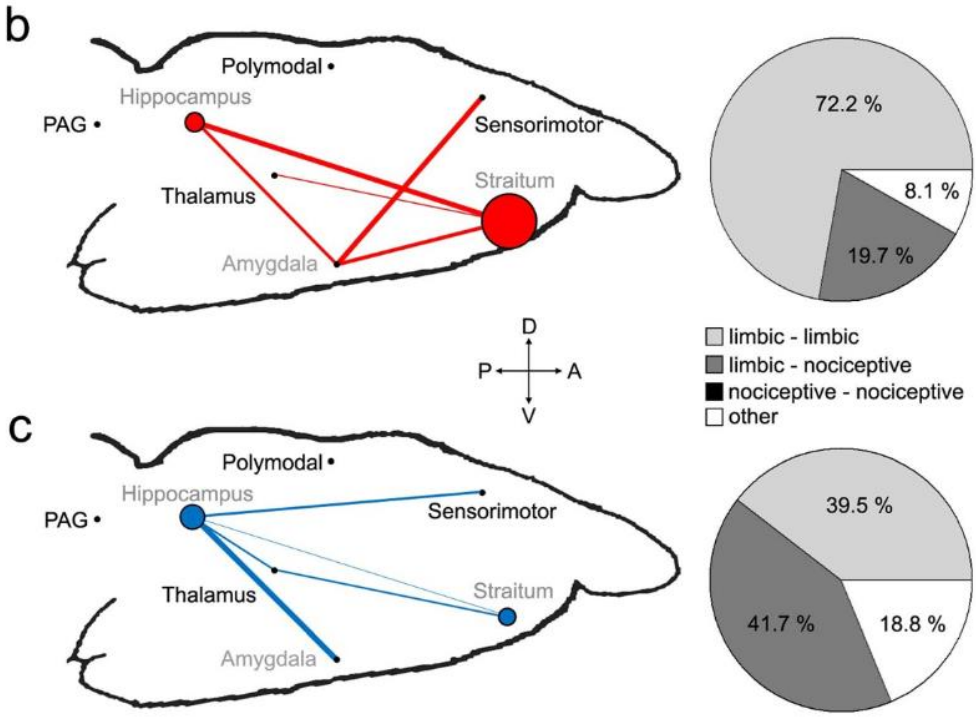

Figure 40: Functional connectivity changes 28 days after SNI are mainly within limbic, and between limbic and nociceptive regions. Significantly (b) increased and (c) decreased functional connectivity are shown relative to sham. Limbic (gray labels) and nociceptive (black labels) ROIs were grouped into two separate functional–anatomical modules, labeled at the approximate brain location. Normalized weighted edges and nodes indicate extent of reorganization between and within the seven regions. Pie charts show the percentages of significantly changed limbic and nociceptive connections relative to the total number of changed connections. There were no connectivity differences between nociceptive regions (M. N. Baliki et al. 2014).

With this study, Baliki and collaborators were able to characterize dysfunctional brain reorganization in a rodent model of neuropathic pain. They found that, in agreement with human studies, the functional neuronal networks are timely reorganized following nerve injury and that, there are more consistent changes in the regions of the limbic system, especially in the late stage. This constitutes a first evidence for time-dependent emergent reorganization of the rodent whole-brain network connectivity during persistent neuropathic pain (M. N. Baliki et al. 2014).

5.3.4.2.3 Alterations of somatomotor functional connectivity

Plastic changes have been primarily reported in S1 and ACC under chronic pain (Komaki et al. 2016; Morris et al. 2018; Spisák et al. 2017; Wells et al. 2017). For example, Spisak and collaborators (2017) compared

the intrinsic connectivity at rest in a chronic pain model (CFA) and reported a decrease in connectivity between the anterior cingulate cortex and the primary motor cortex (Figure 41).

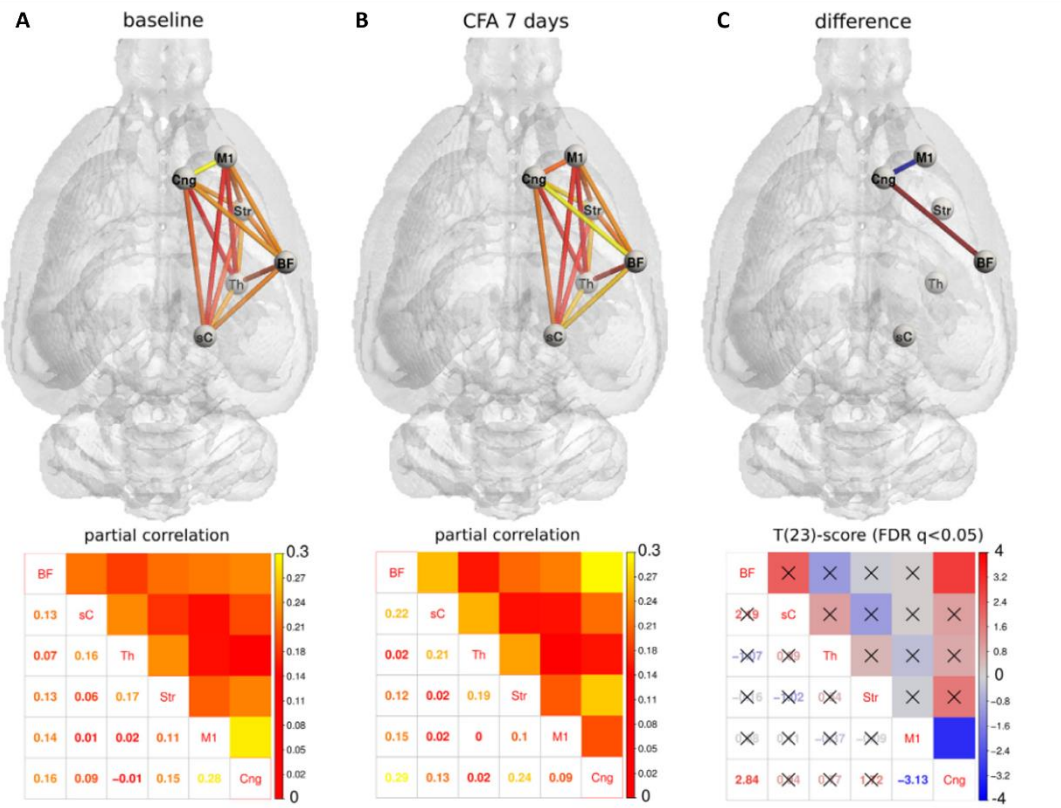

Figure 41: Chronic pain-related changes in functional connectivity. The baseline (A) and long-term (B) functional network and the statistical difference between the two states are visualized in glass-brain plots (top) and as (symmetric) partial correlation matrices (bottom). Colorbar is the same for glass-brain graph and matrix representation and depicts group-mean partial correlation values in the left and middle images and T-scores for the right-side image (degrees of freedom: 23) (Spisák et al. 2017).

Other animal neuroimaging studies have investigated brain reorganization in animal models of chronic pain and, despite the variety of pain models, protocols, neuroimaging techniques, and analysis, a group of brain structures seems to be consistently involved in the chronification of pain (Da Silva and Seminowicz 2019). Those regions involved often the somatomotor areas, prefrontal cortex, anterior cingulate cortex, insular cortex, amygdala and nucleus accumbens.

Other studies have reported an increase in the connectivity of the limbic system in chronic pain, and the ACC may be a key region modulating this network (Komaki et al. 2016; Morris et al. 2018; Spisák et al. 2017; Wells et al. 2017). In addition to receiving afferent nociceptive information, the ACC modulates the

emotional and motivated behaviors of chronic pain through increased connectivity to the striatum, hypothalamus, and mediodorsal thalamus (Komaki et al. 2016; Morris et al. 2018; Spisák et al. 2017). Moreover, additional studies reported enhanced activity of the PFC, ACC, hippocampus, amygdala, basal ganglia, and nucleus accumbens, but not the S1 in chronic pain (Abaei et al. 2016; P.-C. Chang et al. 2017; Jeong and Kang 2018; Komaki et al. 2016; Morris et al. 2018; Spisák et al. 2017; Wells et al. 2017). Taken together, these findings suggest widespread changes in the connectivity in regions involved in emotional, motivational, and cognitive responses associated with chronic pain (Da Silva and Seminowicz 2019).

All the studies cited here reveal significant correspondences in the process of pain chronification between rodent models and humans demonstrating that neuroimaging of pain in animals holds great promises for advancing our knowledge of brain function and allowing us to expand human subject research (Da Silva and Seminowicz 2019).

5.3.5 Studying functional connectivity in anesthetized or awake experimental conditions

5.3.5.1 Side effect of anesthesia in functional connectivity studies

While there are similarities in the brain reorganization between humans and rodents, differences exist in the experimental procedures, particularly concerning the use of anesthesia in animal experiments. Anesthesia has been used in most rodents imaging studies to minimize stress and movement of the animal during the acquisition (Chuang and Nasrallah 2017). However, several studies have documented that anesthetics produce profound changes in cerebral hemodynamics, brain metabolism, neural activity, neurovascular coupling, and functional connectivity compared to the awake states. Anesthesia induces a peculiar neurological state which differs to any natural physiological condition (Gao et al. 2017).

Anesthesia typically affects cardiopulmonary and vascular functions, leading to systemic changes in blood oxygenation, basal cerebral blood flow (CBF), and the consequent hemodynamic response to brain activity (Chuang and Nasrallah 2017). In 2017, Gao and colleagues revised several papers on this topic and they concluded that every published comparison between the awake and anesthetized condition has found substantial differences in every aspect of the hemodynamic response considered (CBV, BOLD, etc.). These studies have found the BOLD, cerebral blood volume (CBV) and cerebral blood flow hemodynamic response function (CBF-HRFs) are slowed in speed and decreased in amplitude by anesthesia (Figure 42) (Logothetis 2008; Aksenov et al. 2015; Chuang and Nasrallah 2017).

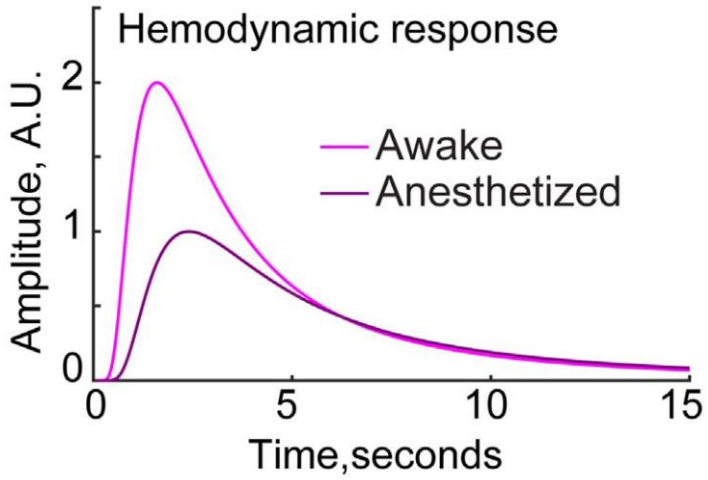

Figure 42. Hemodynamic response in awake and anesthetized conditions. Schematic showing net effects of anesthesia on (BOLD) hemodynamic response function. Anesthesia slows and attenuates the HRF. The awake hemodynamic response is approximately twice as large and has a faster onset compared to the HRF in anesthetized animals (Logothetis 2008; Aksenov et al. 2015; Gao et al. 2017).

Additionally, another negative outcome of the anesthesia is the dampening of the functional connectivity between regions, compared to the awake network. The hypothesis supported is that, in the anesthetized state, brain networks are altered to support different patterns of information transfer. In 2012, Liang and collaborators compared the whole-brain neural networks in awake and anesthetized rodents and their data indicate that connectivity strength was reduced on average in the anesthetized condition and the neural networks were significantly reorganized (Figure 43) (Liang, King, and Zhang 2012).

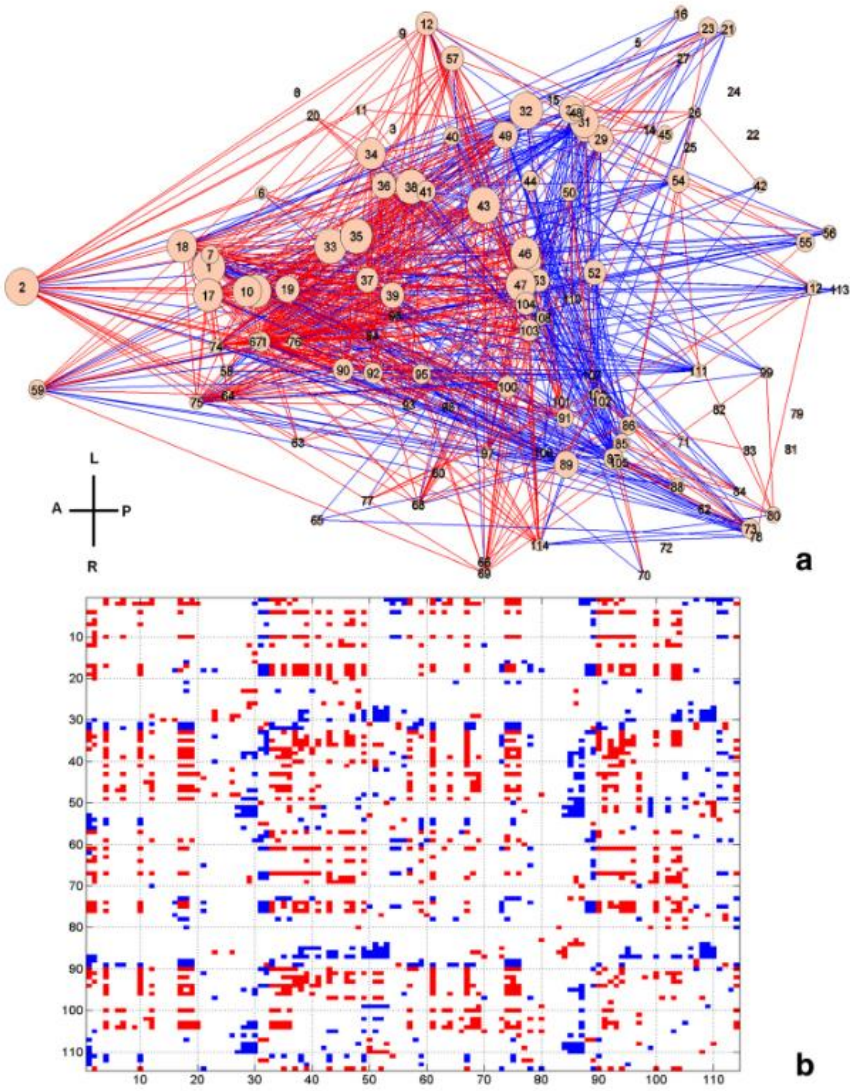

Figure 43: Significantly changed functional connectivity displayed in the dorsal view of the rat brain. (a) Each node represents an anatomical region. Red (blue) lines indicate connections with significantly stronger (weaker) connectivity in the awake condition. The size of each node is proportional to the number of altered connections forth is node. (b) Matrix representation of a. Red (blue) elements are connections with significantly stronger (weaker) connectivity strength in the awake condition (Liang, King, and Zhang 2012).

This study demonstrated that the integrity of the whole-brain network seems conserved in a wide physiologic range from awake to anesthetized states, while local neural networks adapt in new conditions (Liang, King, and Zhang 2012). Moreover, the connectivity strength between cortical and sub-cortical regions was reduced under anesthesia. Considering that anesthetics directly affect several neurotransmitter systems, which may lead to alterations in brain baseline function and responsiveness,

that would explain the changes in the functional connectivity between regions (Paasonen et al. 2017). For example, as most anesthetics bind to the γ-amino butyric acid (GABA) receptors, FC within and between regions of high GABAergic receptor density, such as the thalamus and caudate putamen, is generally weaker. The thalamocortical, frontoparietal and DMN connectivity are as well consistently affected under anesthesia (Hudetz 2012; Chuang and Nasrallah 2017).

The confounding effects observed under anesthesia are influenced by the type of anesthetic, its dosage, mode of administration method and its duration (Paasonen et al. 2017). Indeed, different levels of anesthesia can produce varying degrees of neural suppression and alteration of brain activity patterns. Moreover, different anesthetic agents have distinct mechanisms of action and effects on neural activity. For example, Figure 44 shows the study conducted by Paasonen and colleagues (2017) in which they evaluated the effect of five anesthetics on resting-state FC at two time points (with one-hour interval). Their results suggest that the baseline functional connectivity dynamically changes according to the type of anesthetics and its pharmacodynamics.

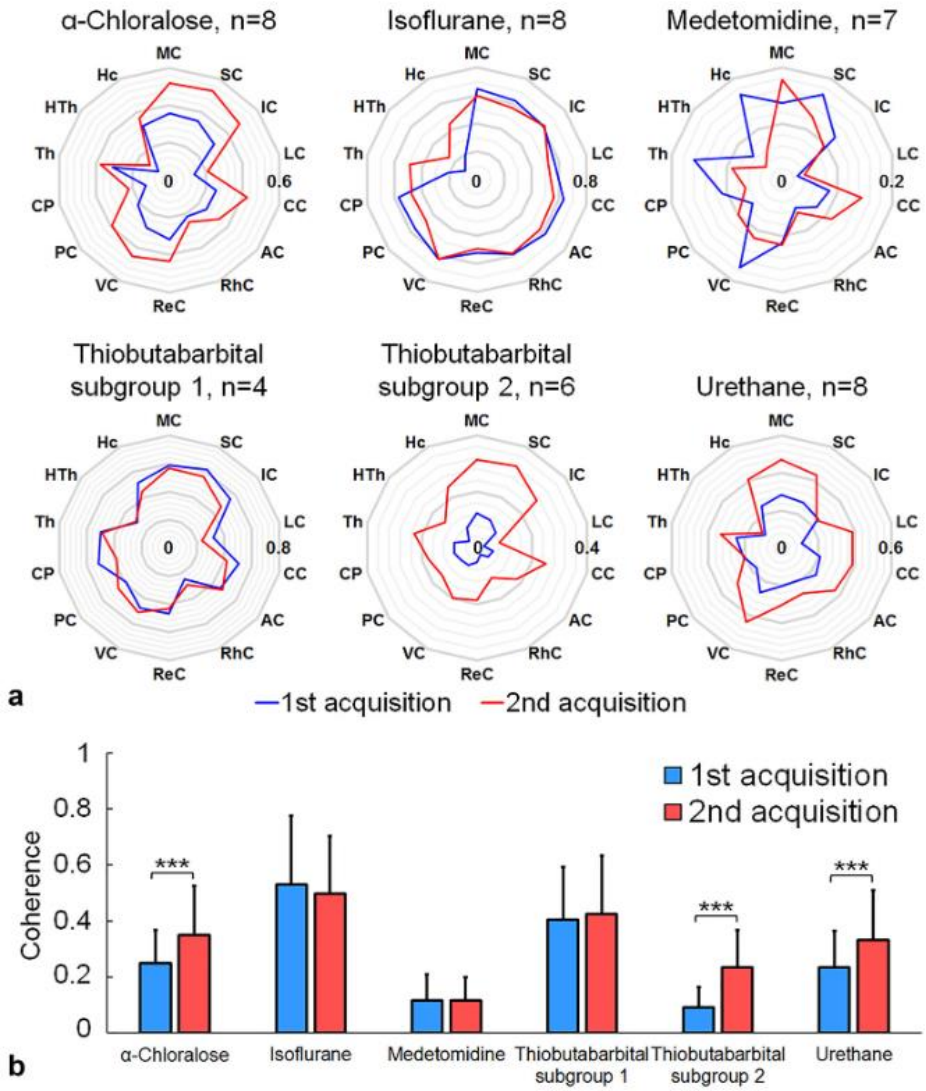

Figure 44: The dosage and the type of anesthesia influences functional connectivity. The anesthetics tested were: α-chloralose (AC), isoflurane (ISO), medetomidine (MED), thiobutabarbital and urethane. Results show an increase in connectivity after 1h in the α-chloralose group, thiobutabarbital subgroup 2 and in the urethane group. Then for the isoflurane group, FC remained stable, although there may have been an increasing trend in some subcortical regions. In the medetomidine group, the FC pattern changed slightly, but not significantly, with the current sample size. In thiobutabarbital subgroup 1, FC remained very stable (Paasonen et al. 2017).

To conclude, studying FC in anesthetized conditions entails some unfavorable effects that alter the connectivity strength, so careful consideration of anesthesia dosage and administration protocols is essential in FC studies to minimize confounding effects.

It is possible to achieve an appropriate balance between maintenance of physiological stability and minimizing the interference with neural activity to obtain reliable FC data, simply by adjusting the dosage

of anesthesia. This concept was demonstrated by Ferrier and colleagues in 2020, in their study they developed a light sedation protocol that preserve near awake levels of FC. In their paper they investigated, using a new imaging technique called functional ultrasound imaging (fUS), the dose-dependent effects of pharmacological sedation in FC (Ferrier et al. 2020). They hypothesized that a very light level of sedation might allow preserving near awake levels of FC. They compared the FC strength in four different states: awake, light sedation, deep sedation and recovery, longitudinally (Figure 45A). The difference between light and deep sedation was the dosage of the same anesthetic (medetomidine). In all conditions, the patterns of FC were similar, with stronger bilateral correlations in awake animals, and lightly sedated. In the deep sedation state the FC strength is strikingly decreased. Upon recovery, after reversal of the sedative effects, the correlation matrix was comparable again to non-sedated mice (Figure 45B) (Ferrier et al. 2020). As in the lightly sedated state, the FC strength is comparable to the connectivity in awake resting animals, this study proposed that by adjusting the dosage of anesthesia, it may be possible to mitigate the adverse effects associated with anesthesia.

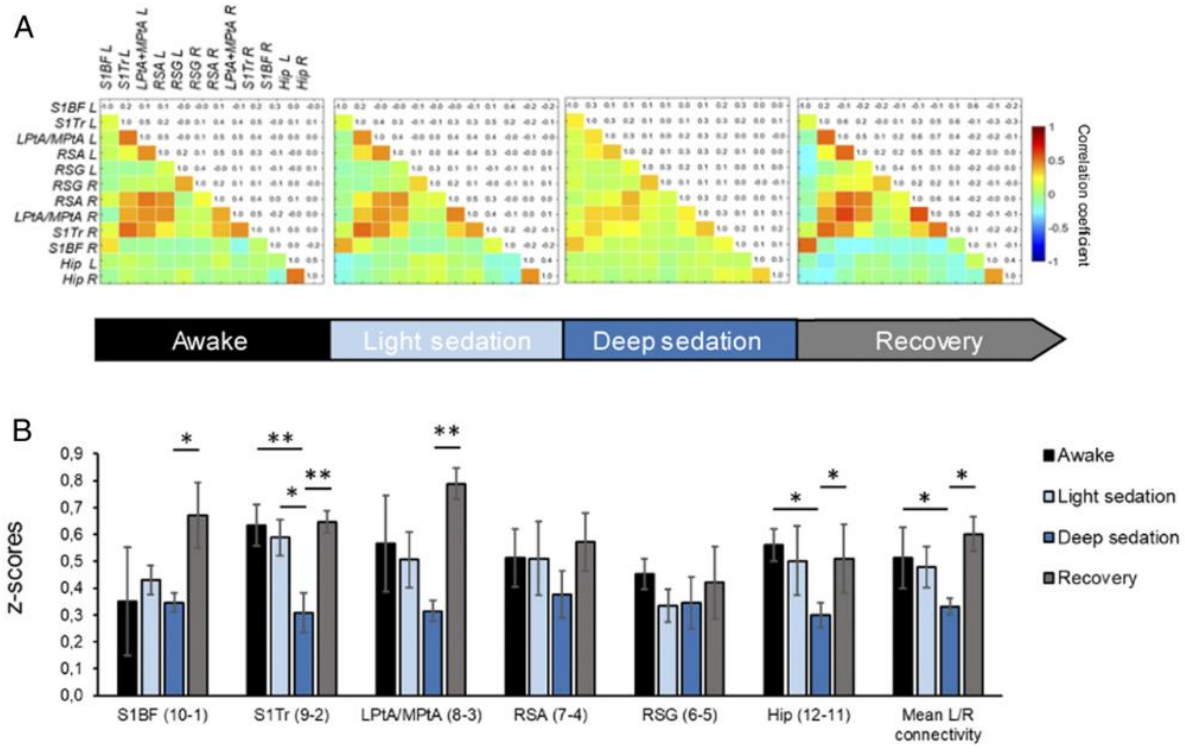

Figure 45: Effect of different levels of anesthesia on resting state functional connectivity using functional ultrasound imaging. (A) Mean correlation matrices at different levels of sedation: At rest (awake), light sedation, deep sedation, and after anesthesia reversal (recovery). (B) Normalized z-scores of interhemispheric correlations for each pair of ROIs in each state of consciousness. (Ferrier et al. 2020).

5.3.5.2 Advantages and limitations of studying functional connectivity in awake animals

We mentioned at the beginning of this section, that, in order to keep the animal in a physiological state and collect reproducible results, two main challenging aspects of imaging experiments in rodents are I) the prevention of animals' movement and II) the potential stress during the imaging session.

Motion artifacts are problematic for several reasons. Firstly, the movement can induce aberration in the signal. This is typically what we observe in fUS imaging and in electrophysiological recordings. Secondly, in fMRI, motion artifacts lead to measurements of the BOLD signal in brain regions surrounding the area of interest, giving rise to poorly reproducible results.
Stress, on the other hand, prevents the acquisition of data under natural physiological conditions. The animals are not only in a different physiological state, in which the 'stress axis' is highly activated, i.e. in which brain areas involved in stress induction and management are functionally activated. Also, within groups, animals display different levels of stress, rendering the results highly variable and difficult to interpret.

Consequently, the initial solution was to anesthetize the animals. However, anesthesia induces significant disruptions in brain activity, and the only way to obtain reliable functional connectivity (FC) data is to achieve a lightly sedated state.
Another potential solution involves conducting imaging experiments under awake conditions while enhancing restraining methods and habituation procedures.
A key advance has been the widespread adoption of head-fixation methods, first developed in the primate neurophysiology community (Wurtz 1969) and then adapted to the use in rodents (Gao et al. 2017). Head-fixation methods significantly reduce movement artifacts but reduce, as well, the possibility to express the natural and physiological behavior of the animal, which induces considerable stress. Consequently, animals require acclimatation and habituation to the head-fixation conditions.
The restriction and habituation procedures depend on species and imaging modalities. An example of restriction methods in MR scanners is shown in Figure 46. The rat head restrainer is usually composed of a bite bar, a pair of adjustable ear bars or ear pads, a nose clamp and a shoulder pad. In terms of acclimation procedure, the rat is first briefly anesthetized to enable secure placement of the animal's head into a head holder with the incisors secured over a bite bar, the nose fixed with a clamp, and ears positioned inside the head holder with adjustable ear pads or ear bars. (Topical application of lidocaine (2%) or EMLA cream is used to relieve any discomfort associated with head-fixation). The animal's

forepaws and hindpaws are loosely taped to prevent any self-injurious behavior (i.e. scratching). The body is then placed in a Plexiglas body tube that allows unrestricted respiration and movement of the trunk and limbs. The animal is exposed to these conditions for 7 days before imaging. The time for exposure during acclimation is increased from 15 min on the first day to 60 min on days 4, 5, 6, and 7, with an increment of 15 min per day (Gao et al. 2017).

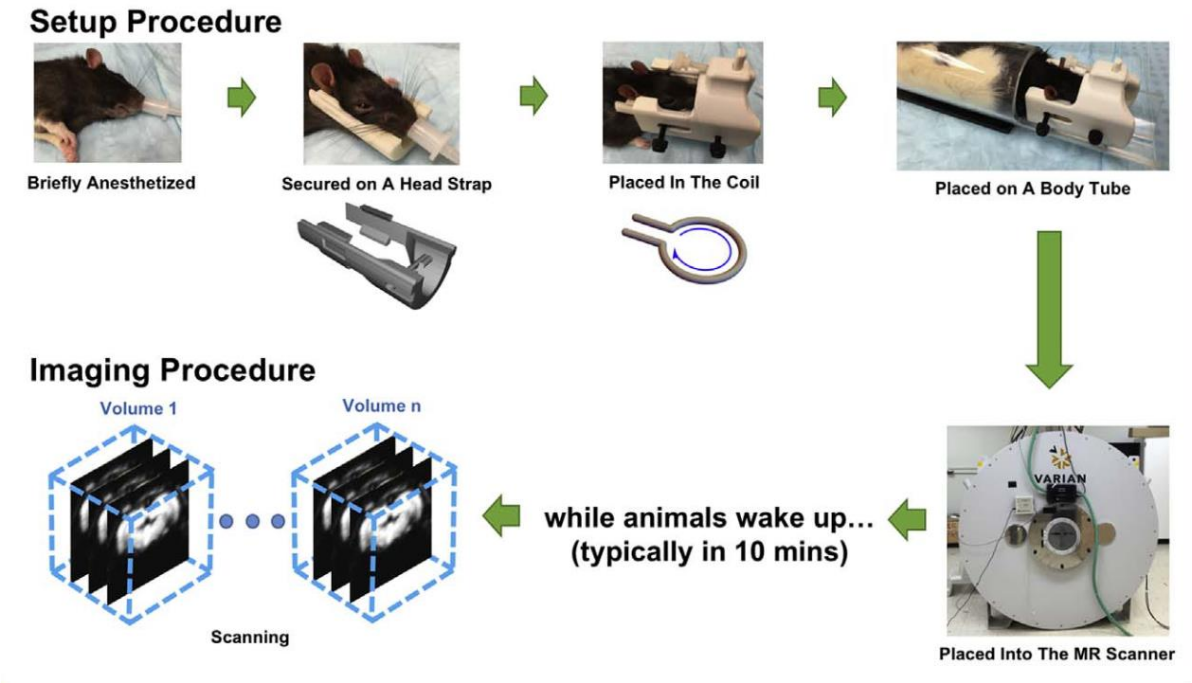

Figure 46: Procedure for imaging an awake rat using MRI. Schematic illustration of the animal setup and imaging procedures. (Gao et al. 2017).

As depicted in the image, the restrictive conditions do not allow for normal animal behavior. The animal is unable to move freely and express its natural and physiological behavior during the experiment. The primary goal of awake experiments is to acquire data under conditions that least perturb the animal's real behavior.

6 NEUROIMAGING

Numerous complementary techniques are used in Neuroscience to investigate the structure, function, development and diseases of the nervous system at various levels, from molecular and cellular to system and behavior.

Neuroimaging is a field of neuroscience that encompasses various imaging techniques used to study the *in vivo* central nervous system (CNS) delineating its structural and functional properties.

In Figure 47, an overview of the principal imaging techniques and their corresponding levels of investigation is proposed. Techniques, such as optical imaging and electrophysiology permit access to the cellular level. Other techniques, such as magnetic resonance imaging (MRI), positron emission tomography (PET), electroencephalography (EEG) and functional ultrasound imaging (fUS), enable to investigate the whole brain at the macroscopic level, non-invasively.

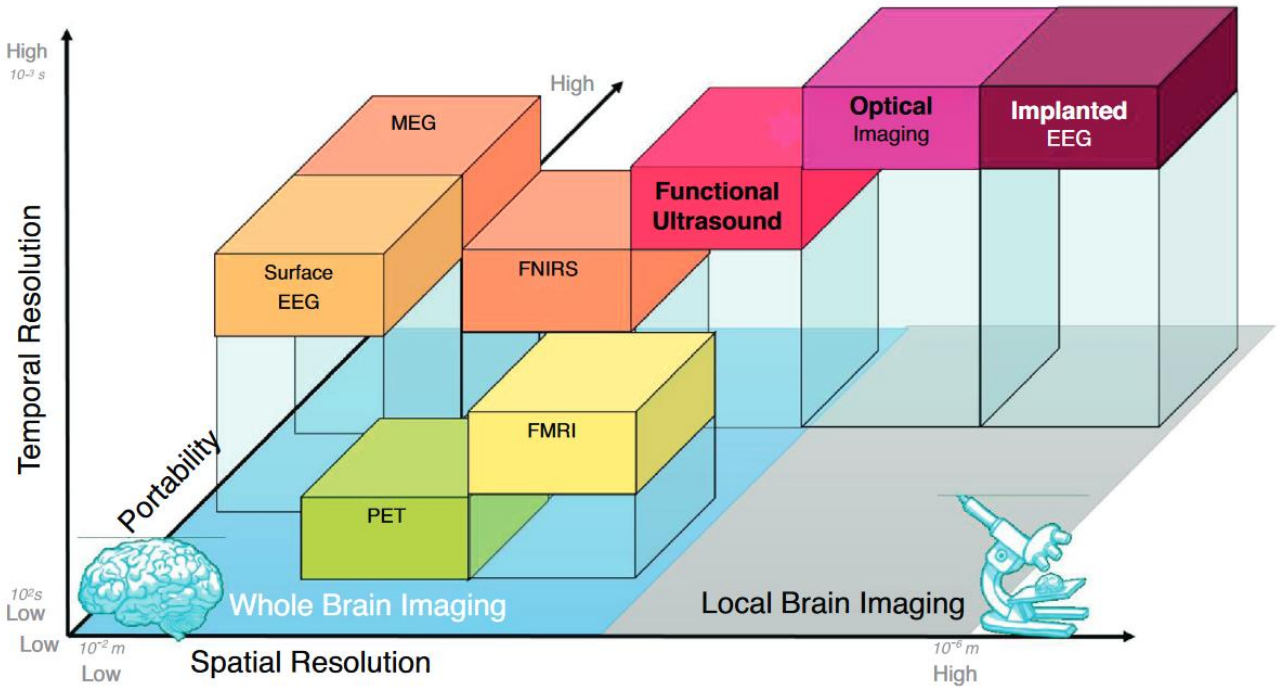

Figure 47: Overview of principal neuroimaging techniques. Main brain functional imaging techniques on a three-axis chart (temporal resolution, spatial resolution, portability). Techniques were separated between local and whole-brain imaging. Functional ultrasound fills a gap between whole brain imaging and microscopy, as well as between fMRI and Optics (Deffieux et al. 2018).

6.1 MICROSCOPIC IMAGING

In the microscopic field of view, optical imaging techniques provide images with excellent spatiotemporal resolution. For example, calcium imaging detects neural firing by monitoring the dynamics of intracellular calcium ions (Ca^{2+}) in neurons *in vivo*. The technique combines two-photon microscopy with calcium-sensitive fluorescent indicators, allowing for real-time imaging of neuronal calcium dynamics. This involves using fluorescent molecules as calcium indicators, as they respond to the binding of Ca^{2+} ions by altering their fluorescence properties. While genetically-engineered animal models are required, it can detect neuron firing with high spatiotemporal resolution (Deffieux, Demené, and Tanter 2021).
Optical-based methods provide the highest spatial and temporal resolutions (~10 µm, ~10 ms) compared to the other neuroimaging techniques. However, they are intrinsically limited to the investigation of the cortex due to the poor penetration of light within the tissues (Mace et al. 2013).

6.2 WHOLE BRAIN IMAGING

Whole brain imaging allows for the non-invasive study of the entire brain *in vivo*. Different types of neuroimaging techniques enable investigation into various aspects of the brain, including its anatomical structure, physiology and functional connectivity between regions (Logothetis 2008; Lenartowicz et al 2010).

The ability to image the living human brain has revolutionized the field of neuroscience, by uncovering the complexity of the brain. From early X-rays to the cutting-edge techniques of today, neuroimaging has transformed neuroscience and continues to shape our understanding of the brain and its functions. The field is still in dynamic evolution with modern and significant technological advancements.
The exploration of *in vivo* brain anatomy started in 1895 with the discovery of X-ray by Wilhem Roentgen. X-ray imaging, at the time, enables only the visualization of the skull (Figure 48A). The technology that enables the visualization of the brain itself arrived later, specifically in 1972, with the advent of X-ray computed tomography (CT). CT provided the first non-invasive method for visualizing the brain's soft tissues in detail. For the first time a non-invasive modality could reveal the ventricular system, separate gray from white matter, outline the deep nuclei, and recognize pathologic changes in the cerebral parenchyma (Figure 48B) (Fulham 2004). CT acquired image by sections, and from this technology, three-dimensional imaging modalities like Emission Computed Tomography (ECT) were developed in its two

forms: Positron Emission Tomography PET (Figure 48E) and Single Photon Emission Computed Tomography SPECT, as well as Magnetic Resonance Imaging (MRI) (Figure 48C and F).

These two imaging modalities measure signals of diverse natures and capture different characteristics of the CNS, MRI acquires physical property of the brain while ET (Emission Tomography), on the other hand, captures the physiological activity associated with neuronal activation.

By this example, we are delineating two categories of brain imaging techniques: structural and functional imaging (Figure 48). Structural imaging techniques delineate brain tissue such as white versus gray matter, vasculature, and bone, based on their physical properties: tissue density or nuclear resonance characteristics. Functional images capture physiological activities in the brain like metabolism, blood flow, chemical composition and absorption which are typically coupled to neuronal firing (Lenartowicz et al 2010).

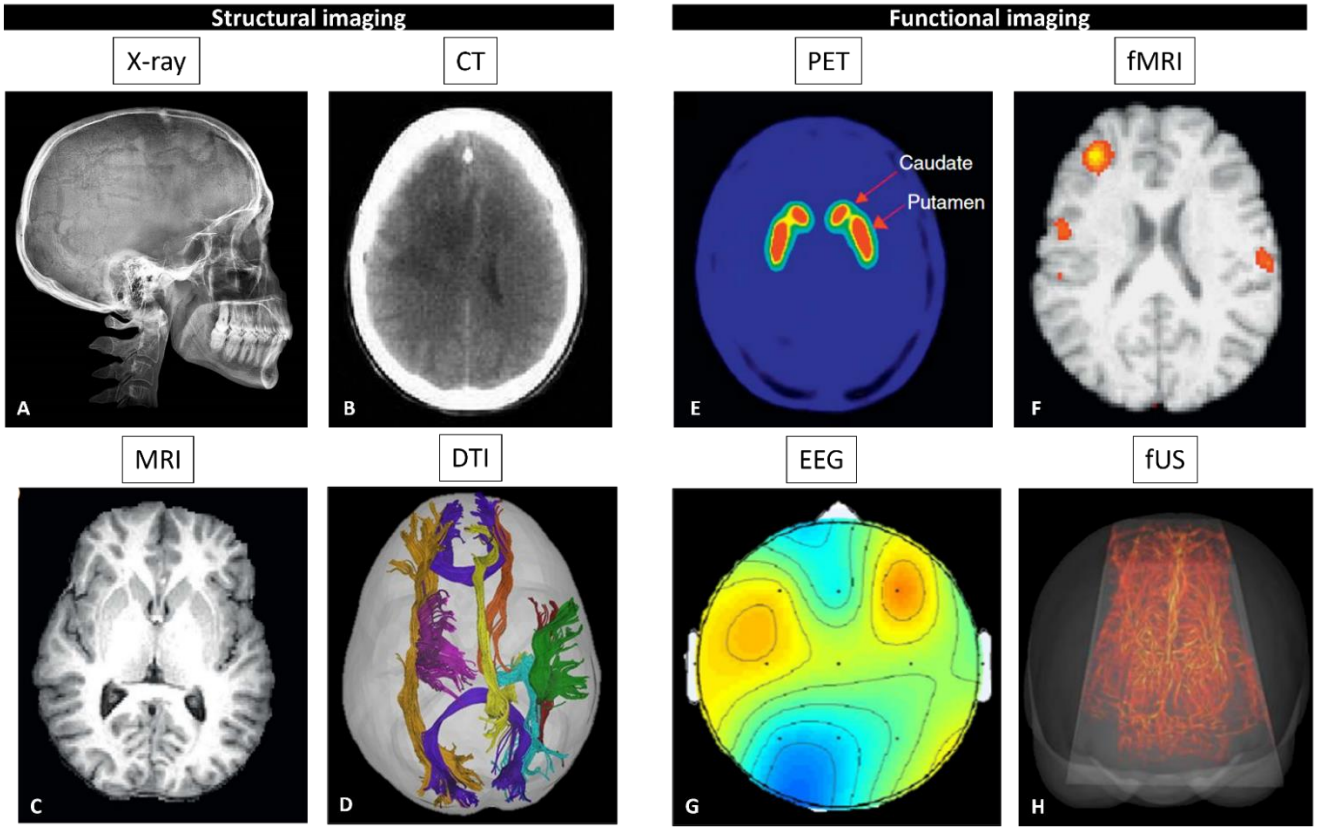

Figure 48: Overview of most common imaging techniques. Subdivided in structural and functional imaging techniques (adapted from M J Fulham, et al 2004; Lenartowicz et al 2010; Baranger et al. 2021).

6.2.1 Structural Imaging techniques

Magnetic Resonance Imaging (MRI) is the most powerful method for structural imaging (Lenartowicz et al 2010). It is based on the principle of nuclear magnetic resonance (NMR), discovered by Felix Boch and Edward Purcell in 1945. Nuclear magnetic resonance results from the magnetic properties of some atomic nuclei, particularly the hydrogen nuclei in water molecules, that tend to resonate when placed in a magnetic field (Fulham 2004).

An electromagnet, typically 1.5–4.0 tesla (T) for human imaging, is first used to produce net nuclear magnetization in hydrogen atoms in the body. Radiofrequency pulses are then applied at the resonant frequency of the hydrogen atoms, which displaces them into a higher-energy state. As the protons then return to their original state, they release energy, creating an oscillating magnetic field that is detected by a conductive coil placed in the field.

Typical MR images capture detailed three-dimensional (3D) structure of the brain, distinguishing between tissues such as gray and white matter, cerebrospinal fluid, bone, fat and air, as well as being able to detect the presence of abnormal tissues such as tumors or cysts (Figure 48C) (Lenartowicz et al 2010).

One advantage of MRI is its extreme flexibility in the types of signals that it can measure. **Diffusion-weighted MRI** (Diffusion Tensor Imaging or **DTI**) is sensitive to the movement of water molecules over time. The measurement of directional diffusion signals allows characterization of white matter structure, which has allowed the development of MRI-based tractography methods for imaging white matter connectivity (Figure 48D) (Lenartowicz et al 2010).

In the 1980s this technology was introduced to the clinic, and since then MRI has assumed a role of unparalleled importance in diagnostic medicine and more recently in basic research. In medicine, MRI is primarily used to produce structural images of organs, including the central nervous system, but it can also provide information on the physico-chemical state of tissues, their vascularization, and perfusion this aspect will be explained in the next section (Logothetis 2008).

6.2.2 Functional Imaging techniques

Functional imaging enables the measurement of brain activity by capturing actual neuronal firing or physiological activities in the brain. Functional imaging modalities fall into two categories: those that

directly detect neuronal activity (EEG/MEG) and those that measure physiological processes associated with neuronal activity (fMRI/PET/fUS) (Lenartowicz et al 2010).

6.2.2.1 Direct measurements of neuronal activity

Direct regcording of neuronal activity consists of measuring the electrical activity produced by neural firing. In the category of whole-brain imaging, techniques that record neural firing include electroencephalography (EEG) and magnetoencephalography (MEG).

6.2.2.1.1 EEG/MEG

Electroencephalography (EEG) was first described by Hans Berger in 1924, by demonstrating that brain activity can be measured directly from the scalp. EEG measures, using electrodes attached to the scalp, electrical signals resulting directly from postsynaptic potentials in the apical dendrites of pyramidal neurons of the cortex (Figure 48H) (Lenartowicz et al 2010).

Perpendicular to the currents detected by EEG, arises a magnetic field that can be measured by **magnetoencephalography (MEG)**, firstly introduced in 1968 by David Choen. With MEG, magnetic fields at the scalp are measured using a superconducting quantum interference device (SQUID) containing highly sensitive detectors that translate the magnetic field back into current values (Lenartowicz et al 2010).

EEG and MEG both record direct neuronal activity, providing excellent temporal resolution. However, their spatial resolution is poor, as they are limited to detecting neuronal signals generated by cortical pyramidal neurons that can be detected from the scalp.

6.2.2.2 Indirect measurements of neuronal activity

As introduced above, neuronal activity can be probed indirectly by techniques that captures physiological activities in the brain metabolism, blood flow, chemical composition and absorption. It has been demonstrated that there is a close relationship between cerebral hemodynamic changes and brain activity. This relationship is referred to as neurovascular coupling.

6.2.2.2.1 Neurovascular coupling

The brain consumes a large amount of energy but, unlike the other organs, lacks a reservoir to store it. Therefore, it constantly receives energy substrates (especially glucose and oxygen) through its blood supply. Complete interruption of the cerebral blood supply for more than a few minutes (for example, with a cerebral artery occlusion in stroke or after cardiac arrest) leads to severe brain damage and death. Understanding how the brain regulates its own blood supply has been a longstanding interest, driven primarily by the need to comprehend the harmful effects of cerebrovascular insufficiency. Additionally, there is recognition that regional changes in cerebral blood flow (CBF) may be linked to brain function (Iadecola 2017).

The relationship between neuronal activity and hemodynamic changes has been first discovered by Angelo Mosso in 1800s. By measuring the changes in brain volume and temperature, he observed that a strong emotional stimulus is linked with cerebral vasodilation and peripheral vasoconstriction. Thereafter, several experiments have further established the close relation in space and time between changes in cerebral blood flow (CBF) and neuronal activity (Iadecola 2004).

Since the brain lacks energy reserves, during neuronal activity, a well-timed delivery of oxygen and glucose in the interested areas is needed, and that explains the increase in CBF in activated brain areas (Iadecola 2017). This coordinated activity results from the proximity between neurons, astrocytes and blood vessels. Together they constitute a functional unit called the neurovascular unit. As shown in Figure 49A, large cerebral arteries branch into smaller arteries and arterioles that run along the surface of the brain (pial arteries). Those consist of an endothelial cell layer, a smooth muscle cell layer and an outer layer of leptomeningeal cells. As the arterioles penetrate deeper into the brain, they lose the layer of leptomeningeal cells and they keep only one layer of smooth muscle cells for the intracerebral arterioles, or pericyte for the capillaries (Figure 49B). Smooth muscle cells and pericytes convert the chemical signals that originate from endothelial cells, neurons and astrocytes into changes in vascular diameter (Iadecola 2004).

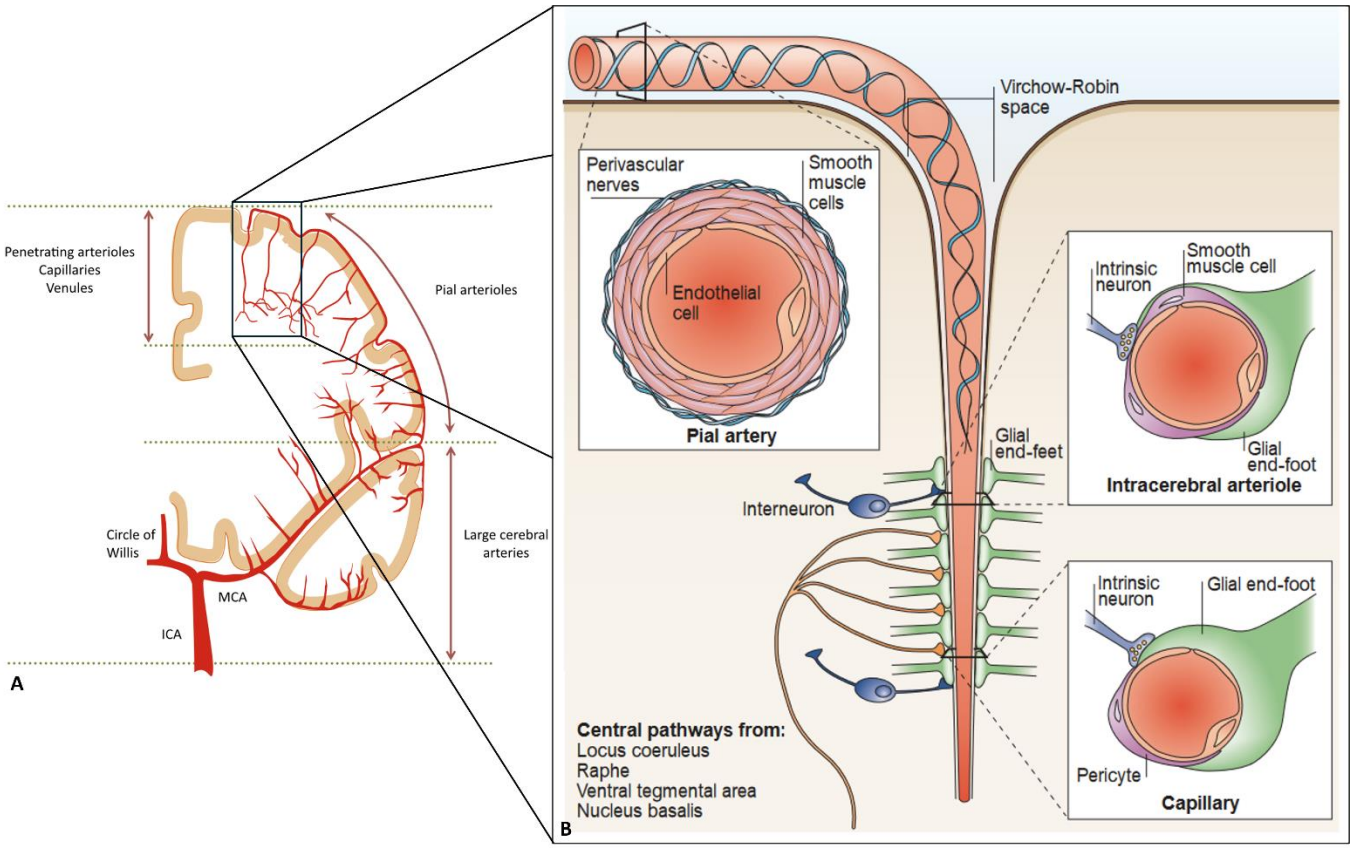

Figure 49: The neurovascular unit. (A) Anatomy of the Cerebrovascular Tree. (B) zoom in of a penetrating arteriole. Large cerebral arteries branch into smaller arteries and arterioles that run along the surface of the brain (pial arteries). These consist of an endothelial cell layer, a smooth muscle cell layer and an outer layer of leptomeningeal cells. As the pial artery penetrates deeper into the brain this space disappears and the vascular basement membrane comes into direct contact with the astrocytic end-feet (intracerebral arterioles and capillaries) (adapted from (Iadecola 2004; 2017).

The release of vasoactive factors from endothelial cells, neurons, and astrocytes is the result of multiple processes consequent to brain activity. These processes are both metabolism and neurotransmitters dependent. These processes take part to a feedback-feedforward model (Figure 50):

- Feedback: synaptic activity increases the local demand for energy, leading to consumption and consequent lack of glucose and oxygen in the activated region. Severe hypoxia and hypoglycemia are potent stimuli of vasodilator release that mediates a local increase of CBF (Iadecola 2004). However, some studies have demonstrated that the CBF increases persist even in the presence of excess glucose or oxygen, suggesting that it is not the only process involved in the flow increase (Attwell and Iadecola 2002).

- Feedforward: based on this evidence, it was suggested that CBF delivery is regulated by a feedforward mechanism. Glutamate is release by the synapse and activates post-synaptic glutamate receptors (GluRs), leading to activation of Ca^{2+}-dependent signaling pathways resulting in the release of vasoactive factors (K+, nitric oxide NO, and prostanoids) that may drive the initial feedforward component (metabolism-independent) of the local vascular response in capillaries and arterioles (Iadecola 2017).

The model suggests that a feedforward mechanism may trigger an exaggerated flow response driven by neurovascular signaling, but feedback mechanisms may also be in place to adjust CBF delivery more closely to the metabolic needs of the tissue. Therefore, both metabolism-dependent (feedback) and independent (feedforward) mechanisms may be involved in functional hyperemia, depending on the timing, intensity, and duration of the activation (Iadecola 2017).

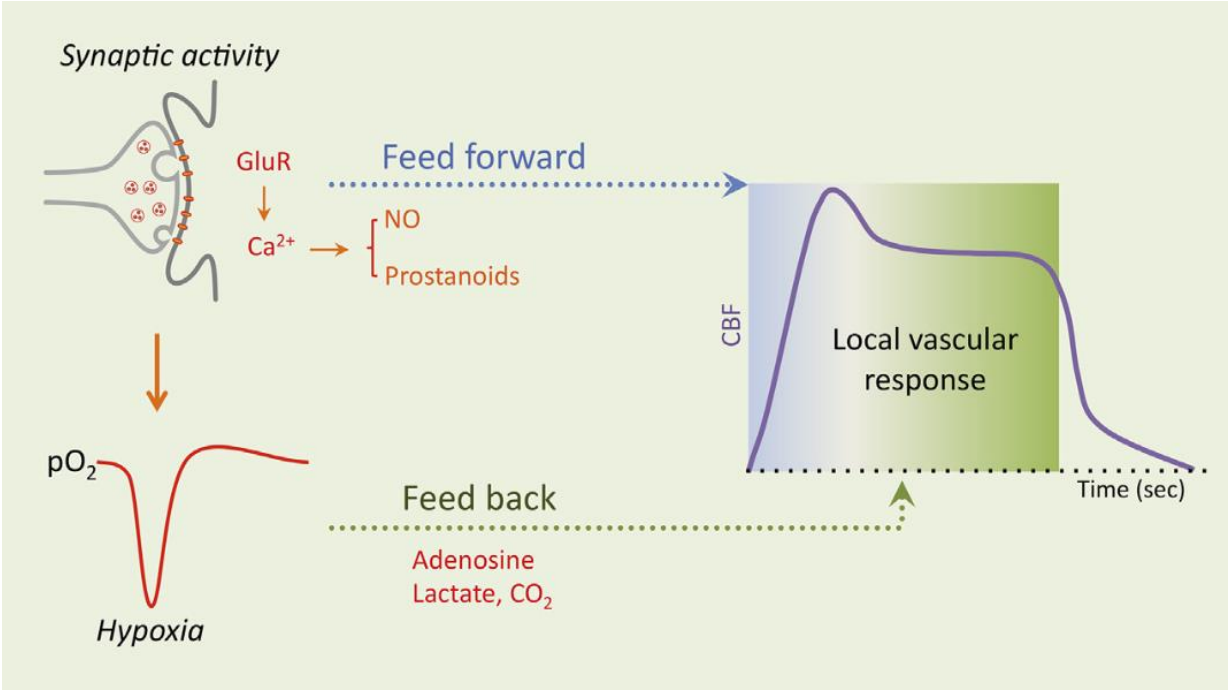

Figure 50: Feedback-feedforward model. Glutamate released by synaptic activity activates post-synaptic glutamate receptors (GluRs), leading to the activation of Ca^{2+}-dependent signaling pathways, resulting in the release of vasoactive factors that may drive the initial feedforward component (metabolism-independent) of the local vascular response in arterioles and capillaries. At the same time, a reduction in tissue O_2 caused by the increased energy consumption induced by activation leads to the accumulation of vasoactive metabolic by-products that may drive a secondary feedback component (metabolism-dependent) to better match the flow response to the metabolic needs of the tissue (Iadecola 2017).

Several neuroimaging techniques such as PET, SPECT, fMRI and fUS rely on the principle of neurovascular coupling to indirectly probe brain activity by detecting hemodynamic changes (Iadecola 2004).

6.2.2.2.2 Emission computed tomography (PET, SPECT)

As already introduced in the previous section, **Emission computed tomography (PET, SPECT)** captures physiological activity associated with neuronal activation. This nuclear imaging method uses injected radioisotopes and combines the principles of the tracer kinetic method and tomographic image reconstruction (Fulham 2004). This technique enables imaging metabolic processes in the brain by detecting the radiation energy emitted from radioactive tracers (isotopes) that are intravenously injected, and subsequently distributed by the circulatory system of the brain. The radiotracer typically binds molecules of interest in the brain and then follows their metabolism by reflecting a specific physiological process. As the radiotracer decay is detected by the PET scanner, a 3D image of the metabolic effects on the radioactive isotope in the brain can be reconstructed (Figure 48E). For instance, glucose labelled with the isotope ^{18}F has been extensively used to measure increased glucose metabolism in visual and auditory sensory cortices in response to visual versus auditory stimuli respectively, and in motor cortex during finger tapping movements. PET is commonly used to study brain metabolism (Lenartowicz et al 2010).
A similar process applies to SPECT. However, in this case, the tracer used is a radionuclide, which has been developed primarily for measurement of cerebral blood flow changes, not metabolic processes (Lenartowicz et al 2010).

Emission Tomography is a powerful and highly sensitive nuclear functional imaging modality but requires dedicated and secured facilities due to the radioactive nature of the tracers used. PET and SPECT suffer from poor spatial and temporal resolution and must be combined with a complementary imaging modality, such as MRI or Computed Tomography (CT), for anatomical imaging (Deffieux et al. 2018).

6.2.2.2.3 fMRI

While MRI has numerous applications in structural imaging, its use was extended to functional imaging in 1990 by Seiji Ogawa and colleagues, who demonstrated that changes in the oxygenation state of blood

hemoglobin cause alterations in the MRI signal (Lenartowicz et al 2010). **Functional Magnetic Resonance Imaging (fMRI)** technique is based on the magnetic difference between deoxyhemoglobin and oxyhemoglobin: since deoxygenated hemoglobin is paramagnetic while oxygenated hemoglobin is diamagnetic, blood deoxygenation introduces a magnetic signal variation, called BOLD (blood oxygen level-dependent) signal (Deffieux et al. 2018). Thanks to the neurovascular coupling, neuronal activation has been demonstrated to be associated with local blood flow and hemoglobin oxygenation increasing (Iadecola 2004), so by measuring the BOLD signal, we can detect hemodynamic changes linked to the enhanced neuronal activity (Figure 48F) (Logothetis 2008).

Imaging cerebral hemodynamic responses with fMRI paved the way for major discoveries in neurosciences. The major advantage of fMRI is that it is non-invasive and, therefore, routinely applicable on humans. However, fMRI also suffers limitations. First, its low temporal resolution and limited sensitivity. Then, its portability, overall costs, maintenance and accessibility, constitute a major drawback, both for preclinical and clinical imaging. Furthermore, in preclinical studies for small-animal imaging, high magnetic fields are needed to reach high spatial resolutions on the order of 150/300 µm (Mace et al. 2013; Deffieux et al. 2018).

As schematized in Figure 47, imaging techniques vary in both spatial and temporal resolution, which constrains the types of questions they can answer within their imaging domain. For structural imaging, spatial resolution is the primary concern, whereas functional imaging requires high spatial and temporal resolution (since neuronal function occurs over milliseconds at a spatial scale of microns).
Among the functional imaging techniques cited so far, none possess both high spatial and temporal resolution. EEG and MEG have high temporal resolution around 0.01 s, but low spatial resolution (~10 mm). Whereas fMRI and PET provide better spatial resolution (fMRI: 1–5mm, PET: 4–8mm) but low temporal resolution (fMRI: 1–6 s, PET: 60–1000 s) (Lenartowicz et al 2010).
A validated alternative to conventional functional neuroimaging modalities is functional ultrasound imaging (fUS), which offers better spatial and temporal resolution compared to the techniques described above. It provides 50–200 µm spatial resolution and a temporal resolution in the tens of milliseconds. As shown in Figure 47, fUS can be positioned right between fMRI and optical techniques on a resolution scale. Furthermore, fUS imaging can image the full depth of the brain and provide 3D angiography (Deffieux et al. 2018). It is a good candidate for real-time in-depth imaging of brain hemodynamics, and a good alternative to fMRI, especially for preclinical studies (Mace et al. 2013).

6.3 FUNCTIONAL ULTRASOUND IMAGING FUS

6.3.1 Conventional Doppler ultrasound imaging

Conventional Doppler ultrasound imaging technique consists in evaluating blood flow dynamics within the body and it is the most commonly used technique in clinical practice to study blood circulation in the heart, arteries, limbs, kidney, and liver (Mace et al. 2013). It relies on similar principles to those of radar and sonar discovered by Paul Langevin at the beginning of the 20th century. Based on this principle, the field of conventional ultrasonography emerged in the 1970s (Mickael Tanter and Fink 2014).
Doppler ultrasound imaging consists in emitting, via a transducer (probe), pulsed focused ultrasonic waves and then detecting the amplitude of the ultrasonic echoes backscattered by tissues or fluids (Deffieux, Demené, and Tanter 2021) (E. Macé et al. 2011). It provides information about the speed, direction, and pattern of blood flow in vessels.

However traditionally, conventional ultrasound imaging has never played a major role in clinical neuroimaging and was limited to a few structural and anatomical characterizations (Bmode images) and blood flow measurements (Transcranial Doppler, TCD) (Deffieux, Demené, and Tanter 2021). Nevertheless, TCD is rarely performed because of the strong attenuation and aberration of the ultrasound beam by the skull that restricts its use to imaging only main cerebral arteries. Moreover, conventional Doppler ultrasound scans the tissue line by line, therefore it suffers from a low sensitivity that limits its use and its potential (Mace et al. 2013).

Recently, our group has developed functional ultrasound (fUS) imaging method which relies on a new sequence for power doppler imaging (E. Macé et al. 2011), called ultrafast doppler (μDoppler), that overcomes the problem of sensitivity and allows in-depth imaging of functional hemodynamic changes (Mace et al. 2013). In particular, in the neuroimaging field, fUS has become a stand-alone ultrasound technique that provides high sensitivity imaging of cerebral blood volume (CBV) changes in the whole brain without contrast agents (Deffieux et al. 2018).

6.3.2 Ultrafast ultrasound imaging

Functional ultrasound imaging (fUS) is based on a new sequence for power doppler imaging which relies on the principle of ultrafast ultrasound imaging, a concept developed from the late 1990s by Mickael Tanter and Mathias Fink (Sandrin et al. 1999; M. Tanter et al. 2002; Mickael Tanter and Fink 2014).

The advantages of this new approach are shown in Figure 51, in comparison with the conventional one.

As briefly mentioned before, conventional ultrasound imaging is based on pulsed focused waves. For each focused wave transmission, the backscattered echoes are recorded, and a beamforming procedure is performed to reconstruct a single line of the image (Figure 51A-B). The complete image is formed by scanning the imaging field line by line.

The ultrafast doppler (µDoppler) sequence is based on a different approach. It uses pulsed plane wave emissions (Figure 51D-E), instead of focused waves. The emission of one plane wave generates backscattered echoes coming from every point of the image, and not from only one line of the image. A full ultrasonic image is then reconstructed from this single emission using a parallel beamforming procedure. The advantage of this strategy is that only one emission is required to produce one ultrasonic image. However, the image quality is poor because the emission wave is not focused. To regain quality, a method called coherent compounding is applied (Montaldo et al. 2009; Bercoff et al. 2011; Mace et al. 2013). It consists of emitting multiple tilted plane waves and coherently summing the resulting set of images (Figure 51F), resulting in a 'compound' ultrasonic image that yields better resolution and lower noise than a conventional doppler image (E. Macé et al. 2011). The comparison between the two methods shows a clear improvement on the µDoppler image, as more vessels are detected and the background noise is reduced (Mace et al. 2013).

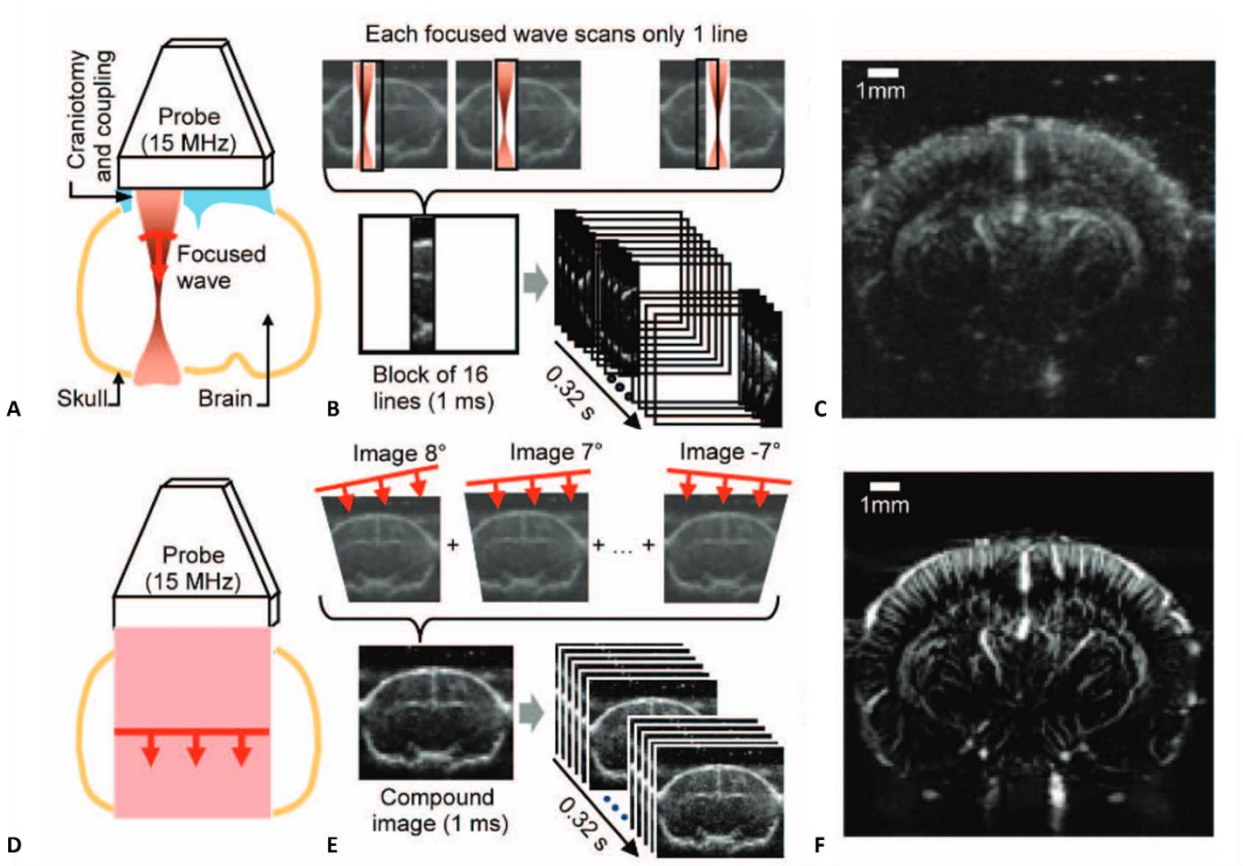

Figure 51: Time-equivalent comparison between conventional doppler and µdoppler modes. (A) schematic description of the experimental setup: The 15-MHz probe is set in the coronal plane above the rat brain exposed by a cranial window. For conventional doppler, focused ultrasonic waves are used. (B) acquisition sequence: The image is subdivided into blocks of 16 lines. one block is small enough to be scanned line by line with focused waves in less than 1 ms. Each block is imaged 40 times at 1 khz for a total acquisition time of 0.32 s. (C) signal processing: a 40-sample-long signal is obtained for each pixel. high pass filtering is applied to reject tissue echoes. The mean intensity of the blood signal is calculated from the blood signal. (D) Power doppler image obtained with conventional doppler mode. (E) schematic description for the µdoppler mode. The experimental setup is the same. For µdoppler, ultrasonic plane waves are emitted. (F) acquisition sequence: 16 plane waves are transmitted with different tilt angles in less than 1 ms to build one compounded image. One µdoppler image results of 320 such compounded images acquired in only 0.32 s. (G) signal processing with 320 time points. (H) µdoppler image (Mace et al. 2013).

The signal detected by the fUS technique is proportional to the local hematocrit (Rubin et al., 1995, Shung et al., 1976), which corresponds to the volume percentage of red blood cells in blood. Consequently, fUS signal is proportional to the local cerebral blood volume (CBV), and to its increases when a vasodilatation occurs (mathematical demonstration in (Deffieux, Demené, and Tanter 2021). By providing high sensitivity imaging of the CBV, fUS imaging can be used to map hemodynamic changes in the brain associated with

changes in brain activity. Moreover, the high temporal and spatial resolution coupled with high penetration depth make fUS an ideal method for performing functional brain imaging, especially in preclinical studies (Mickael Tanter and Fink 2014; E. Macé et al. 2011).

The first *in vivo* proof was done in 2011 by Mace and colleagues. They used fUS to detect task-evoked brain activation. More precisely, they imaged functional changes of cerebral blow volume (CBV) in the trepanned anesthetized rat brain during whisker stimulation (Figure 52) (Mickael Tanter and Fink 2014; E. Macé et al. 2011). Stimulation of groups of vibrissae resulted in an increase in blood volume in the primary somatosensory barrel cortex (S1), with increases in the power Doppler signal correlated with the stimulus pattern (Figure 52A). Activation maps showed a significant activation of S1 during whisker stimuli, as well as a significant activation in the ventral posterior medial nucleus (VPM) of the thalamus (Figure 52B) (E. Macé et al. 2011).

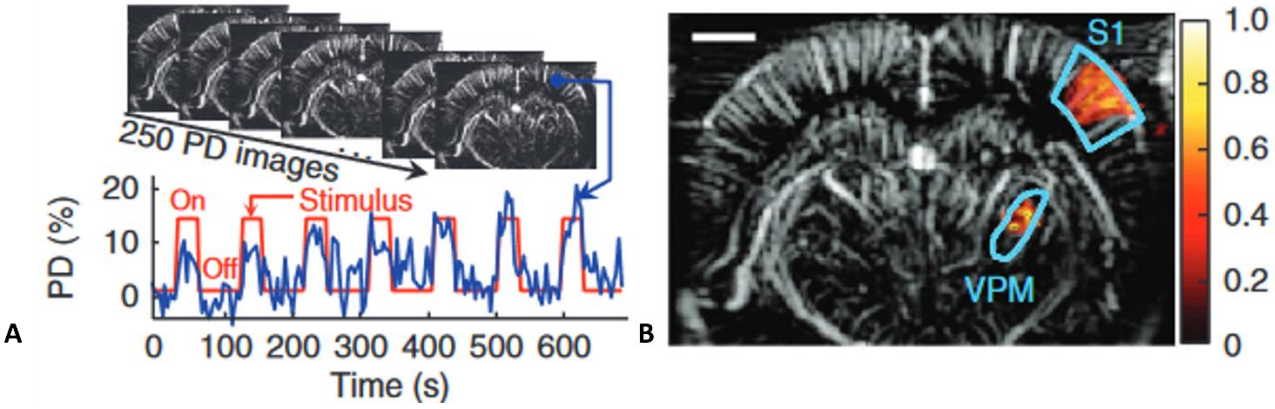

Figure 52: fUS imaging of task-evoked brain activation in the rat brain. (A) Representative example of the Power Doppler (PD) signal (blue) during whisker stimulation (red). (B) Representative example of an activation map obtained when stimulating the left whiskers. The map is calculated as the correlation coefficient between the normalized power Doppler signal and the stimulus pattern. S1, primary somatosensory barrel cortex; VPM, ventral posterior medial nucleus *(E. Macé et al. 2011)*.

This result demonstrated the capability of fUS to image CBV at high spatiotemporal resolution and to record brain activity with high sensitivity and resolution. This first proof of concept illustrates the great potential of fUS imaging and its important implication in different fields of neuroscience.

In preclinical research this modality provides a real-time, portable method for functional deep-brain imaging in small animals with high spatiotemporal resolution (~100 µm, 10 ms) (Mickael Tanter and Fink 2014). It has been applied for several studies in numerous animal models in different configuration:

anesthetized or awake. The following section will delve into the different applications in preclinical research.

In clinical practice it provides a bedside neuro-imaging system for monitoring brain activity of newborns in a non-invasive approach through the fontanel window or to adults during open skull neurosurgery (Deffieux et al. 2018; Demene et al. 2017).

6.3.3 Applications of fUS imaging to preclinical research

Aside from anatomical vascular imaging, the two most common applications of fUS imaging in basic neuroscience are functional mapping and functional connectivity studies.

6.3.3.1 Functional mapping

Functional mapping consists in mapping brain activity during a stimulus (task) compared to baseline (rest). Many sensory stimulations have been used, depending on the type of sensory modality studied: touch using whisker stimulation (Mace et al 2011), visual stimulations (Figure 53A) (Gesnik et al. 2017), olfactory (Boido et al. 2019; Osmanski et al. 2014), auditory (Figure 53C) (Bimbard et al. 2018) and somatosensory cutaneous stimulations (Figure 53B) (Réaux-Le-Goazigo et al. 2022; Claron et al. 2021). Task-evoked brain activity mapping with fUS imaging enable the investigation of different sensory pathways and identify the cerebral regions involved in the task processing with good resolution. For example, in auditory stimulation, the high resolution of fUS signal could capture the responses in specific segregated layer (Bimbard et al. 2018).

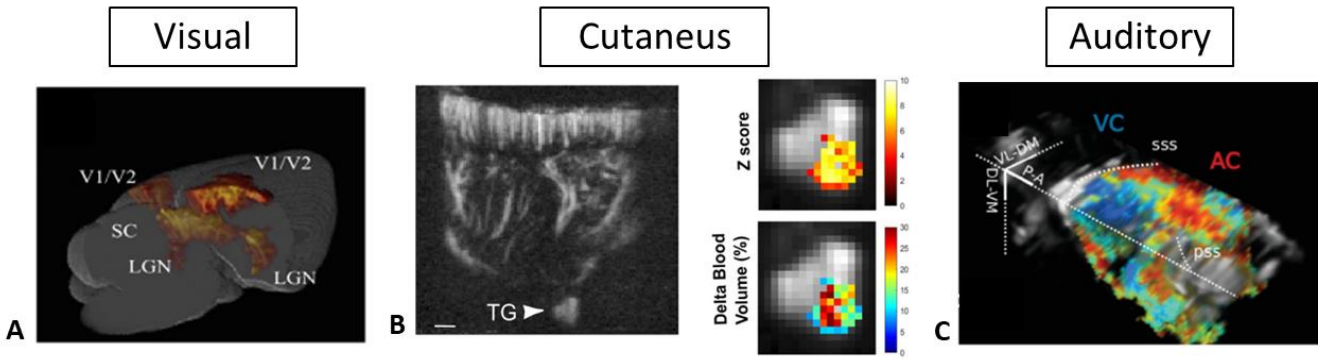

Figure 53: Functional mapping using fUS imaging. Examples of brain activation mapping consequent to three different sensory stimulations: (A) 3D reconstruction of the activated visual system of an anesthetized rat. (C) Map of the auditory cortex of awake ferrets. (adapted (Gesnik et al. 2017; Réaux-Le-Goazigo et al. 2022; Bimbard et al. 2018).

6.3.3.2 Functional connectivity

fUS is also a valuable method for studying functional connectivity by detecting the intrinsic brain activity at rest.

In 2014, Osmanski and colleagues first applied fUS imaging to study the functional connectivity in the anesthetized rat brain. They demonstrated that fUS is capable of detecting correlated patterns in the spontaneous haemodynamic fluctuations between regions that are functionally and anatomically connected (Osmanski et al. 2014). Figure 54 summarizes the results of the study. First, they analysed the Power Doppler signal fluctuations between two contralateral regions. Subsequently, they extended the analysis within more regions to obtain a correlation matrix depicting the correlation factors between the regions of interest.

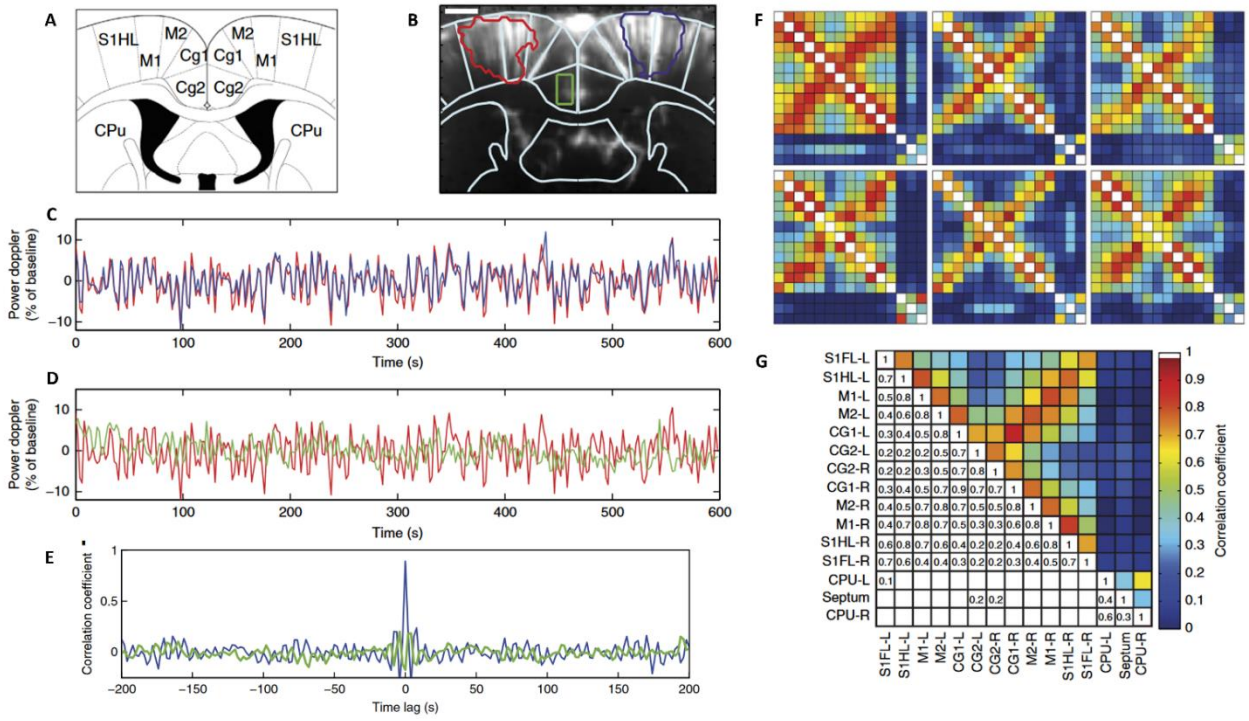

Figure 54: Functional connectivity detected with fUS imaging in anesthetized rats. (A-B) Previously determined seed regions: right (blue) and left (red) S1HL and M1. (C) Spontaneous fUS signals from the bilateral S1HL and M1 were measured at rest, without stimulation, for 10 minutes. As the power doppler signals from the red and the blue regions are in phase, they are highly correlated. (D) the fluctuations of the red and the green signal are not in phase, resulting in low correlation (E). (F) Functional correlation between other pairs of regions located within the plane of interest (Bregma-0.6mm) and the obtained individual correlation matrix. (G) Averaged correlation matrix (Osmanski et al. 2014).

While this seminal work was conducted on anesthetized rats, fUS imaging has been subsequently developed for the study of FC in mice.

In 2020, Ferrier and colleagues demonstrated the feasibility of using fUS for resting-state functional imaging in mice (Figure 55) (Ferrier et al. 2020).

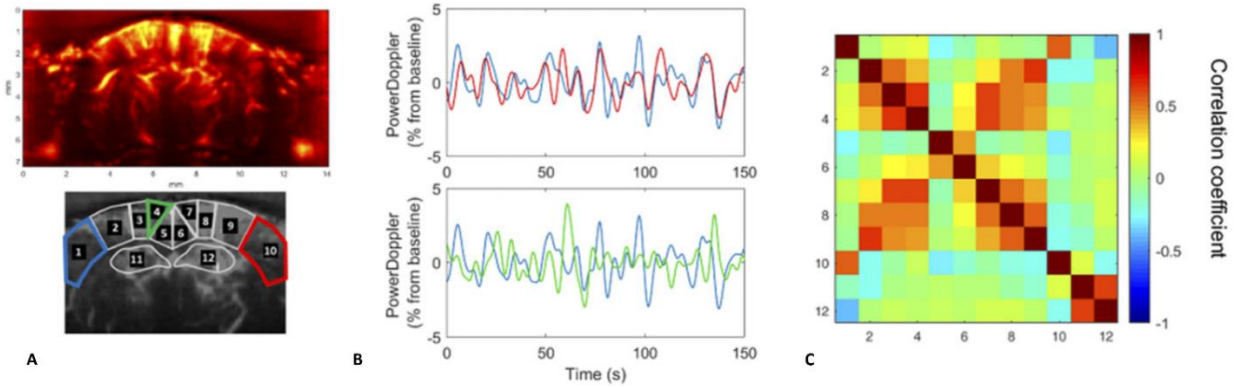

Figure 55: Functional connectivity detected with fUS imaging in awake mice. (A) Representative power Doppler image obtained with the selected ROIs. (B) Power doppler signal of two strongly functionally connected regions and above the signal of two less correlated regions. (C) Resting-state correlation matrix, from a representative awake mouse (adapted from (Ferrier et al. 2020).

This study identified specific RSNs, such as the DMN, comparable to other studies demonstrated using fMRI. It has been demonstrated that the DMN represent a brain state of disconnection, comparable to a task-evoked deactivation (Greicius et al. 2003; Raichle 2015). Therefore, to identify the DMN in this study, the authors investigated the FC during sensory stimulation (whisker stimulation) compared to rest in awake behaving mice. Figure 56 shows the FC matrices obtained during rest and stimulation. The comparison shows drastic suppression of the interhemispheric S1BF connectivity during whisker stimulation, as compared to rest, due to unilateral activation of the left S1BF. Moreover, FC was also weakened between the right and left retrosplenial cortex (RSG) known to be a central hub of the DMN, during stimulation compared to rest, indicating a clear disruption of this midline DMN node (Ferrier et al. 2020).

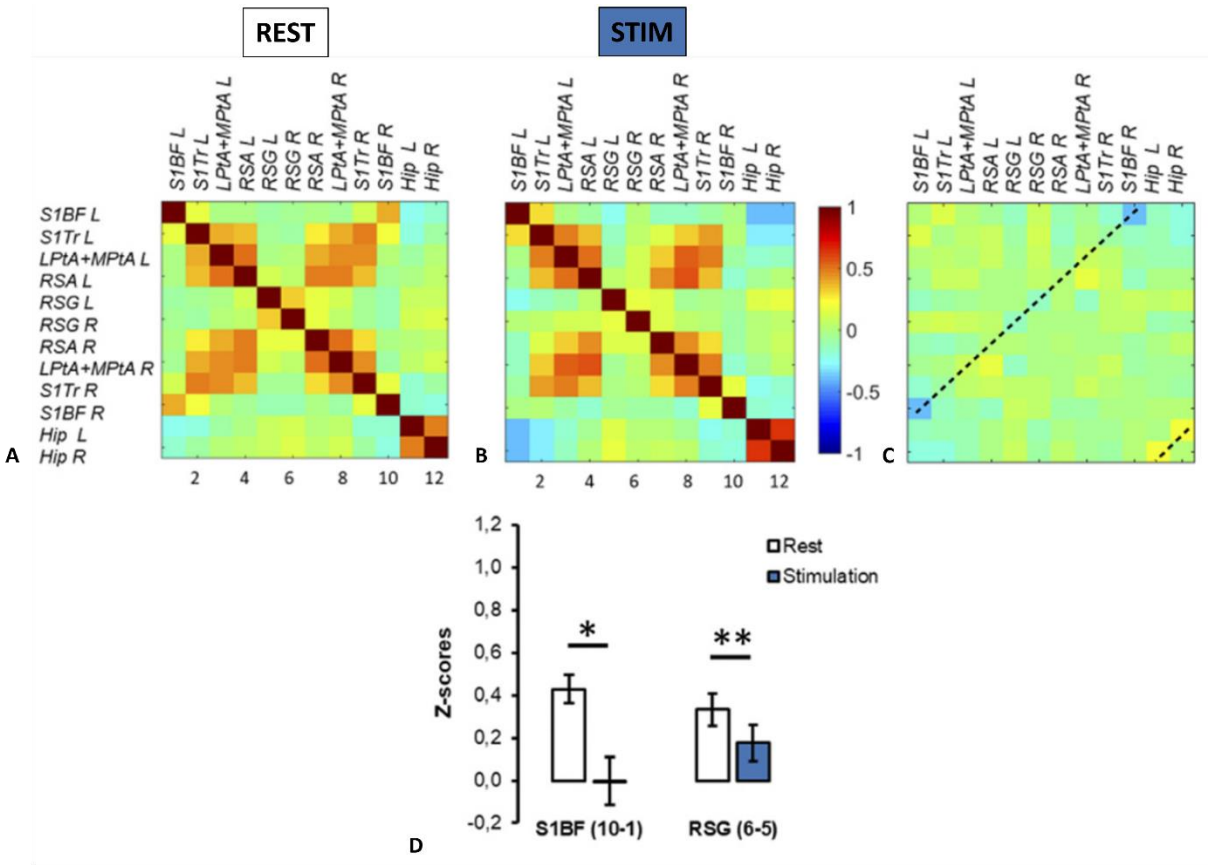

Figure 56: Change in FC in lightly sedated mice at rest and during whisker stimulation. (A) Mean correlation matrices during baseline (REST) and whisker stimulation (STIM). (B) Fisher-transformed z-scores of interhemispheric correlations for each pair of symmetrical ROIs during baseline and whisker stimulation (Ferrier et al. 2020).

These studies, and many others, demonstrated that fUS is a valuable method for studying functional connectivity and it can be used as a valid alternative to fMRI in preclinical research.

Along with these findings, functional ultrasound has been used in several FC studies, for example to investigate brain connectome alterations associated with disease or neurological disorders. For instance, it was shown that, in rat pups, a fetal growth restriction model presented a general decrease of connectivity compared to controls and that early injection of oxytocin could mitigate this effect (Mairesse et al., 2019).

Furthermore, functional connectivity mapping using fUS is a particularly well-suited readout for pharmacological studies and drug discovery (Vidal, Droguerre, Valdebenito, et al. 2020; Vidal, Droguerre, Venet, et al. 2020; Deffieux, Demené, and Tanter 2021; Rabut et al. 2020).

6.3.3.2.1 Functional connectivity studies with fUS in the pain field

One of the numerous applications of fUS FC studies is the study of pain syndromes in rodents' models. Especially, in 2020, Rahal and colleagues in our group conducted an exhaustive study of FC alterations in a rat model of persistent pain using fUS imaging.

This study aimed to investigate the alterations in the brain connectome in a rat model of arthritis. They conducted the experiment in anesthetized rats, and they completed all three modalities of FC analysis, seed-based, static FC and dynamic FC analysis.

With the seed-based analysis approach, a profound reduction in the FC in a part of cortico-cortical networks in arthritic animals was identify (Figure 57) (Rahal et al. 2020).

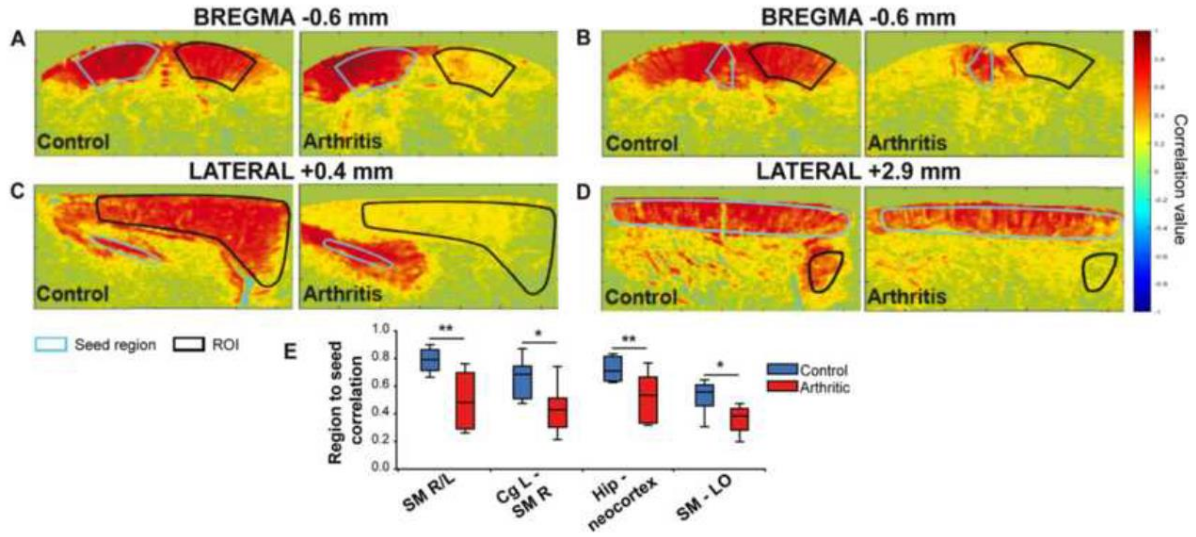

Figure 57: Seed-based analysis of the FC alterations in arthritic animals. (A–E) are typical examples of the correlation between a seed region (ROI delineated in cyan) and the pixels in the imaged plane. The Pearson correlation was then computed in the ROI (delineated in black) (Rahal et al. 2020).

Static FC confirmed the seed-based results, such as an alteration of the FC in some subparts of the somatomotor network (Figure 58A) (Rahal et al. 2020). These results show a reduced connectivity between structures of the DMN, and the strongest changes were observed in a subsection of the somatomotor network, such as the region dedicated to the inflamed paw. This specific and localized plasticity could be due to the increased electrophysiological activity previously described in this model/pathology (Gram et al. 2017; Spisák et al. 2017).

Dynamic FC analysis represents a different approach compared to the previous two. As describe in Figure 58B, one brain state (# 1, which is the most occurrent and is a dynamic pattern of FC, where the signals of the whole SM network and the DMN hub cingulate cortex oscillate in synchrony) was significantly less frequently observed in arthritic animals, whereas on the other hand, two other states (# 2, 3, that are two dynamic patterns, where the primary motor and primary sensory cortex of each side anti-correlate with the rest of the SM network) occurred more frequently in these animals. The lower occurrence of the brain state #1 in arthritic rats shows that the synchronism between the somatosensory, motor and cingulate cortices is highly affected by the pathology. Moreover, this breach of synchronism observed in states 2 and 3 might be an indirect measure of the spontaneous firing of nociceptors, a feature known to induce spontaneous pain. The results indicate a strong and significant alterations of the dynamic of some subnetworks in arthritic animals. Furthermore, this study demonstrated the capability to measure alterations of Dynamic FC resulting from brain function remodelling due to chronic pain using fUS imaging (Rahal et al. 2020).

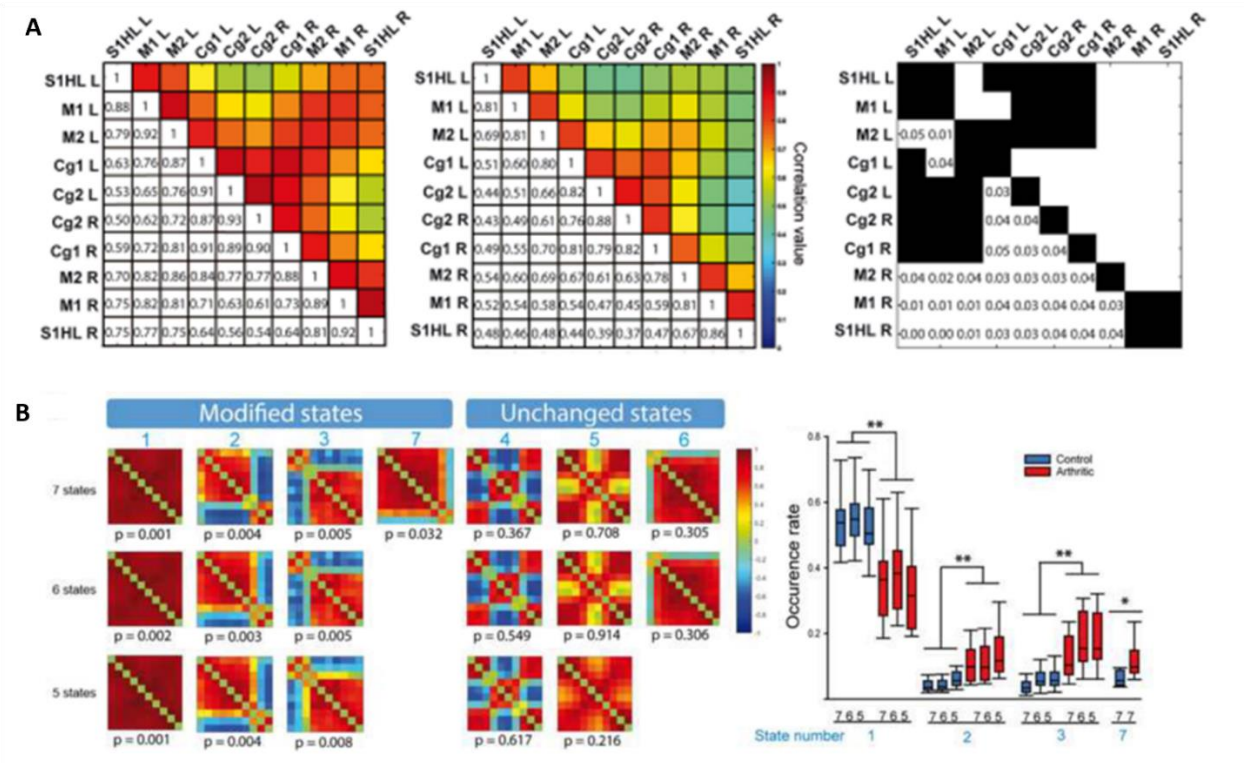

Figure 58: Static and dynamic FC changes in arthritic rats. (A) static FC analysis. Averaged Pearson correlation matrix in the control and arthritic groups. (right) Matrix of significance of the differences between control and arthritic matrices. White squares represent the pairs of ROIs with a significant

alteration in FC between the two groups. (B) Dynamic FC analysis. Decomposition into brain states 5, 6 and 7 obtained by unsupervised k-means clustering of the phase matrices. The decomposition produces robust results, with the matrices obtained for k = 5, 6 or 7 states being very consistent. The p-values written under each matrix show that for four states (states 1, 2, 3 and 7), the occurrence over time is significantly altered between controls and arthritics. (Right) Box plots presenting the occurrence rate of each of the four different states. The first modified state appears significantly more often over time in the control group than in the arthritic group. The other three states appear less frequently over time in the control group than in the arthritic group. While arthritic animals spend less time in the state 1, they spend significantly more time in the states 2 and 3. (Adapted from (Rahal et al. 2020).

Finally, in this study the FC analysis has been correlated with the pain behavior in individual animals, by using individual correlations between FC alterations and several aspects of clinical/pain behavior in arthritic and control animals (mechanical sensitivity, inflammation score or differences in weight gain). The correlation between somatomotor network alterations and weight gain and mechanical hypersensitivity indicate that the somatomotor network is involved in the discriminative aspect of persistent pain. Moreover, the positive correlation in FC alterations between the LO (lateral orbital) cortex and the somatomotor cortex and body weight gain, suggests a link with the emotional and cognitive aspect of pain. Another brain area, whose FC is significantly altered (Hippocampo-Cortical connectivity) and whose changes are linked to changes of behavior, is the hippocampus. The reorganization of the processing within the hippocampus and the cortex, suggest, as previously described in patients with chronic back pain (Mutso et al. 2014), a contributor to the transition from acute to chronic pain and possibly to comorbidities. Overall, these results suggest a correlation between FC alterations and either cognitive or emotional aspect of pain.

This work introduces fUS imaging as a new translational tool for the enhanced understanding of the dynamic pain connectome and brain plasticity in a preclinical model of chronic pain. Moreover, combination with individual behavioral scores showed a clear link between these impairments and some aspects of animal's clinical and/or pain state (Rahal et al. 2020).

6.3.4 Experimental configurations for fUS experiments

Functional ultrasound imaging has been used in numerous animal models such as mice (É. Macé et al. 2018), rats (Gesnik et al. 2017), ferrets (Bimbard et al. 2018), pigeons (Rau et al., 2018) and non-human primates (Dizeux et al. 2019). For each animal model, a specific experimental setup was developed, taking into account the different characteristics of the species. For example, the skull, which protects the brain,

represents a limitation for ultrasound imaging. The skull absorbs and attenuates ultrasound waves, and this effect is associated with the thickness of the bone. To address this issue, several surgical techniques have been developed in the laboratory (Figure 59). These include complete removal of the skull through craniotomy (Figure 59A), thinning the skull (Figure 59B), or replacing the skull with a material transparent to ultrasound waves (Figure 59C). The first two strategies are used for acute experiments, while the third is used for chronic procedures. These surgical procedures have been developed especially for adult rats and larger animals. In mice and young rats, the thinness of the skull minimally affects ultrasound waves, allowing for transcranial experiments (Figure 59D). In non-human primates the thickness of the skull imposes heavier surgical procedures, and fUS has been performed in awake animals by placing the ultrasonic probe within the electrophysiology chamber (Deffieux, Demené, and Tanter 2021; Dizeux et al. 2019; Blaize et al. 2020).

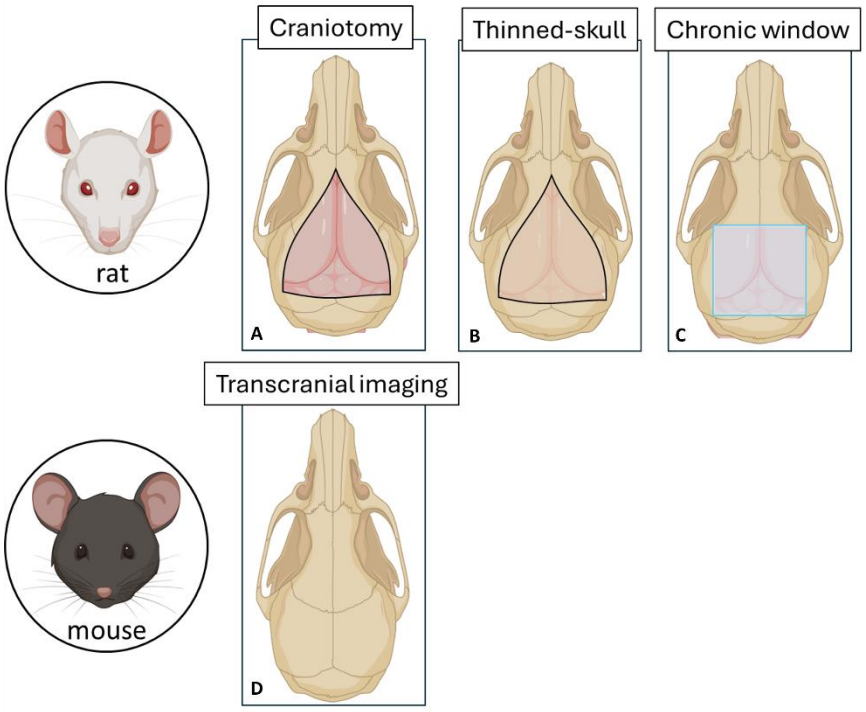

Figure 59: Different surgical approaches in rodents.

fUS experiments can be conducted under various experimental configurations: anesthetized or awake; freely-moving or head-fixed animals.

Due to its experimental ease of use, experiments performed in anesthetized animals are the most common. However, as previously discussed in paragraph 5.3.5.1, in order to study brain activity in behaving animals without the bias of anesthesia, performing awake experiment become important. The

possibility to perform whole brain fUS imaging in behaving rodents has been demonstrated in different conditions: during seizures (Sieu et al. 2015), locomotion or operant tasks (Sieu et al. 2015; Urban et al. 2015) and even during sleep (Bergel et al. 2018).

Two possible configurations for awake fUS imaging have been investigated:

- Freely-moving, which is possible thanks to the miniaturization of ultrasonic probes that can be tethered to the animal's head using a surgically implanted metal frame (Sieu et al. 2015; Urban et al. 2015; Bergel et al. 2018; Rabut et al. 2020).
- Head-fixed, a metal frame surgically implanted on the animal head enables the head-fixation. This configuration is suitable for mice, ferret and primate (É. Macé et al. 2018; Bimbard et al. 2018; Ferrier et al. 2020; Dizeux et al. 2019; Blaize et al. 2020; Brunner et al. 2020) and it enables the use of motorized stage or matrix array for whole brain imaging.

The three most common fUS imaging experimental designs are shown in the figure below (Figure 60), usually for mice and rats it is possible to perform anesthetized, awake head-fixed or freely moving experiments.

Depending on the experimental configuration, there are some limitations concerning the field of view. As depicted in the figure below, freely-moving is restricted to 2D imaging modality. In contrast, in anesthetized and awake head-fixed conditions, access to the entire brain is possible. Figure 60C shows two different modalities to acquire whole-brain imaging, both were used in this project and will be described in the following chapters of the manuscript. These two modalities represent the results of the technological development done by the laboratory in the past fifteen years. Initially ,the acquisitions were limited to a single plane. Later on, new strategies to perform 3D imaging have been developed (Demené et al. 2016; Gesnik et al. 2017; Bimbard et al. 2018; É. Macé et al. 2018; Rau et al., 2018). This was achieved by mechanically translating the 1D transducer. This approach was further optimized using fast scans approach to allow multislice acquisitions (Deffieux, Demené, and Tanter 2021).

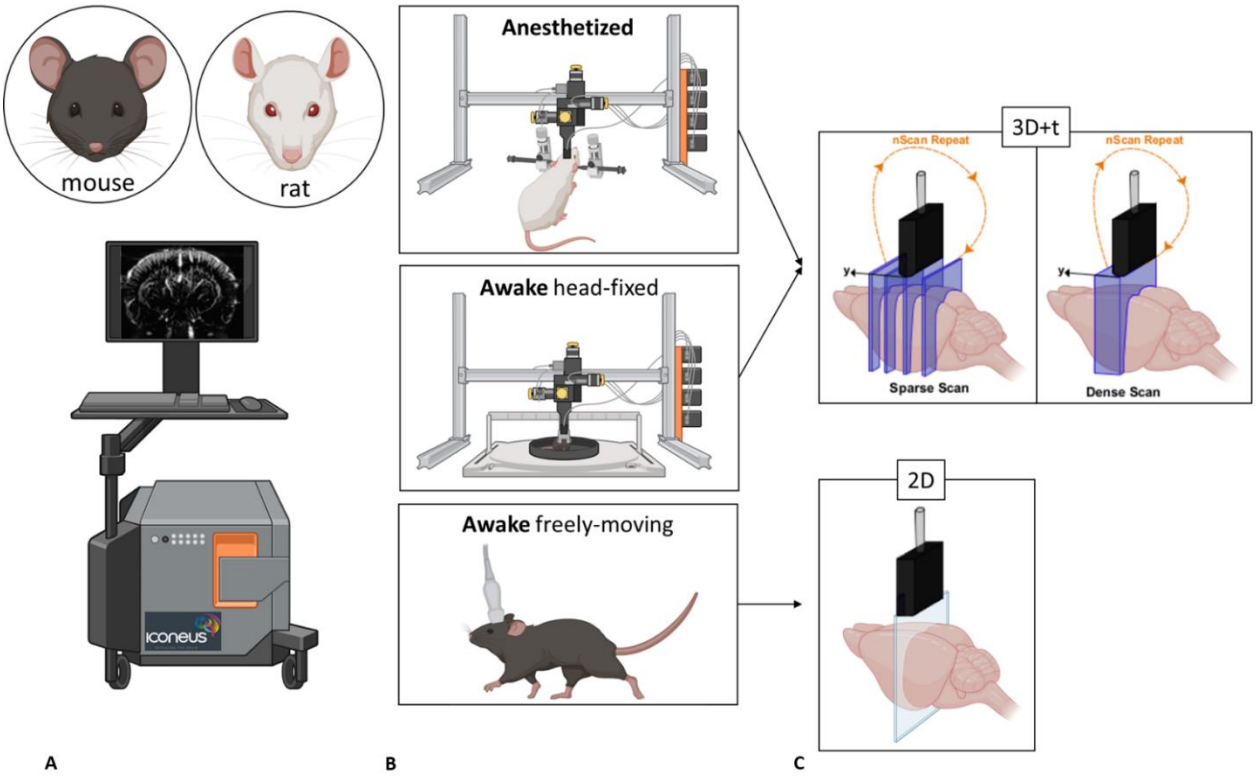

Figure 60: fUS experimental configuration in rodents. (A) Schematic representation of the neuroimaging scanner. (B) Anesthetized, awake head-fixed and freely-moving configuration. (C) imaging modalities.

In conclusion, functional ultrasound imaging enables whole-brain brain activity imaging with high spatio-temporal resolution and high sensitivity. This technique has been used in numerous animal models, from mice to primate, under diverse experimental setups, and it can easily be combined with other neuroscience techniques such as EEG (Sieu et al. 2015; Bergel et al. 2018) or optogenetics (Brunner et al. 2020; Rungta et al. 2017). Moreover, fUS can easily be adapted for awake head-fixed or freely-moving animals and is suitable for pharmacological studies using functional connectivity as a readout (Deffieux, Demené, and Tanter 2021; Rabut et al. 2020).

The various possible configurations suitable for fUS imaging expand the range of investigative possibilities, positioning this technique uniquely between fMRI and optical techniques for studying the brain.

7 OBJECTIVE OF THE THESIS PROJECT

Neuropathic pain is correlated with brain reorganization and consequently FC patterns disruption. Several studies have shown that patients suffering from chronic pain present morphological and functional reorganization in cortical and subcortical areas compared to healthy controls (Bliss et al. 2016; Huang et al. 2019). Preclinical longitudinal studies have demonstrated that those changes are time-dependent and might reflect the development of neuropathic pain symptoms overtime and the apparitions of comorbidities (Yalcin et al. 2011).

The main objective of this thesis was to decipher the temporal link between alterations in cerebral Functional Connectivity and the development of neuropathic pain and/or associated comorbidities in a mouse model of neuropathic pain using functional ultrasound imaging (fUS).

To do so, many technical developments were necessary: experimental protocols to image in awake head fixed animal, with minimal stress, the development of a strategy to image resting-state functional connectivity using fast multislice scanning. This work is presented in **the second chapter of this manuscript**. The experimental protocol developed allows reproducible and standardized fUS imaging in either awake or anesthetized mice. In this work, we developed the experimental protocol for animal handling and imaging.

Then, I used this experimental methodology to test our neurobiological hypothesis. To do this, we measured the resting-state functional connectivity (FC) in awake head-fixed mice, at two time points: I) 2 weeks after induction of neuropathic pain (cuff around the sciatic nerve), II) at 8 weeks post-induction during the emergence of anxiety. This study is presented in **the third chapter**.

During my PhD, the technology of ultrasound probes evolved, offering new opportunities to capture intrinsic connectivity across the entire mouse cerebrum. **In the fourth chapter**, I am presenting the technological development we performed in collaboration with our colleagues at Physics for medicine, to map the brain-wide functional network in 3D, using a multi-array probe.

Finally, I used this newly developed method of imaging in my PhD project to overcome some limitations encountered in chapter 3. Indeed, the novel 3D multi-slice imaging modality, described in chapter 4, was applied for the study of FC alterations in a longitudinal follow-up (T0, 2W, 8W, 12W) of neuropathic pain in a mouse model, in anesthetized conditions. **This study is presented in the fifth chapter**. This approach gave us the opportunity to investigate the alterations of brain changes until a later time point, compared

to the study conducted in chapter 3, 12 weeks post induction of neuropathic pain and to image the brain networks involving the insula, a key structure in pain processing. This was unfortunately not possible in chapter 3.

CHAPTER 2

ARTICLE N°1:

Whole-Brain 3D Activation and Functional Connectivity Mapping in Mice using Transcranial Functional Ultrasound Imaging

INTRODUCTION OF THE ARTICLE N°1

Functional ultrasound (fUS) imaging, as detailed in chapter 1 section 4 is a recently developed neuroimaging technique based on ultrafast doppler that provide high sensitivity imaging of cerebral blood volume changes (Deffieux et al. 2018). As brain perfusion is strongly linked to local neuronal activity, this technique allows the brain mapping by task-induced regional activation as well as by resting-state functional connectivity.

While human fMRI has high reliability and sensibility, fMRI brain mapping in mice, the most used preclinical model in Neuroscience, remains technically challenging due to the small size of the brain and the limited feasibility of imaging in awake conditions. A main advantage of fUS imaging is the full compatibility with imaging the small size of rodents' brains, and additionally, with imaging in awake and behaving conditions.

The first project that I undertook in my PhD, and that lead to the publication attached below (Bertolo and al., 2021, JOVE) aimed at developing and validating several key aspects of fUS imaging in either awake or anesthetized mice. In this work, I developed the experimental protocol for animal handling and imaging. This was necessary for the reproducibility and standardization of the results. I was also actively involved in the development of methods for data collection and signal processing using a commercial fUS system with a motorized linear transducer.

One of the main current limitations of fUS imaging is its 2D feature. In this work, we evaluated a fast plane-switching scanning approach, which involves mechanically translating the 1D transducer using a motorized approach and employing a fast-scanning method to enable multi-slice acquisitions, resulting in a reconstruction of a 3D fUS volume.

This work describes a reproducible protocol for 3D quantification of cerebral hemodynamic variations transcranially in the mouse brain, at rest or in response to sensory stimulation. Whisker stimulation, a standard paradigm to map brain functional activation in rodents, has been selected as an example of sensory stimulation-evoked response. In both configurations, whether anesthetized or awake, we observed a consistent brain activation response that correlated with the sensory stimulus presented. Furthermore, in resting-state conditions we observed, with a static FC analysis, strong interhemispheric connectivity pattern, which is in accordance with findings in the literature (Sforazzini et al. 2014). With seed-based analysis in the dorsal hippocampus we identified a significant interhemispheric connectivity

between right and left hippocampus as well as deep retro-hippocampal regions and piriform cortices. A seed region selected in the S1BF also resulted in a symmetrical (cortico-cortical) correlation pattern, as previously described (Shuler, Krupa, and Nicolelis 2001).

The reproducibility and consistency of the results shown demonstrate the high compatibility of functional ultrasound with the proposed configurations, in anesthetized and awake behaving animals. Moreover, it validates the surgical and the habituation protocols for the awake head-restrained apparatus.

jove

Whole-Brain 3D Activation and Functional Connectivity Mapping in Mice using Transcranial Functional Ultrasound Imaging

Adrien Bertolo[*,1], **Mohamed Nouhoum**[*,1], **Silvia Cazzanelli**[*,1], **Jeremy Ferrier**[*,3], **Jean-Charles Mariani**[2], **Andrea Kliewer**[4,2], **Benoit Belliard**[1], **Bruno-Félix Osmanski**[3], **Thomas Deffieux**[*,1], **Sophie Pezet**[*,1], **Zsolt Lenkei**[*,2], **Mickael Tanter**[*,1]

[1] Physics for Medicine Paris, ESPCI Paris, INSERM, CNRS, PSL Research University [2] Institute of Psychiatry and Neurosciences of Paris, INSERM U1266, Université de Paris [3] Iconeus [4] Department of Pharmacology and Toxicology, Jena University Hospital - Friedrich Schiller University Jena

[*] These authors contributed equally

Corresponding Author

Jeremy Ferrier

jeremy.ferrier@iconeus.com

Citation

Bertolo, A., Nouhoum, M., Cazzanelli, S., Ferrier, J., Mariani, J.C., Kliewer, A., Belliard, B., Osmanski, B.F., Deffieux, T., Pezet, S., Lenkei, Z., Tanter, M. Whole-Brain 3D Activation and Functional Connectivity Mapping in Mice using Transcranial Functional Ultrasound Imaging. *J. Vis. Exp.* (168), e62267, doi:10.3791/62267 (2021).

Date Published

February 24, 2021

DOI

10.3791/62267

URL

jove.com/video/62267

Abstract

Functional ultrasound (fUS) imaging is a novel brain imaging modality that relies on the high-sensitivity measure of the cerebral blood volume achieved by ultrafast doppler angiography. As brain perfusion is strongly linked to local neuronal activity, this technique allows the whole-brain 3D mapping of task-induced regional activation as well as resting-state functional connectivity, non-invasively, with unmatched spatio-temporal resolution and operational simplicity. In comparison with fMRI (functional magnetic resonance imaging), a main advantage of fUS imaging consists in enabling a complete compatibility with awake and behaving animal experiments. Moreover, fMRI brain mapping in mice, the most used preclinical model in Neuroscience, remains technically challenging due to the small size of the brain and the difficulty to maintain stable physiological conditions. Here we present a simple, reliable and robust protocol for whole-brain fUS imaging in anesthetized and awake mice using an off-the-shelf commercial fUS system with a motorized linear transducer, yielding significant cortical activation following sensory stimulation as well as reproducible 3D functional connectivity pattern for network identification.

Introduction

Over the last two decades, neuroimaging has become an important tool for studying brain function and organization, enabling researchers to make important discoveries in the field of neuroscience. Today, functional magnetic resonance imaging (fMRI) has become the gold standard clinical neuroimaging technique to assess task or drug-evoked brain activation and to map functional connectivity at rest. While human fMRI has high reliability and sensibility, mouse fMRI remains technically challenging for numerous reasons[1]. First, fMRI has a poor spatial and temporal resolution.

The small size of the mouse brain necessitates the use of strong magnetic fields using expensive scanners to achieve reasonable spatial resolution. Second, maintaining stable physiological parameters within the narrow range allowing efficient neuro-vascular coupling is very difficult in anesthetized mice. Finally, the blood oxygen level dependent (BOLD) signal on which fMRI studies rely has relatively poor sensitivity, leading to low signal-to-noise ratio when applied to mice and often requires repeated stimulus presentation over long acquisition to detect small variations. The mouse being the most widely used animal model in biomedical preclinical research, these limitations are partly responsible for the translational gap in neuropsychiatry, hindering new promising therapeutic targets on the bench to be transposed into effective treatments on bedside.

Functional ultrasound (fUS) is a recently developed neuroimaging technique based on ultrafast doppler[2]. By directly sampling cerebral blood volume, this technique allows probing brain activity in real-time through the neurovascular coupling. Compared to other neuroimaging techniques, fUS yields a spatial resolution of 100 µm and a temporal resolution in the tens of milliseconds. This technique allows whole-brain imaging of complete coronal sections of the mouse brain, completely non-invasively. Furthermore, it is fully compatible with conscious and behaving animals[3,4,5]. One of the main current limitations of fUS is its 2D feature, allowing to record a single coronal plane at the same time. While volumetric 3D fUS using 2D matrix array transducers has already been successfully demonstrated in rats[6] and confirmed in mice[7], its current lack of sensitivity requires a full craniotomy as well as averaging an important number of trials to detect a slight change of activity. Alternatively, linear transducers can be stepped across multiple positions and perform functional imaging plane by plane to cover the whole brain. However, this technique requires numerous experimental paradigm repetitions and as such long acquisition times (3-4 hours for the mouse brain)[8,9].

In the present work, we describe a robust experimental platform including a commercially available functional ultrasound scanner and a fast plane-switching linear transducer with procedures to acquire 3D fUS data in anesthetized and awake mice, allowing volumetric and transcranial functional mapping of the mouse brain, non-invasively, without contrast-agent and within short acquisition times. We illustrate this feature by mapping somatosensory cortex activation following whisker stimulation as well as resting-state functional connectivity. Aside from animal preparation and data collection, we also describe the procedure for visualization, atlas registration and analysis of real-time fUS signals.

Protocol

All the procedures presented here have been performed in agreement with the European Community Council Directive of 22 September 2010 (010/63/UE) and our local ethics committee (Comité d'éthique en matière d'expérimentation animale number 59, 'Paris Centre et Sud', project #2017-23). Adult mice (male C57BL/6 Rj, age 2-3 months, 20-30 g, from Janvier Labs, France) were housed 4 per cage with a 12h light/dark cycle, constant temperature at 22 °C and food and water ad libitum. Before the beginning of the experiments, animals are given a one-week minimum acclimatization period to housing conditions.

1. Animal preparation for anesthetized fUS imaging

1. Anesthesia

1. Weigh the mouse.
2. Prepare a mixture of ketamine and xylazine at 10 mg/mL and 2 mg/mL, respectively, in sterile saline. Administer 0.2 mL of the ketamine/xylazine solution intraperitoneally using a 26 gauge needle and 1 mL disposable syringe. After a few minutes, position the animal onto the stereotaxic frame, making sure that the head is flat.
3. Administer a second volume of anesthetics to reach a total dose of 100 mg/kg ketamine and 20 mg/kg xylazine (taking the initial dose into account).
   NOTE: Anesthesia should last for 1 h. To maintain a steady sedation for a longer time, inject 0.05 mL of the ketamine/xylazine mixture every 30 min intraperitoneally.

2. **Animal preparation for anesthetized imaging session**

1. Apply some eye ointment (e.g., Ocry-Gel) to the mouse eyes to avoid any cataract formation during the imaging session. Shave the mouse head using a trimmer. Apply some depilatory cream and rinse after a couple of minutes. Repeat until the hair is completely removed.
2. Insert subcutaneous pins in the limbs for electrocardiogram (ECG) recording. Place centrifuged ultrasound gel (1500 rpm, 5 min) on the head.
3. Monitor the depth of anesthesia during the complete duration of the experiments (anesthesia induction included). Maintain the temperature of the animals at 37 °C by using a heating blanket coupled to a rectal probe.
4. Monitor the following physiological parameters which are indirect indicators of the depth of anesthesia: Heart rate (220-250 beats per minute - monitored through the electrocardiogram thin electrodes implanted subcutaneously), and Respiratory rate (130-140 breaths per minute - monitored using a spirometer connected to the ECG acquisition system).
   NOTE: A description of the experimental setup is depicted in **Figure 1**.

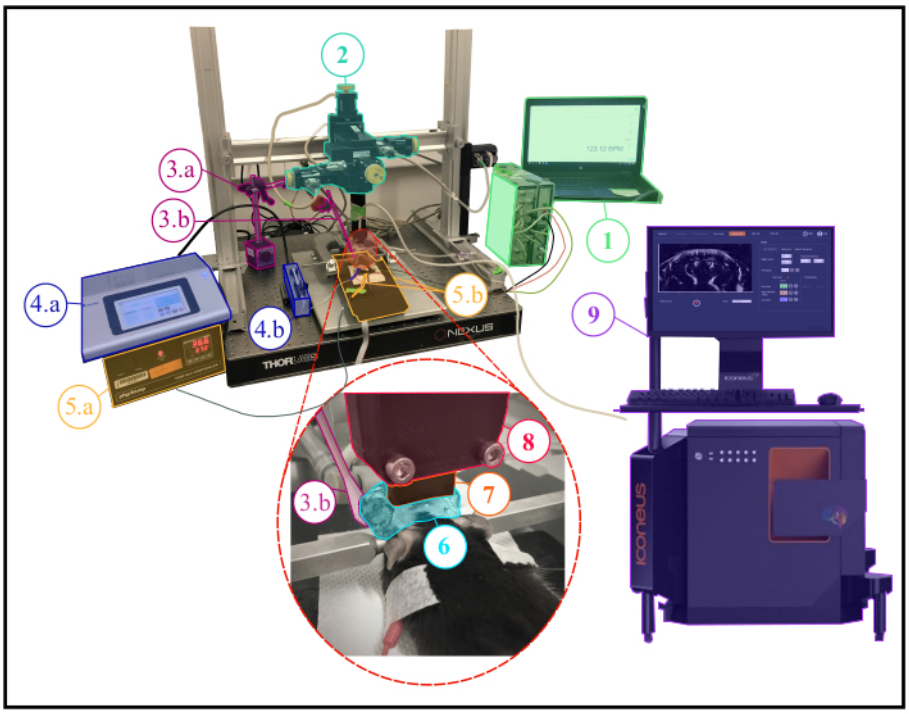

Figure 1: Experimental setup for anesthetized fUS experiments. Description of the experimental setup showing all the scientific equipment needed during an anesthetized experiment. **1.** Physiological monitoring : live display of both respiratory and cardiac frequencies. **2.** Four-axis motor module (three translations and one rotation) monitored by Iconeus One system (**9**) and allowing to perform transcranial 3D tomographic scans or 4D acquisitions. **3a.** Servo-Motor driving the whisker stimulator (**3b.**) The servo-motor is controlled by an arduino uno card which is interfaced with the Iconeus One system (**9**) in order to synchronize stimulation patterns with imaging sequences. **4.a.** Syringe pump controller. **4.b.** Syringe holder. **5.a.** Temperature plate monitor controlling the heating plate. **5.b.** Heating plate and rectal thermometer interfaced with the temperature plate monitor (**5.a.**). **6.** Ultrasound gel placed between the animal's head and the ultrasound probe, providing acoustic coupling between them. **7.** 15 MHz ultrasound probe. **8.** Probe holder linking the probe (**7**) to the motor module (**2**). **9.** Iconeus One equipment and software, allowing programing different imaging sequences and controlling the motors module (**2**) driving the probe (**7**). Please click here to view a larger version of this figure.

2. Animal preparation for awake head-fixed mice experiments

1. Headplate surgery

1. Place the anesthetized animal (steps 1.1-1.2) in the stereotaxic frame on a heating pad (37 °C). Apply protective gel for the eyes and administer lidocaine s.c. (0.2 mL, 2 %) under the scalp skin using a 26-gauge needle and wait a few minutes.

NOTE: Monitor the anesthesia level every 10-30 min by response (absence of) to a firm toe pinch.

2. Perform an incision following the sagittal suture from behind the occipital bone to the beginning of the nasal bone. Using surgical scissors, excise the skin over both hemispheres.

3. Clean the skull with 1% iodine solution and remove any remaining periosteum. Using the headplate as a template, drill two holes (1 mm diameter) in the skull to position the anchoring screws.
   CAUTION: Be careful not to drill completely through the skull to avoid any brain damages or dura inflammation

4. Position the headplate with the screws. Use dental cement to fix the screws and the headplate in front and in the back of the frame to maintain good grip of the implant.
   CAUTION: Be careful to not apply cement inside the frame window as it greatly diminishes signal quality. Cover the skull with a thin layer of surgical glue to protect the bone and seal the wounds on the side of the imaging window.

5. Remove the animal from the stereotaxic frame after the cement is dry and reverse the anesthesia by a subcutaneous injection of atipamezole at 1 mg/kg. A prophylactic administration of meloxicam (5 mg/kg/day, s.c.) is administered for post-operative pain.

6. Place the animal in a recovery cage on a heating pad (37 °C). The mouse can return its home cage with littermates within a few hours. Place a magnetic 3D-printed cap (polyactic acid material with magnet inserts) over the headplate for protection (**Figure 2A**). Leave the mouse to recover for 4 to 6 days before the beginning of the habituation to the mobile home cage (MHC).
   NOTE: The total weight of the cap and the headplate is 2.8 g.

2. Handling and habituation

   1. On day 1 post-recovery (PR), gently hold the mouse in hand for 5-10 min several times a day.

   2. On day 2 PR, repeat handling as in day 1 and leave the animal for 5-10 min exploring freely MHC.
      NOTE: Playing some background music in the room can help reduce animal's stress.

   3. On day 3 PR, let the animal freely explore the MHC for 5-10 min. Afterwards, carefully grab the headplate and gently place it in the clamp, moving manually the carbon cage to accompany the mouse. Habituate the animal in the head-fixed position for 5-10 min. Clean the MHC in between training sessions with 70% ethanol solution and rinse with tap water.
      NOTE: Make sure that the MHC receives a sufficient air flow as recommended by the manufacturer. The height of the head clamp needs to be manually adjusted to provide a comfortable position.

   4. On day 4 and 5 PR, repeatedly clamp the mouse MHC and gradually increase the head-fixed time, starting from 5 min and up to 30 min. Apply some saline and ultrasound gel on the imaging window to habituate.

   5. On day 6 PR, repeat the protocol from day 4/5 PR and position the probe above the animal's head following step 3.1.

   6. On the day of the experiment, proceed as described above. Then, humidify the imaging window with

saline and apply some ultrasound gel. Start the tracking of the animal and proceed to the probe positioning (see below).

NOTE: Clamping in the MHC may also be done by wrapping the mouse in a rag. In that case, mice need to be habituated to the wrapping procedure before head-fixation. A description of a complete experimental setup for awake imaging is provided in **Figure 2B**.

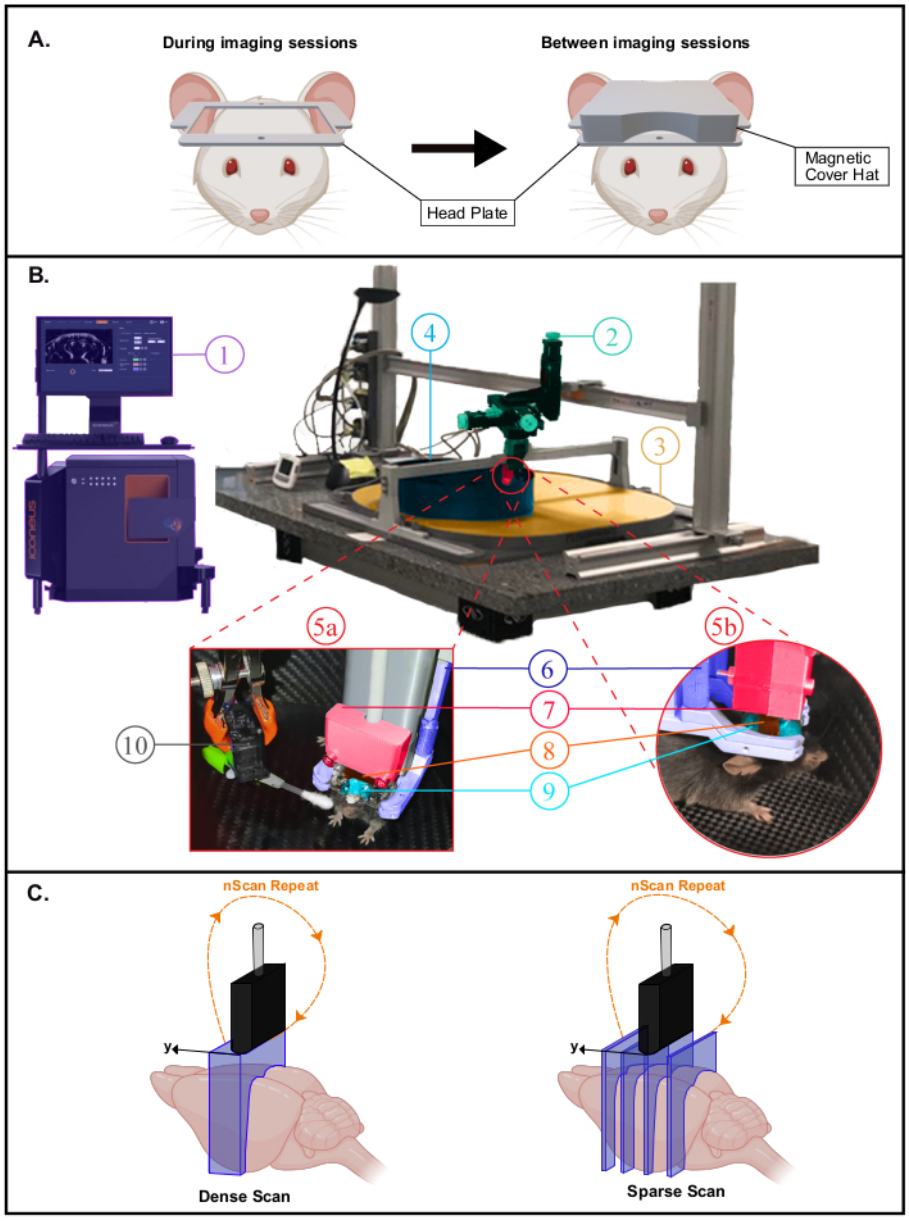

Figure 2: Experimental setup for awake fUS experiments. A. Schematic illustration of the headplate magnetic cover protecting the imaging window (created with BioRender.com). During imaging sessions (Left), the cover is removed to scan the brain in the large aperture offered by the head plate. **B.** Photograph of the experimental setup for transcranial awake imaging in head-fixed freely-behaving mice. **1.** Iconeus One system and software, allowing to set up different imaging sequences and controlling the motors module. **2.** Four-axis motors module (three translations and one rotation) monitored by Iconeus One system (**1**) and allowing 3D tomographic scans or 4D acquisitions. **3.** Air dispensing table. **4.** Mobile Home Cage (MHC). **5a,5b.** Photographs showing closer views of the animal's environment inside the MHC. **6.** Head fixation system

clamping the head plate. **7.** Probe holder linking the probe to the motor module (2). **8**. 15 MHz ultrasonic probe. **9.** Ultrasound gel placed between the mouse head and the ultrasound probe, providing acoustic coupling between them. **10.** Servo-Motor driving the whisker stimulator. The Servo-Motor is controlled by an Arduino Uno card which is interfaced with the Iconeus One system through TTL signal (1) in order to synchronize stimulation patterns with imaging sequences. **C.** Illustration of the different spatial sampling possibilities (created with BioRender.com): in each case, the probe is stepped from the first position to the last one and a Doppler image is recorded at each position to reconstruct the stacked volume. This process is continuously repeated during the whole acquisition time. Dense Scan (left): the step between slices must be small enough (typically 400 µm, which corresponds to the elevation resolution) to allow volumetric imaging. Sparse Scan (right): if distant functional regions are targeted (at different positions), it is also possible to decrease spatial sampling to image different slices that intersect these regions while not compromising the temporal sampling. Please click here to view a larger version of this figure.

3. Probe positioning

1. Start the software (e.g., IcoScan) and create an experiment session. Go to the **Move Probe** menu to adjust the position of the ultrasound probe using the navigation keyboard.
   NOTE: The probe should be positioned approximately 1 mm above the animal's head. It is crucial to ensure that the probe is in contact with ultrasound gel before starting any imaging sequence.
2. Start the **Live View** acquisition and adjust probe position if needed via real time imaging of the animal CBV (cerebral blood volume). Align the brain at the center of the image. Optimize the imaging parameters to capture the highest signal-to-noise ratio.
   NOTE: In awake mice experiments, the aperture size needs to be reduced to avoid artefacts induced by lateral muscles contraction.

4. Angiographic scan and atlas registration

1. Open the **Angio 3D** option in the acquisition software. On the preset panel, adjust the scanning parameters (first slice, last slice and step size) in order to scan the whole brain (**Figure 3A, B**), and start the acquisition.
   NOTE: When setting up the scan parameters, make sure that the scan will cover the posterior part of the brain
2. Leave the acquisition software open and start the software for data analysis and visualization (e.g., IcoStudio), and load the angio 3D scan. Navigate through the acquisition volume using the 3-views panel and select the **Coronal Scan Direction**: antero-posterior or postero-anterior.
3. Go to the **Brain Registration Panel**. Load the mouse reference template that will be needed for the registration process. Register the scan on the **Allen Mouse Common Coordinates Framework** using the fully automatic or the manual registration modes (**Figure 3C**).
4. Check the result by looking at the superposition of the angio 3D scan and the reference template or by looking at the superposition of the scan and the Allen reference atlas using the **Atlas Manager** panel (**Figure 3D**). Save the registration as a .bps file.

NOTE: The registration file can be reused for any other acquisition performed during the same experiment session.

5. Brain Positioning System (BPS)

1. In the IcoStudio software, make sure that the angiographic scan and its .bps file (generated in **step 4.4**) are loaded.
2. Go to the **Brain Navigation Panel**. In the **Atlas Manager** panel, navigate through the mouse **Allen brain atlas** with the parent/child tree navigator. Find the anatomical targeted regions and select them to superimpose them to your scan in the 3-views.
3. Visualize the targeted regions in the 3-view panel and choose an imaging plane that overlaps the targeted regions for the experiment. To do so, manually set two markers on the coronal position that includes the regions of interest.
4. Click on **Brain Positioning System** (BPS) to extract the resulting motor coordinates. These coordinates correspond to the probe position which allows to image the targeted plane. Check the preview of the image which is computed from the angio scan.
5. In the IcoScan software, enter the **Probe positioning** panel and click on **Enter BPS coordinates**. Apply the coordinates given in **step 5.4**. The probe moves and aligns on the targeted imaging plane.
6. Perform a live view acquisition and check that the current imaging plane corresponds to the prediction given in **step 5.4**.

   NOTE: It is also possible to select parasagittal/non orthogonal planes.

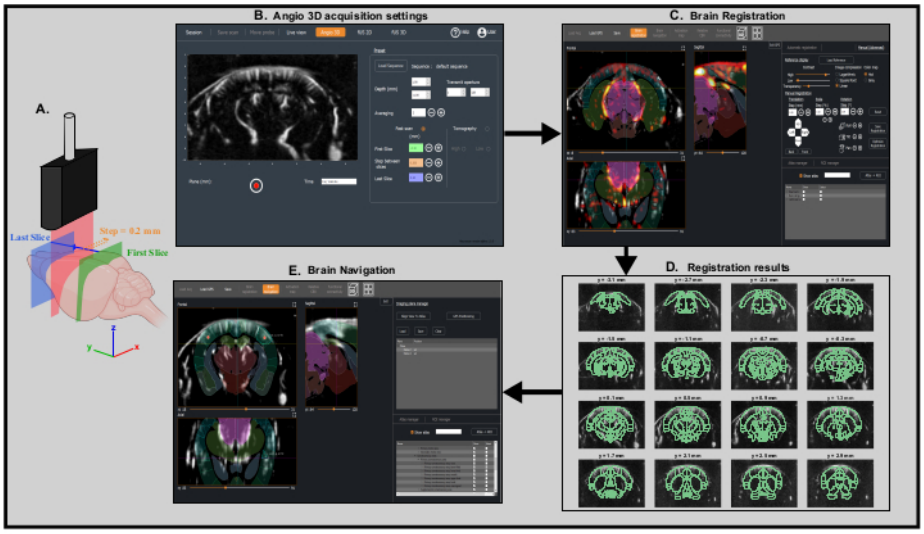

Figure 3: Fast transcranial angiographic Scan and Brain registration for precise probe positioning. A. Schematic representation of the mouse brain being scanned transcranially by the ultrasonic probe from the first coronal slice (green) to the last coronal slice (blue) during a fast angiographic scan. The current imaged slice (represented in red) moves step by step from the back (green) to the front (blue) of the brain. Created with BioRender.com **B.** Screenshot of IcoScan acquisition software in the Angio 3D panel. The preset parameters on the right configure the fast scan. The positions in mm of the first slice, the last slice and the step size must be well chosen to scan linearly the whole brain. **C.** Screenshot of the IcoStudio processing software. The fast Angio 3D scan is automatically registered to a reference template of the mouse brain. The three-views (left) shows the superposition of the vasculature and the mouse brain Allen atlas in the coronal, sagittal and axial views. **D.** Linear lay-out (montage) of 16 slices (out of 31) from the 3D angio scan, with the registered Allen reference atlas superimposed onto the vasculature. **E.** Screenshot of the Brain Navigation panel showing the predicted imaging plane corresponding to the motor coordinates computed by the software thanks to the two markers placed at the center of the left and right primary somatosensory cortex, barrel fields region. Please click here to view a larger version of this figure.

6. Task-evoked experiment: whisker stimulation

1. Predefine the stimulation sequence, including time of stimulation, inter-stimulation time and number of repetitions.
2. Run a 3D fUS sequence by defining the total time of acquisition, the number of positions as well as the dead-time between positions. In case of automatic stimulation synchronized with the acquisition system through TTL input, select the **Trig-IN** option before starting the acquisition.

NOTE: For the results presented in this work, stimulation was delivered using cotton swab positioned such as to allow deflection of most of the whiskers in the dorsal/ventral direction. It was fixed on a servo-motor driven by an Arduino UNO card, linked to the Iconeus One

system to ensure synchronization. The recommended parameters for stimulation are 30 s ON, 30 s OFF, amplitude of 20° and 4 Hz frequency. Alternatively, the stimulation can also be delivered manually by deflecting the whiskers at the defined times during the acquisition.

3. Open the acquisition in IcoStudio software and enter the **Activation map** menu. Fill the activation pattern field with start and end times and compute the activation map. Adjust the display parameters for visualization. Export the activation map as a .h5 file for off-line analysis.
   NOTE: Activation is estimated using a generalized linear model (GLM) approach with the stimulus convolved by a default mouse hemodynamic response (HRF). Alternatively, activation can be visualized directly by estimating the Pearson correlation between the stimulation pattern and the hemodynamic signal from each voxel.

7. 4D functional connectivity

1. Run a 3D fUS sequence by defining the total time of acquisition, the number of imaging plane positions as well as the dead-time between positions.
   NOTE: For 4D functional connectivity, we recommend acquisition time between each volume < 2.5 s (sampling frequency of at least 0.4 Hz) and a total acquisition time of at least 10 min (number of time points > 180).
2. Save the acquisition and load it in the IcoStudio software. If necessary, load the .bps file and the Allen mouse brain coordinate framework. In the **Atlas manager**, select regions of the atlas as regions of interest (ROI).
3. Enter the **Functional Connectivity** menu and select the desired regions in the ROI manager. Visualize the results as connectivity matrix (supervised analysis) or seed-based correlation map (unsupervised). Select and adjust the bandwidth filters as desired and export correlation results for statistical analysis.
   NOTE: In 3D fUS imaging mode, the relative probe positions are set manually. Hence, two types of scans are possible and can be chosen depending on the functional application: dense scans versus sparse scans (**Figure 2C**).

Representative Results

This protocol describes the 3D quantification of cerebral hemodynamic variations transcranially in the mouse brain, at rest or in response to sensory stimulation. Whisker stimulation, a standard paradigm to map brain functional activation in rodents, has been selected as an example of sensory stimulation-evoked response. **Figure 4** shows a representative activation map in response to mechanical whisker stimulation in an anesthetized mouse obtained using transcranial fUS imaging. The total trial time was 760 s, with a 60 s baseline (before and after the stimulation), an 80 s stimulation and a 60 s recovery time, repeated 5x. Significant activation was determined with the resolution of a general linear model (GLM) using a default mouse hemodynamic response function (HRF). The activated regions (Z scores with p-value >0.0000006 after stringent Bonferroni correction for multiple comparison) are displayed as color-coded values overlaid onto the Allen common coordinate framework template. Voxel-wise time course of the contralateral primary somatosensory cortex, barrel field region (S1BF) revealed a 15-20% increase of the CBV compared to baseline.

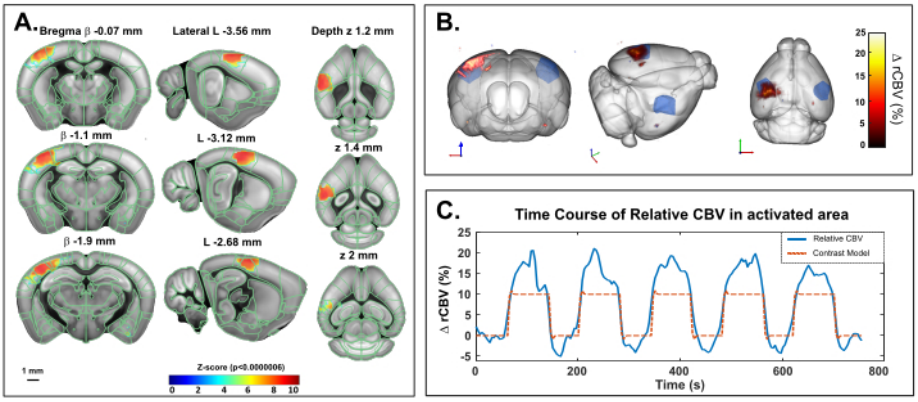

Figure 4: Transcranial activation Maps and rCBV time course following whiskers stimulation in ketamine/xylazine anesthetized mouse. A. Activation map showing significantly activated voxels following mechanical stimulation of the right whiskers (80 s ON, 60 s OFF ,5x) under ketamine/xylazine anesthesia. Maps were obtained by computing Z-scores based on general linear model analysis (GLM) with Bonferroni correction for multiple comparison. Z-scores (color coded) are overlaid on the Allen brain 3D template (after registration with the brain positioning system) and displayed in three-views: coronal (left), sagittal (middle) and axial (right). Anatomical regions from the Allen mouse brain common coordinate framework are displayed for reference. Activated voxels are well located inside the left S1BF cortex. Scale bar: 1 mm. Each sample volume was scanned over 2.8 mm (corresponding to 7 slices in the elevation direction) in 3.85 s allowing to record 20 volumic samples during each functional response. **B.** 3D rendering of whisker stimulation-evoked relative cerebral blood volume (rCBV) increase compared to baseline level. The anatomical delineation of the S1BF is indicated in blue. **C.** Time course of CBV variations in the left S1BF (blue) and the corresponding stimulus applied (red). Please click here to view a larger version of this figure.

The same paradigm has been applied in a head-fixed behaving mouse in the mobile homecage using the awake preset of IcoScan. **Figure 5** presents the activation map after a multiple whisker stimulation experiment using the experimental setup described in **Figure 2**. A few posterior and caudal whiskers were stimulated with the following pattern: 30 s baseline followed by five consecutive trials of 30 s ON (4 Hz) and 30 s OFF (**Figure 5C**). Stimulation was delivered using a servo-motor driven by an Arduino UNO card triggering the image acquisition sequence for synchronization. Significant activation was determined with the resolution of a general linear model (GLM) using a default mouse hemodynamic response function (HRF). Multiple comparison correction was performed with the Bonferroni method. Conventional alpha level of 0.05 was normalized by the total number of voxels in the acquisition volume, resulting in a final stringent threshold of 0.000003.

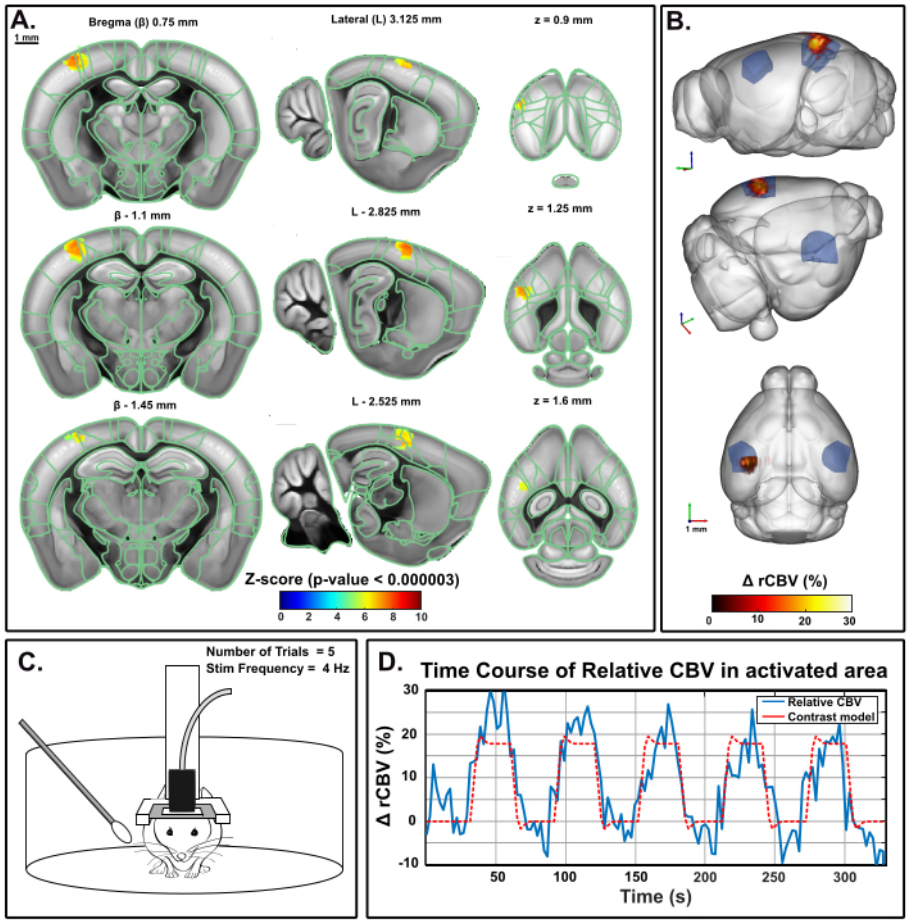

Figure 5: Activation Maps and rCBV time course following whiskers stimulation in awake behaving mouse. A. Activation map showing significantly activated voxels following mechanical stimulation of the right whiskers (30 s ON, 30 s OFF, 5x) in an awake mouse in the mobile homecage. Maps were obtained by computing Z-scores based on general linear model analysis (GLM) with Bonferroni correction for multiple comparison (normalization by the total number of voxels). Z-scores (color coded) are overlaid on the Allen brain 3D template (after registration with the Brain Positioning System) and displayed in three-views: coronal (left), sagittal (middle) and axial (right). Anatomical regions from the Allen Mouse Brain Common Coordinate Framework are displayed for reference. Activated voxels are well located inside the left S1BF cortex. Scales bars, 1 mm. Each sample volume was scanned over 1.6 mm (corresponding to 3 slices in the elevation direction) in 3.85 s allowing to record 17 volumic samples during each functional response. **B.** 3D rendering of whisker stimulation-evoked relative Cerebral Blood Volume (rCBV) increase compared to baseline level. The anatomical delineation of the S1BF is indicated in blue. **C.** Illustration of the mouse in the mobile homecage during the right whisker stimulation experiment, during which five 30 s trials were performed for a total acquisition time of 330 s. **D.** Instantaneous relative CBV time course

extracted inside the activated area (blue), with the corresponding stimulus superimposed (red). Please click here to view a larger version of this figure.

Figure 6 shows the temporal correlations of normalized low-frequency (<0.2 Hz) spontaneous CBV fluctuations between 3D brain regions (identified from registration to the Allen common coordinate framework) in a ketamine-xylazine anesthetized mouse. Total acquisition time was 20 min (1200 s). Atlas-supervised analysis revealed strong interhemispheric connectivity patterns, with resulting correlation coefficient values up to 0.8. Seed-based analysis in the dorsal hippocampus revealed a significant interhemispheric connectivity between right and left hippocampus as well as deep retro-hippocampal regions and piriform cortices. A seed region selected in the S1BF also resulted in a symmetrical (cortico-cortical) correlation pattern, as previously described.

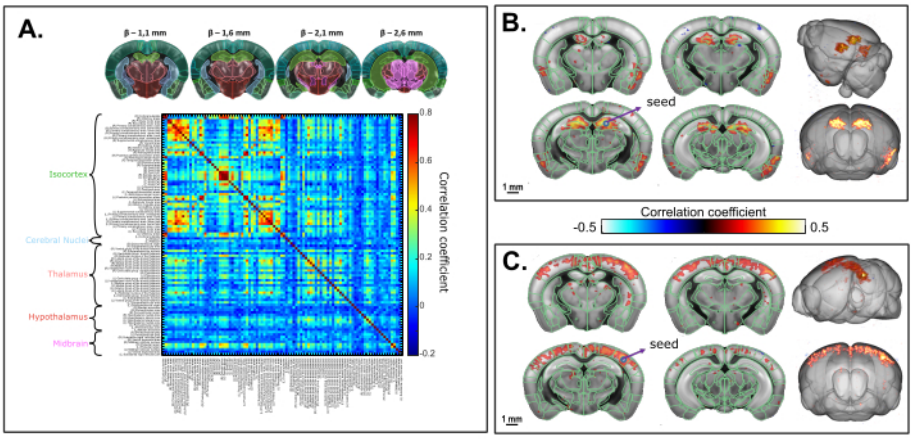

Figure 6: Transcranial volumetric resting-state functional connectivity of the mouse brain under ketamine/xylazine anesthesia assessed on a 20 min 3D fUS acquisition. A. Correlation matrix based on 3D regions of the Allen common coordinate framework registered on the transcranial functional acquisition. The matrix is obtained by computing the normalized Pearson's correlation of spontaneous low-frequency fluctuations (<0.1 Hz) of the average time signals from all the voxels included in each identified ROI after slice timing correction. Each sampled volume was scanned over 1.6 mm in the elevation direction (corresponding to 4 slices) acquired over 2.2 s. **B**. Seed-based analysis projected onto a 3D template. The seed was selected within the right dorsal hippocampus at β - 2.1 mm. Correlation map is obtained by computing the Pearson Correlation coefficient between the temporal signals of the seed and each voxel of the whole acquisition after slice timing correction. **C.** 3D correlation map based on seed-based analysis with seed region selected within the S1BF at β - 2.1 mm. Scale bars: 1 mm. Please click here to view a larger version of this figure.

Discussion

Whole brain imaging methods are crucial tools to better understand brain physiology and pathology. The method described here allows the precise quantification of hemodynamic signals in the living brain directly at the bench. The unmatched sensitivity and spatio-temporal resolution of functional ultrasound is particularly well suited for the mouse physiology. Functional responses and resting-state networks can be mapped within short acquisition times, longitudinally and without having to average trials or subjects to obtain a reliable measure. The relevant combination of high sensitivity ultrasonic linear probes and fast motorized setups enables one to perform transcranial volumetric fUS imaging in mice within reasonable acquisition times. This protocol can be performed either on anesthetized or awake mice using a mobile home cage.

Whisker stimulation, the sensory stimulus used as an illustrating example in this manuscript, is a standard functional activation paradigm in rodents and a reliable read-out to study sensory processing, neurovascular coupling and their alterations[5,6,10,11]. While coarse manual brushing of the whiskers may be preferred for its ease of use, this method lacks spatial and temporal precision. The use of an automatic stimulator, such as the one described here triggered with the fUS imaging scanner, allows for a better control of several parameters including the time of onset, the amplitude displacement, the frequency as well as the angle of the Q-tip/comb, resulting in a better inter-animal reproducibility. Additionally, a more precise timing of stimulation enables the modeling of the Hemodynamic Response Function (HRF) by determining the time to onset and time to peak parameters[12,13]. To ensure better precision on the number of whiskers deflected during the stimulation (and thus the area of the activated region), more sophisticated stimulators can be adapted to this protocol. Many other stimuli such as light[8], sound[14] or odor presentation[15] can be implemented using the same protocol.

The compatibility of functional ultrasound with awake and behaving animals is an important advantage compared to other neuroimaging techniques, enabling functional activation mapping without the anesthesia bias. Using an air-lifted mobile homecage is a good alternative to other existing head-fixed apparatus such as linear or spherical treadmills. While being firmly head-fixed, the motion of the homecage gives the mouse the illusion to navigate the environment, allowing a wide-range of behavioral testings to be coupled to fUS imaging[16]. However, the habituation procedure to head-fixing constitutes an important step to decrease stress, especially for experiments where it can be considered a confounding factor. The procedure detailed here (6-days of handling and habituation to head fixation) gives robust results for sensory stimulation and resting-state functional connectivity. However, it might be necessary to extend the habituation period for more refined behavioral tests[17].

Disclosures

Jeremy Ferrier and Bruno-Félix Osmanski are employees of Iconeus. Thomas Deffieux, Zsolt Lenkei, Bruno-Félix Osmanski, and Mickael Tanter are co-founders and shareholders of Iconeus.

Acknowledgments

This work was supported by the European Research Council (ERC) Advanced Grant N° 339244-FUSIMAGINE, the National Agency for Research funding 'Pinch' (ANR-18-CE37-005), the Inserm Research Technology Accelerator in Biomedical Ultrasound, the ElfUS technical core of the IPNP, Inserm U1266, the European research program FUSIMICE of

the Human Brain Project, and EMBO Short-Term Fellowship 8439 to Andrea Kliewer.

References

1. Hoyer, C., Gass, N., Weber-Fahr, W., Sartorius, A. Advantages and challenges of small animal magnetic resonance imaging as a translational tool. *Neuropsychobiology.* **69** (4), 187-201 (2014).
2. Deffieux, T., Demene, C., Pernot, M., Tanter, M. Functional ultrasound neuroimaging: a review of the preclinical and clinical state of the art. *Current Opinion in Neurobiology.* **50**, 128-135 (2018).
3. Rabut, C. et al. Pharmaco-fUS: Quantification of pharmacologically-induced dynamic changes in brain perfusion and connectivity by functional ultrasound imaging in awake mice. *NeuroImage.* **222**, 117231 (2020).
4. Tiran, E. et al. Transcranial functional ultrasound imaging in freely moving awake mice and anesthetized young rats without contrast agent. *Ultrasound in Medicine and Biology.* **43** (8), 1679-1689 (2017).
5. Ferrier, J., Tiran, E., Deffieux, T., Tanter, M., Lenkei, Z. Functional imaging evidence for task-induced deactivation and disconnection of a major default mode network hub in the mouse brain. *Proceedings of the National Academy of Sciences of the United States of America.* **117** (26), 15270-15280 (2020).
6. Rabut, C. et al. 4D functional ultrasound imaging of whole-brain activity in rodents. *Nature Methods.* **16** (10), 994-997 (2019).
7. Brunner, C. et al. A platform for brain-wide volumetric functional ultrasound imaging and analysis of circuit dynamics in awake mice. *Neuron*. **108** (5), 861-875.e7 (2020).
8. Gesnik, M. et al. 3D functional ultrasound imaging of the cerebral visual system in rodents. *NeuroImage.* **149**, 267-274 (2017).
9. Macé, É. et al. Whole-brain functional ultrasound imaging reveals brain modules for visuomotor integration. *Neuron.* **100** (5), 1241-1251.e7 (2018).
10. Macé, E., Montaldo, G., Cohen, I., Baulac, M., Fink, M., Tanter, M. Functional ultrasound imaging of the brain. *Nature Methods.* **8** (8), 662-664 (2011).
11. Tiran, E. et al. Transcranial functional ultrasound imaging in freely moving awake mice and anesthetized young rats without contrast agent. *Ultrasound in Medicine and Biology.* **43** (8), 1679-1689 (2017).
12. Claron, J. et al. Large scale functional ultrasound imaging of the spinal cord reveals in depth spatiotemporal responses of spinal nociceptive circuits in both normal and inflammatory state. *Pain.* (*In Press.*) (2020).
13. Aydin, A.K. et al. Transfer functions linking neural calcium to single voxel functional ultrasound signal. *Nature Communications.* **11** (1), 2954 (2020).
14. Bimbard, C. et al. Multi-scale mapping along the auditory hierarchy using high-resolution functional ultrasound in the awake ferret. *eLife.* **7**, e35028 (2018).
15. Boido, D. et al. Mesoscopic and microscopic imaging of sensory responses in the same animal. *Nature Communications.* **10** (1), 1110 (2019).
16. Kislin, M. et al. Flat-floored air-lifted platform: A new method for combining behavior with microscopy or electrophysiology on awake freely moving rodents. *Journal of Visualized Experiments.* (88), 51869 (2014).

17. Juczewski, K., Koussa, J.A., Kesner, A.J., Lee, J.O., Lovinger, D.M. Stress and behavioral correlates in the head-fixed method: stress measurements, habituation dynamics, locomotion, and motor-skill learning in mice. *Scientific Reports.* **10** (1), 12245 (2020).

CHAPTER 3

ARTICLE N°2:

Resting state-fUS imaging of functional connectivity in awake mice with neuropathic pain: insights into pain and stress networks

INTRODUCTION OF THE ARTICLE N°2

In the study presented in the previous chapter, we validated the experimental methodology for conducting multislice fUS imaging in awake head-fixed mice. Building upon this validation, I applied this experimental approach to investigate potential alterations in a mouse model of neuropathic pain.

As introduced in chapter 1 section 5, neuropathic pain is correlated with brain reorganization and consequently FC patterns disruption. Several studies have shown that patients suffering from chronic pain present morphological and functional reorganization in cortical and subcortical areas compared to healthy controls (Bliss et al. 2016; Huang et al. 2019). Preclinical longitudinal studies have demonstrated that those changes are time-dependent and might reflect the development of the neuropathic pain symptoms overtime and the apparitions of comorbidities (Yalcin et al. 2011).

The aim of this work was to study the temporal link between alterations in cerebral FC and the development of neuropathic pain and/or associated comorbidities in a mouse model of neuropathic pain. To do this, we measured the resting-state functional connectivity (FC) in awake head-fixed mice, at two time points: I) 2 weeks after induction of neuropathic pain (cuff around the sciatic nerve), II) at 8 weeks post-induction during the emergence of anxiety (8W).

One of the advantages of fUS imaging technique is the compatibility with awake and behaving animals, as demonstrated in the paper presented in chapter 2 (Bertolo et al. 2021).

In order to avoid the bias induced by the anesthesia, we performed our study in awake head-fixed conditions. We chose an alternative head-fixation apparatus called Mobile HomeCage (Neurotar, https://www.neurotar.com/the-mobile-homecage/), which consists of an air-lifted mobile homecage that follows the movement of the animal. While being firmly head-fixed, the mouse has the illusion of navigating and exploring the environment because of the motion of the homecage. With this apparatus minimizing the disruption of normal behavior under head-restrained conditions, coupled with the extended habituation protocol (see Materials and Methods), we minimized the stress typically associated with such constraints.

The results of the study show FC alterations in a wide-range network between regions known to be involved in pain processing. Statistical analysis investigating the correlations between couple of regions identify alterations in the connectivity between Infralimbic and Hypothalamus specific for the neuropathic group at 2W. Furthermore, at 8W we identify a disconnection between regions within the somatomotor

areas and connected with it, like the Amygdala and the Thalamus. A second effect identified at 8W is the reinforced connection between the NAc and M2 and the NAc and the Thalamus.

As one of the main articles of my PhD, I performed all the experiments and signal analysis, as well as statistical analysis and wrote the article. Some colleagues (such as S. Diebold) were involved in the improvement of signal analysis. Due to the time taken in this analysis, this study has not been published yet, but will be submitted in the coming months.

Resting state-fUS imaging of functional connectivity in awake mice with neuropathic pain: insights into pain and stress networks

Silvia Cazzanelli[1,2], Samuel Le Meur Diebolt[1,2], Youenn Travert-Jouanneau[1], Luc Eglin[2], Adrien Bertolo[2], Thomas Deffieux[1], Mickael Tanter[1], Bruno-Felix Osmanski[2], Jeremy Ferrier[2] and Sophie Pezet[1]

[1] Physics for Medicine Paris, INSERM, ESPCI Paris, CNRS, PSL Research University - Paris, France.

[2] Iconeus, 27 Rue du Faubourg Saint-Jacques, 75014 Paris, France

1 ABSTRACT

Neuropathic pain poses a significant clinical challenge, necessitating a comprehensive understanding of its underlying neurobiological mechanisms. In this study, we investigated alterations in resting-state functional connectivity (FC) in awake mice suffering from neuropathic pain, aiming to elucidate changes within the pain matrix of the contralateral brain hemisphere, at 2 and 8 weeks post nerve injury.

Using functional ultrasound (fUS) imaging, we observed pronounced disconnections within somatomotor networks, including S1HL/M2 and S1Tr/Thalamus, consistent with findings in both rodent models and human patients with persistent pain conditions. Interestingly, reinforcement of FC was noted between the nucleus accumbens (NAc) and the thalamus at 8 weeks post-lesion, highlighting dynamic adaptations in reward circuitry associated with neuropathic pain. The increased FC observed in neuropathic animals suggests active reinforcement of the hypothalamic-pituitary-adrenal (HPA) axis in response to ongoing spontaneous pain. Finally, our results also suggest that surgical intervention induces FC alterations between subdivisions of the prefrontal cortex and either the hippocampus or anterior cingulate cortex.

These observations highlight the complex adaptive changes that take place over time at the level of the cerebral brain networks involved in the sensory, emotional and stress in persistent painful conditions.

2 INTRODUCTION

Neuropathic pain is an abnormal pain sensation that persists longer than the temporal course of natural healing. It is a major health issue all over the world since it affects 7–10% of the general population (Colloca et al. 2017). Neuropathic pain is caused by a nerve lesion under different disease conditions and can lead to altered and disordered transmission of sensory signals into the spinal cord and the brain. The altered sensory transmission leads to a distinct set of symptoms; the most common two being allodynia and hyperalgesia. Allodynia consists in a nociceptive response to a normally non-nociceptive stimulus and hyperalgesia is an enhanced response to noxious stimuli (Zhuo 2008). In addition to sensory symptoms, mood disorders such as anxiety and depression are frequently observed in patients suffering from neuropathic pain.

The abnormal function of the somatosensory system is due to maladaptive plasticity within the nociceptive pathways. Multiple alterations distributed widely across the nervous system contribute to generate an abnormal processing of the sensory stimuli. These alterations include ectopic generation of action potentials, facilitation and disinhibition of synaptic transmission, loss of synaptic connectivity and formation of new synaptic circuits (Costigan, Scholz, and Woolf 2009). Those plastic changes not only take place in peripheral nociceptors, spinal dorsal horn and subcortical areas but also in cortical areas involved in the processing of painful information (Zhuo 2008).

Treating neuropathic pain requires a deeper understanding of the plastic changes in somatosensory pathways and to do so, different rodent models have been developed for preclinical research. These models derive from known etiologies, thus reproducing peripheral nerve injuries, central injuries, and metabolic-, infectious- or chemotherapy-related neuropathies. Murine models of peripheral nerve injury often target the sciatic nerve which is easy to access and allows nociceptive tests on the hind paw (Yalcin et al. 2014). This study has been conducted on a sciatic nerve cuffing model, which results in chronic mechanical allodynia and time dependent mood disorders as anxiety-like and depressive-like behavior (Sellmeijer et al. 2018).

It has been previously shown that the anxiodepressive-like consequences of neuropathic pain evolve over time, with a much later onset than sensitive symptoms (Yalcin et al. 2011; Suzuki et al. 2007; Gonçalves et al. 2008). According to the literature, in the cuff model, mechanical hypersensitivity immediately develops following nerve injury. On the other hand, mice develop anxiety-related behaviors 3 to 4 weeks

later, while depression-related behaviors are observed after 6 to 8 weeks (Yalcin et al., 2011; Sellmeijer et al. 2018). These apparent discrepancies suggest that the time factor could be a decisive parameter when studying the affective consequences of neuropathic pain.

This article aimed at characterizing cortical plastic changes associated with neuropathic pain using a relatively new technique of neuroimaging: functional ultrasound (fUS) imaging. fUS imaging allows the precise measurement of relative changes in cerebral blood volume with an excellent spatial (100–300 µm) and temporal resolutions (10 ms). In a similar way to blood oxygen level-dependent functional magnetic resonance imaging (BOLD-fMRI), fUS imaging relies on the neurovascular coupling to infer brain activity indirectly from measurement of hemodynamic signals (Bertolo et al. 2023). It is particularly sensitive to measure task-evoked hemodynamic changes in the corticex (Macé et al. 2011). It was then further used to perform functional studies in humans (Demene et al. 2017; Soloukey et al. 2020), non-human primates (Dizeux et al. 2019) and rodents (Sieu et al. 2015; Urban et al. 2015; Bergel et al. 2018; Rahal et al. 2020; (Macé et al. 2011). fUS imaging can also measure resting-state hemodynamic fluctuations between brain areas over time; this last approach enables the identification of intrinsic functional connectivity (FC) patterns (Osmanski et al. 2014). In this study, we investigated how FC within pain-related brain regions is altered over time, in association with neuropathic pain and the associated comorbidities.

We measured the functional connectivity (FC) at rest in awake, head-fixed mice: I) naïve, II) sham operated and iii) in mice subjected to neuropathic pain (2W cuffing of the sciatic nerve), or during the emergence of anxiety-like behavior (8W). Our results show significant changes in FC in major pain-related brain regions in accordance with the development of neuropathic pain symptoms. These findings suggest that the regions involved in pain processing undergo a maladaptive plasticity following nerve injury which may participate in pain chronification. Moreover, the connectivity alterations change across the investigated timepoints, and this could be correlated with the subsequent apparition of the comorbidities.
Our study provides a novel imaging approach to investigate and follow overtime FC alterations associated with neuropathic pain.

3 MATERIALS AND METHODS

Animals

All the experiments were performed in agreement with the European Community Council Directive of 22nd September (010/63/UE) and the local ethics committee ("Comité d'éthique en matière d'expérimentation animale n°59, 'Paris Centre et Sud'", project agreement APAFIS#19701 2019031020578789 V5).

The experiments were performed on 59 male C57BL/6 mice (Charles River Lab). Mice arrived at the laboratory one week before the beginning of the experiments at the age of 7 weeks and weighed between 20-25g. Animals were socially housed in well-ventilated cages. The housing room was kept at a constant temperature of 22°C and relative humidity was kept at 45-50%. Food and water were available *ad libitum*. The housing room was kept under a 12h light/dark reverse cycle (light 8 pm – 8 am) and all the experiments were done during the dark phase, under red light.

Experimental design (Figure 1)

In order to investigate the functional connectivity changes associated with neuropathic pain, we developed an experimental approach allowing the monitoring of intrinsic brain connectivity in a mouse model of neuropathic pain over time. Our investigation focused on key stages of symptoms development and comorbidity progression within the disease.

This study was conducted by integrating procedures to induce and assess neuropathic pain symptoms in a mouse model, along with an imaging experimental protocol conducted under awake head-restrained conditions (Figure 1A).

The study started with the evaluation of the mechanical sensitivity threshold by the Von Frey test in naïve conditions. After the assessment of a robust threshold the cohort underwent the procedure for the induction of neuropathic pain, called cuff surgery (Figure 1B). At this point, we divided the cohort into three subgroups: the neuropathic group, which underwent the complete surgery including the implantation of the cuff; the sham group, which underwent the same surgical protocol but did not receive the cuff implantation; and finally, the naïve group, which did not undergo any surgical procedures.

In order to allow for head-fixation, a metal plate was implanted on the skull of the animal. All three subgroups underwent the same surgical procedure (Figure 1C).

Following the experimental protocol previously validated in a prior publication (Bertolo et al. 2021) we performed imaging sessions in awake head-restrained mice. In this configuration we acquired data in

three different sagittal planes using a motorized approach that enabled a volumetric reconstruction of the imaged sections (Figure 1D-E). This approach facilitates imaging numerous brain regions simultaneously, opening up the possibility of conducting functional connectivity studies across a wide range of regions. To control for the surgery bias, each group of mice were implanted with head-posts 3 weeks before the imaging session.

The imaging session was conducted under resting-state conditions and lasted for 20 minutes. Each animal underwent multiple imaging sessions during each timepoint.

Surgical procedures

Surgical procedures were performed under ketamine/domitor anesthesia Médétomidine (Domitor®, 0,5 mg/kg) and Kétamine (Imalgène®, 60 mg/kg).

Neuropathic pain model

Neuropathic pain was induced by implanting a 2 mm section of PE-20 polyethylene tubing around the main branch of the sciatic nerve of the right leg (Figure 1B) (Benbouzid et al. 2008; Yalcin et al. 2014; Barrot 2012). Animals in the sham group underwent the same procedure without cuff implantation, mice in the naïve group did not undergo any surgery procedure.

Implantation of metal plate for head-fixation

In order to perform fUS imaging in head-fixed animals, a metal plate with an imaging window of 13 x 21 mm^2 was surgically implanted on the skull of the mouse (Figure 1C).

The animal was anesthetized by an intramuscular (IM) injection and placed on a heating pad. Once the animal was completely asleep, the skin was shaved and disinfected with betadine® and anesthetized locally with lidocaïne (4 mg/kg). The eyes of the mouse were protected using an ointment (Ocry-gel, TVM, UK). Then the animal was placed on the stereotaxic frame and using surgical scissors an incision was performed following the sagittal suture from behind the occipital bone to the beginning of the nasal bone. The body temperature was constantly monitored with a rectal probe connected to a heating pad set at 37°C. The metal plate was implanted on the skull using two anchoring screws and dental cement. The detailed procedure has been described previously in Bertolo et al. 2021

The anesthesia was reversed with a SC injection of Atipamezole (Antisedan®, 1 mg/kg) and Meloxicam (5 mg/kg) was injected subcutaneously along with 0.1 ml of 5% Glucose as post-surgery treatment. A protective cap was attached to the metal plate using magnets to protect the

skull and to keep the field of imaging intact for 4–6 weeks. Altogether, the metal plate and the cap did not interfere with the normal behavior of the mice (Bertolo et al. 2021).

Habituation to the head-restrained set-up

The mice were habituated to be head-restrained in the Mobile HomeCage (MHC, Neurotar, Finland). This head-fixation platform combines a stable head-fixation with an air-lifted carbon cage. The cage is suspended on an air cushion, allowing the mouse to move and explore the environment while being headfixed. This set-up provides a familiar environment that the animal can explore and navigate while being head-restrained.

The training procedure consists of 2 phases: regular handling by the experimenter and progressive habituation to the head-restrained conditions. The handling started two days after the surgery and lasted at least 4 days. Each day, the handling lasted for 10 to 15 minutes. At the end of the procedure, the animal was left free to explore the carbon cage of the MHC. Next, the habituation to head fixation lasted for a minimum of 5 days. The mouse was clamped every day and each time, the head-fixed time was gradually increased, starting from 15 min on the first day to 2 hours on the last day. The total duration of the training protocol to the Mobile HomeCage must be adjusted based on each mouse's individual performance and wellbeing. Most mice are considered ready for imaging after 5 days of habituation but some of them may require a 2-days extension if any sign of stress is observed (Bertolo et al. 2021).

Mice were weighed daily during the habituation period to monitor their wellbeing. Any animals that experienced a weight loss exceeding 20% were excluded from the experiments. To reduce stress during the head-restrained experiments, positive reinforcement training was used; after each handling, habituation, and experimental session, a treat was given to the mouse as a reward. To mitigate the stress caused by the noise of the machine and the set-up, background music was constantly playing during both the training and the experimental sessions.

Mechanical sensitivity (Von Frey) test.

This test was performed to assess the mechanical sensitivity of the hind paws of the mice. Mice were placed in Plexiglas boxes (9 cm x 7 cm x 7 cm) with a wire mesh floor (Figure *2*A). The mechanical sensitivity was tested with thin calibrated plastic filaments (Von Frey filaments) that were applied to the plantar surface of the hind paw. The mice were left in the set-up for a 45-minutes habituation period, after which each hind paw of the animals were stimulated by applying a series of filaments with increasing gauges or stiffness (from 0.16g to 10g). When reaching the sensitivity threshold, the mouse responded by

withdrawing its paw away from the stimulus. Each filament was tested 5 times per paw, applied until bent (Yalcin et al. 2014; Barthas et al. 2015). The threshold was defined as 3 or more withdrawals observed out of the 5 trials. Mice were tested before the cuff surgery, and then two and eight weeks after the cuff surgery.

fUS imaging session

Using a prototype ultrasonic ultrafast neuroimaging system (Iconeus, Paris, France - ART Inserm Ultrasons Biomédicaux) equipped with a linear ultrasound probe (128 elements, 15 MHz central frequency, 100 µm spatial pitch, Vermon, Tours, France) attached to a 4-axis motorized stage (Physik Instrumente, Germany), we performed resting-state FC acquisitions in awake head-fixed mice (Figure 1D) at 2 and 8 weeks post-neuropathic pain induction.

After head-fixation in the MHC, the skull was gently covered with previously centrifuged echographic gel. A coronal scan of the entire window (Bregma to Lambda) was performed, enabling the reconstruction of a 3D angiographic volume. By using the Iconeus software IcoStudio (Iconeus, Paris, France) we can automatically align the 3D angiography with the templates of the Allen Mouse Brain (Nouhoum et al. 2021). This alignment allowed us to position the probe in the desired plane of interest and then perform from 4 to 6 scans of 1200s each, using a 4-axis motor. Three different parasagittal planes on the left hemisphere were targeted. The imaging session was conducted under resting-state conditions and lasted for 20 minutes. Each animal underwent multiple 20-min runs at each imaging session.

Choice of imaging planes.

Functional ultrasound (fUS) imaging enables the measurement of the CBV with high sensitivity and high spatiotemporal resolutions in the rat and mice brain (Osmanski et al. 2014; Gesnik et al. 2017; Macé et al. 2011; Errico et al. 2015; 2016). However, compared to fMRI, fUS imaging suffers so far, a lack of simultaneous imaging in the three dimensions of space. Nevertheless, due to the speed of the 4-axis motor used and the accurate registration of the Iconeus software, it was possible to image repetitively in three planes, at a speed that would allow the measurement of FC (adjusted sampling rate of 0.55 Hz). The detailed procedure has been previously described in Bertolo et al., 2021.

Based on previous studies of FC alterations in neuropathic pain in human patients and rodent models, we chose to focus our study on 18 specific brain regions, which are located across three different parasagittal planes in the left hemisphere. Plane1: L=0.5 mm, plane2: L=1.5mm and

plane3: L=3.5mm (Figure 1E). The brain regions studied were identified from on-the-fly registrations of the brain fUS volume to the Allen common coordinate framework (Nouhoum et al. 2021). The selected regions of interest (ROI) included the frontal area subdivided into prelimbic (PL), infralimbic (IL), anterior cingulate (ACC) and retrosplenial area (RSA, lateral agranular part); the insular cortex, subdivided into the dorsal (AID), posterior (AIP) and ventral (AIV) part; the somatomotor area divided in primary somatosensory area, lower limb (S1HL) and trunk (S1Tr), primary (M1) and secondary (M2) motor area; the hippocampal region (HIP); the interbrain regions subdivided in thalamus (THAL) and hypothalamus (HYP); and finally, the striatum consisting of the caudoputamen (CPU), nucleus accumbens (NAC), lateral septal complex (LS) and striatum-like amygdalar nuclei (sAMY).

fUS imaging sequences

The fUS imaging sequence consisted of eleven successive tilted ultrasonic plane waves with an angle ranging from −10° to 10° emitted at a 5.5 kHz Pulse Repetition Frequency (PRF). The backscattered echoes were recorded by the transducer array and beamformed to produce a block of 200 consecutive ultrafast images with a framerate of 500 Hz. In order to filter the Cerebral Blood Volume (CBV) and to remove the tissue signal, we used a clutter filter based on Singular Value Decomposition (SVD) applied to 200 successive frames by removing the 35 first singular vectors which mainly correspond to the tissue space (Demene et al. 2015). Finally, a Power Doppler image was obtained by integrating the energy of the filtered frames, resulting in a Power Doppler image every 400 ms. After probe positioning along the sagittal midline, the functional scans were programmed as follows: 3 para-sagittal slices were sequentially acquired over 400 ms each with a dead time of 0.2 s to step the probe using the motors. This resulted in a final time resolution of 1.8 s after slice timing correction.

Power Doppler denoising

Prior to statistical analysis, power Doppler signals were denoised using the IcoLab software (ICONEUS, Paris) to mitigate the effects of motion artifacts (in awake acquisitions) and hemodynamic variations from non-neuronal sources. The denoising process involved the following steps:

1. Computation of confounding time series through principal component analysis (PCA) of the most variable time series obtained from white matter voxels, following the method outlined by Behzadi

et al. (2007). Specifically, the top 5% most variable voxels were selected for PCA fitting, with the top 5 principal components retained as confounding variables.

2. Detection of high motion volumes in awake acquisitions by identifying volumes where the smoothed global signal (i.e., the average power Doppler signal from brain voxels, smoothed using a 5-sample moving average) deviated by more than 5% from its baseline. The global signal baseline was determined using least trimmed square regression. Only periods of low motion lasting at least 20 seconds were retained, with any remaining volumes interpolated to prevent bias in subsequent temporal filtering.
3. Temporal filtering of power Doppler signals and confounding time series using a Butterworth forward-backward bandpass filter with a frequency range of [0.01, 0.1] Hz and an order of 8.
4. Regression of filtered confounding time series from the power Doppler signals to remove confounding effects.

The denoising approach frequently discards entire acquisitions due to excessive noise, resulting in the exclusion of many acquisitions. As a result, the number of animals that could be included in the study drastically diminished. The study began with a cohort of 59 mice, yet only 24 animals were ultimately included in the analysis of the ultrasound data and subsequent statistical analyses (n=24; 2w n=12 and 8W n=12).

Correlation matrix analysis and statistical approach

Thanks to the registration procedure, the Allen Mouse Brain Atlas segmentation could be used to perform automatic region-based CBV extraction over more than 18 brain regions of interest (ROI). After normalization and slice timing correction, the Pearson correlation coefficient was computed between every pre-processed and spatially averaged signal (in each ROI). Subject-level FC matrices were Fisher-transformed and averaged across subjects (2W n=12: naive n=2 sham n=5 np n=5; 8W n=12 naive n=5 sham n=5 np n=2).

These results are represented as a correlation matrix displaying the correlation coefficient between every couple of regions in a color-coded range. Alternatively, the correlations between regions were also represented as a circular plot (Figure 3B-D) where line thickness and color correspond to the correlation coefficient value between the two nodes.

In order to test the connectivity differences in selected pairs of ROIs between the neuropathic and the control groups across different time points, we performed a two-way ANOVA test using mixed models. If a significant effect of treatment, time or time/treatment interaction was evidenced ($p<0.05$), a post-hoc

Tukey's test with multiple comparisons correction has been applied. The pairs of ROIs that showed significant differences in the correlation coefficients between the neuropathic and the control group are reported in the results section.

During the imaging sessions the animals were imaged several times resulting in a numerous acquisition for each animal. For the analysis n=103 acquisitions were included, corresponding to n=54 for the 2W time point (naive n=15, sham n=18, np n=21) and n=49 for the 8W time point (naive n=20, sham n=14, np n=15).

4 RESULTS

Neuropathic allodynia

The nerve injury caused by the cuff implantation resulted in mechanical allodynia in the lesioned paw of the neuropathic group compared to Sham or naïve mice (Figure 2).

Mechanical sensitivity was assessed for the three groups, naïve, sham and np, before the cuff surgery (T0). No differences in mechanical threshold were observed between groups, nor between contralateral and ipsilateral paws within each group (Figure 2B-C).

At 2 and 8 weeks after surgery, we observed a significant decrease in the mechanical sensitivity thresholds of the neuropathic group's ipsilateral paw in, compared to the control groups' ipsilateral paws (ipsiSHAM/ipsiNAIVE vs ipsiNP $p<0.0001$, Figure 2B) (ipsiSHAM/ipsiNAIVE vs ipsiNP $p= 0.0089$, Figure 2C). There is a significant difference between the threshold assessed in the ipsilateral paw within the neuropathic group before and after the surgery ($p<0.0001$, Figure 2B) ($p=0.0427$, Figure 2C). We also observed a significant decrease in the mechanical sensitivity threshold between contralateral and ipsilateral paw within the neuropathic group at both 2 weeks (contraNP vs ipsiNP $p<0.0001$, Figure 2B) and 8 weeks (contraNP vs ipsiNP $p=0.0015$, Figure 2C). This result indicates the presence of mechanical allodynia in the lesioned paw of the neuropathic group at both time points. This initial assessment of unilateral mechanical allodynia suggests that the neuropathic group exhibited typical neuropathic pain symptoms during the imaging sessions.

FC alterations in a wide-range network

The fUS imaging set-up configuration allowed for data acquisition in three sagittal planes and then the reconstruction of the volume of the three imaged sections.

After removing motion artifacts, the time series from each ROI were extracted from the recording session (20min) and a correlation matrix was obtained. Next, the correlation matrices of all the acquisitions were averaged within each group to obtain the six matrices shown in Figure 3, corresponding to one correlation matrix per group resulting in a total of three matrices per time point (Figure 3A-C). In Figure 3B and C the correlation matrices are alternatively represented as a circular network. The averaged correlation coefficients were depicted as links connecting the different ROIs with varying thickness and colors, proportional to the strength of the correlation (see Materials and Methods).

The matrices and the circular networks illustrate the intrinsic brain connectivity, inferred by the temporal correlation of the spontaneous CBV fluctuations, among 18 selected brain regions. This method allows the broad characterization of the functional connectivity network across groups and time points.

At both time points (2W and 8W) the intrinsic connectivity of each group shows a consistent pattern of correlation with a distinctive variability in the strength of correlations among groups. The connectivity pattern reveals three distinct clusters: interconnections between the different subparts of the insular cortex, the somatomotor area and the striatum-interbrain cluster.

The insular cluster shows a strong correlation between its three different subdivisions with a stronger variability across groups at 2W (AIP-AID naive: 0.76 ± 0.29SD, sham: 0.42 ± 0.36SD, np: 0.37 ± 0.23SD).

The second cluster is characterized by a robust connection among somatomotor regions, including the somatosensory cortex (S1HL and S1TR), the primary and secondary motor areas. There is a strong connection between S1TR and M1 with S1HL, consistently observed across groups and time points, with a greater variability across groups at 8W (S1HL-M1 naive: 0.63 ± 0.23SD, sham: 0.38 ± 0.26SD, np: 0.73 ± 0.39SD). While strong correlations persist within M2, they are less consistent across groups and time points.

A third cluster consists in the interconnection between the striatum and the interbrain. The connections within this cluster are not as strong as those in the somatomotor and insula clusters. However, there are few subgroups of connections where correlations fluctuate across groups and time points. For example, the connection between the NAc and the interbrain is stronger at 8W compared to 2W.

These results demonstrate a consistent pattern of connectivity, indicating robust reproducibility across groups and time points. The robustness of this pattern enables us to identify specific clusters of variability in the strength of connections across groups.

Functional connectivity alterations in specific subnetworks at 2W

To further investigate the variability in the strength of connections across groups we conducted a Two-way ANOVA analysis using mixed-models in which we compared the strength of correlations of a couple of regions across groups and timepoints. With this approach, we identified specific subnetworks showing significant differences in the connectivity between groups.

Regarding the specific alterations in connectivity occurring during the early stages of neuropathic pain (2W after the cuff surgery), we have identified two distinct subnetworks of significant alterations. These alterations involve connectivity between the frontal area, hippocampus, insular cortex, and interbrain (Figure 4A).

In these subnetworks, we discern two distinct patterns of variation, as depicted in panels B and C. One pattern aligns with the expected effects of our neuropathic pain model, potentially linked to neuropathic pain itself. The other pattern, however, appears unrelated to neuropathic pain and likely reflects variations attributable to other factors. The graphs were obtained after Fisher transformation of the Pearson correlation coefficient of the correlation matrices described in the paragraph above.

In the graphs shown in panel B we report a neuropathic pain specific effect in link with the cuff lesion. The connectivity between the infralimbic region and the hypothalamus is significantly increased in the NP groups compared to the control groups, naïve ($p=0.0069$) and sham ($p=0.0152$).

These results highlight the presence of alterations in the connectivity between neuropathic and control groups at 2 weeks after the surgery. There is an increased connectivity between the frontal area and the hypothalamus associated with the neuropathic lesion.

In panel C, the three graphs display differences in connectivity that suggest what we refer to as a nonspecific effect, as differences between groups do not align with our initial hypothesis and cannot be attributed to neuropathic pain. Graph 1 shows alterations in the interconnection within the frontal area, between Infralimbic cortex (IL) and Anterior Cingulate Cortex (ACC). There is a significant difference between the connectivity of the naïve group compared to the sham and the np group (NAÏVE-SHAM $p= 0.0314$, NAÏVE-NP $p= 0.002$). Interestingly there is no difference between sham and np and the graph shows a gradual increase of connectivity. Moreover, there is a time effect within the neuropathic and the naïve group. In the neuropathic group the connectivity decreased at 8W compared to 2W ($p=0.0451$). On the contrary in the naïve group the connectivity increased at 8W compared to what registered in the 2W naïve group ($p=0.0328$).

Graph 2 depicts the connectivity between ACC and Hip and shows a specific behavior of the sham group. The connectivity is increased, compared to naïve ($p=0.035$) and np ($p=0.0254$). Furthermore, there is a significant time effect concerning the sham group, the sham group at 8W shows a decrease in connectivity compared to 2W ($p=0.0008$).

Graph 3 represents the interconnection between subparts of the insular cortex. The connectivity between AIP and AID in the sham ($p=0.0062$) and np ($p=0.0008$) group is decreased compared to the naïve. There are no differences between sham and np.

Functional connectivity alterations in specific subnetworks at 8W

Eight weeks after the cuff surgery, as already shown in the global comparison (Figure 3), significant alterations in the FC can be observed in neuropathic mice compared to 2W.

A specific subnetwork of significant alterations in connectivity has been identified. It is centered around the somatomotor area and involves connections between the amygdala, striatum, and interbrain (Figure 5). Within this network, we identified two centers of plasticity illustrated respectively in panel B and C.

In Figure 5B we identify changes in connectivity strength among somatomotor areas, and between somatomotor areas and amygdala and thalamus. The neuropathic group shows a significant decrease in the connections between S1HL-M2 ($p=0.0033$), M1-Amy ($p=0.0014$) and finally S1TR-Thal (sham $p=0.0034$, naïve $p=0.0344$) compared to the control groups. These variations were also significantly different from the neuropathic group imaged at 2W (NP 2Wvs8W: S1HL-M2 $p<0.0001$, M1-Amy $p= 0.0019$, S1TR-Thal $p= 0.0008$). These results show a disconnection within the somatomotor areas, and between the amygdala and the thalamus due to neuropathic pain 8 weeks after the cuff surgery.

In figure 5C, we found the opposite effect. The neuropathic group shows an increase of connectivity in regions connected with the striatum, more precisely the NAc. In the connection between NAc and M2, and between NAc and thalamus, the neuropathic group shows a stronger correlation compared to the control groups (SHAM $p= 0.0002$, NAÏVE $p= 0.0319$) and the connectivity showed by the np group imaged at 2W ($p<0.0001$).

These results highlight an opposite plasticity effect concerning two different subnetworks. The neuropathic lesion is associated with a disconnection in the regions linked with the somatomotor cortex and a stronger connection between regions linked with the striatum, 8 weeks after the cuff surgery.

5 DISCUSSION

Imaging techniques play a crucial role in unraveling the complex neurobiology underlying chronic pain conditions such as neuropathic pain (Thomson and Bushnell, 2012). In this study, we employed functional ultrasound (fUS) imaging in awake mice to investigate alterations in brain connectivity associated with neuropathic pain. Our findings shed light on the dynamic changes in functional networks within the brain and provide insights into the pathophysiology of chronic pain.

Alterations of the FC in link with post-surgical pain

Within the statistically significant changes of FC observed at 2 weeks post lesion, two regions, namely the Infralimbic cortex (IL) and the hippocampus, showed increased FC with the anterior cingulate cortex (ACC) in both the sham and neuropathic groups, suggesting an effect of post-surgical pain. Additionally, a third pair of regions, comprising two subparts of the insula, also showed specific FC changes associated with post-surgical pain. The ACC plays a pivotal role in the affective and motivational aspects of pain (Becerra et al. 2013; Navratilova, Atcherley, and Porreca 2015; Neugebauer et al. 2009), receiving nociceptive inputs from the medial thalamus and integrating them with motivational and affective information from other brain areas of, such as the insular cortex, medial prefrontal cortex (mPFC), and basolateral amygdala (BLA) (Navratilova, Atcherley, and Porreca 2015; Bushnell, Čeko, and Low 2013; Williams, Crossman, and Slater 1977; Marwan N. Baliki and Apkarian 2015). This integration leads to the generation of affective and motivational pain responses through its projections to the amygdala, nucleus accumbens (NAc), and mPFC (Navratilova, Atcherley, and Porreca 2015; Marwan N. Baliki and Apkarian 2015; M. N. Baliki et al. 2006). On the other hand, the insular cortex represents a central hub for pain processing, both for sensory and emotional processing (Labrakakis 2023). Although more specific experiments are required to confirm these observations, together with the increased connectivity within the insula, these results suggest that surgical intervention induces early and short-lasting changes in the pain matrix.

Alterations of the IL/ Hypothalamus FC specifically in neuropathic pain animals

At 2 weeks post lesion, when the neuropathic pain peaks, the FC between the infralimbic cortex and the hypothalamus is statistically significantly increased in neuropathic animals compared to all control groups. The IL and hypothalamus are crucial for pain modulation and homeostatic regulation, with the hypothalamus involved in regulating autonomic, endocrine, and behavioral responses to pain (Schaeuble and Myers 2022), while the IL is implicated in emotional regulation related to pain. Previous studies

demonstrate anatomical links between the IL and hypothalamus, with a high density of IL afferents in the PH (Myers et al. 2016). Optogenetic stimulation of IL afferents activates neurons in the PH (Wood et al. 2019), indicating functional connectivity, especially in stress-related responses. The PH is involved in stress integration, receiving inputs from various forebrain regions and projecting to stress-related nuclei like the paraventricular nucleus (PVN) (Ulrich-Lai et al. 2011). The increased FC observed in neuropathic animals suggests active reinforcement of the hypothalamic-pituitary-adrenal (HPA) axis in response to ongoing spontaneous pain.

Disconnections of the somatomotor network 8 weeks post lesion

Our study also revealed disconnections in the somatomotor networks, including the S1HL/M2, and S1Tr/Thalamus (Figure 5). Several studies have previously described such disconnections in somatomotor regions in persistent pain conditions, both in rodents and humans. Using the same technology of imaging as our study, but in anesthetized rats, we previously demonstrated alterations in various subparts of the somatomotor cortex contralateral to the inflamed paw in a model of persistent inflammatory pain (Rahal et al., 2020). By correlating FC alterations (static or dynamic FC) with clinical/pain behaviors in arthritic and control animals, we found a significant correlation between somatomotor network alterations and weight gain reduction (an indirect index of disease burden on animal physiology) and mechanical hypersensitivity (Rahal et al. 2020).

Abnormalities within the somatomotor network was also observed in CRPS patients compared with healthy control subjects (Hotta et al. 2023), as well as in patients with chronic back pain (Zhu et al. 2024). Consistent with our findings, both studies in humans also reported changes in the connectivity of the somatomotor with the thalamus and with the periaqueductal gray (PAG) or the insula(Hotta et al. 2023; Zhu et al. 2024). Surprisingly, these adaptive changes of brain network involved in sensitivity and pain are observed in our study at 8 weeks post lesion (and not earlier). We hypothesize that these long-lasting rearrangements of the somatomotor network may require several weeks of altered electrophysiological changes to take place, as observed in neuropathic pain by Leblanc and colleagues (LeBlanc et al. 2016).

Reinforcement of the FC between NAc and the thalamus at 8 weeks post lesion

The NAc, a central component of the brain's reward circuitry, comprises a core and shell region (Marwan N Baliki et al. 2013). While the shell is associated with value predictions for monetary gambles, the core is activated during the anticipation of cessation of thermal pain, which is a reward value of pain relief. The NAc is causally involved in the transition to chronic pain in humans (Marwan N Baliki et al. 2012) and is

necessary for full expression of neuropathic pain-like behavior in rodents (M. N. Baliki et al. 2014). Notably, only the core NAc has connections to the thalamus in humans, while in rodents, only the shell NAc has strong thalamic connections (M. N. Baliki et al. 2014; Chang et al. 2014).

Persistent pain induces significant structural rearrangements of the NAc. In subacute back pain, NAc volume decreases significantly before the development of chronic pain and remains unchanged at follow-up, suggesting that it plays a role in risk for development of chronic pain. In addition, a shift in the electrophysiological properties of the NAc takes place. These alterations in low-frequency (0.01 to 0.027 Hz) oscillations at rest, are a signature of the state of chronic pain in this condition (Makary et al. 2020).

Increased excitatory neurotransmitters content in the thalamus in neuropathic pain conditions contributes to both sensitization and mechanical allodynia (Wang et al. 2020). Moreover, alteration of the FC between the right core NAc and left thalamus was evidenced in patients with fibromyalgia, with a reduced FC in these conditions, in which the reduced reward towards pain relief is well established (Park et al. 2022). In our study, a reinforcement of the FC between the NAc (core and shell parts) and the thalamus was observed specifically in neuropathic animals. Both these regions are involved in emotional processing and regulation. The dysregulated connectivity observed between these regions may contribute to emotional disturbances and mood disorders associated with neuropathic pain.

Limitations of our study

While animal models offer strengths, there are notable limitations, especially regarding differences in experimental conditions compared to human studies. Preclinical imaging often involves anesthesia to minimize stress and movement, impacting physiological and neuronal activity. To mitigate anesthesia bias, our study was conducted in awake conditions, facilitated by fUS imaging's compatibility with both freely-moving and head-fixed animals (Bertolo et al. 2021). However, head-restrained conditions can induce stress, mitigated in our study by using an alternative head-fixation apparatus called Mobile HomeCage. This apparatus minimizes disruption to normal behavior while ensuring head fixation (Kislin et al. 2014). Nonetheless, head-restrained configuration presents limitations due to the invasiveness of head-plate implantation, affecting sterility conditions. Additionally, motion artifacts in awake experiments frequently lead to the exclusion of acquisitions, reducing the number of animals included in the analysis. Despite starting with a cohort of 59 mice, only 24 were ultimately included in the analysis. Furthermore, longitudinal studies under awake conditions were hindered by challenges in maintaining clear cranial windows, resulting in separate cohorts for each time point.

In conclusion, the observed changes in connectivity patterns provide novel perspectives on the pathophysiology of neuropathic pain. Notably, the reinforcement of functional connectivity between the nucleus accumbens (NAc) and the thalamus at 8 weeks post-lesion suggests dynamic adaptations in reward circuitry associated with neuropathic pain. Overall, our findings contribute to a deeper understanding of the complex neural mechanisms underlying neuropathic pain and provide a foundation for future research to better elucidate the precise role of NAc and shed light on potential targets for therapeutic intervention.

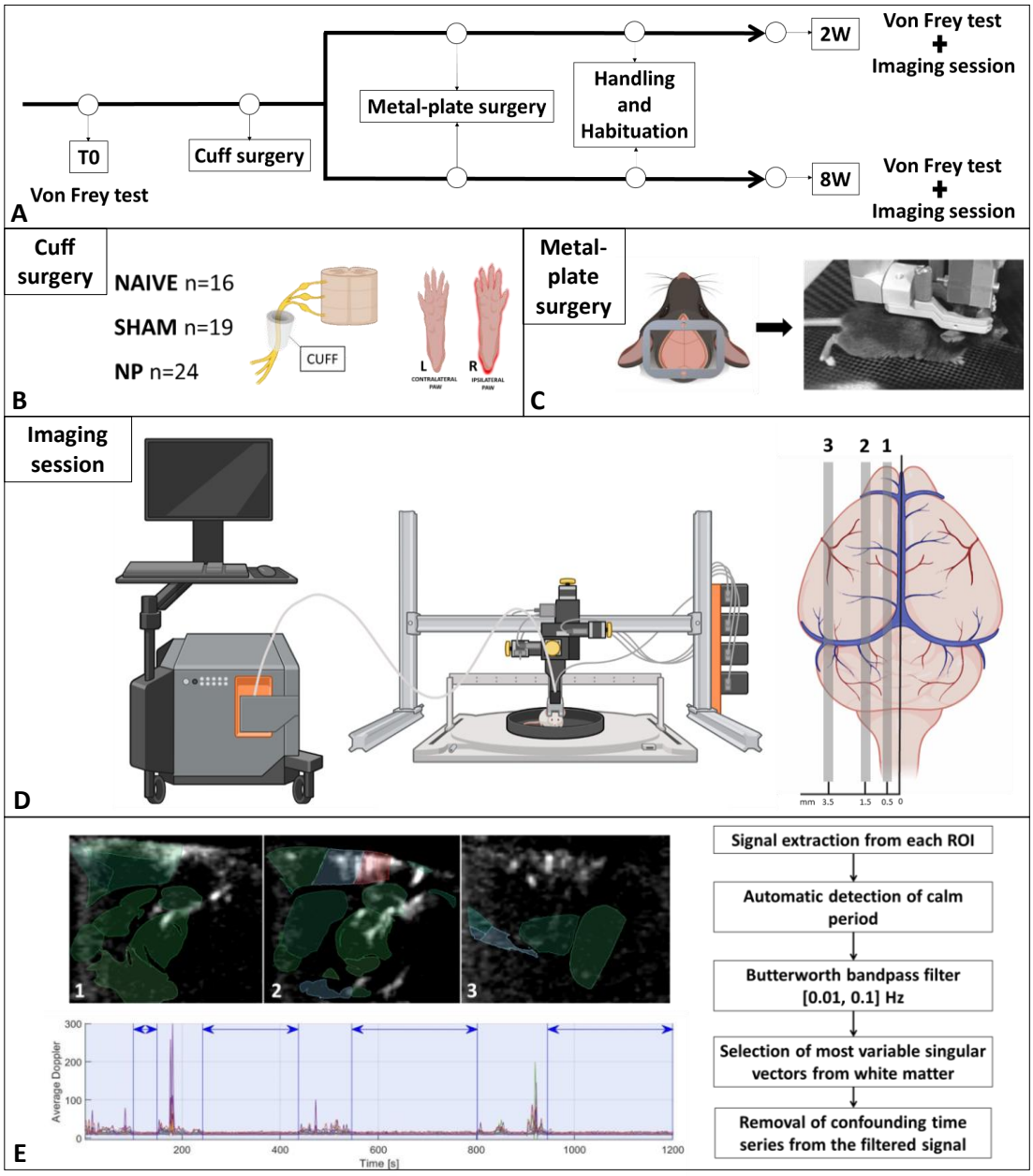

Figure 1: Experimental design. (A) Experimental timeline. Von Frey test was performed at baseline before cuff surgery. Depending on the attributed time point of the cohort the cuff surgery was performed either 2 weeks or 8 weeks before the imaging session. The metal-plate was implanted, for each time point, three weeks before the imaging session. After a week of recovery, two weeks of handling and habituation followed. Imaging was then performed for one week; each animal was imaged multiple times. (B) Schematic representation of the cuff surgery and the size of the dataset. (C) Schematic representation of the head-plate implantation that allows head fixation. (D) Schematic illustration of the experimental setup for fUS imaging on head-fixed freely behaving mice using the air-floated Mobile HomeCage (Neurotar ref). Representation of the three sagittal planes imaged. (E) Representative power Doppler image with corresponding regions of interest automatically positioned by the atlas registration performed by the Iconeus software. Selection of quiet periods and signal denoising protocol. (Created with Biorender.com).

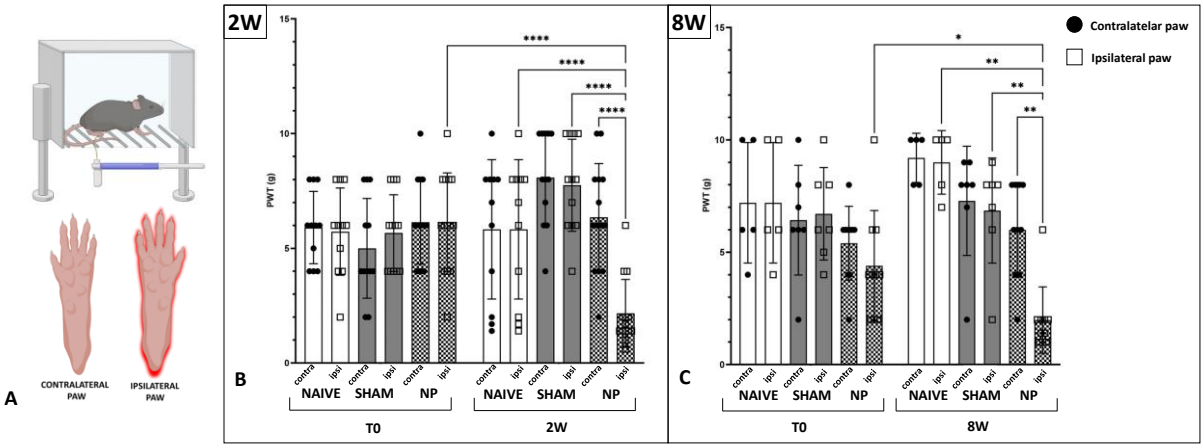

Figure 2: Cuff implantation induces mechanical allodynia. (A) Schematic description of a mouse in the Von Frey set-up and below the illustration of contralateral and ipsilateral paw showing the ipsilateral as the lesioned paw in the neuropathic group. (B) Von Frey test conducted at baseline (T0) and 2W showing the presence of mechanical allodynia in the neuropathic group's ipsilateral paw at 2W. Data are expressed as mean ± SD (****p<0.0001) (Naïve n=11, Sham n=12, NP n=14). (C) Von Frey test conducted at baseline (T0) and 8W showing mechanical allodynia in the neuropathic group's ipsilateral paw at 8W. Data are expressed as mean ± SD (contraNP vs ipsiNP **p=0.0015, ipsiSHAM/ipsiNAIVE **p= 0.0089, * p=0.0427) (Naïve n=5, Sham n=7, NP n=10). (Created with Biorender.com).

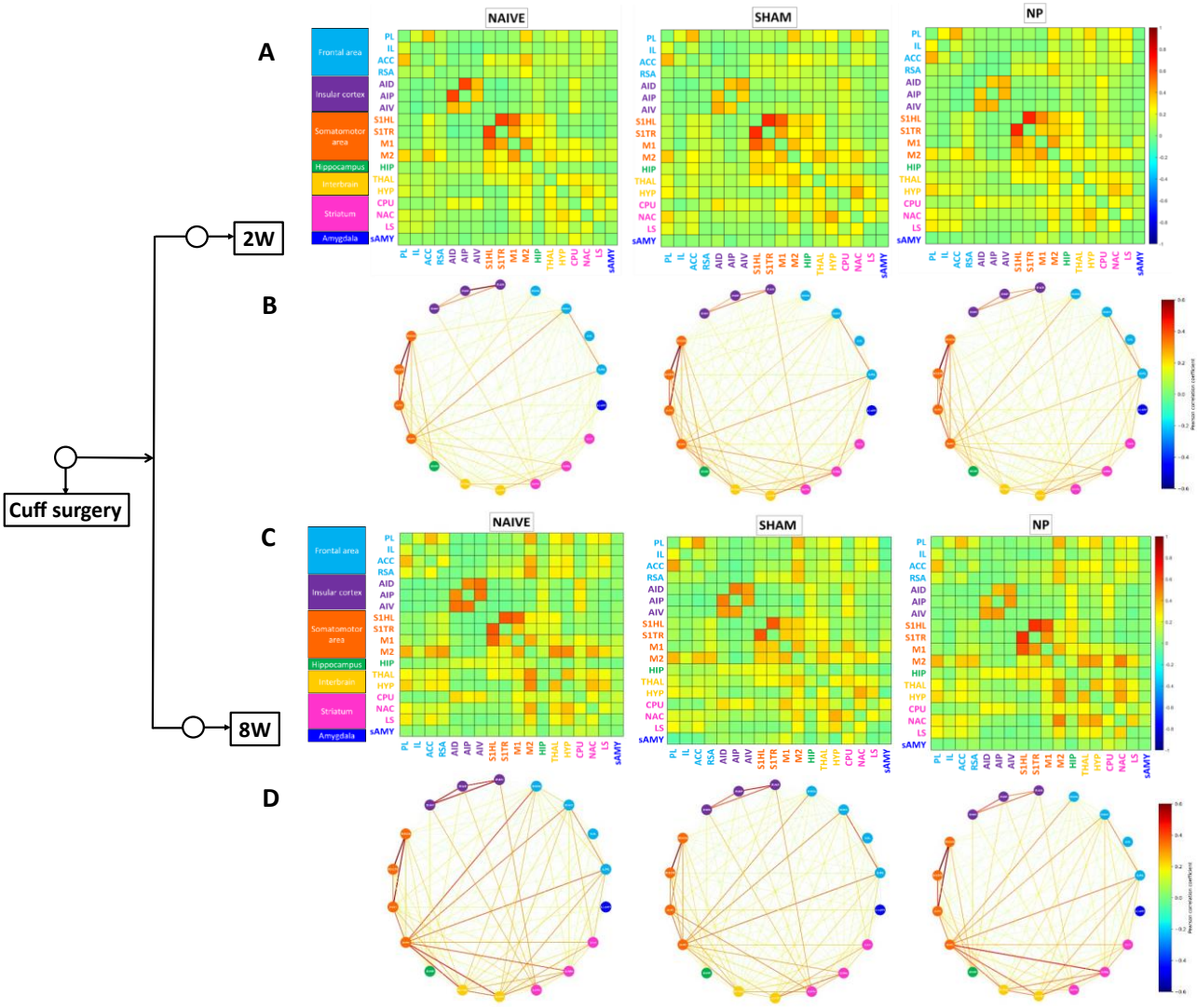

Figure 3: Functional Connectivity alterations in a wide-range network. (A-C) Resting-state correlation matrices, displaying the mean Pearson correlation coefficient between 18 selected ROIs in a color-coded range from -1 to 1. (B-D) Alternative representation of the correlation matrix as a circular network with the 18 ROIs displayed in a circular layout and the connection between them illustrated as links with thickness and color corresponding to the correlation coefficient between the two nodes.

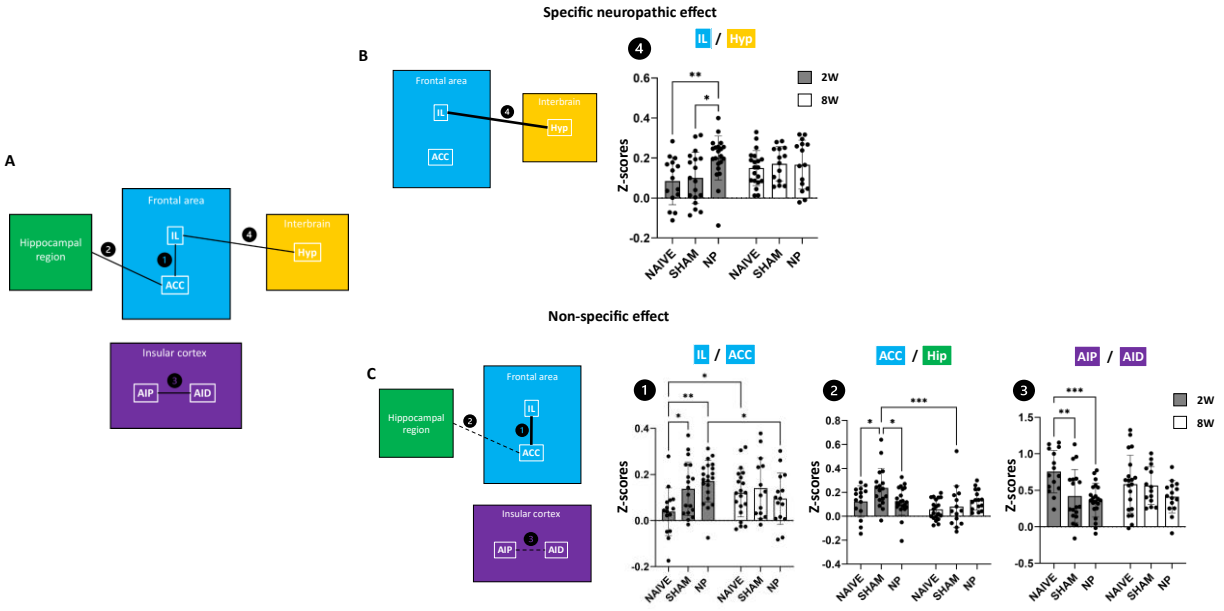

Figure 4: Functional connectivity alterations in specific subnetworks at 2W. (A) Schematized illustration of the two subnetworks showing significant functional connectivity alterations. Frontal area, hippocampal region and the interbrain and the interconnections between the posterior and the dorsal part of the insular cortex. (B-C) Division of subnetwork showing a non-specific effect (B) and a specific effect (C). The increase in connectivity is illustrated as a bold line and the decrease as a dotted line. The changes illustrated refer to the alterations detected in the neuropathic group compared to the sham group. Graphs 1, 2, 3 and 4 represent Fisher-transformed z-score of correlations between pairs of ROIs at 2 and 8 weeks. Data are presented as mean ± SD (*p<0.05, **p<0.01, ***p<0.001). Mice n=12, acquisitions n=54.

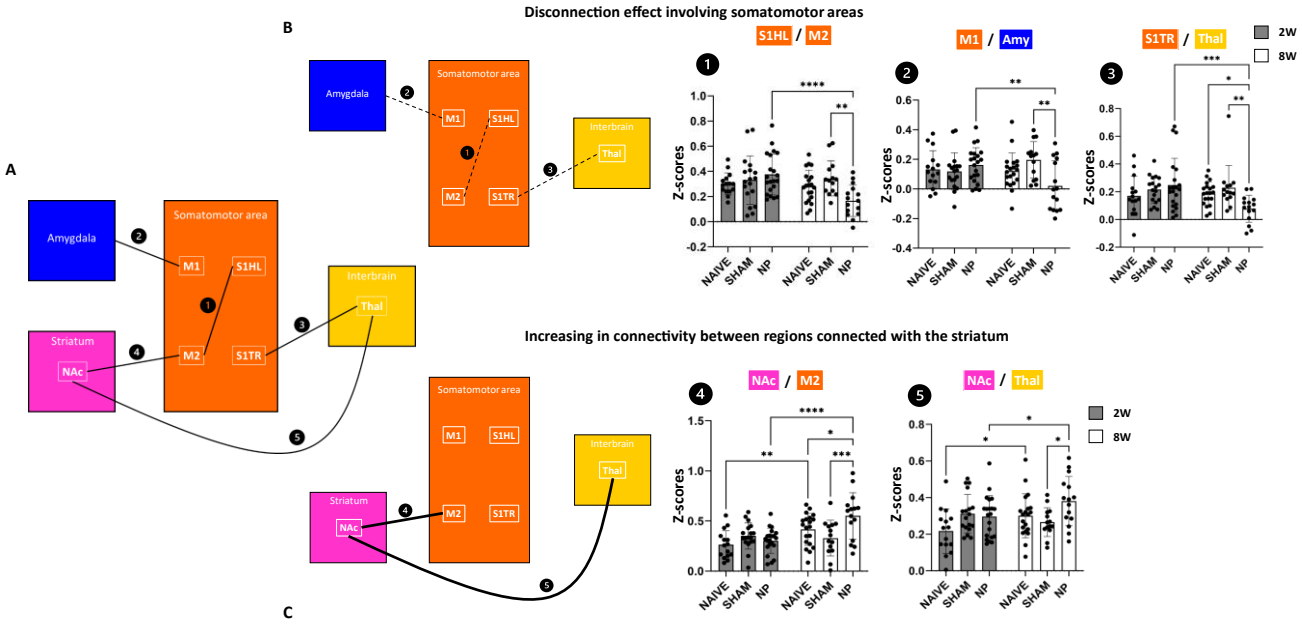

Figure 5: Functional connectivity alterations of a specific subnetwork at 8W. (A) Schematized illustration of the subnetworks showing significant functional connectivity alterations. Somatomotor area, interbrain, amygdala and striatum. (B-C) Division of subnetworks showing a disconnection effect involving somatomotor areas (B) and an increase in the connectivity between regions connected to the striatum (C). The increase in connectivity is illustrated as a bold line and the decrease as a dotted line. The changes illustrated refer to the alterations detected in the neuropathic group compared to the sham group. Graphs 1, 2, 3, 4 and 5 represent Fisher-transformed z-scores of correlations between pairs of ROIs at 2 and 8 weeks. Data are presented as mean ± SD (*p<0.05, **p<0.01, ***p<0.001, ****p<0.0001). Mice n=12, acquisitions n=49.

Conflict of interest

MT, BFO and TD are co-founders and shareholders of Iconeus company. AB, BFO and JF are employees of Iconeus. MT, BFO and TD are co-inventors of several patents in the field of neurofunctional ultrasound and ultrafast ultrasound. MT; BFO and TD do not have any other financial conflict of interest, nor any non-financial conflict of interests. All the other authors do not have any financial or non-financial conflict of interests.

Authors contribution statement

SP and SC designed the experimental paradigm.

SC, YT were involved in the awake functional ultrasound imaging and behavioral experiments.

SC performed the experiments and analyzed the ultrasound data.

SC, SP and JF wrote the manuscript.

JF and BFO supervised the signal processing of the ultrasound data.

SC and SP performed the statistical analysis.

SD, LE, AB, TD were involved in the signal processing.

SP and JF were involved in the interpretation of the data and wrote some parts of the manuscript.

Acknowledgments

The authors wish to thank Nathalie Ialy-Radio for animal husbandry and the CNRS, INSERM and ESPCI for their financial support. This work was supported by funding from ANRT and the Agence Nationale de la recherche (Project 'PINCH', 18-CE37-0005-01). SG's PhD was co-funded by Iconeus.

6 REFERENCES

Baliki, M. N., P. C. Chang, A. T. Baria, M. V. Centeno, and A. V. Apkarian. 2014. “Resting-State Functional Reorganization of the Rat Limbic System Following Neuropathic Injury.” *Scientific Reports* 4 (1): 6186. https://doi.org/10.1038/srep06186.

Baliki, M. N., D. R. Chialvo, P. Y. Geha, R. M. Levy, R. N. Harden, T. B. Parrish, and A. V. Apkarian. 2006. “Chronic Pain and the Emotional Brain: Specific Brain Activity Associated with Spontaneous Fluctuations of Intensity of Chronic Back Pain.” *Journal of Neuroscience* 26 (47): 12165–73. https://doi.org/10.1523/JNEUROSCI.3576-06.2006.

Baliki, Marwan N, Ali Mansour, Alex T Baria, Lejian Huang, Sara E Berger, Howard L Fields, and A Vania Apkarian. 2013. “Parceling Human Accumbens into Putative Core and Shell Dissociates Encoding of Values for Reward and Pain.” *The Journal of Neuroscience : The Official Journal of the Society for Neuroscience* 33 (41): 16383–93. https://doi.org/10.1523/JNEUROSCI.1731-13.2013.

Baliki, Marwan N, Bogdan Petre, Souraya Torbey, Kristina M Herrmann, Lejian Huang, Thomas J Schnitzer, Howard L Fields, and A Vania Apkarian. 2012. “Corticostriatal Functional Connectivity Predicts Transition to Chronic Back Pain.” *Nature Neuroscience* 15 (8): 1117–19. https://doi.org/10.1038/nn.3153.

Baliki, Marwan N., and A. Vania Apkarian. 2015. “Nociception, Pain, Negative Moods, and Behavior Selection.” *Neuron* 87 (3): 474–91. https://doi.org/10.1016/j.neuron.2015.06.005.

Barrot, M. 2012. “Tests and Models of Nociception and Pain in Rodents.” *Neuroscience* 211 (June):39–50. https://doi.org/10.1016/j.neuroscience.2011.12.041.

Barthas, Florent, Jim Sellmeijer, Sylvain Hugel, Elisabeth Waltisperger, Michel Barrot, and Ipek Yalcin. 2015. “The Anterior Cingulate Cortex Is a Critical Hub for Pain-Induced Depression.” *Biological Psychiatry* 77 (3): 236–45. https://doi.org/10.1016/j.biopsych.2014.08.004.

Becerra, L., E. Navratilova, F. Porreca, and D. Borsook. 2013. “Analogous Responses in the Nucleus Accumbens and Cingulate Cortex to Pain Onset (Aversion) and Offset (Relief) in Rats and Humans.” *Journal of Neurophysiology* 110 (5): 1221–26. https://doi.org/10.1152/jn.00284.2013.

Benbouzid, Malika, Viviane Pallage, Mathieu Rajalu, Elisabeth Waltisperger, Stéphane Doridot, Pierrick Poisbeau, Marie José Freund-Mercier, and Michel Barrot. 2008. “Sciatic Nerve Cuffing in Mice: A Model of Sustained Neuropathic Pain.” *European Journal of Pain* 12 (5): 591–99. https://doi.org/10.1016/j.ejpain.2007.10.002.

Bergel, Antoine, Thomas Deffieux, Charlie Demené, Mickaël Tanter, and Ivan Cohen. 2018. “Local Hippocampal Fast Gamma Rhythms Precede Brain-Wide Hyperemic Patterns during Spontaneous Rodent REM Sleep.” *Nature Communications* 9 (1): 5364. https://doi.org/10.1038/s41467-018-07752-3.

Bertolo, Adrien, Jeremy Ferrier, Silvia Cazzanelli, Samuel Diebolt, Mickael Tanter, Sophie Pezet, Mathieu Pernot, Bruno-Félix Osmanski, and Thomas Deffieux. 2023. “High Sensitivity Mapping of Brain-Wide Functional Networks in Awake Mice Using Simultaneous Multi-Slice fUS Imaging.” *Imaging Neuroscience*, October. https://doi.org/10.1162/imag_a_00030.

Bertolo, Adrien, Mohamed Nouhoum, Silvia Cazzanelli, Jeremy Ferrier, Jean-Charles Mariani, Andrea Kliewer, Benoit Belliard, et al. 2021. “Whole-Brain 3D Activation and Functional Connectivity Mapping in Mice Using Transcranial Functional Ultrasound Imaging.” *Journal of Visualized Experiments*, no. 168 (February), 62267. https://doi.org/10.3791/62267.

Bushnell, M. Catherine, Marta Čeko, and Lucie A. Low. 2013. “Cognitive and Emotional Control of Pain and Its Disruption in Chronic Pain.” *Nature Reviews Neuroscience* 14 (7): 502–11. https://doi.org/10.1038/nrn3516.

Chang, Pei-Ching, Sarah Lynn Pollema-Mays, Maria Virginia Centeno, Daniel Procissi, Massimo Contini, Alex Tomas Baria, Marco Martina, and Apkar Vania Apkarian. 2014. “Role of Nucleus Accumbens in Neuropathic Pain: Linked Multi-Scale Evidence in the Rat Transitioning to Neuropathic Pain.” *PAIN* 155 (6): 1128. https://doi.org/10.1016/j.pain.2014.02.019.

Colloca, Luana, Taylor Ludman, Didier Bouhassira, Ralf Baron, Anthony H. Dickenson, David Yarnitsky, Roy Freeman, et al. 2017. “Neuropathic Pain.” *Nature Reviews Disease Primers* 3 (1): 17002. https://doi.org/10.1038/nrdp.2017.2.

Costigan, Michael, Joachim Scholz, and Clifford J. Woolf. 2009. “Neuropathic Pain: A Maladaptive Response of the Nervous System to Damage.” *Annual Review of Neuroscience* 32 (1): 1–32. https://doi.org/10.1146/annurev.neuro.051508.135531.

Demene, Charlie, Jérome Baranger, Miguel Bernal, Catherine Delanoe, Stéphane Auvin, Valérie Biran, Marianne Alison, et al. 2017. “Functional Ultrasound Imaging of Brain Activity in Human Newborns.” *Science Translational Medicine* 9 (411): eaah6756. https://doi.org/10.1126/scitranslmed.aah6756.

Demene, Charlie, Thomas Deffieux, Mathieu Pernot, Bruno-Felix Osmanski, Valerie Biran, Jean-Luc Gennisson, Lim-Anna Sieu, et al. 2015. “Spatiotemporal Clutter Filtering of Ultrafast Ultrasound Data Highly Increases Doppler and fUltrasound Sensitivity.” *IEEE Transactions on Medical Imaging* 34 (11): 2271–85. https://doi.org/10.1109/TMI.2015.2428634.

Dizeux, Alexandre, Marc Gesnik, Harry Ahnine, Kevin Blaize, Fabrice Arcizet, Serge Picaud, José-Alain Sahel, Thomas Deffieux, Pierre Pouget, and Mickael Tanter. 2019. “Functional Ultrasound Imaging of the Brain Reveals Propagation of Task-Related Brain Activity in Behaving Primates.” *Nature Communications* 10 (1): 1400. https://doi.org/10.1038/s41467-019-09349-w.

Errico, Claudia, Bruno-Félix Osmanski, Sophie Pezet, Olivier Couture, Zsolt Lenkei, and Mickael Tanter. 2016. “Transcranial Functional Ultrasound Imaging of the Brain Using Microbubble-Enhanced Ultrasensitive Doppler.” *NeuroImage* 124 (January):752–61. https://doi.org/10.1016/j.neuroimage.2015.09.037.

Errico, Claudia, Juliette Pierre, Sophie Pezet, Yann Desailly, Zsolt Lenkei, Olivier Couture, and Mickael Tanter. 2015. “Ultrafast Ultrasound Localization Microscopy for Deep Super-Resolution Vascular Imaging.” *Nature* 527 (7579): 499–502. https://doi.org/10.1038/nature16066.

Gesnik, Marc, Kevin Blaize, Thomas Deffieux, Jean-Luc Gennisson, José-Alain Sahel, Mathias Fink, Serge Picaud, and Mickaël Tanter. 2017. “3D Functional Ultrasound Imaging of the Cerebral Visual System in Rodents.” *NeuroImage* 149 (April):267–74. https://doi.org/10.1016/j.neuroimage.2017.01.071.

Gonçalves, Leonor, Rui Silva, Filipa Pinto-Ribeiro, José M. Pêgo, João M. Bessa, Antti Pertovaara, Nuno Sousa, and Armando Almeida. 2008. “Neuropathic Pain Is Associated with Depressive Behaviour and

Induces Neuroplasticity in the Amygdala of the Rat." *Experimental Neurology* 213 (1): 48–56. https://doi.org/10.1016/j.expneurol.2008.04.043.

Hotta, Jaakko, Jukka Saari, Hanna Harno, Eija Kalso, Nina Forss, and Riitta Hari. 2023. "Somatotopic Disruption of the Functional Connectivity of the Primary Sensorimotor Cortex in Complex Regional Pain Syndrome Type 1." *Human Brain Mapping* 44 (17): 6258–74. https://doi.org/10.1002/hbm.26513.

Kislin, Mikhail, Ekaterina Mugantseva, Dmitry Molotkov, Natalia Kulesskaya, Stanislav Khirug, Ilya Kirilkin, Evgeny Pryazhnikov, et al. 2014. "Flat-floored Air-lifted Platform: A New Method for Combining Behavior with Microscopy or Electrophysiology on Awake Freely Moving Rodents." *JoVE (Journal of Visualized Experiments)*, no. 88 (June), e51869. https://doi.org/10.3791/51869.

Labrakakis, Charalampos. 2023. "The Role of the Insular Cortex in Pain." *International Journal of Molecular Sciences* 24 (6): 5736. https://doi.org/10.3390/ijms24065736.

LeBlanc, Brian W., Paul M. Bowary, Yu Chieh Chao, Theresa R. Lii, and Carl Y. Saab. 2016. "Electroencephalographic Signatures of Pain and Analgesia in Rats." *Pain* 157 (10): 2330–40. https://doi.org/10.1097/j.pain.0000000000000652.

Macé, Emilie, Gabriel Montaldo, Ivan Cohen, Michel Baulac, Mathias Fink, and Mickael Tanter. 2011. "Functional Ultrasound Imaging of the Brain." *Nature Methods* 8 (8): 662–64. https://doi.org/10.1038/nmeth.1641.

Makary, Meena M., Pablo Polosecki, Guillermo A. Cecchi, Ivan E. DeAraujo, Daniel S. Barron, Todd R. Constable, Peter G. Whang, et al. 2020. "Loss of Nucleus Accumbens Low-Frequency Fluctuations Is a Signature of Chronic Pain." *Proceedings of the National Academy of Sciences* 117 (18): 10015–23. https://doi.org/10.1073/pnas.1918682117.

Myers, Brent, Eduardo Carvalho-Netto, Dayna Wick-Carlson, Christine Wu, Sam Naser, Matia B. Solomon, Yvonne M. Ulrich-Lai, and James P. Herman. 2016. "GABAergic Signaling within a Limbic-Hypothalamic Circuit Integrates Social and Anxiety-Like Behavior with Stress Reactivity." *Neuropsychopharmacology: Official Publication of the American College of Neuropsychopharmacology* 41 (6): 1530–39. https://doi.org/10.1038/npp.2015.311.

Navratilova, Edita, Christopher W. Atcherley, and Frank Porreca. 2015. "Brain Circuits Encoding Reward from Pain Relief." *Trends in Neurosciences* 38 (11): 741–50. https://doi.org/10.1016/j.tins.2015.09.003.

Neugebauer, Volker, Vasco Galhardo, Sabatino Maione, and Sean C. Mackey. 2009. "Forebrain Pain Mechanisms." *Brain Research Reviews*, A Decade of Pain Research: New Approaches, New Targets, 60 (1): 226–42. https://doi.org/10.1016/j.brainresrev.2008.12.014.

Nouhoum, M., J. Ferrier, B.-F. Osmanski, N. Ialy-Radio, S. Pezet, M. Tanter, and T. Deffieux. 2021. "A Functional Ultrasound Brain GPS for Automatic Vascular-Based Neuronavigation." *Scientific Reports* 11 (1): 15197. https://doi.org/10.1038/s41598-021-94764-7.

Osmanski, Bruno-Félix, Sophie Pezet, Ana Ricobaraza, Zsolt Lenkei, and Mickael Tanter. 2014. "Functional Ultrasound Imaging of Intrinsic Connectivity in the Living Rat Brain with High Spatiotemporal Resolution." *Nature Communications* 5 (1): 5023. https://doi.org/10.1038/ncomms6023.

Park, Su Hyoun, Anne K. Baker, Vinit Krishna, Sean C. Mackey, and Katherine T. Martucci. 2022. “Altered Resting-State Functional Connectivity within Corticostriatal and Subcortical-Striatal Circuits in Chronic Pain.” *Scientific Reports* 12 (1): 12683. https://doi.org/10.1038/s41598-022-16835-7.

Rahal, Line, Miguel Thibaut, Isabelle Rivals, Julien Claron, Zsolt Lenkei, Jacobo D. Sitt, Mickael Tanter, and Sophie Pezet. 2020. “Ultrafast Ultrasound Imaging Pattern Analysis Reveals Distinctive Dynamic Brain States and Potent Sub-Network Alterations in Arthritic Animals.” *Scientific Reports* 10 (1): 10485. https://doi.org/10.1038/s41598-020-66967-x.

Schaeuble, Derek, and Brent Myers. 2022. “Cortical–Hypothalamic Integration of Autonomic and Endocrine Stress Responses.” *Frontiers in Physiology* 13 (February). https://doi.org/10.3389/fphys.2022.820398.

Sellmeijer, Jim, Victor Mathis, Sylvain Hugel, Xu-Hui Li, Qian Song, Qi-Yu Chen, Florent Barthas, et al. 2018. “Hyperactivity of Anterior Cingulate Cortex Areas 24a/24b Drives Chronic Pain-Induced Anxiodepressive-like Consequences.” *The Journal of Neuroscience* 38 (12): 3102–15. https://doi.org/10.1523/JNEUROSCI.3195-17.2018.

Sieu, Lim-Anna, Antoine Bergel, Elodie Tiran, Thomas Deffieux, Mathieu Pernot, Jean-Luc Gennisson, Mickaël Tanter, and Ivan Cohen. 2015. “EEG and Functional Ultrasound Imaging in Mobile Rats.” *Nature Methods* 12 (9): 831–34. https://doi.org/10.1038/nmeth.3506.

Soloukey, Sadaf, Arnaud J. P. E. Vincent, Djaina D. Satoer, Frits Mastik, Marion Smits, Clemens M. F. Dirven, Christos Strydis, et al. 2020. “Functional Ultrasound (fUS) During Awake Brain Surgery: The Clinical Potential of Intra-Operative Functional and Vascular Brain Mapping.” *Frontiers in Neuroscience* 13 (January):1384. https://doi.org/10.3389/fnins.2019.01384.

Suzuki, Takahiro, Mitsuyuki Amata, Gaku Sakaue, Shinya Nishimura, Takaya Inoue, Masahiko Shibata, and Takashi Mashimo. 2007. “Experimental Neuropathy in Mice Is Associated with Delayed Behavioral Changes Related to Anxiety and Depression.” *Anesthesia & Analgesia* 104 (6): 1570–77. https://doi.org/10.1213/01.ane.0000261514.19946.66.

Ulrich-Lai, Yvonne M., Kenneth R. Jones, Dana R. Ziegler, William E. Cullinan, and James P. Herman. 2011. “Forebrain Origins of Glutamatergic Innervation to the Rat Paraventricular Nucleus of the Hypothalamus: Differential Inputs to the Anterior versus Posterior Subregions.” *The Journal of Comparative Neurology* 519 (7): 1301–19. https://doi.org/10.1002/cne.22571.

Urban, Alan, Clara Dussaux, Guillaume Martel, Clément Brunner, Emilie Mace, and Gabriel Montaldo. 2015. “Real-Time Imaging of Brain Activity in Freely Moving Rats Using Functional Ultrasound.” *Nature Methods* 12 (9): 873–78. https://doi.org/10.1038/nmeth.3482.

Wang, Zhifu, Sheng Huang, Xiangmei Yu, Long Li, Minguang Yang, Shengxiang Liang, Weilin Liu, and Jing Tao. 2020. “Altered Thalamic Neurotransmitters Metabolism and Functional Connectivity during the Development of Chronic Constriction Injury Induced Neuropathic Pain.” *Biological Research* 53 (1): 36. https://doi.org/10.1186/s40659-020-00303-5.

Williams, D. J., A. R. Crossman, and P. Slater. 1977. “The Efferent Projections of the Nucleus Accumbens in the Rat.” *Brain Research* 130 (2): 217–27. https://doi.org/10.1016/0006-8993(77)90271-2.

Wood, Miranda, Othman Adil, Tyler Wallace, Sarah Fourman, Steven P. Wilson, James P. Herman, and Brent Myers. 2019. “Infralimbic Prefrontal Cortex Structural and Functional Connectivity with the

Limbic Forebrain: A Combined Viral Genetic and Optogenetic Analysis." *Brain Structure & Function* 224 (1): 73–97. https://doi.org/10.1007/s00429-018-1762-6.

Yalcin, Ipek, Yohann Bohren, Elisabeth Waltisperger, Dominique Sage-Ciocca, Jerry C. Yin, Marie-José Freund-Mercier, and Michel Barrot. 2011. "A Time-Dependent History of Mood Disorders in a Murine Model of Neuropathic Pain." *Biological Psychiatry* 70 (10): 946–53. https://doi.org/10.1016/j.biopsych.2011.07.017.

Yalcin, Ipek, Salim Megat, Florent Barthas, Elisabeth Waltisperger, Mélanie Kremer, Eric Salvat, and Michel Barrot. 2014. "The Sciatic Nerve Cuffing Model of Neuropathic Pain in Mice." *Journal of Visualized Experiments*, no. 89 (July), 51608. https://doi.org/10.3791/51608.

Zhu, Kun, Jianchao Chang, Siya Zhang, Yan Li, Junxun Zuo, Haoyu Ni, Bingyong Xie, et al. 2024. "The Enhanced Connectivity between the Frontoparietal, Somatomotor Network and Thalamus as the Most Significant Network Changes of Chronic Low Back Pain." *NeuroImage* 290 (April):120558. https://doi.org/10.1016/j.neuroimage.2024.120558.

Zhuo, Min. 2008. "Cortical Excitation and Chronic Pain." *Trends in Neurosciences* 31 (4): 199–207. https://doi.org/10.1016/j.tins.2008.01.003.

CHAPTER 4

ARTICLE N°3:

High sensitivity mapping of brain-wide functional networks in awake mice using simultaneous multi-slice fUS imaging

INTRODUCTION OF THE ARTICLE N°3

As discussed in the introduction, one of the main limitations of fUS imaging was its 2D feature. To circumvent this limitation, several studies in the laboratory proposed different strategies to image in pseudo or real 3 dimensions. In a previous study (Bertolo et al. 2021), presented in chapter 2, we used a volumetric fUS using 2D transducer, thanks to a motorized linear array. Such approach allowed multiple brain slices to be scanned rapidly and repeatedly. This approach allows for 3D fUS imaging at a framerate which remains compatible with resting-state FC measurement. Using this method, FC measurements were feasible for a volumetric reconstruction of maximum 4 planes imaged repetitively.

In the following study, (in which I was involved in the development of the experimental design and the execution of all experiments), we proposed a new approach to perform 3D imaging, enabling high-sensitivity mapping of brain-wide functional network.

This new hybrid solution is dedicated to brain-wide transcranial FC studies in mice, based on a newly developed multi-array probe, consisting of four combined linear arrays, allowing simultaneous multi-slicing of the entire mouse cerebrum. Allowing for resting-state FC analysis across the entire brain.

In this study we demonstrated the reproducibility of this new 3D imaging modality by describing its capability to detect task-evoked (visual stimulation) brain responses in anesthetized mice, and furthermore to evaluate resting-state FC in awake head-fixed animals. We measured functional connectivity imaging over 16 complete coronal slices, providing a more comprehensive view of brain functional networks in the whole mouse brain through the skull. Seed-based and multivariate analyses revealed reliable detection of bilateral connectivity, including long-range connections in both cortical and subcortical brain regions.

Imaging Neuroscience
an open access journal

Research Article

High sensitivity mapping of brain-wide functional networks in awake mice using simultaneous multi-slice fUS imaging

Adrien Bertolo[a,b], Jeremy Ferrier[b], Silvia Cazzanelli[a,b], Samuel Diebolt[a,b,c], Mickael Tanter[a], Sophie Pezet[a], Mathieu Pernot[a,*], Bruno-Félix Osmanski[b,*], Thomas Deffieux[a,*]

[a]Physics for Medicine Paris, ESPCI Paris, INSERM, CNRS, PSL Research University, Paris, France.
[b]Iconeus, Paris, France.
[c]Institute of Psychiatry and Neuroscience of Paris, INSERM, University of Paris, France

*Colast authors.

Corresponding Authors: Adrien Bertolo (adrien.bertolo@espci.fr), Thomas Deffieux (thomas.deffieux@inserm.fr)

ABSTRACT

Functional ultrasound (fUS) has received growing attention in preclinical research in the past decade, providing a new tool to measure functional connectivity (FC) and brain task-evoked responses with single-trial detection capability in both anesthetized and awake conditions. Most fUS studies rely on 2D linear arrays to acquire one slice of the brain. Volumetric fUS using 2D matrix or row-column arrays has recently been demonstrated in rats and mice but requires invasive craniotomy to expose the brain due to a lack of sensitivity. In a previous study, we proposed the use of motorized linear arrays, allowing imaging through the skull in mice for multiple slices with high sensitivity. However, the tradeoff between the field of view and temporal resolution introduced by motorized scanning prevents acquiring brain-wide resting-state FC data with a sufficient volume rate for resting-state FC analysis. Here, we propose a new hybrid solution optimized and dedicated to brain-wide transcranial FC studies in mice, based on a newly developed multi-array transducer allowing simultaneous multi-slicing of the entire mouse cerebrum. We first demonstrate that our approach provides a better imaging quality compared to other existing methods. Then, we show the ability to image the whole mouse brain non-invasively through the intact skin and skull during visual stimulation under light anesthesia to validate this new approach. Significant activation was detected along the whole visual pathway, at both single and group levels, with more than 10% of augmentation of the cerebral blood volume (CBV) signal during the visual stimulation compared to baseline. Finally, we assessed resting-state FC in awake head-fixed animals. Several robust and long-ranged FC patterns were identified in both cortical and sub-cortical brain areas, corresponding to functional networks already described in previous fMRI studies. Together, these results show that the multi-array probe is a valuable approach to measure brain-wide hemodynamic activity in mice with an intact skull. Most importantly, its ability to identify robust resting-state networks is paving the way towards a better understanding of the mouse brain functional organization and its breakdown in genetic models of neuropsychiatric diseases.

Keywords: volumetric imaging, functional ultrasound, brain imaging, visual pathway, functional connectivity, awake mice, connectomics

1. INTRODUCTION

Functional ultrasound (fUS) imaging is a recent modality that is able to probe the brain activity at a high spatiotemporal resolution (Mace et al., 2013; B.-F. Osmanski et al., 2014). In a similar way to blood oxygen level-dependent functional magnetic resonance imaging (BOLD-fMRI), fUS imaging relies on the neurovascular coupling to infer brain activity indirectly from measurement of hemodynamic

Received: 12 July 2023 Revision: 12 October 2023 Accepted: 13 October 2023 Available Online: 23 October 2023

signals. This is achieved by combining multiple echoes from thousands of ultrasound plane waves emitted at an ultrafast frame rate. The resulting Power Doppler (PD) signal is directly proportional to the CBV, that is, the amount of blood flowing through the voxel at a point in time.

fUS is particularly suited for studying neural networks in the mouse brain, the most common preclinical model in neuroscience. Using an emission frequency of 15 MHz, fUS images yield an in-plane spatial resolution of 100 × 100 µm (and ~500 µm slice thickness). The direct visualization of blood flow through the Doppler effect also gives fUS imaging a remarkable sensitivity to hemodynamic variations and specifically to those of neuronal origin. A growing body of evidence is now showing that fUS signals faithfully report multi-unit neuronal activity in mice through the neurovascular coupling (Aydin et al., 2020; Boido et al., 2019; Nunez-Elizalde et al., 2022), despite open questions regarding single unit activity uncoupling in primates at rest (Claron et al., 2023).

Most importantly, fUS is seamlessly compatible with awake behaving animals, whether head-fixed (Ferrier et al., 2020; Macé et al., 2018) or freely moving (Rabut et al., 2020; Sieu et al., 2015; Tiran et al., 2017) thanks to the miniaturization of ultrasonic linear arrays (2D imaging) which can now be tethered to the animal's head using an implanted frame. Hence, fUS has been successfully applied to characterize many task-based (Gesnik et al., 2017; Macé et al., 2011, 2018; B. F. Osmanski et al., 2014) and resting-state functional systems (Ferrier et al., 2020; B.-F. Osmanski et al., 2014; Rabut et al., 2020).

However, a main restriction compared to fMRI is the 2D limitation, due to the geometry of current ultrasonic probes (1D linear arrays). While sequential scanning of the entire brain has been proposed using a motorized stage, it involves long acquisition time (>2 h per animal) and repeated stimulus presentation at each position to cover the whole brain (Gesnik et al., 2017; Macé et al., 2018). As multiple sessions must be repeated at each position to capture the whole brain, one limitation of this method is also that the animal's behavior may vary from one session to another, and thus across slices. Most importantly, this approach is incompatible with the study of resting-state functional connectivity networks as it is inherently based on the synchronous measure of spontaneous oscillatory activity within spatially distributed brain regions (Coletta et al., 2020). We recently introduced an alternative approach using fast plane-switching transducers to significantly reduce the scanning time (Bertolo, Nouhoum, et al., 2021). However, the tradeoff between the number of positions imaged and the time resolution limits the field of view to a section of a few millimeters only.

On the other hand, full-3D volumetric fUS has been successfully achieved in rodents using fully populated matrix (FPM) arrays and row-column addressing (RCA) transducers. However, this approach suffers from a significant lack of sensitivity, calling for a surgery to expose the brain (Brunner et al., 2020; Rabut et al., 2019; Sauvage et al., 2019). In this context, further developments are needed to improve the spatial coverage of fUS imaging to achieve a more global view of the brain without compromising on resolution, frame rate, or sensitivity.

Here, we introduce a new multi-array probe consisting of four combined linear arrays, allowing simultaneous multi-slice (SMS) fUS imaging of the mouse brain. This new type of transducer increases fUS time resolution by a factor of four without compromising on sensitivity and spatial resolution. We first show that the multi-array probe can achieve almost brain-wide coverage in mice at 100 × 100 × 525 µm in under 2.4 s, non-invasively through the skin and bone. By comparing the imaging quality across different methods on the same animal before and after craniotomy, we provide evidence that the multi-array probe is more sensitive than FPM and RCA transducers. We then validate the ability of SMS-fUS imaging to spatially map brain activity using a simple visual activation paradigm in lightly anesthetized animals, showing significant CBV increases in areas of the visual pathway. Finally, this approach is extended to resting-state functional connectivity mapping in awake head-fixed mice. Seed-based and multivariate analyses reveal reliable detection of bilateral connectivity, including long-range connections in both cortical and subcortical brain regions.

2. MATERIALS AND METHODS

2.1. Ethics

Twelve male C57BL/6 mice (7-8 weeks old, Janvier Labs, France) were used with approval from our local ethics committee (Comité d'éthique en matière d'expérimentation animale number 59, "Paris Centre et Sud", project #2017-23). Animals were housed four per cage with a 12 h light/dark cycle, a constant temperature at 22°C, and unlimited access to food and water. Before beginning the experiments, animals are given a 1-week minimum acclimatization period to housing conditions. All experiments have been performed in agreement with the

European Community Council Directive of 22 September 2010 (010/63/UE).

Methods were carried out following relevant guidelines and regulations and in compliance with ARRIVE guidelines (Percie du Sert et al., 2020).

2.2. Visual stimulation experiments in lightly anesthetized mice

Visual stimulation experiments were performed in a dark room, with mice in a lightly anesthetized condition (Fig. 1(ii)). All acquisitions (one per animal, n = 6) were considered in the statistical analysis.

2.2.1. Animal preparation

Mice were anesthetized by an initial intraperitoneal (IP) injection of ketamine and xylazine mixture at 100 mg/kg and 10 mg/kg, respectively. The hair was shaved using depilatory cream, and the mouse was positioned on a stereotaxic frame. Anesthesia was maintained with a low isoflurane supply throughout the imaging session (0.5% administered through a nose cone in an 80/20 air/oxygen stream). The eyes of the mouse were protected using an ointment (Ocry-gel, TVM, UK). Body temperature was controlled with a rectal probe connected to a heating pad set at 37°C. Respiration and heart rate were monitored using a PowerLab data acquisition system with the LabChart software (ADInstruments, USA). Additional IP ketamine/xylazine doses (25 mg/kg and 2.5 mg/kg, respectively) were infused intermittently (every 90 to 120 min), as deemed necessary based on changes in physiological parameters.

2.2.2. Visual stimulation protocol

Visual stimulation was delivered using a white LED light positioned 30 cm from the mouse (measured luminance of 15 lux). After a baseline of 60 s, eight stimuli (30 s of flickered light consisting of 200 ms pulses with a 4 Hz frequency) were repeated every 90 s, resulting in a total acquisition duration of 780 s.

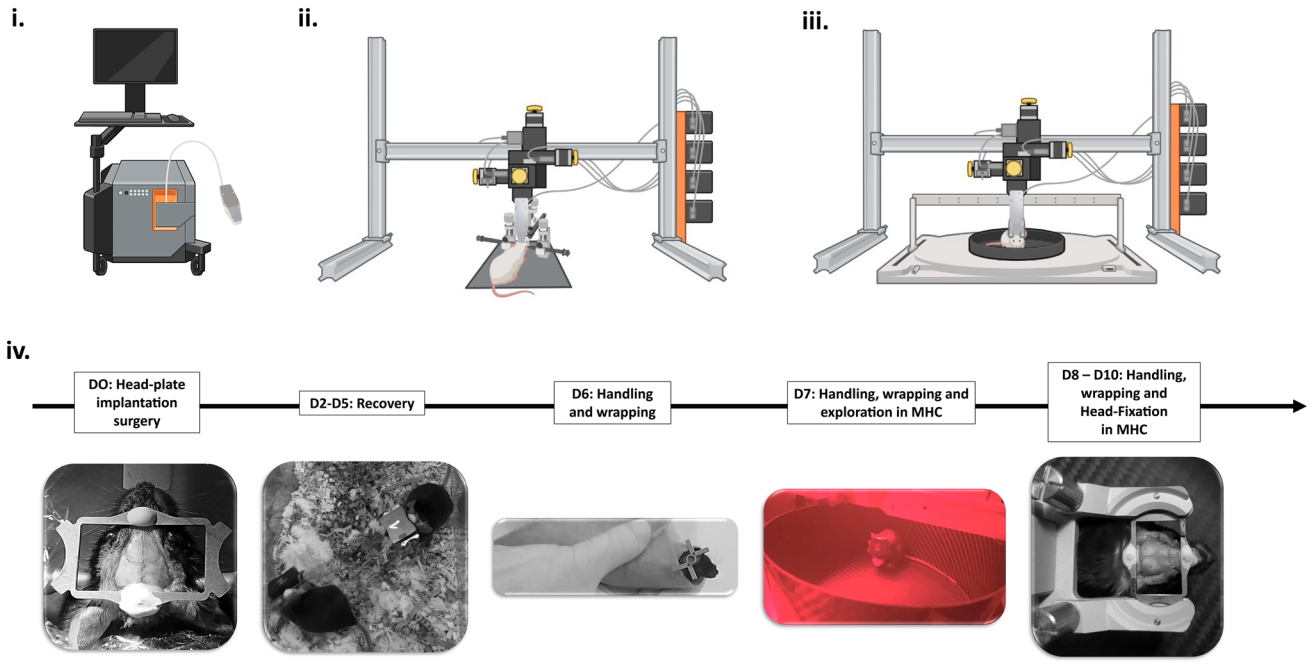

Fig. 1. Experimental designs used for both anesthetized experiments (ii) and awake (iii, iv) experiments. (i) Iconeus One scanner (256 channels ultrasound system) driving the multi-array probe. (ii) Experimental setup for visual stimulation in lightly anesthetized mice. The anesthetized mouse is shaved and placed in a stereotaxic frame. The multi-array probe is mounted on a 4-axis motorized stage. A white LED is placed 30 cm from the mouse's eyes for visual stimulation. (iii) Experimental setup for resting-state functional connectivity in awake mice. The multi-array probe is mounted on the 4-axis motor stage, and placed just above the head of the mouse, in the MHC. (iv) Different steps of the animal habituation protocol (post-surgery recovery, handling, wrapping for installation in the MHC, head-fixed exploration in the MHC). The first imaging session can be set at D11.

2.3. Resting-state functional connectivity in awake mice

Resting-state FC acquisitions (1200 s) were performed in awake head-fixed conditions (Fig. 1(iii)). Two animals (out of six) underwent a second imaging session as the rate of calm periods was considered as too short (more details can be found in Section 2.6).

2.3.1. Surgical implantation of metal plate

A headpost with an imaging window of 13 × 21 mm² was surgically implanted for head fixation. The procedure has been described in detail previously (Bertolo, Nouhoum, et al., 2021). Briefly, mice were anesthetized using ketamine (100 mg/kg) and medetomidine (1 mg/kg). After hair shaving and skin disinfection, lidocaine was administered under the scalp, and the skin was excised. The head plate (Neurotar, Model 14) was attached to the skull using two anchoring screws and dental cement (Superbond, C&B). The imaging window was sealed using Kwik-cast, and anesthesia was reversed by a subcutaneous atipamezole injection (1 mg/ml). Meloxicam (5 mg/kg, IP) was administered for postoperative pain, and the mice were recovered in their home cage.

2.3.2. Habituation and training

A head-restrained imaging setup was used for awake imaging (Mobile HomeCage, Neurotar, Finland). The mice were head-fixed with a rigid metal clamp and positioned in a floating round carbon-fiber cage, allowing them to explore the environment freely. Six days after the surgery, mice were repeatedly manipulated by the experimenter for a couple days and left to freely explore the Mobile HomeCage (MHC). From day 3, the animals were habituated to head fixation in the MHC by gradually increasing the time of each session, from 5 min initially, rising to 60 on day 6 (the day of the imaging session). The critical experimental design time points are listed in Figure 1(iv).

2.4. The multi-array probe

A 15 MHz multi-array probe was developed consisting in four compact linear arrays of 64 elements, with a pitch of 110 µm (IcoPrime-4D Multi-array, Iconeus, Paris, France). The high sensitivity of this probe is due to several factors, including the large active surface of each element (1.5 mm width), the small pitch (~λ), and the presence of an acoustic lens under each array enabling the acoustic energy to be focused on a slice of approximately 500 microns (minimum thickness at 8 mm depth) similarly to linear arrays. The four independent linear arrays were designed to be tightly assembled with only 2.1 mm from each other to minimize acoustical cross-talk (see Supplementary Fig. 3) and optimize the field of view. The total number of elements can be addressed simultaneously with a 256-channel scanner such as the Iconeus One system (256 channels).

The dedicated imaging sequence and the live Doppler reconstruction procedure were implemented in a live acquisition software (IcoScan, Iconeus, Paris, France), as described in the following sub-sections.

2.4.1. Imaging sequence and beamforming with the multi-array probe

The imaging sequence was implemented using the same ultrafast plane wave transmission and reception scheme replicated for each of the four linear arrays. Four images (one per array) were simultaneously obtained from 4 × 200 compounded frames acquired at 500 Hz ($T_{integration} = 0.4s$) using 4 × 8 tilted plane waves acquired at a pulse repetition frequency of 4 kHz (-12°, -8.57°, -5.14°, -1.71°, 1.71°, 5.14°, 8.57°, 12°). To compensate for the limited lateral aperture size (64 elements compared to 128 in conventional linear arrays), we used a trapezoidal beamforming grid with $\theta_{max} = 12°$, allowing the field of view to be extended on both sides and enabling the retrieval of deeper lateral brain regions.

2.4.2. Clutter filtering

Each block of 0.4 s was filtered using a Singular Value Decomposition (SVD) clutter filter to separate tissue signal from blood signal and form a PD image (Demene et al., 2015).

Briefly, the signal matrix from a Doppler block $S\left(N_x, N_y, N_z, N_t\right)$ was first reshaped to a Casorati matrix $M_c\left(N_x.N_y.N_z, N_t\right)$ and decomposed by an SVD procedure as follows:

$$M_c = U.S.V^* \tag{1}$$

where S is a diagonal matrix with coefficients λ_i, corresponding to the ordered singular values associated with a spatial singular vector U_i whose temporal variations are described by the temporal singular vector V_i. The signal associated with blood can be expressed as:

$$S_{blood} = \sum_{N_{cut}+1}^{200} U_i.\ \lambda_i.V_i^* \tag{2}$$

as the first N_{cut} spatiotemporal modes are associated with tissue with high energy. For anesthetized experiments (as there isn't any motion), we used a fixed threshold $N_{cut} = 60$ (Demene et al., 2015). For awake experiments (episodic motion), the threshold N_{cut} was set adaptively for each Doppler block using a fixed energy threshold (Baranger et al., 2018; Maresca et al., 2018).

2.4.3. Motorized fast scanning with the multi-array probe

As illustrated in Figure 2(i), the four arrays are separated by 2.1 mm, and the acoustic lenses allow four acoustic beams to focus along the elevation direction with a full-width half-maximum (FWHM) of 0.5 mm. By translating the probe at four positions separated by 0.525 mm (a quarter of the inter-array distance, Fig. 3(i) and (ii)), we can achieve a final volume of 16 contiguous slices with a repetition time (TR) of 2.4 s (Fig. 3(iii) and (iv)). Up to a step of 0.525 mm, the scanning is considered non-interrupted slicing, ensuring that the whole-brain volume is sampled without any gaps between the slices. The TR of 2.4 s not only considers the integration time ($T_{integration} = 0.4\,s$), but also considers the dead time during which the probe is translated ($T_{translation} = 0.2\,s$) and the number of positions (four). To avoid long displacements and make sure that $T_{translation}$ does not last more than 200 ms between the last position and the first one (before starting each new volume), the scanning order of the different positions was optimized to limit the maximum displacement to two steps (1.050 mm) using an interleaved sequence (1-3-4-2 if $n_{positions} = 4$). Regarding this maximum displacement and considering the configuration of our motor setup, the maximal translation time was estimated at 0.1 s. All sequence parameters are summarized in Table 1, and the whole procedure is described in Figure 3.

If $n_{positions} > 1$, TR can be expressed as:

$$TR = n_{positions}\left(T_{integration} + T_{translation}\right) \quad (4)$$

$n_{positions}$ and $T_{integration}$ parameters can be set to different values, and we will discuss the implications of temporal resolution and SNR later in the Section 4.

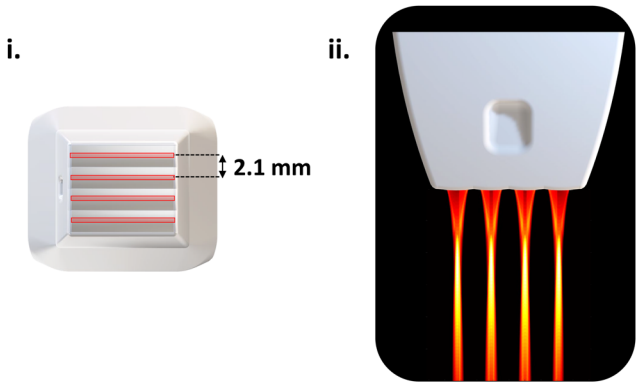

Fig. 2. Multi-array probe. (i) Top view of the multi-array probe. The schematic of the probe head shows four acoustic lenses, separated by 2.1 mm. The slice thickness (0.5 mm) is represented with the red rectangles in the center of each array. (ii) Lateral view of head of the multi-array probe. The emitted pressure field, simulated with Field II software, is represented under each array, and thresholded at -6 dB.

2.4.4. Comparison with RCA and matrix transducers

We performed acquisitions of 180 s with the MUX-FPM, the RCA, and the multi-array probes on the same animal, before and after craniotomy (removal of the skull) and compared the image quality.

For the surgery and the following brain imaging session, the mouse was anesthetized with an initial intraperitoneal injection of ketamine and xylazine mixture. Then, anesthesia was maintained with a 1.5% isoflurane supply and the animal physiology was monitored following the protocol already described in Section 2.2.1. An additional subcutaneous injection of buprenorphine (0.1 mg/kg) was administered to provide analgesia, A 1 × 1 cm skull window was removed by drilling (Foredom) at low speed using a microdrill steel burr (Burr number 19007-07, Fine Science Tools) while leaving the dura intact.

The imaging sequence parameters for the RCA and MUX-FPM are detailed in Supplementary Table 1. All the probes were centered at 15 MHz.

For the RCA sequence, 20 tilted plane-wave were transmitted alternatively with the rows and the columns, while backscattered echoes were always received with the orthogonal aperture. We used the XDoppler approach (Bertolo, Sauvage, et al., 2021) to obtain an isotropic PSF with reduced side-lobe levels. The MUX-FPM sequence was designed to drive one sub-aperture of 32 × 8 piezo elements (representing a quarter of the whole aperture) at a time, and the back-scattered echoes were received on the whole aperture after four transmissions and receptions, thus allowing a frame rate of 333 Hz for nine tilted plane waves. The MUX FPM and RCA volumes were further averaged over 2.4 s to match the volume rate of the multi-array acquisition scheme.

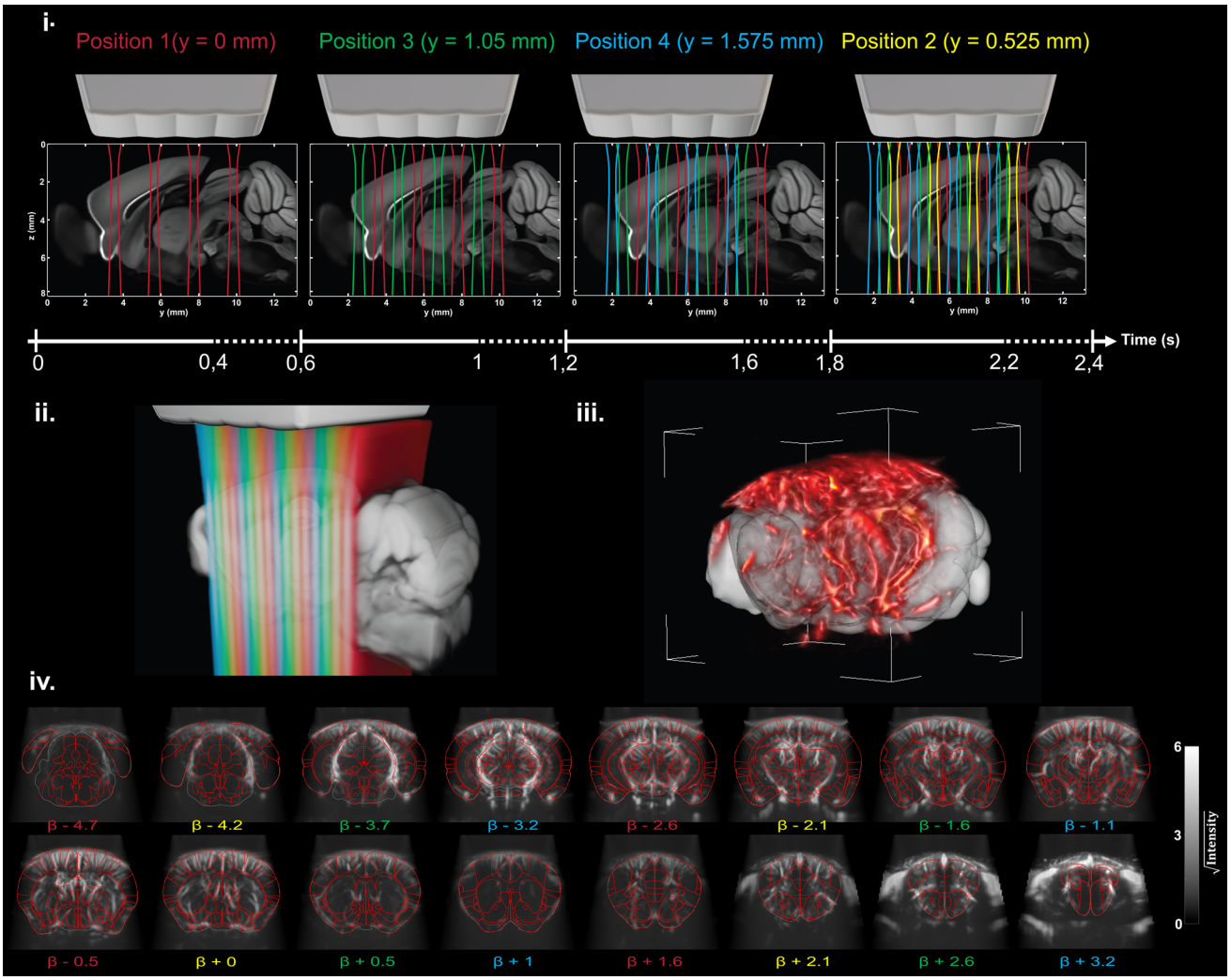

Fig. 3. Principle of motorized fast scanning for whole-brain transcranial fUS imaging. (i) The probe is translated at each position following the order 1-3-4-2 (with interleaving) to minimize the translation distance and keep the translation time below 0.2 s. The step between slices is set to 0.525 mm, allowing homogeneous scanning of the dead volume between two arrays (2.1 mm). At each position, the probe rests for 0.4 s to acquire 4 × 200 compounded frames at 500 Hz. The resulting pressure field (simulated with Field II (Jensen, 1997)) is represented under each array, and overlaid on the two-photon Allen template. Every 2.4 s, the 16 continuous slices (ii) are beamformed, processed, and concatenated to form a 3D volume (iii). These 16 PD slices are also depicted in (iv) with their corresponding anatomical coordinate relative to Bregma coordinates (in mm) and overlaid with the envelope of the main Allen atlas regions. This cycle is repeated constantly during the whole acquisition. The PD scan represented in (iv) was performed on an anesthetized mouse.

Table 1. Summary of the recommended sequence parameters for whole-brain SMS fUS imaging.

Spatial specifications					Temporal specifications			
Field of view	Depth	In-plane resolution	Number of slices	Step between slices	Frame rate	Doppler integration	Pause duration	Repetition time
β-4.9 to β+3	1 mm to 11 mm	100 µm × 100 µm	16	525 µm	500 Hz	0.4 s	0.2 s	2.4 s

All volumes were registered and resampled in the same space to allow the extraction of PD intensity profiles along the same voxels, and Contrast to Noise Ratio (CNR) estimation from the same vessel and background regions of interest for the different acquisitions.

2.5. Automatic atlas registration, and ROI segmentation

All volumetric scans were co-registered to an average scan and aligned to a standard Doppler reference template, already pre-aligned with the Allen Mouse Brain Atlas common coordinates framework (Nouhoum et al., 2021; Wang et al., 2020) (Fig. 3(iii)). An initial affine transformation matrix was first determined using a convolutional neuronal network (Blons et al., 2022) trained to identify nine vascular landmark locations in an angiographic scan. From the identification of these landmarks in both the scan and the reference template, we could estimate a first affine transformation aligning the scan to the Doppler reference. A refined affine transformation was finally determined from this initial transformation by running an iterative intensity-based registration algorithm (Nouhoum et al., 2021).

An indirect evaluation of the registration was proposed by introducing a "matching score". This score is defined as the average correlation between the registered scan and the averaged template from the whole dataset. This score is reported for each session in Supplementary Figure 1.

2.6. Scans pre-processing pipeline

The entire pre-processing pipeline is illustrated in Figure 4, and further details about every step are provided in this section. Slice timing correction (STC) was systematically applied by resampling the data on a common time basis (first position) to consider the delays in slices, using linear interpolation.

Then, the baseline low-frequency drift was estimated (voxel-wise) with *polyfit* function (MATLAB), using a polynomial of degree 3, and subtracted from the fUS signal.

Despite adaptative clutter filtering, a variable portion of certain acquisitions had to be removed in each scan because of the high motion. Calm "resting" periods were automatically determined from the whole-brain global signal (GS) Doppler profile. The baseline of the GS was first estimated with a linear regression. Then, periods were considered as calm when the GS standard variations were kept below 5% of the GS baseline level for at least 60 s, and a calm score was computed as the total useful duration corresponding to resting periods during a whole acquisition. This score is reported in Supplementary Figure 1. Two acquisitions with less than 10 min of calm periods were removed from the resting-state analysis. For the corresponding animals, another imaging session led to less artefactual acquisitions, and was thus considered in the FC analysis.

To study the slow CBV fluctuations associated with resting-state FC, the fUS signal of each calm period was first standardized before applying a bandpass filter. According to the fMRI literature (Biswal et al., 1995) and recent fUS studies (Nunez-Elizalde et al., 2022) characterizing these low-frequency oscillations, the frequency band was chosen between 0.01 Hz and 0.1 Hz. Then, all the filtered calm periods were temporally concatenated. Finally, the GS of the resulting pre-processed scan was derived and considered as a confounding variable to reduce non-neuronal sources of variance for awake resting-state FC data. The choice to integrate the global signal regression (GSR) procedure for the processing of our awake dataset will be discussed later in the manuscript.

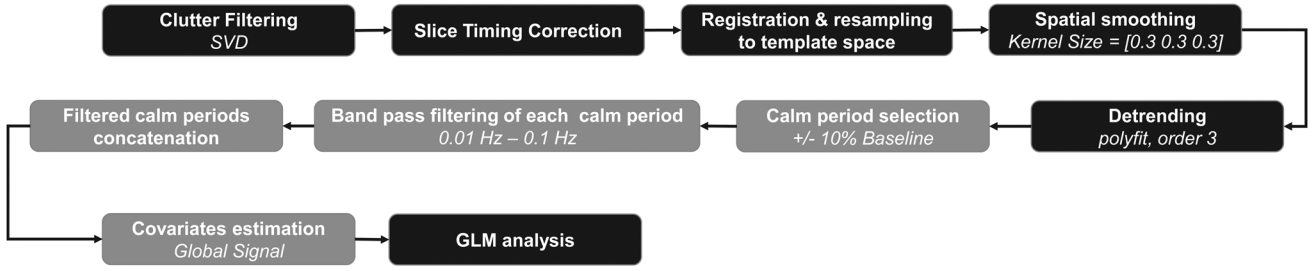

Fig. 4. Block diagram describing each step of the processing pipeline. Steps represented in gray blocks are specific to awake resting-state data pre-processing.

2.7. Statistical analysis

2.7.1. General linear model (GLM) for visual stimulation activation maps and resting-state FC seed-based maps estimation

Activation maps (visual stimulation) and seed-based maps (resting-state FC) were computed using a GLM applied on pre-processed scans.

For visual stimulation, the stimulus response was modeled by convolving the stimulus pattern with a four half-cosine canonical hemodynamic response function. This signal was rescaled so that its value was zero when there was no stimulus and one during the stimulus. The baseline could then be directly extracted from our model from the intercept value.

For seed-based maps, the expected signal was taken as the average CBV time course in the seed ROI. A t-statistic with its corresponding p-value was derived for each voxel to assess the GLM significance, comparing the baseline condition (contrast = 0) and the stimulus (contrast = 1).

The familywise error rate (FWER) for subject-level analysis was controlled by the Bonferroni procedure, adopting a false discovery rate of 0.05.

Group-level significance was assessed with a one-sample Student t-test performed on the individual t-maps, with a false discovery rate of 0.05. Correction for multiple comparisons was done with maximal statistic permutation testing combined with threshold free cluster enhancement (TFCE) (Smith & Nichols, 2009).

2.7.2. Average relative CBV (rCBV) profiles in activated areas during visual stimulation experiments

Hemodynamic responses to visual stimulation were estimated by computing the relative change in CBV (rCBV) in percentage, obtained by subtracting the CBV baseline and dividing by the CBV baseline afterwards.

The rCBV time profiles were extracted in 228 Allen regions of interest (Supplementary Table 2) and represented through temporal raster plots (Fig. 6(ii)). The percentage of significantly activated voxels in each of these regions was determined by overlapping the Allen segmentation to the p-value map obtained with the GLM analysis (gray-scale colorbars on raster plots). We also plotted the rCBV of significantly activated voxels in important regions of the visual pathway (Fig. 6(iv)).

For each subject, the inter-trial rCBV was estimated by averaging the eight trials within an imaging session (Fig. 6(ii, v)). Finally, the inter-subject (n = 6) and inter-trial rCBV was finally derived by averaging inter-trial rCBV profiles of each subject (Fig. 7(iii, iv)).

2.7.3. Functional connectivity matrix estimation

Thanks to the registration procedure, the Allen atlas segmentation could be used to perform automatic Allen-based CBV extraction over more than 200 brain regions of interest (ROI) distributed in the whole brain (listed in Supplementary Table 2). The Pearson correlation coefficient was computed between every pre-processed and spatially averaged signal (in each ROI). Subject-level FC matrices were Fisher-transformed and averaged across subjects (n = 6). The group-average matrix was finally re-transformed to Pearson correlations. We also performed a one-sample t-test (two-tailed, $p < 0.05$, FDR corrected) to test whether the average coefficients were different from zero.

For each session, the value of the correlation between two symmetric regions taken in the somatosensory cortex (SS), and between the somatosensory cortex and the anterior cingulate cortex (ACA) was taken as a quality control metric, describing the specific or unspecific character of functional connectivity (Supplementary Fig. 1) (Grandjean et al., 2017).

2.7.4. Independent component analysis (ICA) for functional networks identification

Independent components (ICs) were estimated by running *fastICA* 100 times with *icasso* stabilization MATLAB algorithms (Himberg & Hyvarinen, 2003; Ntekouli, 2019) on co-registered pre-processed and temporally concatenated resting-state FC scans (awake condition, n = 6). Different dimensionalities were tested: 15, 25, and 35. We chose to set the number of ICs to 25, as it was found to best represent the heterogeneity of our dataset with a good stability. Finally, plausible FC networks were classified manually by following the same rules as the ones proposed by Zerbi *et al.* (2015) and Grandjean *et al.* (2017) fMRI studies. The general assumption behind this identification is: if there are active functional networks, those functional network components will closely match known structural networks among vascular or noise components. Out of the 25 group-level ICs, we identified 16 spatial components associated with functional systems. To enhance functional regions visualization, each spatial map was scaled to Z-scores and thresholded to $|Z| > 3$ (corresponding to $p < 0.001$).

Finally, volumetric representations were constructed by extracting the boundary surface of the resulting binarized mask.

3. RESULTS

3.1. The multi-array probe is more sensitive than RCA and matrix arrays

The results of the image quality comparison between the MUX-FPM, the RCA and the multi-array probes are presented in Figure 5. We focused our comparisons on three coronal slices, intersecting β-3.3 mm, β-2.3 mm, and β + 0.15 mm. The sensitivity was assessed by comparing CNR estimations from the same vascular and background regions for all acquisitions. Vessel's intensity profiles were also extracted along the same voxels.

In both trepanned and transcranial conditions, the multi-array provides a better image quality than MUX-FPM and RCA probes, with higher CNR values. Higher peak amplitude and more small vessels were revealed with PD intensity profiles for the multi-array.

In transcranial condition, the vascular signal is completely lost with the MUX-FPM, and the multi-array offers a better contrast compared to the RCA on the vessel's intensity profiles.

Interestingly, the CNR obtained with the multi-array in transcranial condition is still better than the one measured with the MUX-FPM without the skull.

3.2. Functional hyperaemia induced by visual stimulation in lightly anesthetized mice

To validate the multi-array approach, we first evaluated the ability to detect CBV responses in the whole brain during visual stimuli.

Figure 6 shows the visual responses obtained in one representative mouse after one experiment of 780 s. Activation maps obtained with GLM analysis revealed significant activation in all regions of the visual pathway: the lateral geniculate nucleus (LGN), the superior colliculus (SC), the primary visual cortex (V1), and the retrosplenial cortex (RS), as represented in Figure 6(i). The raster plot in Figure 6(ii) shows the rCBV response in the whole brain. The percentage of activated voxels was derived in each of the 228 segmented Allen regions (Supplementary Table 2) and is represented with the gray colorbar. Moreover, the rCBV time profile shows single-trial detection in each region. On average (across trials), the rCBV increase reached 5% in the LGN, 7% in the SC, 16% in the V1, and 9% in RS in this experiment.

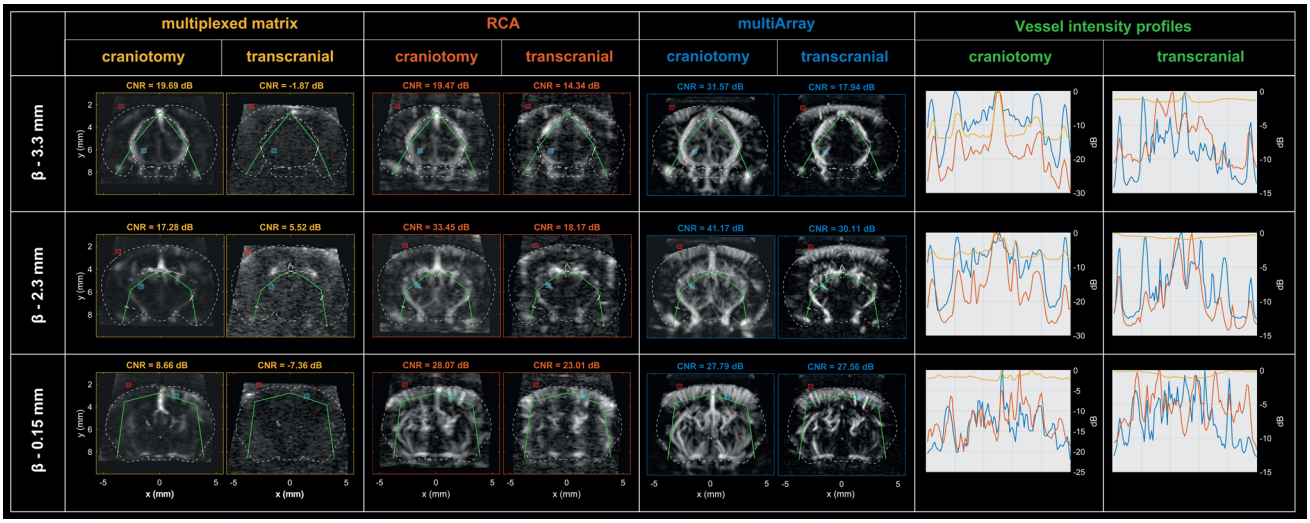

Fig. 5. Assessing the imaging quality before and after craniotomy: comparative analysis of the multi-array probe against RCA and MUX-FPM probes. Comparisons were focused on three coronal slices, represented in each row of this comparative table. For each probe, the first column represents PD images after craniotomy whereas the second one represents PD images before craniotomy. For each slice, the vessel ROI is represented with the cyan square whereas the background ROI is represented with the red square. The green line indicates the voxels along which PD profiles were extracted for contrast comparison (last column). Whereas the multi-array probe provides the best imaging quality before and after craniotomy, the MUX-FPM is not sensitive enough to detect blood flow through the skull.

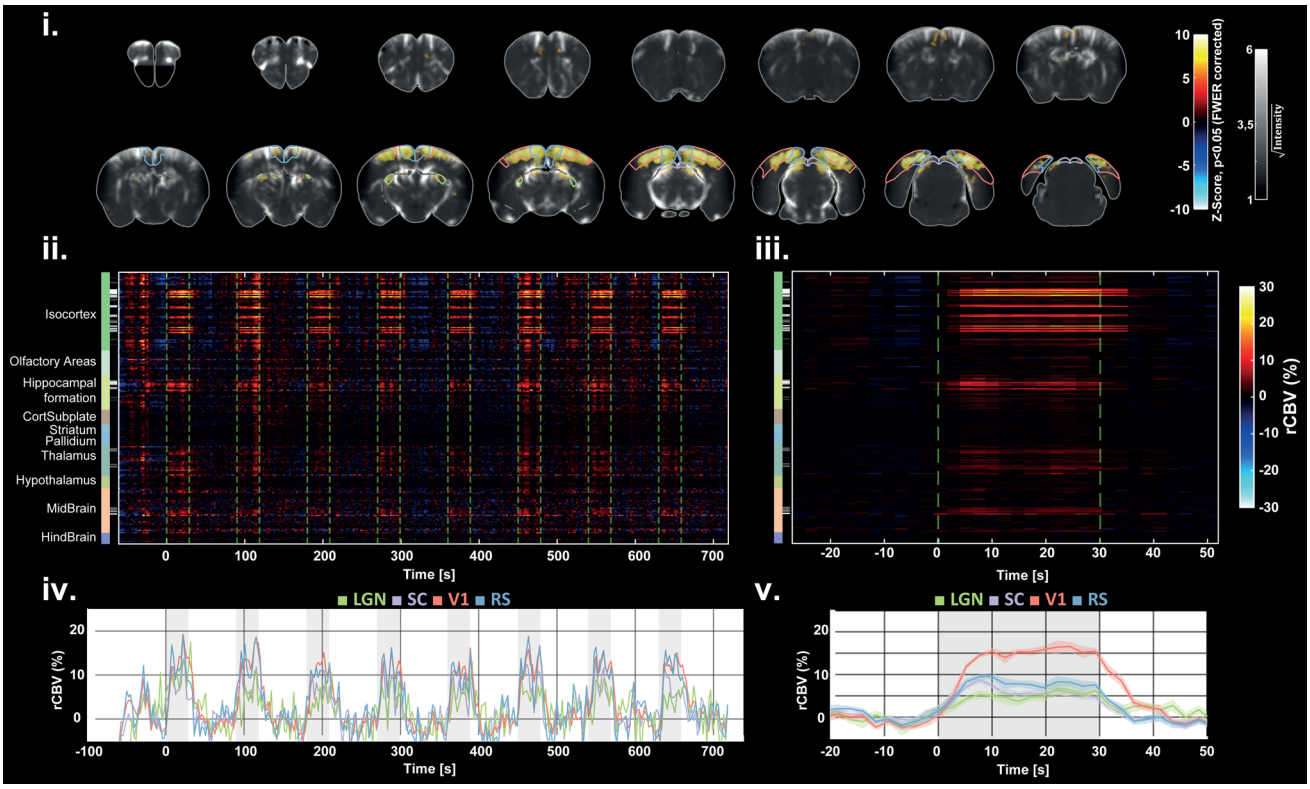

Fig. 6. Subject-level response after visual stimulation. (i) Subject-level activation map ($p < 0.05$, FWER corrected with Bonferroni procedure) overlaid with the PD angiography from the most anterior (top left) to the most posterior acquired slice (bottom right), reveals significant activation in major brain areas of the visual system: contours for the V1, RS, SC, and LGN regions are depicted on each slice. (ii) Raster plot of rCBV time course extracted in 228 Allen regions covering the whole brain. The gray-scale colorbar indicates the percentage of activated voxels in each region (black = 0%, white = 100 %). Green dashed lines indicate the beginning and the end of each stimulus. (iii) Cross-trial averaged raster plot. (iv) rCBV curves extracted in V1, RS, SC, and LGN, showing single-trial detections at each stimulus. (v) The average rCBV curves (cross-trial) show an increase of the rCBV from 5% for the LGN to 15% for V1 during the ON-time.

A second-level statistical analysis was then performed on a population of six subjects. Voxels with significant activation are represented on coronal slices (Fig. 7(i)) and in 3D renderings (Fig. 7(ii)). Significant activation was detected in the Thalamus, in the Midbrain, in the Hippocampal formation, and in the Isocortex. The percentage of activation in each of the 228 Allen regions (gray colorbar in Fig. 7(iii)) is reported in Supplementary Table 2. On average (cross-trials and subjects), the rCBV increase reached 4% in the LGN, 6% in the SC, 7.5% in the RS, and 12% in the V1 during the ON-time (Fig. 7(iv)).

3.3. Resting-state functional connectivity in awake mice

To study the dataset associated with resting-state functional connectivity in awake conditions (n = 6), we performed different statistical analyses. First, we performed a seed-based analysis, then we derived the average functional connectivity matrix, and we finally investigated spatial ICA to identify functional networks.

The seed-based analysis revealed significant and long-range functional connectivity patterns across the awake dataset. When the seed was placed in the upper limb region of the primary somatosensory area (SSp-ul), strong FC was measured in the contralateral region, and in other regions of the primary somatosensory cortex, such as the trunk (SSp-t), lower limbs (SSp-ll), the secondary motor cortex (MOs), and the hippocampal region (HPC, Fig. 8(i)). The specific midline associative cortices hub involved in the default mode network (DMN) previously described in the fUS (Grandjean et al., 2017) and fMRI (Gozzi & Schwarz, 2016; Grandjean et al., 2017; Sforazzini et al., 2014) literature was then identified by placing the seed in the dorsal part of the anterior cingulate area (ACA, Fig. 8(ii)). Finally, sub-cortical inter-hemispheric FC was also

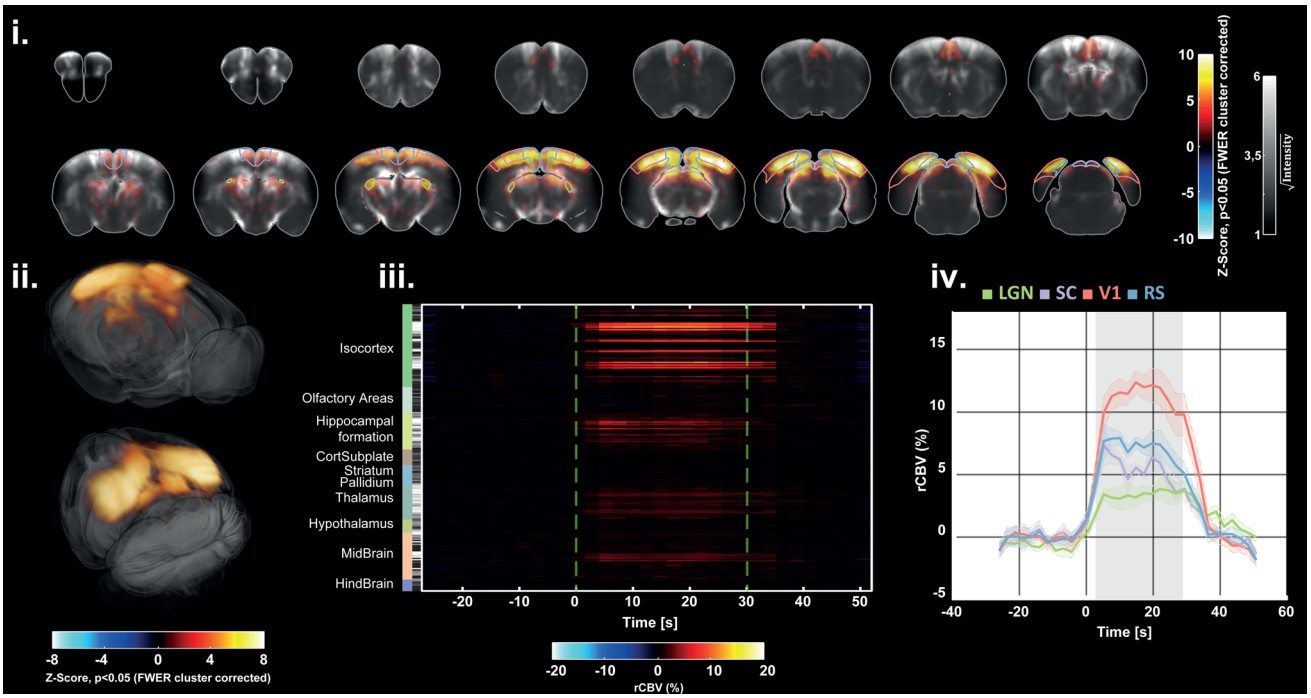

Fig. 7. Group-level response after visual stimulation (n = 6). (i) Average activation map (two-tailed t-test, $p < 0.05$, FWE corrected using TFCE and maximal statistic permutation testing), overlaid with the average PD angiography (cross-subject), from the most anterior slice (top left) to the most posterior slice (bottom right). (ii) 3D renderings (Amira software) of the average activation map, thresholded with significant voxels. (iii) Raster plot of averaged rCBV profiles (cross-trial and cross-subjects) extracted in 228 Allen regions. The gray color bar indicates the percentage of significant voxels in each region (black = 0%, white = 100 %). (iv) Average rCBV (cross-trial and cross-subjects) profiles extracted from important regions of the visual pathway show an increase of the rCBV going from 4% for the LGN to 12% for V1 during the ON-time.

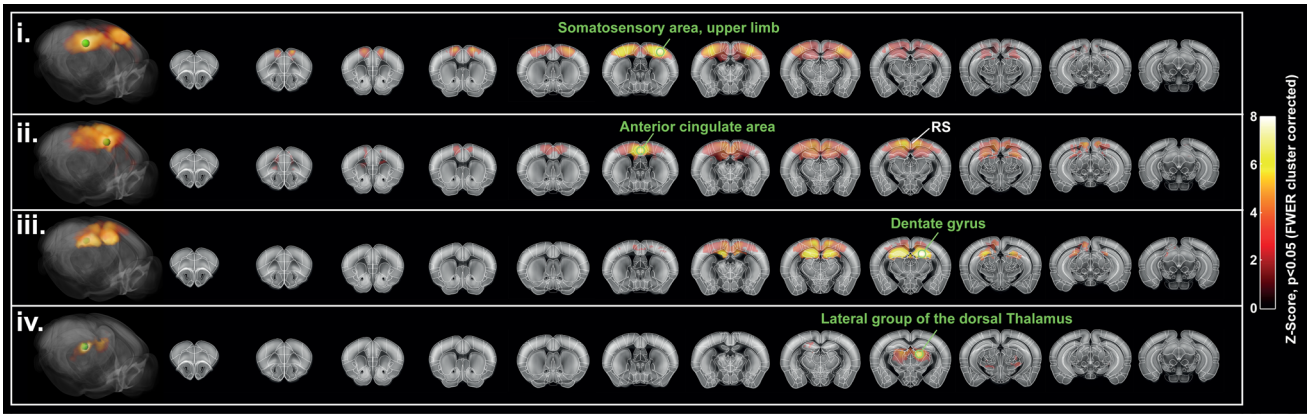

Fig. 8. Seed-based analysis reveals long-range FC patterns (n = 6). Each row represents an average seed-based map across the awake dataset (n = 6), thresholded with significant connectivity (one-tailed t test), $p < 0.05$, FWER cluster corrected using TFCE. Seed regions are denoted by the green legends: (i) somatosensory area, upper limb, (ii) Anterior cingulate area, (iii) Dentate gyrus, (iv) Lateral group of the dorsal Thalamus. Maps were resampled in the Allen mouse template. Volume renderings (left) are performed with Amira software. Activation maps are also represented on coronal slices overlaid with the two-photon Allen mouse template.

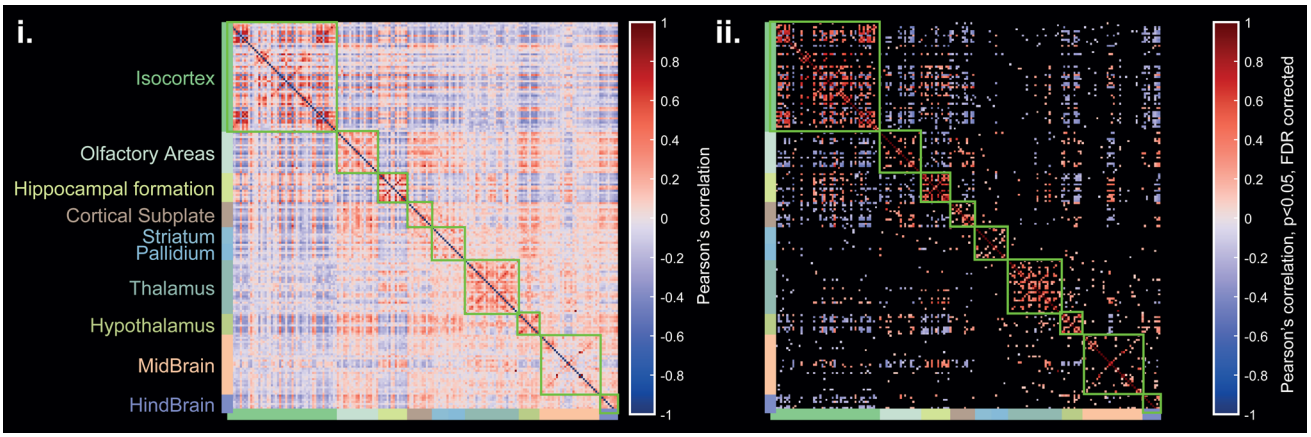

Fig. 9. Average functional connectivity matrix (n = 6) derived for more than 200 Allen cortical and subcortical structures which are listed in Supplementary Table 2 (i). Strong inter-hemispheric FC (anti-diagonals in green squares) is measured in both cortical and sub-cortical regions. Significant coefficients (one-sample t-test, $p < 0.05$, FDR corrected) are represented on the right matrix (ii).

found in both hippocampal and thalamic regions when placing the seed in the dentate gyrus or in the lateral group of the dorsal thalamus, respectively (Fig. 8(iii)). The map obtained with the DG seed also revealed hippocampo-cortical connections. These patterns were also identified at the subject level, as demonstrated in Supplementary Figure 2.

Then, the average functional connectivity matrix provided a global view of the whole brain FC (Fig. 9). The Allen-based and mirrored (left/right) segmentation of ROIs allowed different FC patterns in each major brain region to be exposed. The strongest inter-hemispheric correlation coefficients were observed in the isocortex, the hippocampal formation, the olfactory areas (OA), the thalamus (TH), and the hypothalamus (HT). Interestingly, the OA region was found to be highly functionally connected with different sub-cortical structural regions such as the cortical subplate (CS), the striatum (ST), and the HT, in good agreement with the results shown in a recent fMRI study in awake mice (Gutierrez-Barragan et al., 2022).

Finally, group-ICA revealed the presence of 16 resting-state functional networks. Five of them were classified as cortical networks (Fig. 10(i)), one as a hippocampal network (Fig. 10(ii)), and five as sub-cortical networks (Fig. 10(iii)). These networks span various brain regions defined by the Allen brain atlas and correlate with the brain structural connectivity with a systematic bilateral organization. Resting-state networks previously described in the fMRI literature were identified in our volumetric fUS data, involving the same anatomical regions. The identification of the DMN, the latero-cortical network (LCN), and the medial part of the salience network (SN) is in good agreement with the triple-network organization for the mouse brain previously proposed (Mandino et al., 2022). For the SN, the absence of activation in the agranular insular is argued in the discussion

Fig. 10. Functional networks identified with ICA. Identified networks were classified in three different groups (cortical (i), hippocampal (ii), and sub-cortical (iii)). Each network (labeled in the first column and represented in 3D in the second column) comprises at least one independent component. For each component, abbreviations of overlapped structural regions are captioned. In the last column, coronal sections of spatial maps are overlaid with the two-photon Allen template. RS = retrosplenial area, ACA = anterior cingulate area, MOp = primary motor area, SSp = primary somatosensory, ul = upper limb, ll = lower limb, bf = barrel field, PFC = prefrontal cortex, Mos = secondary motor cortex, VISa = anterior visual area, VISam = anteromedial visual area, VISrl = rostrolateral visual area, VISp = primary visual area, VISl = lateral visual area, ORB = orbital cortex, ACB = nucleus accumbens, HPC = hippocampus, CA = cornu ammonis, DG = dentate gyrus, AM = anteromedial nucleus, VAL = ventral anterior-lateral complex of the thalamus, VPM = ventral posteromedial nucleus, LP = lateral posterior nucleus of the thalamus, PO = posterior complex of the thalamus, SN = substantia nigra, VTA = ventral tegmental area, SC = superior colliculus, PRT = pretectal region, ACB = nucleus accumbens, OB = olfactory bulb, AON = anterior olfactory nucleus, BMA = basomedial amygdalar nucleus, medial amygdalar nucleus, PAA = Piriform-amygdalar area, COA = cortical amygdalar area.

part. The large field of view allowed the complete mapping of the visual network. Deeper networks were also characterized, including the hippocampus (HPC) and several sub-cortical networks, namely the thalamus (TH), the midbrain (MB), the basal forebrain (BF), the olfactory (OF) and the amygdala (Amy) networks. The presence of BF and OF networks is in good agreement with previous fMRI observations, supporting that high functional activity in these arousal regions is related to conscious wakefulness (Gutierrez-Barragan et al., 2022). Several networks were described with more than one IC. The DMN was decomposed into a first component

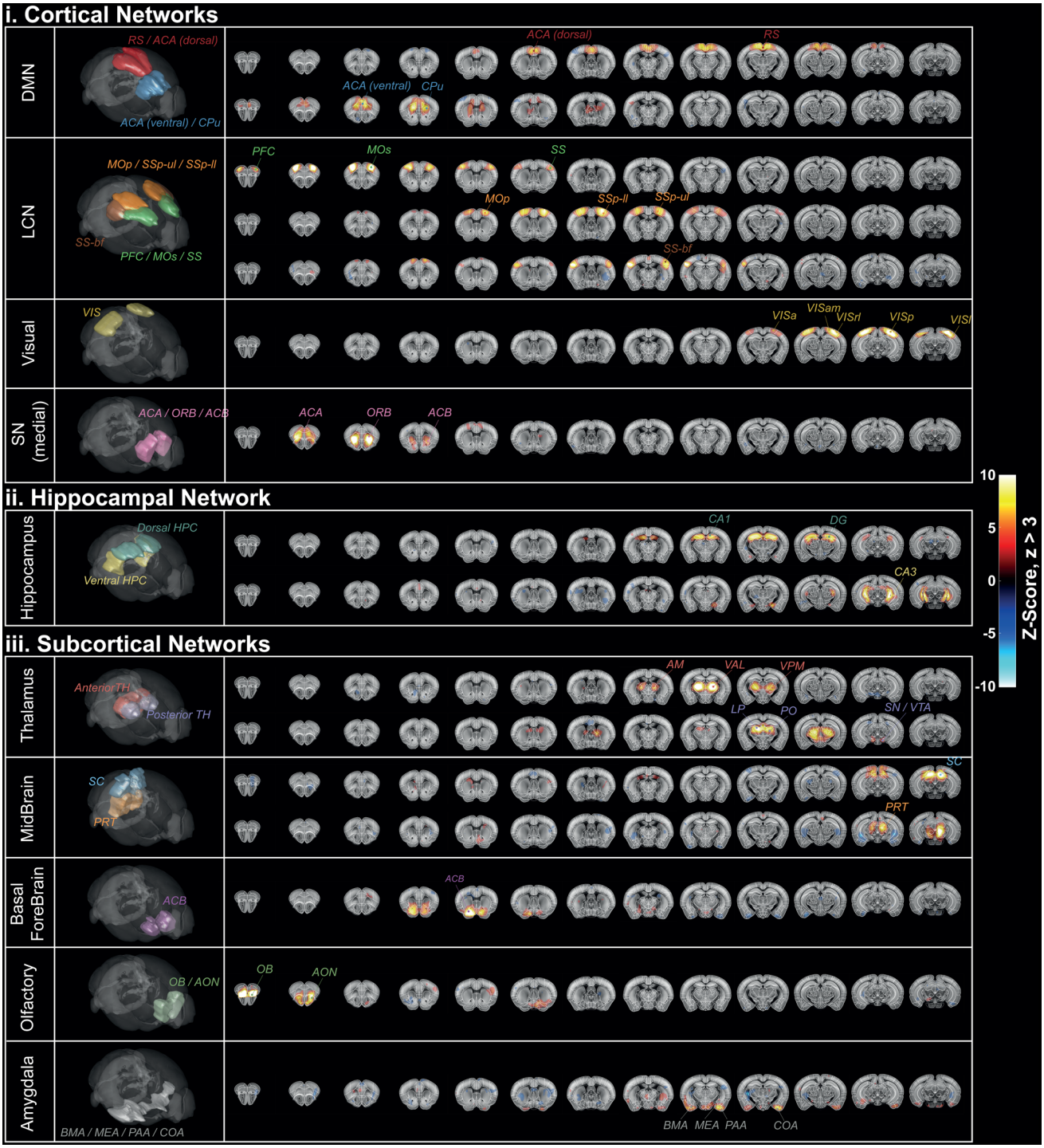

connecting the ACA and the RS together and a second one that was more specific to anterior ACA, as was previously observed in fMRI studies (Grandjean et al., 2017; Zerbi et al., 2015). The LCN was associated with three different components. The more anterior one was found to connect the prefrontal cortex (PFC), the secondary motor cortex (MOs), and the somatosensory cortex (SS). Among the two anterior components, a first one involved the primary motor cortex (MOp), the upper-limb and lower-limb regions of the primary SS cortex (SSp-ul and SSp-ll) whereas the more lateral one matched the barrel-field cortex (SS-bf). HPC and MB networks were described by two dorsal/ventral submodules, and the TH network was decomposed into two lateral/ventral submodules, matching with different sub-cortical nuclei specified in Figure 10(iii).

The elevation extent of each network is reported in Supplementary Table 3.

4. DISCUSSION

Compared to other preclinical neuroimaging modalities, fUS imaging benefits from several advantages such as a high spatial resolution, a high sampling rate, and a full-depth, non-invasive penetration into the mice brain. However, monitoring resting-state functional connectivity (rsFC) with brain-wide coverage in mice with an intact skull had, up to now, never been performed because of sensitivity and volume-rate issues (15-17, 35). In this study, we present the use of a new simultaneous multi-slice (SMS) approach based on a multi-array probe to perform transcranial brain-wide fUS imaging of functional activity and connectivity in anesthetized and awake mice. This new method allows for an acceleration in data acquisition equal to the number of simultaneously insonified slices (four), without compromising the sensitivity when compared to classic linear ultrasound arrays.

The sensitivity of our approach was highlighted by the comparison of the imaging quality with other methods in the same animal. Compared to the images acquired with the RCA and MUX-FPM probes, the multi-array images provided higher CNR values and better contrasts on vessel intensity profiles, in both trepanned and transcranial conditions.

Our hybrid approach using a multi-linear array allows for functional connectivity imaging over 16 complete coronal slices, providing a more comprehensive view of brain functional networks in the whole mouse brain through the skull.

We first conducted SMS-fUS acquisitions to investigate task-based functional activation and obtained reliable hyperemia in different brain regions of the visual system in response to light stimuli in lightly anesthetized mice. Notably, we found statistically significant activations in the lateral geniculate nuclei, the superior colliculi, the primary visual cortex, and, more surprisingly, within the retrosplenial area at both the subject level and group level. While the retrosplenial cortex is not typically found to be activated following visual stimulation in fMRI studies (Dinh et al., 2021; Niranjan et al., 2016), this brain region has been shown to exhibit visual responses using GCaMP imaging techniques (Murakami et al., 2015), and has been included in an extended retinotopic organization of the mouse brain (Zhuang et al., 2017). Consistently, significant hyperemia has already been demonstrated in the retrosplenial area using fUS in awake head-fixed mice, independently of stimulus directions or the presence of an optokinetic reflex (Macé et al., 2018). Taken together, these observations further support the high sensitivity of fUS imaging and its ability to faithfully report neuronal activity. In this study, we used a simple flashing LED stimulus, but more complex visual tasks could be performed using the same approach such as multi-directional drifting grating stimuli (Macé et al., 2018). Similarly, this paradigm could be straightforwardly transposed to the mapping of the brain correlates of complex behavior or cognitive tasks in awake mice in future studies.

Resting-state functional connectivity was then evaluated in awake head-fixed mice under stimulus-free conditions. Leveraging our previously published automatic registration to the Allen Mouse Brain Atlas (Nouhoum et al., 2021), we performed seed-based analysis, derived an average functional connectivity matrix over 200 segmented regions, and identified large-scale functional connections spanning several coronal slices. Expanding previous work using fMRI (Gutierrez-Barragan et al., 2022; Tsurugizawa et al., 2020), our work provides a fine-grained comprehensive description of the organization of mouse brain functional networks during wakefulness. Unsupervised multivariate ICA analysis has revealed 16 functional networks that cover the whole brain and that strikingly resemble those previously described in the fMRI literature. We found relevant inter-hemispheric connectivity within the cortical, hippocampal, basal ganglia, and sub-cortical regions at both subject and group levels. Based on previously published fMRI studies (Grandjean et al., 2017; Mandino et al., 2022; Zerbi et al., 2015), relevant components have been manually classified into major networks identified in the mouse brain: the default

mode network (including midline and associative regions), the lateral cortical network (including somatosensory-motor executive areas), the visual network, as well as the salient network (including the most anterior part of the anterior cingulate and orbitofrontal cortices). Subcortical components included the hippocampal network, the thalamic network, as well as modes within the midbrain, the basal forebrain, the olfactory nucleus, and the amygdala. We found two independent hippocampal networks corresponding to the dorsal and ventral hippocampus, as described in the literature (Zerbi et al., 2015), as well as two independent thalamic networks corresponding to the anterior and posterior thalamus, less often described in the fMRI literature. Together, these observations attest to the high sensitivity of our approach through its ability to detect reliable spontaneous coactivations in the deepest regions of the mouse brain, even in the transcranial setting. More advanced analyses such as dynamic functional connectivity and coactivated patterns (CAPs) could help provide a more accurate description of the mouse functional connectome and facilitate comparisons with fMRI datasets.

Several limitations must be considered when interpreting the results. First, certain areas of the brain remain more difficult to image due to stronger skull aberrations, mostly linked to the skull shape or presence of sutures. This includes the cerebellum, the auditory cortex, temporal areas, and insular cortex. This explains the absence of significant functional connectivity in these regions. Applying aberration correction techniques to the ultrasound field may help recover signals in those areas. Second, the current field of view, which was specifically optimized for the adult mouse brain, would be too restricted for rats or larger animals. Future development of 512-channel scanners with higher computational power will enable the conceptualization of larger multi-arrays transducers to overcome this limitation. Alternatively, larger piezo elements with reduced central frequency could be considered to increase the probe aperture, but with a tradeoff on in-plane spatial resolution.

Moreover, the use of global signal regression (GSR) as a preprocessing step for resting-state signals is highly debated in the fMRI literature. GSR was used in the present study to reduce contributions from non-neuronal sources, notably motion artifacts, in awake resting-state signals (Rabut et al., 2020). However, as GSR has been shown to introduce spurious negative correlation values in FC networks (Murphy & Fox, 2017), great care should be taken when interpreting negatively correlated regions in seed-based maps and GLM analyses. Note that the preprocessing of task-evoked data from anesthetized mice did not require GSR as there were no motion artifacts.

Overall, our approach showed promising results with a TR of 2.4 s—a theoretical limit for resting-state functional connectivity (with respect to Nyquist-Shannon theorem and considering an upper frequency of 0.2 Hz for the RS bandwidth)—but it is still slower than what could be reached using a matrix or row-column array (Brunner et al., 2020; Rabut et al., 2019; Sauvage et al., 2019). In our study and others (Aydin et al., 2020; Bertolo, Nouhoum, et al., 2021; Boido et al., 2019; Ferrier et al., 2020; Gesnik et al., 2017; Macé et al., 2018; Nunez-Elizalde et al., 2022; B. F. Osmanski et al., 2014; B.-F. Osmanski et al., 2014; Rabut et al., 2020; Sieu et al., 2015; Tiran et al., 2017), high sensitivity Doppler frames were computed over 200 compounded ultrasonic images acquired over 0.4 s so that several cardiac cycles are sampled and averaged. This leads to a more efficient rejection of tissue echoes (such as arterial pulsatility). A higher frame rate could theoretically be achieved by reducing the number of images down to 50, yielding a TR of ~1 s. However, one should expect a significant SNR penalty on fUS signals due to systemic physiological noise contamination, the extent of which would require further investigations.

In conclusion, our results show that the SMS approach using a multi-array fUS probe is a very promising method for studying 3D connectomics in awake or anesthetized mice, non-invasively through the skull. Along with its seamless compatibility with awake behaving animals, we believe that this approach will pave the way for more advanced studies to help shed new light on the spatio-temporal organization of spontaneous or evoked activity of the mouse brain and its breakdown in neuropsychiatric diseases.

DATA AND CODE AVAILABILITY

Data and code that support the findings of this study are available from the corresponding author upon reasonable request. Researchers wishing to obtain the raw data must contact the Office of Research Contracts at INSERM to initiate a discussion on the proposed data transfer or use.

AUTHOR CONTRIBUTIONS

Adrien Bertolo, Jeremy Ferrier, and Silvia Cazzanelli (experiments); Adrien Bertolo (processing); Samuel Diebolt (discussions); Mathieu Pernot, Thomas Deffieux, and

Bruno-Félix Osmanski (supervising); Sophie Pezet, Mickael Tanter (study conception and discussions (physics and neurobiology)).

FUNDING

This project has received funding from the European Union's Horizon 2020 research and innovation program under grant agreement No 874721. INSERM also supported this work through a Biomedical Ultrasound Technology Research Accelerator (ART).

DECLARATION OF COMPETING INTEREST

Mickael Tanter, Mathieu Pernot, Bruno-Félix Osmanski, and Thomas Deffieux are share-holders and co-founders of the Iconeus company. Adrien Bertolo, Jeremy Ferrier, Samuel Diebolt, and Bruno-Félix Osmanski are employees of the Iconeus company.

SUPPLEMENTARY MATERIALS

Supplementary material for this article is available with the online version here: https://doi.org/10.1162/imag_a_00030.

REFERENCES

Aydin, A.-K., Haselden, W. D., Goulam Houssen, Y., Pouzat, C., Rungta, R. L., Demené, C., Tanter, M., Drew, P. J., Charpak, S., & Boido, D. (2020). Transfer functions linking neural calcium to single voxel functional ultrasound signal. *Nature Communications*, *11*(1), 2954. https://doi.org/10.1038/s41467-020-16774-9

Baranger, J., Arnal, B., Perren, F., Baud, O., Tanter, M., & Demene, C. (2018). Adaptive spatiotemporal SVD clutter filtering for ultrafast Doppler imaging using similarity of spatial singular vectors. *IEEE Transactions on Medical Imaging*, *37*(7), 1574–1586. https://doi.org/10.1109/TMI.2018.2789499

Bertolo, A., Nouhoum, M., Cazzanelli, S., Ferrier, J., Mariani, J.-C., Kliewer, A., Belliard, B., Osmanski, B.-F., Deffieux, T., Pezet, S., Lenkei, Z., & Tanter, M. (2021). Whole-brain 3D activation and functional connectivity mapping in mice using transcranial functional ultrasound imaging. *Journal of Visualized Experiments*, *168*, 62267. https://doi.org/10.3791/62267

Bertolo, A., Sauvage, J., Tanter, M., Pernot, M., & Deffieux, T. (2021). XDoppler: Cross-correlation of orthogonal apertures for 3D blood flow imaging. *IEEE Transactions on Medical Imaging*, *40*(12), 1–1. https://doi.org/10.1109/TMI.2021.3084865

Biswal, B., Zerrin Yetkin, F., Haughton, V. M., & Hyde, J. S. (1995). Functional connectivity in the motor cortex of resting human brain using echo-planar MRI. *Magnetic Resonance in Medicine*, *34*(4), 537–541. https://doi.org/10.1002/mrm.1910340409

Blons, M., Bertolo, A., Deffieux, T., Osmanski, B.-F., Tanter, M., & Berthon, B. (2022, March 18). 3D vascular landmarks localization in Dopper images of mouse brains using a deep convolutional neural network enables precise volumetric registration. *EMIM 2022, Poster*. https://www.eventclass.org/contxt_emim2022/online-program/session?s=104#e641

Boido, D., Rungta, R. L., Osmanski, B.-F., Roche, M., Tsurugizawa, T., Le Bihan, D., Ciobanu, L., & Charpak, S. (2019). Mesoscopic and microscopic imaging of sensory responses in the same animal. *Nature Communications*, *10*(1), 1110. https://doi.org/10.1038/s41467-019-09082-4

Brunner, C., Grillet, M., Sans-Dublanc, A., Farrow, K., Lambert, T., Macé, E., Montaldo, G., & Urban, A. (2020). A platform for brain-wide volumetric functional ultrasound imaging and analysis of circuit dynamics in awake mice. *Neuron*, *108*(5), 861–875.e7. https://doi.org/10.1016/j.neuron.2020.09.020

Coletta, L., Pagani, M., Whitesell, J.D., Harris, J.A., Bernhardt, B., & Gozzi, A. Network structure of the mouse brain connectome with voxel resolution. (2020). *Science Advances*, *6*(51), eabb7187. https://doi.org/10.1126/sciadv.abb7187

Claron, J., Provansal, M., Salardaine, Q., Tissier, P., Dizeux, A., Deffieux, T., Picaud, S., Tanter, M., Arcizet, F., & Pouget, P. (2023). Co-variations of cerebral blood volume and single neurons discharge during resting state and visual cognitive tasks in non-human primates. *Cell Reports*, *42*(4), 112369. https://doi.org/10.1016/j.celrep.2023.112369

Demene, C., Deffieux, T., Pernot, M., Osmanski, B.-F., Biran, V., Gennisson, J.-L., Sieu, L.-A., Bergel, A., Franqui, S., Correas, J.-M., Cohen, I., Baud, O., & Tanter, M. (2015). Spatiotemporal clutter filtering of ultrafast ultrasound data highly increases Doppler and fUltrasound sensitivity. *IEEE Transactions on Medical Imaging*, *34*(11), 2271–2285. https://doi.org/10.1109/TMI.2015.2428634

Dinh, T. N. A., Jung, W. B., Shim, H.-J., & Kim, S.-G. (2021). Characteristics of fMRI responses to visual stimulation in anesthetized vs. Awake mice. *Neuroimage*, *226*, 117542. https://doi.org/10.1016/j.neuroimage.2020.117542

Ferrier, J., Tiran, E., Deffieux, T., Tanter, M., & Lenkei, Z. (2020). Functional imaging evidence for task-induced deactivation and disconnection of a major default mode network hub in the mouse brain. *Proceedings of the National Academy of Sciences U S A*, *117*(26), 15270–15280. https://doi.org/10.1073/pnas.1920475117

Gesnik, M., Blaize, K., Deffieux, T., Gennisson, J.-L., Sahel, J.-A., Fink, M., Picaud, S., & Tanter, M. (2017). 3D functional ultrasound imaging of the cerebral visual system in rodents. *Neuroimage*, *149*, 267–274. https://doi.org/10.1016/j.neuroimage.2017.01.071

Gozzi, A., & Schwarz, A. J. (2016). Large-scale functional connectivity networks in the rodent brain. *Neuroimage*, *127*, 496–509. https://doi.org/10.1016/j.neuroimage.2015.12.017

Grandjean, J., Zerbi, V., Balsters, J. H., Wenderoth, N., & Rudin, M. (2017). Structural basis of large-scale functional connectivity in the mouse. *The Journal of Neuroscience*, *37*(34), 8092–8101. https://doi.org/10.1523/JNEUROSCI.0438-17.2017

Gutierrez-Barragan, D., Singh, N. A., Alvino, F. G., Coletta, L., Rocchi, F., De Guzman, E., Galbusera, A., Uboldi, M.,

Panzeri, S., & Gozzi, A. (2022). Unique spatiotemporal fMRI dynamics in the awake mouse brain. *Current Biology*, *32*(3), 631–644.e6. https://doi.org/10.1016/j.cub.2021.12.015

Himberg, J., & Hyvarinen, A. (2003). Icasso: Software for investigating the reliability of ICA estimates by clustering and visualization. In: *2003 IEEE XIII Workshop on Neural Networks for Signal Processing (IEEE Cat. No.03TH8718)* (pp. 259–268). https://doi.org/10.1109/NNSP.2003.1318025

Jensen, J. A. (1997). Field: A program for simulating ultrasound systems. *Medical & Biological Engineering & Computing*, *34*(sup. 1), 351–353.

Macé, E., Montaldo, G., Cohen, I., Baulac, M., Fink, M., & Tanter, M. (2011). Functional ultrasound imaging of the brain. *Nature Methods*, *8*(8), 662–664. https://doi.org/10.1038/nmeth.1641

Mace, E., Montaldo, G., Osmanski, B.-F., Cohen, I., Fink, M., & Tanter, M. (2013). Functional ultrasound imaging of the brain: Theory and basic principles. *IEEE Transactions on Ultrasonics, Ferroelectrics and Frequency Control*, *60*(3), 492–506. https://doi.org/10.1109/TUFFC.2013.2592

Macé, É., Montaldo, G., Trenholm, S., Cowan, C., Brignall, A., Urban, A., & Roska, B. (2018). Whole-brain functional ultrasound imaging reveals brain modules for visuomotor integration. *Neuron*, *100*(5), 1241–1251.e7. https://doi.org/10.1016/j.neuron.2018.11.031

Mandino, F., Vrooman, R. M., Foo, H. E., Yeow, L. Y., Bolton, T. A. W., Salvan, P., Teoh, C. L., Lee, C. Y., Beauchamp, A., Luo, S., Bi, R., Zhang, J., Lim, G. H. T., Low, N., Sallet, J., Gigg, J., Lerch, J. P., Mars, R. B., Olivo, M., … Grandjean, J. (2022). A triple-network organization for the mouse brain. *Molecular Psychiatry*, *27*(2), 865–872. https://doi.org/10.1038/s41380-021-01298-5

Maresca, D., Correia, M., Tanter, M., Ghaleh, B., & Pernot, M. (2018). Adaptive spatiotemporal filtering for coronary ultrafast Doppler angiography. *IEEE Transactions on Ultrasonics, Ferroelectrics, and Frequency Control*, *65*(11), 2201–2204. https://doi.org/10.1109/TUFFC.2018.2870083

Murakami, T., Yoshida, T., Matsui, T., & Ohki, K. (2015). Wide-field Ca2+ imaging reveals visually evoked activity in the retrosplenial area. *Frontiers in Molecular Neuroscience*, *08*, 20. https://doi.org/10.3389/fnmol.2015.00020

Murphy, K., & Fox, M. D. (2017). Towards a consensus regarding global signal regression for resting state functional connectivity MRI. *Neuroimage*, *154*, 169–173. https://doi.org/10.1016/j.neuroimage.2016.11.052

Niranjan, A., Christie, I. N., Solomon, S. G., Wells, J. A., & Lythgoe, M. F. (2016). fMRI mapping of the visual system in the mouse brain with interleaved snapshot GE-EPI. *Neuroimage*, *139*, 337–345. https://doi.org/10.1016/j.neuroimage.2016.06.015

Nouhoum, M., Ferrier, J., Osmanski, B.-F., Ialy-Radio, N., Pezet, S., Tanter, M., & Deffieux, T. (2021). A functional ultrasound brain GPS for automatic vascular-based neuronavigation. *Scientific Reports*, *11*(1), 15197. https://doi.org/10.1038/s41598-021-94764-7

Ntekouli, M. (2019). *Investigating brain function and anatomy through ICA-based functional ultrasound imaging*. http://resolver.tudelft.nl/uuid:d4786d82-9836-4eb4-a8cc-775f9e5bd83f

Nunez-Elizalde, A. O., Krumin, M., Reddy, C. B., Montaldo, G., Urban, A., Harris, K. D., & Carandini, M. (2022). Neural correlates of blood flow measured by ultrasound. *Neuron*, *110*(10), 1631–1640.e4. https://doi.org/10.1016/j.neuron.2022.02.012

Osmanski, B. F., Martin, C., Montaldo, G., Lanièce, P., Pain, F., Tanter, M., & Gurden, H. (2014). Functional ultrasound imaging reveals different odor-evoked patterns of vascular activity in the main olfactory bulb and the anterior piriform cortex. *Neuroimage*, *95*, 176–184. https://doi.org/10.1016/j.neuroimage.2014.03.054

Osmanski, B.-F., Pezet, S., Ricobaraza, A., Lenkei, Z., & Tanter, M. (2014). Functional ultrasound imaging of intrinsic connectivity in the living rat brain with high spatiotemporal resolution. *Nature Communications*, *5*(1), 5023. https://doi.org/10.1038/ncomms6023

Percie du Sert, N., Ahluwalia, A., Alam, S., Avey, M. T., Baker, M., Browne, W. J., Clark, A., Cuthill, I. C., Dirnagl, U., Emerson, M., Garner, P., Holgate, S. T., Howells, D. W., Hurst, V., Karp, N. A., Lazic, S. E., Lidster, K., MacCallum, C. J., Macleod, M., … Würbel, H. (2020). Reporting animal research: Explanation and elaboration for the ARRIVE guidelines 2.0. *PLoS Biology*, *18*(7), e3000411. https://doi.org/10.1371/journal.pbio.3000411

Rabut, C., Correia, M., Finel, V., Pezet, S., Pernot, M., Deffieux, T., & Tanter, M. (2019). 4D functional ultrasound imaging of whole-brain activity in rodents. *Nature Methods*, *16*(10), 994–997. https://doi.org/10.1038/s41592-019-0572-y

Rabut, C., Ferrier, J., Bertolo, A., Osmanski, B., Mousset, X., Pezet, S., Deffieux, T., Lenkei, Z., & Tanter, M. (2020). Pharmaco-fUS: Quantification of pharmacologically-induced dynamic changes in brain perfusion and connectivity by functional ultrasound imaging in awake mice. *Neuroimage*, *222*, 117231. https://doi.org/10.1016/j.neuroimage.2020.117231

Sauvage, J., Deffieux, T., Poree, J., Rabut, C., Ferin, G., Flesch, M., Rosinski, B., Nguyen-Dinh, A., Tanter, M., & Pernot, M. (2019). 4D Functional imaging of the rat brain using a large aperture row-column array. *IEEE Transactions on Medical Imaging*, 1–1. https://doi.org/10.1109/TMI.2019.2959833

Sforazzini, F., Schwarz, A. J., Galbusera, A., Bifone, A., & Gozzi, A. (2014). Distributed BOLD and CBV-weighted resting-state networks in the mouse brain. *Neuroimage*, *87*, 403–415. https://doi.org/10.1016/j.neuroimage.2013.09.050

Sieu, L.-A., Bergel, A., Tiran, E., Deffieux, T., Pernot, M., Gennisson, J.-L., Tanter, M., & Cohen, I. (2015). EEG and functional ultrasound imaging in mobile rats. *Nature Methods*, *12*(9), 831–834. https://doi.org/10.1038/nmeth.3506

Smith, S., & Nichols, T. (2009). Threshold-free cluster enhancement: Addressing problems of smoothing, threshold dependence and localisation in cluster inference. *Neuroimage*, *44*(1), 83–98. https://doi.org/10.1016/j.neuroimage.2008.03.061

Tiran, E., Ferrier, J., Deffieux, T., Gennisson, J.-L., Pezet, S., Lenkei, Z., & Tanter, M. (2017). Transcranial functional ultrasound imaging in freely moving awake mice and anesthetized young rats without contrast agent. *Ultrasound in Medicine & Biology*, *43*(8), 1679–1689. https://doi.org/10.1016/j.ultrasmedbio.2017.03.011

Tsurugizawa, T., Tamada, K., Ono, N., Karakawa, S., Kodama, Y., Debacker, C., Hata, J., Okano, H., Kitamura, A., Zalesky, A., & Takumi, T. (2020). Awake functional MRI detects neural circuit dysfunction in a mouse model of

autism. *Science Advances*, *6*(6), eaav4520. https://doi.org/10.1126/sciadv.aav4520

Wang, Q., Ding, S.-L., Li, Y., Royall, J., Feng, D., Lesnar, P., Graddis, N., Naeemi, M., Facer, B., Ho, A., Dolbeare, T., Blanchard, B., Dee, N., Wakeman, W., Hirokawa, K. E., Szafer, A., Sunkin, S. M., Oh, S. W., Bernard, A., … Ng, L. (2020). The Allen Mouse Brain Common Coordinate Framework: A 3D reference atlas. *Cell*, *181*(4), 936–953. e20. https://doi.org/10.1016/j.cell.2020.04.007

Zerbi, V., Grandjean, J., Rudin, M., & Wenderoth, N. (2015). Mapping the mouse brain with rs-fMRI: An optimized pipeline for functional network identification. *Neuroimage*, *123*, 11–21. https://doi.org/10.1016/j.neuroimage.2015.07.090

Zhuang, J., Ng, L., Williams, D., Valley, M., Li, Y., Garrett, M., & Waters, J. (2017). An extended retinotopic map of mouse cortex. *eLife*, *6*, e18372. https://doi.org/10.7554/eLife.18372

CHAPTER 5

ARTICLE N°4:

Longitudinal fUS imaging of functional connectivity during neuropathic pain development in mice revealed long lasting alterations of pain and stress networks

INTRODUCTION OF THE ARTICLE N°4

In this next chapter, leveraging the benefits offered by the newly developed multi-array fUS probe, we designed a new study to overcome some limitations encountered in chapter 3.
First, we aimed at investigating the FC alterations in the cuff model at the whole-brain level, without any a priori regarding the brain imaging sections or restrict our observations to a single brain hemisphere. Second, we adopted a longitudinal approach to better control for individual variability, each animal being its own control. To do so, this work had to be conducted in anesthetized conditions. This approach gave us the opportunity to investigate the alterations of brain changes until a later time point, 12W. Furthermore, the study was built on the technological development described in chapter 4. The novel 3D multi-slice imaging modality has been applied for the study of FC alterations in a longitudinal follow-up of neuropathic pain in a mouse model, in anesthetized conditions.

The results of the study show FC alterations in a wide-range network between regions known to be involved in pain processing and adaptation to stress.

I performed all aspects of the work presented in this article: the experiments, the signal and statistical analysis and the redaction of the article.

Longitudinal fUS imaging of functional connectivity during neuropathic pain development in mice revealed long lasting alterations of pain and stress networks

Silvia Cazzanelli[1,2], Youenn Travert-Jouanneau[1], Samuel Diebolt[1,2], Luc Eglin[2], Adrien Bertolo[2], Thomas Deffieux[1], Mickael Tanter[1], Bruno-Felix Osmanski[2], Jeremy Ferrier[2] and Sophie Pezet[1]

[1]Physics for Medicine Paris, INSERM, ESPCI Paris, CNRS, PSL Research University - Paris, France.

[2] Iconeus, 27 Rue du Faubourg Saint-Jacques, 75014 Paris, France

1 ABSTRACT

Chronic pain is known to induce significant morphological and functional alterations in the human brain, as evidenced by various imaging studies. However, comparatively fewer investigations have explored the dynamic changes in neural networks at the rodent level.

In this study, we used functional Ultrasound (fUS) Imaging, a cutting-edge neuroimaging technique renowned for its sensitivity to blood volume changes, high spatial resolution (100 um), rapid temporal resolution (400 ms), and wide field of view. Our aim was to elucidate the potential alterations in brain functional connectivity throughout the progression of neuropathic pain in mice, comparing against two control groups (naive and sham-operated).

Through our longitudinal approach, we observed significant changes in functional connectivity within key brain regions implicated in emotional and cognitive processing, notably the infralimbic area and the amygdala. These changes manifested from 2 weeks post-surgery in both sham-operated and neuropathic animals, with a notable persistence in the latter group at 8 weeks post-lesion, suggesting persisting pain-related mechanisms. Additionally, our study revealed heightened functional connectivity between the insula and the prelimbic area specifically in neuropathic animals at 2 weeks post-lesion. Given the established roles of these regions in stress regulation, particularly in chronic stress scenarios, our findings suggest profound adaptive changes within pain and stress processing networks in neuropathic mice. In summary, our findings illuminate the dynamic alterations within neural networks during the development of neuropathic pain in rodents, emphasizing the significance of comprehending the intricate interplay between pain, stress, and neural circuitry in preclinical models.

2 INTRODUCTION

Neuropathic pain is an abnormal pain sensation, due to nerve lesion, that persists longer than the temporal course of natural healing. The altered and intact sensory neurons convey disordered sensory signals into the spinal cord and the brain, leading to distinct sets of symptoms, such as allodynia and hyperalgesia (Costigan, Scholz, and Woolf 2009). In chronic pain states, long-lasting electrophysiological, structural and functional changes take place in the various relays of the pain pathways inducing a maladaptive plasticity, (Zhuo 2008). These central mechanisms of plasticity are believed to be pivotal for the development of mood disorders, such as anxiety and depression, that are frequently observed in chronic pain patients (Petrovic et al. 2000).

Pain is a complex sensory and emotional experience that can vary between people and even within an individual, depending on the context and meaning of the pain, but also the psychological state of the person. Cognitive and emotional factors have a major impact on pain perception (M. Catherine Bushnell, Čeko, and Low 2013). Both in humans and animals, pain can be negatively modulated when attention is given outside the painful experience (Villemure and Bushnell 2009; Longe et al. 2001; Jonathan C.W. Brooks et al. 2002; Valet et al. 2004). While exacerbation of pain is due to an enhanced activation of some pain-related areas, such as the S1, ACC and insula (Villemure and Bushnell 2009; M. C. Bushnell et al. 1999; Ploner et al. 2011), reduction of pain by alteration of the pain by distraction from pain is due to a reduction in activity of both the insula and S1. Modulation of the emotional state (such as inducing a negative emotional state by looking at emotional faces) alters several brain areas, but most consistently the ACC (Villemure and Bushnell 2009; Ploner et al. 2011; Roy et al. 2009; Berna et al. 2010).

As chronic pain alters the brain, the descending inhibitory mechanism, which is the natural mechanism of coping to various types of stimuli (Ossipov, Dussor, and Porreca 2010), are chronically impaired in chronic pain patients, leading to central sensitization, allodynia and hyperalgesia (Gracely et al. 2002). Functional brain imaging studies in patients with chronic pain, such as in fibromyalgia patients, also supported that endogenous pain modulatory systems may be dysfunctional in these patients (Jensen et al. 2009; Berman et al. 2008).

The insula is an important hub for the integration of multimodal information (Gogolla 2017). The strong interconnection between the insular cortex and the limbic system indicates an essential role of the insula

in emotion. Recent studies demonstrate its involvement in aversive behaviors (Gehrlach et al. 2019), including fear (Klein et al. 2021) and anxiety (Méndez-Ruette et al. 2019; Paulus and Stein 2006).

The insula also has a crucial role in pain processing: it is activated in an intensity-dependent manner (Robert C. Coghill et al. 1999) by noxious stimulations (R. C. Coghill et al. 1994; Garcia-Larrea and Peyron 2013), suggesting its involvement in intensity coding. Finally, the spatial location of activation follows somatotopic organization (Henderson, Gandevia, and Macefield 2007; J.C.W. Brooks et al. 2005).

Clinical studies also emphasized the role of the insular cortex in chronic pain (Labrakakis 2023), showing a relationship between alterations in insular activity (Hsieh et al. 1995), structure (Gustin et al. 2011), and pain chronification. In contrast, animal research on the role of the posterior insula in pain has been limited (Labrakakis 2023). While its role in the development of mechanical allodynia (Benison et al. 2011) and in the aversive aspect of pain were well described (Tan et al. 2017), a comprehensive view of the functional interplay between the insula and other pain-related areas in the context of chronic pain is still missing.

In order to fulfill this need, this study aimed at characterizing the changes in pain-related brain networks, with a special attention on the insula), through the measurements of brain functional connectivity in a mice model of neuropathic pain, using a relatively new technique of neuroimaging: functional ultrasound (fUS) imaging. fUS imaging allows the precise measurement of relative changes in cerebral blood volume with an excellent spatial (100–300 µm) and temporal resolutions (10 ms). It was used in many functional studies in human (Demene et al. 2017; Soloukey et al. 2020), non-human primates (Dizeux et al. 2019) and rodents (Macé et al. 2011; Sieu et al. 2015; Urban et al. 2015; Bergel et al. 2018; Rahal et al. 2020). fUS imaging can also measure resting-state hemodynamic fluctuations between brain areas over time; this last approach enables the identification of intrinsic functional connectivity (FC) patterns (Osmanski et al. 2014), which is a functional measure of the strength of the brain networks (Fox and Raichle 2007). In this study, we investigated how the FC between pain-related brain regions is altered in link with neuropathic pain and the associated comorbidities.

We measured the functional connectivity (FC) at rest in anesthetized mice: I) naïve, II) subjected to neuropathic pain (2W cuffing of the sciatic nerve), III) during the emergence of anxiety-like behavior (8W), IV) during the emergence of depressive-like behavior (12W). Our results show significant changes in FC in major pain-related brain regions in accordance with the development of neuropathic pain symptoms. These findings suggest that the regions involved in pain processing undergo a maladaptive plasticity following nerve injury which may participate in pain chronification. Moreover, the connectivity alterations

change across the investigated timepoints, and this could be correlated with the subsequent apparition of the comorbidities.

Our study provides a novel imaging approach to investigate and follow overtime FC alterations associated with neuropathic pain.

3 MATERIALS AND METHODS

Animals

All the experiments were performed in agreement with the European Community Council Directive of 22nd September (010/63/UE) and the local ethics committee ("Comité d'éthique en matière d'expérimentation animale n°59, 'Paris Centre et Sud'", project agreement APAFIS#19701 2019031020578789 V5).

The experiments were performed on 24 male C57BL/6 mice (Charles River Lab). Mice arrived at the laboratory one week before the beginning of the experiments at the age of 5 weeks and weighed between 20-25g. Animals were socially housed in well-ventilated cages. The housing room was kept at a constant temperature of 22°C and relative humidity was kept at 45-50%. Food and water were available *ad libitum*. The housing room was kept under a 12h light/dark reverse cycle (light 8 pm – 8 am) and all the experiments were done during the dark phase, under red light.

Experimental design (Figure 1)

In order to investigate the functional connectivity changes associated with neuropathic pain, we developed an experimental approach allowing the monitoring of intrinsic brain connectivity in a mouse model of neuropathic pain over time. Following a longitudinal approach, we investigated key stages of symptoms development and comorbidity progression within the disease. This study was conducted by integrating procedures to induce and assess neuropathic pain symptoms in a mouse model, along with an imaging experimental protocol conducted under anesthetized conditions (Figure 1A).

The study started with the evaluation of the mechanical sensitivity threshold by the Von Frey test in naïve conditions. After the assessment of a robust threshold the cohort underwent the first imaging session. Subsequently the neuropathic pain was induced by a procedure called cuff surgery (procedure detailed in the following paragraphs). The cohort was divided into three subgroups: the neuropathic group, which underwent the complete surgery including the implantation of the cuff; the sham group, which underwent the same surgical protocol but did not receive the cuff implantation; and finally, the naïve group, which did not undergo any surgical procedures. Throughout the longitudinal study some mice died recovering from anesthesia (2W n=1, 8W n= 2, 12W n=2).

Following the experimental protocol previously validated in a prior publication (Bertolo et al 2023) we performed imaging sessions in anesthetized mice (Figure 1B). In this configuration we acquired data with

a newly developed multi-array transducer allowing simultaneous multi-slicing of the entire mouse cerebrum (Figure 1C). This approach facilitates imaging numerous brain regions simultaneously, opening the possibility of conducting functional connectivity studies across the whole-brain.
The imaging session was conducted under resting-state conditions and lasted for 20 minutes. Each animal underwent sequential imaging sessions at each time point, for a total of four sessions.

Neuropathic pain model

Neuropathic pain was induced by implanting a 2 mm section of PE-20 polyethylene tubing around the main branch of the sciatic nerve of the right leg (**Figure *1***B) (Benbouzid et al. 2008; Barrot 2012; Yalcin et al. 2014). All procedures were performed under ketamine/medetomidine anesthesia Medetomidine (Domitor®, 0.5 mg/kg) and Ketamine (Imalgène®, 60 mg/kg). Animals in the sham group underwent the same procedure without cuff implantation, mice in the naïve group did not undergo any surgical procedure.

Mechanical sensitivity (Von Frey) test.

This test was performed to assess the mechanical sensitivity of the hind paws of the mice.
Mice were placed in Plexiglas boxes (9 cm x 7 cm x 7 cm) on a wire mesh surface (Figure 2A). The mechanical sensitivity was tested with thin calibrated plastic filaments (Von Frey filaments) that were applied to the plantar surface of the hind paw. The mice were left for 45 min to habituate to the set-up, after which each hind paw of the animals were sequentially stimulated by applying a series of filaments with increasing gauges or stiffness (from 0.16g to 10g). When the sensitivity threshold was reached, the mouse responded by withdrawing its paw away from the stimulus. Each filament was tested 5 times per paw, and was applied until it bent (Yalcin et al. 2014; Barthas et al. 2015). The threshold was defined as 3 or more withdrawals observed out of the 5 trials per filament. Mice were tested before the cuff surgery (baseline) and then at two, eight and twelve weeks after the cuff surgery.

Animal preparation

Mice were anesthetized by an initial intraperitoneal (IP) injection of ketamine and xylazine mixture at 80 mg/kg and 8 mg/kg, respectively. Anesthesia was maintained throughout the imaging session with an intramuscular perfusion of ketamine (15 mg/kg) and xylazine (1.5 mg/kg) using a syringe pump and with a low isoflurane supply (0.5% administered through a nose cone in an 100%/0% air/oxygen stream).

The hair of the mouse was shaved using depilatory cream, the skin disinfected with betadine® and anesthetized locally using injectable lidocaïne (4 mg/kg). The mouse was positioned on a stereotaxic frame and the scalp was incised along the sagittal suture, from behind the occipital bone to the beginning of the nasal bone. In this longitudinal study, the same animal underwent sequential imaging sessions at each time point, for a total of four sessions. Therefore, the skin was cut to avoid the development of ingrown hair between imaging sessions. The presence of ingrown hair would result in a thicker skin layer, hindering the ultrasound penetration.

The eyes of the mice were protected using an ointment (Ocry-gel, TVM, UK). Body temperature was monitored with a rectal probe connected to a heating pad set at 37°C. Respiration and heart rate were monitored using a PowerLab data acquisition system with the LabChart software (ADInstruments, USA).

fUS imaging session

Using an IconeusOne functional ultrasound system (Iconeus, France) we performed 20-min resting-state FC acquisitions (Figure 1B). The skull was gently covered with previously centrifuged echographic gel for ultrasonic coupling with the probe. A 15 MHz multi-array probe, consisting of four compact linear arrays of 64 piezo elements with a pitch of 110 µm (IcoPrime 4D-MultiArray, Iconeus, Paris, France) was used. The four independent linear arrays are designed to be tightly assembled with a 2.1 mm gap between each to minimize acoustical cross-talk and optimize the field of view. This study has followed the same procedure previously described in Bertolo et al. 2023. The probe was mounted on a 4-axis linear motor stage allowing a precise probe positioning and fast scanning of the brain.

A coronal scan of the entire window (Bregma to Lambda) was first performed to reconstruct a 3D angiographic volume of the brain. By using the IcoStudio software (Iconeus, Paris, France), we automatically aligned each individual 3D angiography with the Allen Mouse Brain common coordinate framework (Nouhoum et al. 2021) to ensure that the same fUS volume was acquired for each animal and at each imaging session.

fUS Imaging sequence

The imaging sequence was implemented using the same ultrafast plane wave transmission and reception scheme replicated for each of the four linear arrays. Four images (one per array) were simultaneously obtained from 4 × 200 compounded frames acquired at 500 Hz ($T_{integration}$ = 0.4s) using 4 × 8 tilted plane waves acquired at a pulse repetition frequency of 4 kHz (-12°, -8.57°, - 5.14°, 1.71°, 1.71°, 5.14°, 8.57°, 12°). To compensate for the limited lateral aperture size (64 elements compared to 128 in conventional

linear arrays), we used a trapezoidal beamforming grid with θmax = 12°, allowing the field of view to be extended on both sides and enabling the retrieval of deeper lateral brain regions (Bertolo et al. 2023).

In order to filter the Cerebral Blood Volume (CBV) and remove the tissue signal, a Singular Value Decomposition (SVD) was applied to 200 successive frames by removing the 60 first singular vectors, which correspond mainly to the tissue space (Demene et al. 2015). Finally, a Power Doppler image was obtained by integrating the energy of the filtered frames, resulting in four Power Doppler images captured in 400 ms.

For functional scans, the probe was sequentially stepped by 0.515 mm along the antero-posterior axis within a 0.2 duration, allowing the acquisition of a full volume of 10 x 8.1 x 9 mm3 comprised of 16 Power Doppler images of 100 x 100 x 515 µm3 resolution, as described previously (Bertolo et al. 2023). After slice timing correction, each full mouse brain volume was acquired in 2.4 s.

Power Doppler denoising

Prior to statistical analysis, power Doppler signals were denoised using the IcoLab software (ICONEUS, Paris) to mitigate the effects of motion artifacts (in awake acquisitions) and hemodynamic variations from non-neuronal sources. The denoising process involved the following steps:

1. Computation of confounding time series through principal component analysis (PCA) of the most variable time series obtained from white matter voxels, following the method outlined by Behzadi et al. (2007). Specifically, the top 5% most variable voxels were selected for PCA fitting, with the top 5 principal components retained as confounding variables.
2. Detection of high motion volumes in awake acquisitions by identifying volumes where the smoothed global signal (i.e., the average power Doppler signal from brain voxels, smoothed using a 5-sample moving average) deviated by more than 5% from its baseline. The global signal baseline was determined using least trimmed square regression. Only periods of low motion lasting at least 20 seconds were retained, with any remaining volumes interpolated to prevent bias in subsequent temporal filtering.
3. Temporal filtering of power Doppler signals and confounding time series using a Butterworth forward-backward bandpass filter with a frequency range of [0.01, 0.1] Hz and an order of 8.
4. Regression of filtered confounding time series from the power Doppler signals to remove confounding effects.

Correlation matrix analysis and statistical approach

Thanks to the registration procedure, the fUS brain volumes segmentation was performed using the Allen Mouse Brain atlas to extract mean rCBV signals over more than 40 brain regions of interest (ROI).

The selected 40 regions of interest (ROI) are grouped into 6 macro-regions that include the right and the left part of the Isocortex, the Hippocampus, the Striatum, the Interbrain and the Amygdala.

The Isocortex includes: Frontal pole, cerebral cortex (FRP), Primary motor area (M1), Secondary motor area (M2), Primary somatosensory area, hind-limb (S1HL), Primary somatosensory area, trunk (S1TR), Anterior cingulate cortex (ACC), Prelimbic area (PL), Infralimbic area (IL), Orbital area (OA), Agranular insular area, dorsal part (AID), Agranular insular area, posterior part (AIP), Agranular insular area, ventral part (AIV), Retrosplenial area (RSA). The hippocampal region (HIP). The Striatum includes: Caudoputamen (CPu), Nucleus accumbens (NAc), Lateral septal complex (LS). The interbrain includes Thalamus (THAL) and Hypothalamus (HYP). The Amygdala (sAMY).

The Pearson correlation coefficient was calculated between every pre-processed and normalized time-series (from each ROI). Subject-level FC matrices were Fisher-transformed and averaged across subjects (n=24; naïve n=8, sham n=8, np n=8).

These results are represented as a correlation matrix that displays the static Pearson's correlation coefficients between each possible pair of regions, ranging from -1 to 1. Alternatively, the correlation coefficients have been represented as a circular plot (Figure 4). The ROIs were arranged in a circular layout and the connection between them were illustrated as links with thickness corresponding to the correlation coefficient between the two nodes.

In order to test the connectivity differences in selected pairs of ROIs between the neuropathic and the control groups across different time points, we performed a two-way ANOVA test using mixed models. Following a significant effect of phenotype (NAIVE, Sham or NP), time (baseline, 2-weeks, 8-weeks or 12-weeks), or interaction between time and phenotype, a post-hoc Tukey's test was applied to reveal statistical differences between groups after correction for multiple comparisons. The pairs of ROIs that showed significant differences in the correlation coefficients between the neuropathic and the control group are reported in the results section.

4 RESULTS

Neuropathic allodynia

The nerve injury caused by the cuff implantation results in mechanical allodynia in the lesioned paw of the neuropathic group (Yalcin et al. 2014) (Figure 2).

Mechanical sensitivity was assessed for the three groups, naïve, sham and NP, before the cuff surgery at T0. No differences in mechanical sensitivity threshold were observed between groups at baseline (Figure 2B-C).

In the neuropathic group, starting from 2 weeks after the surgery, the ipsilateral paw's mechanical threshold showed a decrease compared to the ipsilateral paws of the control groups (2W p= 0.0002). This effect remains consistent at both 8 weeks (p= 0.0021) and 12 weeks (p= 0.0003). Moreover, the neuropathic group exhibited a significantly decreased paw withdrawal threshold compared to the threshold assessed before the surgery (T0 vs 2W p<0.0001, T0 vs 8W p= 0.0002, T0 vs 12W p=0.0001) (Figure 2C). On the other hand, there were no differences observed between the groups in the mechanical sensitivity of the contralateral paw (Figure 2B).

This result indicates the presence of mechanical allodynia in the lesioned paw of the neuropathic group, beginning at 2 weeks and persisting consistently at 8 and 12 weeks. The assessment of unilateral mechanical allodynia suggests that the neuropathic group exhibited typical neuropathic pain symptoms during the imaging sessions.

FC alterations in a wide-range network

The fUS imaging set-up configuration used in this study allows for whole-brain imaging. This approach facilitates imaging numerous brain regions simultaneously, opening to the possibility of conducting functional connectivity studies across all brain regions. In this study, we chose to investigate the bilateral functional connectivity across 40 brain regions, grouped into 6 macro-regions (Figure 3). In Figure 4 the correlation matrices are alternatively represented as a circular network. The averaged correlation coefficients were depicted as links connecting the different ROIs with varying thickness and colors, proportional to the strength of the correlation.

The matrices and the circular networks, respectively, show a consistent pattern of correlations between groups and timepoints. The pattern is mostly characterized by a cluster representing the strong inter-hemispheric connections within the isocortex. This cluster can be subdivided into three subclusters within

which the strength of connectivity varies between groups and overtime. The somatomotor area in the right hemisphere, the bilateral part of the retrosplenial cortex and the somatomotor connections in the left hemisphere. Those three clusters show strong correlation at baseline, followed by a decrease at 2W and a strong increase at 8W and 12W.

The correlation pattern is also characterized by the strong interconnection within the interbrain regions, which is slightly less prominent at 2W for all phenotypes.

These results demonstrate a consistent pattern of connectivity, indicating a good reproducibility of the measure between groups and time points. The robustness of this pattern enabled us to identify specific clusters of variability in the strength of connections across groups.

Functional connectivity alterations in a specific subnetwork

Statistical analysis revealed significant differences in the functional connectivity between the somatomotor and the striatum, the frontal area and the amygdala, the frontal area and the insular cortex (*Figure 5*A).

First, at 2W after nerve injury, the connectivity between the right primary motor cortex (R-M1) and the left nucleus accumbens (L-NAc) was significantly reinforced in NP mice compared to the sham group ($p=0.0225$) and compared to the correlation found at T0 in the same group ($p=0.0151$). Moreover, at 8W and 12W this connectivity significantly decreases in NP mice compared to that at 2W ($p=0.0337$ and $p=0.0443$, respectively). This enhanced connectivity between (R)-M1 and (L)-NAc returns to baseline values for the subsequent time points (*Figure 5*B).

Secondly, some networks exhibited a biphasic change in connectivity in NP mice compared to control groups (Figure 5C), characterized by an initial increase followed by a decrease: the correlation between the left infralimbic cortex (L-IL) and the right amygdala (R-Amy) was significantly higher in the NP group at 8W compared to sham ($p=0.0075$). However, at 12W the connectivity between those two regions was significantly lower compared to both control groups (SHAM $p=0.022$, NAÏVE $p=0.0338$). We can observe a similar evolution regarding the connectivity strength between the right prelimbic cortex (R-PL) and the right anterior insular cortex (R-AIV): at 2W, the correlation is significantly enhanced in NP mice compared to both control groups (SHAM $p=0.0289$, NAÏVE $p=0.0032$), and its Z-score value at baseline (T0) ($p<0.0001$). At 8W, the connections between R-PL and R-AIV in the neuropathic groups returned to baseline levels but was significantly lower than the sham group ($p=0.0031$) and significantly decreased compared to values at 2W ($p=0.032$).

These results highlight the presence of some alterations in the functional connectivity between neuropathic and control groups. We identified a biphasic effect overtime that involved a reinforced connection between frontal area and amygdala or insular cortex, at early stages of the neuropathic pain (2W-8W), followed by a decrease in the late stage (12W).

Insights into insular cortex connectivity trends in neuropathic mice

While the two-way ANOVA analysis did not reveal any significant effect of phenotype or time, the right insular cortex displayed notable shifts in connectivity patterns with several regions over time in neuropathic mice (Figure 6A).

As indicated by the arrow on the graph (Figure 6B-4), an increased correlation between the right dorsal insular cortex (R-AID) and the right prelimbic cortex (R-PL) is observed in neuropathic mice compared to sham and naïve at 2 weeks post nerve injury (+ 53% vs. sham; +56% vs. naïve). Although this increase did not reach statistical significance due to a lack of statistical power, both control groups, namely naive and sham, exhibited consistent connectivity level on average compared to baseline.

Moreover, when looking at the connectivity pattern between the ventral part of right the insular cortex (R-AIV) and the right amygdala (R-Amy) a late disconnection can be also observed at 12 weeks compared to controls (-70% vs. sham; -75% vs naïve, Figure 6B-5), although not reaching statistical significance. The same disconnection tendency can be observed in the latest time point between R-AIV and the right caudate putamen (R-CPu) in neuropathic mice (-49% vs. sham; -51% vs naïve, Figure 6B-6).

Taken together, these findings suggest that the ipsilateral insular cortex represents a central hub that is differentially affected during neuropathic pain development, showing both signs of hyper- and hypo connectivity depending on the regions considered and the time point following nerve injury.

5 DISCUSSION

Chronic pain patients suffer a disrupted quality of life, not only from the experience of pain itself, but also from comorbid symptoms such as depression, anxiety, cognitive impairment, and sleep disturbances. The heterogeneity of these symptoms support the idea of a major involvement of the cerebral cortex in the chronic pain condition. This study aimed at quantifying potential changes in brain resting-state functional connectivity during the development of neuropathic pain. Through longitudinal measurements of the brain functional connectivity in anesthetized naive, sham operated or lesioned mice (suffering from neuropathic pain), our study brings forward specific changes in brain networks involved in the emotional aspect of pain, but also in the adaptive response to psychological stress.

Circumventing limitations in preclinical neuroimaging studies

Imaging human patients was the first approach employed to reveal dysfunctional brain reorganization. These studies have been critical for identifying the brain circuitry involved in pain processing and modulation, and for understanding the disruption of those circuits in chronic pain. Despite the important information provided by imaging human subjects, there are many limitations. For example, longitudinal or lifespan studies in controlled conditions in humans are very difficult to perform. Conversely, in animal models, especially in rodent imaging studies, it is possible to overcome many of these limitations and provide a mechanism for back-translation of findings from humans to rodent models (Thompson and Bushnell 2012). In animal models more detailed, controlled, and invasive analysis can be performed. Therefore, we chose to conduct this study in a mouse model of neuropathic pain and longitudinally follow key stages of symptoms development and comorbidity progression within the disease.

For a longitudinal approach, the optimal configuration for fUS imaging experiments is under anesthetized conditions. The anesthetized configuration usually allows transcranial imaging through the shaved skin. The skin needs to be shaved with a depilatory cream; however, this procedure cannot be repeated multiple times due to hair regrowth, particularly ingrown hair. This would result in a thicker skin layer that could affect the quality of the image. Therefore, the skin was cut and sutured at each imaging session.

Another limitation of the anesthetized approach is in the repeated anesthesia injections. The animals were anesthetized five times with a mixture of ketamine and xylazine, which may have an effect on the

functional connectivity (Scheidegger et al. 2012; Martin 2014; Chuang and Nasrallah 2017). The global increase in FC overtime observed in Figure 3, might be due to the repeated doses of ketamine that we hypothesized could have brain-wide long-lasting effects on neural activity.

Biphasic changes of FC between the Infralimbic area and the Amygdala

The pairs of structures whose FC is modified in our study are involved in the affective-emotional aspects of pain. The biphasic alteration of their FC observed during the course of model development is possibly a sign of adaptive changes of brain networks during the chronification of pain and the development of comorbidities (anxiety and depression) that was previously described in this model (Yalcin et al. 2014; Barthas et al. 2015).

The amygdala plays a key role in processing emotional aspects of pain, such as fear, anxiety, and stress responses (Neugebauer 2020; Ji et al. 2024). The IL, on the other hand, is implicated in cognitive processes such as attentional control, decision-making, and extinction learning, which can modulate the experience of pain. Anatomical studies in rodents and other animals have demonstrated direct projections from the IL to different nuclei within the amygdala, including the basolateral amygdala (BLA) and the central nucleus of the amygdala (CeA) (Wood et al. 2019). These IL afferents modulate amygdalar activity. Conversely, the amygdala also sends projections back to the IL, forming reciprocal connections between these regions. This bidirectional connectivity allows for the integration of emotional information processed by the amygdala with cognitive and executive functions mediated by the IL.

The medial PFC undergoes dynamic changes in chronic pain conditions, with an overall deactivation, due to both an input-specific depression of excitatory glutamatergic inputs, and potentiation of GABAergic inhibition (Jefferson, Kelly, and Martina 2021). Both the prelimbic area (PL) and the amygdala play important roles in the processing of physical stress (Godoy et al. 2018). The central nucleus of the amygdala (CeA) participates in autonomic response integration. The mPFC is also actively involved in different stress responses in general, PL and Infralimbic (IL) regions coordinate a top-down control in these mechanisms. The amygdaloid complex also participates in psychological stress circuitry and with PFC disruption its involvement becomes more prevalent, and the circuitry switches to a bottom-up control.

In our study, the FC between the IL and the amygdala changed over the course of the disease, with a significant reduction in both sham and neuropathic animals at 2 weeks post lesion, compared to naïve

mice. As these changes are common to both groups of animals who undergo post-surgical pain, our hypothesis is that such an increase is due to post-surgical pain.
Interestingly, at 8 weeks post lesion, these changes disappear in sham animals but persist in neuropathic pain animals, suggesting long-lasting pain-related mechanisms. At this time point, the FC is surprisingly increased compared to both control groups (naïve and sham). Finally, at 12 weeks post lesion, the FC between the IL and the amygdala is decreased again compared to control groups.

Considering previous clinical observations of enhanced FC between the amygdala and multiple cortical, subcortical regions in pediatric CRPS patients compared to controls (Simons et al. 2014), and alteration of the FC between the PrL and the amygdala in stress-induced visceral pain in rats (Wang et al. 2013), we hypothesize that the biphasic changes we observe in our study is due to adaptation of the mechanism of pain and affective processing, leading to other negative emotions.

Biphasic changes of FC between the Prelimbic area and the Insula

The insula is involved in the sensory-discriminative and affective-motivational aspects of pain processing, while the PL is implicated in cognitive and emotional regulation of pain.
The PL, a region of the prefrontal cortex, and the insula, located within the cerebral cortex, are interconnected through neural pathways that support their functional interactions.

These connections involve both direct and indirect pathways: Anatomical studies in rodents and non-human primates have demonstrated direct projections from the PL to the insula. These projections typically originate from layers V and VI of the PL and terminate in various regions of the insula (Gehrlach et al. 2020), including its anterior, middle, and posterior divisions. These direct connections provide a means for the PL to influence the activity and function of the insula. Conversely, the PL receives glutamatergic inputs from the ipsilateral agranular insular cortex (Hoover and Vertes 2007).

In our study, the FC between the PrL and the insula was increased specifically in neuropathic animals, exclusively at 2 weeks post lesion. Due to the known involvement of insula in the central autonomic network (Saper 1982; Shoemaker and Goswami 2015) and the common role for the PrL and the insula in stress-regulated mechanism, and in particular doing chronic stress, where long-term excitatory/inhibitory balance of the insular cortices have significant implications for visceral regulation, (Schaeuble and Myers 2022; Godoy et al. 2018), our hypothesis is that this altered FC may be due to a state of long-lasting stress

in neuropathic animals that inevitably leads to functional rearrangement of the insula and an increased communications between these areas involved in stress and autonomic functions.

It must be noted that other changes of FC were observed in neuropathic pain animals. However as these alterations were robust, but of modest sample size, the ANOVA showed no statistical changes overall (Figure 6). These changes involve always a part of the insula and another structure of either the limbic system (the amygdala), the mPFC (PL) or the reward system (CPu) tendencies. These changes are likely to be indicative of an adaptive plasticity in the brain networks involved in pain, its modulation and of stress and its physiological consequences.

To conclude, this study revealed biphasic changes in functional connectivity between key brain regions implicated in pain processing and emotional regulation, namely the infralimbic area and the amygdala, as well as the prelimbic area and the insula. These alterations suggest adaptive changes in brain networks during the chronification of pain and the development of comorbidities, shedding light on the underlying mechanisms involved. These findings offer valuable implications for understanding the neurobiological basis of chronic pain and for the development of targeted therapeutic interventions aimed at alleviating both the physical and emotional burden experienced by chronic pain patients.

6 FIGURES

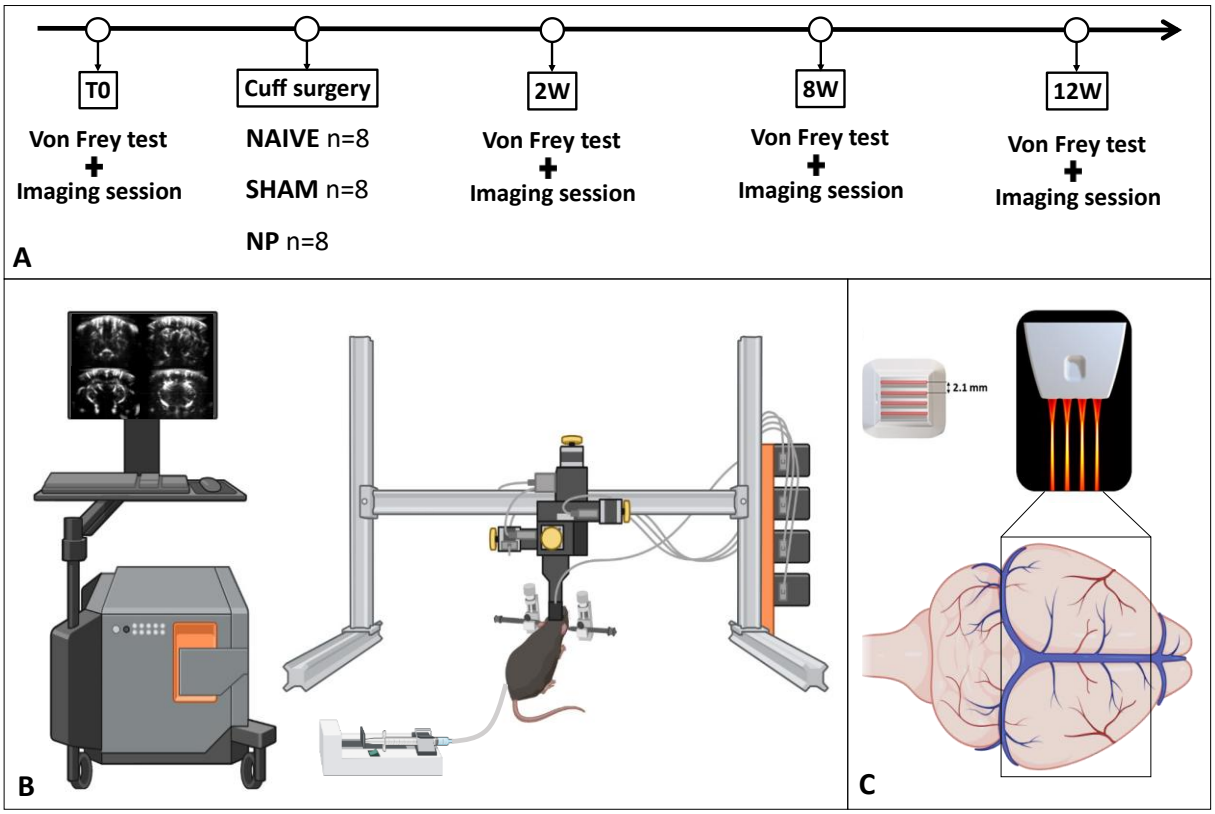

Figure 1: Experimental design. (A) Experimental timeline. Von Frey test was performed at baseline before cuff surgery. Imaging and Von Frey test was repeated at each time point. (B) Schematic illustration of the experimental setup for fUS imaging on anesthetized mice. (C) schematic illustration of the multi-array probe which includes four acoustic lenses, separated by 2.1 mm.

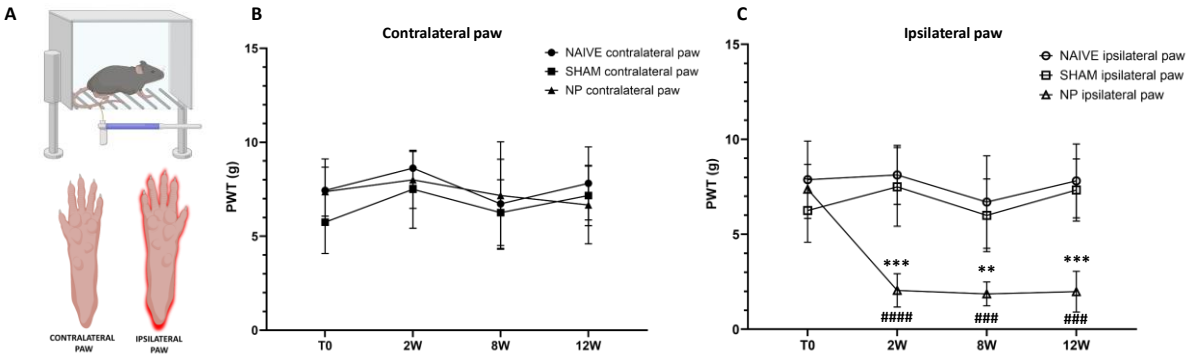

Figure 2: Figure 2: Cuff implantation induced mechanical allodynia. (A) Schematic description of a mouse in the Von Frey set-up and below the illustration of contralateral and ipsilateral paw showing the ipsilateral as the lesioned paw in the neuropathic group. (B) Von Frey test on contralateral paw at each time point. (C) Von Frey test on ipsilateral paw at each time point. Showing mechanical allodynia in the neuropathic group's ipsilateral paw starting at 2W, then following at 8W and 12W. Data are expressed as mean ± SD (* comparison between NP and Sham ipsilateral paws, ** p<0.01, *** p<0.001) (# comparison with NP at T0, ### p<0.001, #### p<0.0001) (T0: Naïve n=8, Sham n=8, NP n=8; 2W: Naïve n=8, Sham n=7, NP n=8; 8W: Naïve n=8, Sham n=7, NP n=6; 12W: Naïve n=7, Sham n=6, NP n=6).

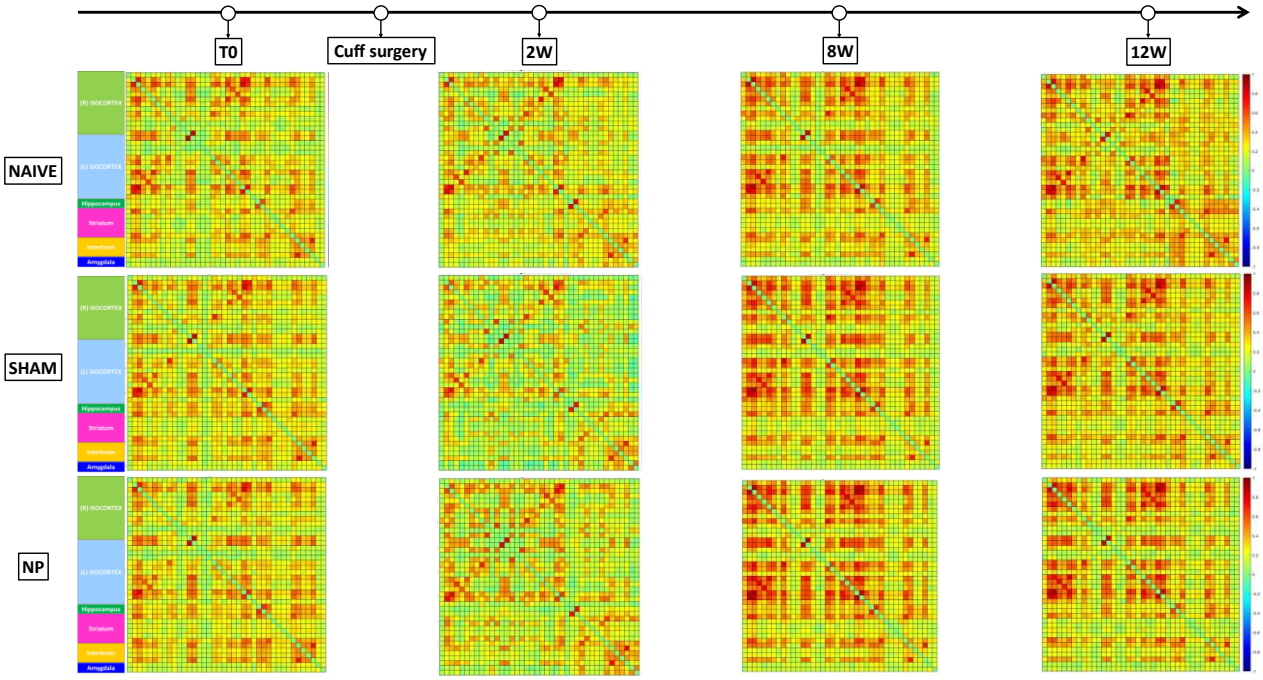

Figure 3: Functional Connectivity alterations in a wide-range network. Correlation matrices representation. Resting-state correlation matrices, displaying the mean Pearson correlation coefficient between 40 selected ROIs in a color-coded range from -1 to 1.

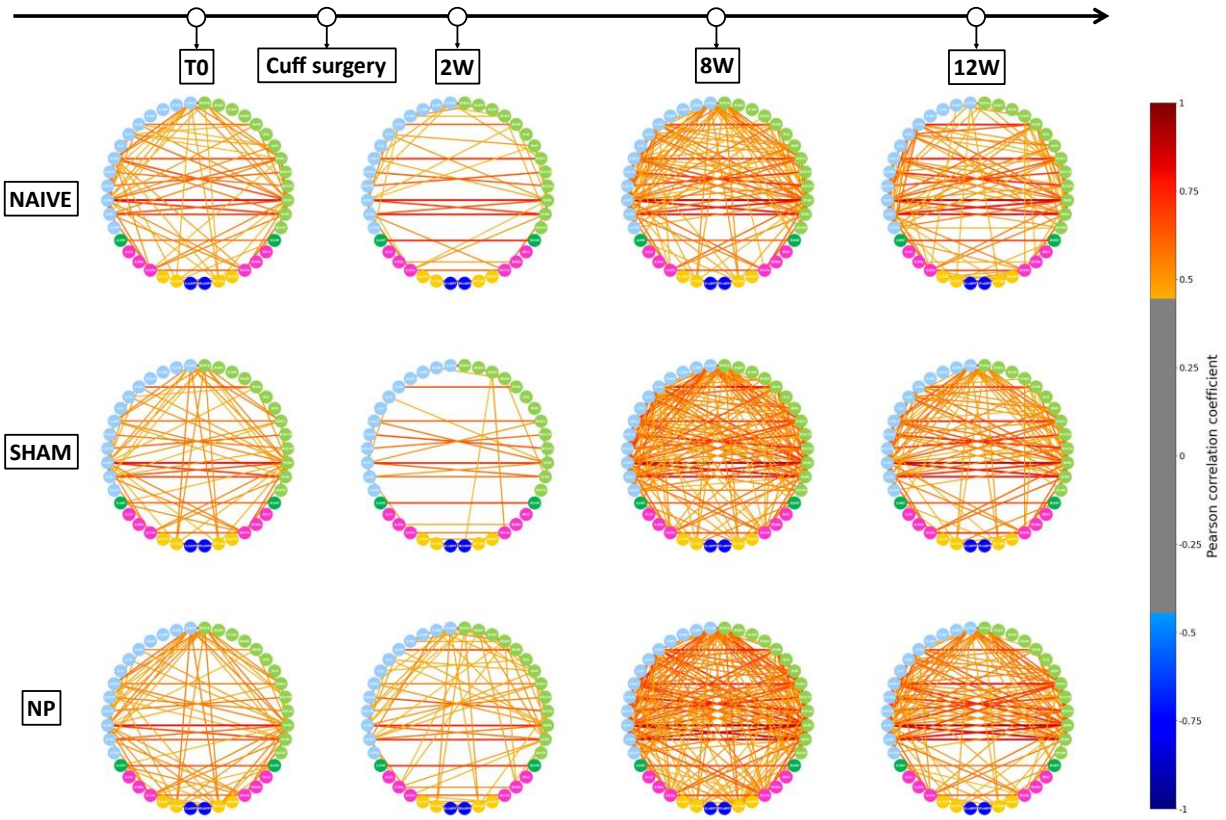

Figure 4: Functional Connectivity alterations in a wide-range network. Circular network representation. Alternative representation of the correlation matrix as a circular network with the 40 ROIs displayed in a circular layout and the connection between them illustrated as links with thickness corresponding to the correlation coefficient between the two nodes.

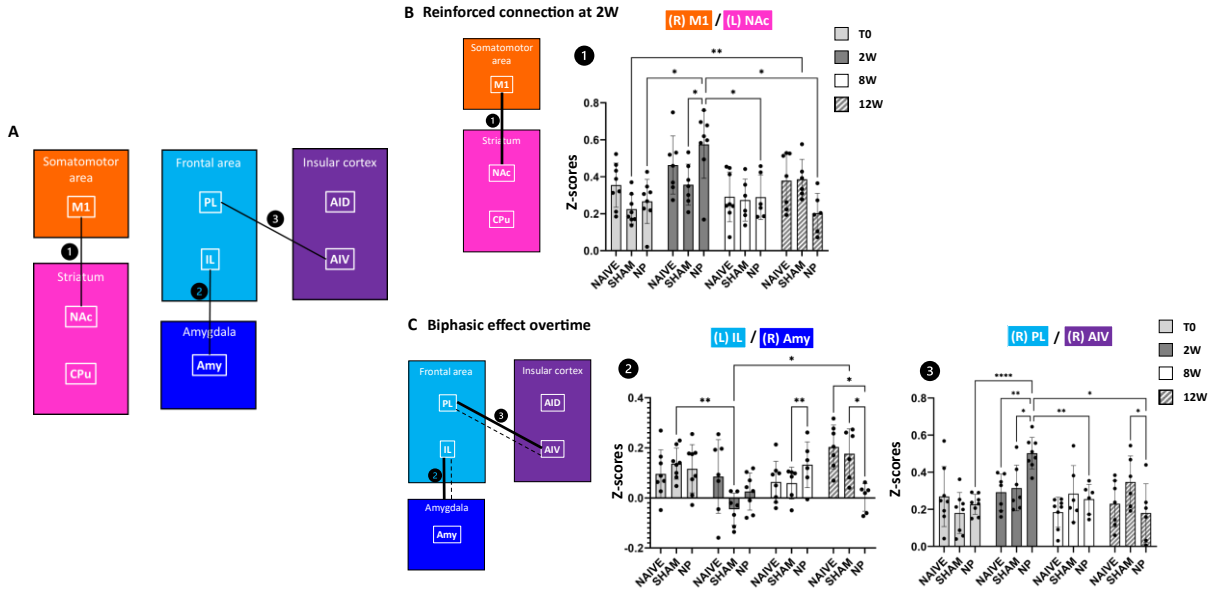

Figure 5: Functional connectivity alterations in a specific subnetwork. (A) Schematized illustration of two subnetworks showing significant functional connectivity alterations. Somatomotor area and striatum. Frontal area, amygdala and insular cortex. (B-C) Division of subnetwork showing a reinforced connection at 2W (B) and a biphasic effect overtime (C). The increase in connectivity is illustrated as a bold line and the decrease as a dotted line. The changes illustrated refer to the alterations detected in the neuropathic group compared to the sham group. Graphs 1, 2 and 3 represent Fisher-transformed z-score of correlations between pairs of ROIs at four time points (T0, 2, 8 and 12 weeks). Data are presented as mean ± SD. *p<0.05, **p<0.01, ****p<0.0001. T0: Naïve n=8, Sham n=8, NP n=8; 2W: Naïve n=7, Sham n=7, NP n=8; 8W: Naïve n=8, Sham n=6, NP n=6; 12W: Naïve n=7, Sham n=6, NP n=6.

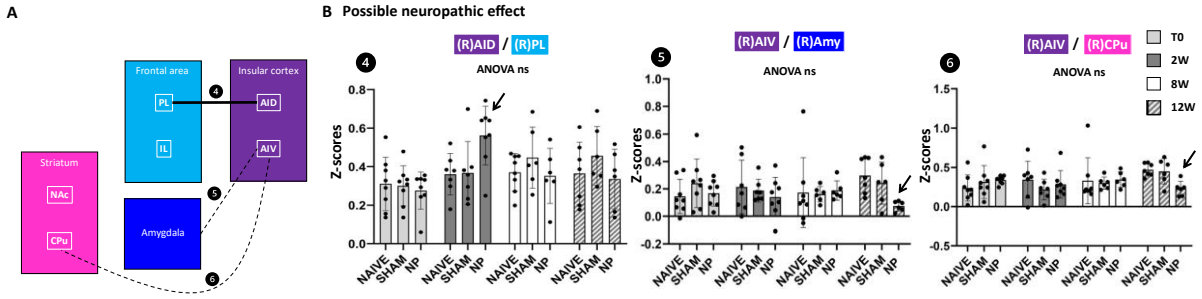

Figure 6: Possible neuropathic effect in the connection between the insular cortex, without significant changes. (A) Schematized illustration of one subnetwork showing a possible neuropathic effect. The increase in connectivity is illustrated as a bold line and the decrease as a dotted line. The changes illustrated refer to the alterations detected in the neuropathic group compared to the sham group. (B) Graphs 1, 2 and 3 represent Fisher-transformed z-score of correlations between pairs of ROIs at four time points (T0, 2, 8 and 12 weeks). The two-way ANOVA did not show any significant differences between groups, but the data show a clear trend of connectivity alterations in the neuropathic group compared to

the control groups (arrow). T0: Naïve n=8, Sham n=8, NP n=8; 2W: Naïve n=7, Sham n=7, NP n=8; 8W: Naïve n=8, Sham n=6, NP n=6; 12W: Naïve n=7, Sham n=6, NP n=6.

Conflict of interest

MT, BFO and TD are co-founders and shareholders of Iconeus company. AB, BFO and JF are employees of Iconeus. MT, BFO and TD are co-inventors of several patents in the field of neurofunctional ultrasound and ultrafast ultrasound. MT and TD do not have any other financial conflict of interest, nor any non-financial conflict of interest. All the other authors do not have any financial or non-financial conflict of interest.

Authors contribution statement

SP, SC and JF designed the experimental paradigm.

SC, YT were involved in functional ultrasound imaging and behavioral experiments.

SC, SP and JF wrote the manuscript.

SC performed the experiments and analyzed the ultrasound data.

JF and BFO supervised the signal processing of the ultrasound data.

SC and SP performed the statistical analysis.

SD, LE were involved in the signal processing.

SP and JF were involved in the interpretation of the data and wrote some parts of the manuscript.

Acknowledgments

The authors wish to thank Nathalie Ialy-Radio for animal husbandry and the CNRS, INSERM and ESPCI for their financial support. This work was supported by funding from ANRT and the Agence Nationale de la recherche (Project 'PINCH', 18-CE37-0005-01). SC's PhD was co-funded by Iconeus.

7 REFERENCES

Barrot, M. 2012. “Tests and Models of Nociception and Pain in Rodents.” *Neuroscience* 211 (June):39–50. https://doi.org/10.1016/j.neuroscience.2011.12.041.

Barthas, Florent, Jim Sellmeijer, Sylvain Hugel, Elisabeth Waltisperger, Michel Barrot, and Ipek Yalcin. 2015. “The Anterior Cingulate Cortex Is a Critical Hub for Pain-Induced Depression.” *Biological Psychiatry* 77 (3): 236–45. https://doi.org/10.1016/j.biopsych.2014.08.004.

Benbouzid, Malika, Viviane Pallage, Mathieu Rajalu, Elisabeth Waltisperger, Stéphane Doridot, Pierrick Poisbeau, Marie José Freund-Mercier, and Michel Barrot. 2008. “Sciatic Nerve Cuffing in Mice: A Model of Sustained Neuropathic Pain.” *European Journal of Pain* 12 (5): 591–99. https://doi.org/10.1016/j.ejpain.2007.10.002.

Benison, A. M., S. Chumachenko, J. A. Harrison, S. F. Maier, S. P. Falci, L. R. Watkins, and D. S. Barth. 2011. “Caudal Granular Insular Cortex Is Sufficient and Necessary for the Long-Term Maintenance of Allodynic Behavior in the Rat Attributable to Mononeuropathy.” *Journal of Neuroscience* 31 (17): 6317–28. https://doi.org/10.1523/JNEUROSCI.0076-11.2011.

Bergel, Antoine, Thomas Deffieux, Charlie Demené, Mickaël Tanter, and Ivan Cohen. 2018. “Local Hippocampal Fast Gamma Rhythms Precede Brain-Wide Hyperemic Patterns during Spontaneous Rodent REM Sleep.” *Nature Communications* 9 (1): 5364. https://doi.org/10.1038/s41467-018-07752-3.

Berman, Steven M., Bruce D. Naliboff, Brandall Suyenobu, Jennifer S. Labus, Jean Stains, Gordon Ohning, Lisa Kilpatrick, et al. 2008. “Reduced Brainstem Inhibition during Anticipated Pelvic Visceral Pain Correlates with Enhanced Brain Response to the Visceral Stimulus in Women with Irritable Bowel Syndrome.” *The Journal of Neuroscience: The Official Journal of the Society for Neuroscience* 28 (2): 349–59. https://doi.org/10.1523/JNEUROSCI.2500-07.2008.

Berna, Chantal, Siri Leknes, Emily A. Holmes, Robert R. Edwards, Guy M. Goodwin, and Irene Tracey. 2010. “Induction of Depressed Mood Disrupts Emotion Regulation Neurocircuitry and Enhances Pain Unpleasantness.” *Biological Psychiatry* 67 (11): 1083–90. https://doi.org/10.1016/j.biopsych.2010.01.014.

Bertolo, Adrien, Jeremy Ferrier, Silvia Cazzanelli, Samuel Diebolt, Mickael Tanter, Sophie Pezet, Mathieu Pernot, Bruno-Félix Osmanski, and Thomas Deffieux. 2023. “High Sensitivity Mapping of Brain-Wide Functional Networks in Awake Mice Using Simultaneous Multi-Slice fUS Imaging.” *Imaging Neuroscience*, October. https://doi.org/10.1162/imag_a_00030.

Brooks, J.C.W., L. Zambreanu, A. Godinez, A.D. (Bud) Craig, and I. Tracey. 2005. “Somatotopic Organisation of the Human Insula to Painful Heat Studied with High Resolution Functional Imaging.” *NeuroImage* 27 (1): 201–9. https://doi.org/10.1016/j.neuroimage.2005.03.041.

Brooks, Jonathan C.W., Turo J. Nurmikko, William E. Bimson, Krish D. Singh, and Neil Roberts. 2002. “fMRI of Thermal Pain: Effects of Stimulus Laterality and Attention.” *NeuroImage* 15 (2): 293–301. https://doi.org/10.1006/nimg.2001.0974.

Bushnell, M. C., G. H. Duncan, R. K. Hofbauer, B. Ha, J.-I. Chen, and B. Carrier. 1999. “Pain Perception: Is There a Role for Primary Somatosensory Cortex?” *Proceedings of the National Academy of Sciences* 96 (14): 7705–9. https://doi.org/10.1073/pnas.96.14.7705.

Bushnell, M. Catherine, Marta Čeko, and Lucie A. Low. 2013. “Cognitive and Emotional Control of Pain and Its Disruption in Chronic Pain.” *Nature Reviews Neuroscience* 14 (7): 502–11. https://doi.org/10.1038/nrn3516.

Chuang, Kai-Hsiang, and Fatima A. Nasrallah. 2017. “Functional Networks and Network Perturbations in Rodents.” *NeuroImage* 163 (December):419–36. https://doi.org/10.1016/j.neuroimage.2017.09.038.

Coghill, R. C., J. D. Talbot, A. C. Evans, E. Meyer, A. Gjedde, M. C. Bushnell, and G. H. Duncan. 1994. “Distributed Processing of Pain and Vibration by the Human Brain.” *Journal of Neuroscience* 14 (7): 4095–4108. https://doi.org/10.1523/JNEUROSCI.14-07-04095.1994.

Coghill, Robert C., Christine N. Sang, Jose Ma. Maisog, and Michael J. Iadarola. 1999. “Pain Intensity Processing Within the Human Brain: A Bilateral, Distributed Mechanism.” *Journal of Neurophysiology* 82 (4): 1934–43. https://doi.org/10.1152/jn.1999.82.4.1934.

Costigan, Michael, Joachim Scholz, and Clifford J. Woolf. 2009. “Neuropathic Pain: A Maladaptive Response of the Nervous System to Damage.” *Annual Review of Neuroscience* 32 (1): 1–32. https://doi.org/10.1146/annurev.neuro.051508.135531.

Demene, Charlie, Jérome Baranger, Miguel Bernal, Catherine Delanoe, Stéphane Auvin, Valérie Biran, Marianne Alison, et al. 2017. “Functional Ultrasound Imaging of Brain Activity in Human Newborns.” *Science Translational Medicine* 9 (411): eaah6756. https://doi.org/10.1126/scitranslmed.aah6756.

Demene, Charlie, Thomas Deffieux, Mathieu Pernot, Bruno-Felix Osmanski, Valerie Biran, Jean-Luc Gennisson, Lim-Anna Sieu, et al. 2015. “Spatiotemporal Clutter Filtering of Ultrafast Ultrasound Data Highly Increases Doppler and fUltrasound Sensitivity.” *IEEE Transactions on Medical Imaging* 34 (11): 2271–85. https://doi.org/10.1109/TMI.2015.2428634.

Dizeux, Alexandre, Marc Gesnik, Harry Ahnine, Kevin Blaize, Fabrice Arcizet, Serge Picaud, José-Alain Sahel, Thomas Deffieux, Pierre Pouget, and Mickael Tanter. 2019. “Functional Ultrasound Imaging of the Brain Reveals Propagation of Task-Related Brain Activity in Behaving Primates.” *Nature Communications* 10 (1): 1400. https://doi.org/10.1038/s41467-019-09349-w.

Fox, Michael D., and Marcus E. Raichle. 2007. “Spontaneous Fluctuations in Brain Activity Observed with Functional Magnetic Resonance Imaging.” *Nature Reviews Neuroscience* 8 (9): 700–711. https://doi.org/10.1038/nrn2201.

Garcia-Larrea, Luis, and Roland Peyron. 2013. “Pain Matrices and Neuropathic Pain Matrices: A Review.” *Pain* 154 (Supplement 1): S29–43. https://doi.org/10.1016/j.pain.2013.09.001.

Gehrlach, Daniel A., Nate Dolensek, Alexandra S. Klein, Ritu Roy Chowdhury, Arthur Matthys, Michaela Junghänel, Thomas N. Gaitanos, et al. 2019. “Aversive State Processing in the Posterior Insular Cortex.” *Nature Neuroscience* 22 (9): 1424–37. https://doi.org/10.1038/s41593-019-0469-1.

Gehrlach, Daniel A, Caroline Weiand, Thomas N Gaitanos, Eunjae Cho, Alexandra S Klein, Alexandru A Hennrich, Karl-Klaus Conzelmann, and Nadine Gogolla. 2020. “A Whole-Brain Connectivity Map of Mouse Insular Cortex.” *eLife* 9 (September):e55585. https://doi.org/10.7554/eLife.55585.

Godoy, Lívea Dornela, Matheus Teixeira Rossignoli, Polianna Delfino-Pereira, Norberto Garcia-Cairasco, and Eduardo Henrique De Lima Umeoka. 2018. “A Comprehensive Overview on Stress Neurobiology: Basic Concepts and Clinical Implications.” *Frontiers in Behavioral Neuroscience* 12 (July):127. https://doi.org/10.3389/fnbeh.2018.00127.

Gogolla, Nadine. 2017. “The Insular Cortex.” *Current Biology* 27 (12): R580–86. https://doi.org/10.1016/j.cub.2017.05.010.

Gracely, Richard H., Frank Petzke, Julie M. Wolf, and Daniel J. Clauw. 2002. “Functional Magnetic Resonance Imaging Evidence of Augmented Pain Processing in Fibromyalgia.” *Arthritis and Rheumatism* 46 (5): 1333–43. https://doi.org/10.1002/art.10225.

Gustin, Sylvia M., Chris C. Peck, Sophie L. Wilcox, Paul G. Nash, Greg M. Murray, and Luke A. Henderson. 2011. “Different Pain, Different Brain: Thalamic Anatomy in Neuropathic and Non-Neuropathic Chronic Pain Syndromes.” *Journal of Neuroscience* 31 (16): 5956–64. https://doi.org/10.1523/JNEUROSCI.5980-10.2011.

Henderson, L. A., S. C. Gandevia, and V. G. Macefield. 2007. “Somatotopic Organization of the Processing of Muscle and Cutaneous Pain in the Left and Right Insula Cortex: A Single-Trial fMRI Study.” *PAIN* 128 (1): 20. https://doi.org/10.1016/j.pain.2006.08.013.

Hoover, Walter B., and Robert P. Vertes. 2007. “Anatomical Analysis of Afferent Projections to the Medial Prefrontal Cortex in the Rat.” *Brain Structure & Function* 212 (2): 149–79. https://doi.org/10.1007/s00429-007-0150-4.

Hsieh, Jen-Chuen, Måns Belfrage, Sharon Stone-Elander, Per Hansson, and Martin Ingvar. 1995. “Central Representation of Chronic Ongoing Neuropathic Pain Studied by Positron Emission Tomography.” *PAIN* 63 (2): 225. https://doi.org/10.1016/0304-3959(95)00048-W.

Jefferson, Taylor, Crystle J. Kelly, and Marco Martina. 2021. “Differential Rearrangement of Excitatory Inputs to the Medial Prefrontal Cortex in Chronic Pain Models.” *Frontiers in Neural Circuits* 15 (December). https://doi.org/10.3389/fncir.2021.791043.

Jensen, Karin B., Eva Kosek, Frank Petzke, Serena Carville, Peter Fransson, Hanke Marcus, Steven C. R. Williams, et al. 2009. “Evidence of Dysfunctional Pain Inhibition in Fibromyalgia Reflected in rACC during Provoked Pain.” *Pain* 144 (1–2): 95–100. https://doi.org/10.1016/j.pain.2009.03.018.

Ji, Guangchen, Peyton Presto, Takaki Kiritoshi, Yong Chen, Edita Navratilova, Frank Porreca, and Volker Neugebauer. 2024. “Chemogenetic Manipulation of Amygdala Kappa Opioid Receptor Neurons Modulates Amygdala Neuronal Activity and Neuropathic Pain Behaviors.” *Cells* 13 (8): 705. https://doi.org/10.3390/cells13080705.

Klein, Alexandra S., Nate Dolensek, Caroline Weiand, and Nadine Gogolla. 2021. “Fear Balance Is Maintained by Bodily Feedback to the Insular Cortex in Mice.” *Science* 374 (6570): 1010–15. https://doi.org/10.1126/science.abj8817.

Labrakakis, Charalampos. 2023. “The Role of the Insular Cortex in Pain.” *International Journal of Molecular Sciences* 24 (6): 5736. https://doi.org/10.3390/ijms24065736.

Longe, S. E., R. Wise, S. Bantick, D. Lloyd, H. Johansen-Berg, F. McGlone, and I. Tracey. 2001. “Counter-Stimulatory Effects on Pain Perception and Processing Are Significantly Altered by Attention: An fMRI Study.” *Neuroreport* 12 (9): 2021–25. https://doi.org/10.1097/00001756-200107030-00047.

Macé, Emilie, Gabriel Montaldo, Ivan Cohen, Michel Baulac, Mathias Fink, and Mickael Tanter. 2011. “Functional Ultrasound Imaging of the Brain.” *Nature Methods* 8 (8): 662–64. https://doi.org/10.1038/nmeth.1641.

Martin, Chris. 2014. “Contributions and Complexities from the Use of in Vivo Animal Models to Improve Understanding of Human Neuroimaging Signals.” *Frontiers in Neuroscience* 8:211. https://doi.org/10.3389/fnins.2014.00211.

Méndez-Ruette, Maxs, Sergio Linsambarth, Rodrigo Moraga-Amaro, Daisy Quintana-Donoso, Luis Méndez, Giovanni Tamburini, Francisca Cornejo, Rodrigo F. Torres, and Jimmy Stehberg. 2019. “The Role of the Rodent Insula in Anxiety.” *Frontiers in Physiology* 10 (March). https://doi.org/10.3389/fphys.2019.00330.

Neugebauer, Volker. 2020. “Amygdala Physiology in Pain.” *Handbook of Behavioral Neuroscience* 26:101–13. https://doi.org/10.1016/b978-0-12-815134-1.00004-0.

Nouhoum, M., J. Ferrier, B.-F. Osmanski, N. Ialy-Radio, S. Pezet, M. Tanter, and T. Deffieux. 2021. “A Functional Ultrasound Brain GPS for Automatic Vascular-Based Neuronavigation.” *Scientific Reports* 11 (1): 15197. https://doi.org/10.1038/s41598-021-94764-7.

Osmanski, Bruno-Félix, Sophie Pezet, Ana Ricobaraza, Zsolt Lenkei, and Mickael Tanter. 2014. “Functional Ultrasound Imaging of Intrinsic Connectivity in the Living Rat Brain with High Spatiotemporal Resolution.” *Nature Communications* 5 (1): 5023. https://doi.org/10.1038/ncomms6023.

Ossipov, Michael H., Gregory O. Dussor, and Frank Porreca. 2010. “Central Modulation of Pain.” *The Journal of Clinical Investigation* 120 (11): 3779–87. https://doi.org/10.1172/JCI43766.

Paulus, Martin P., and Murray B. Stein. 2006. “An Insular View of Anxiety.” *Biological Psychiatry* 60 (4): 383–87. https://doi.org/10.1016/j.biopsych.2006.03.042.

Petrovic, P., K. M. Petersson, P. H. Ghatan, S. Stone-Elander, and M. Ingvar. 2000. “Pain-Related Cerebral Activation Is Altered by a Distracting Cognitive Task.” *Pain* 85 (1–2): 19–30. https://doi.org/10.1016/s0304-3959(99)00232-8.

Ploner, Markus, Michael C. Lee, Katja Wiech, Ulrike Bingel, and Irene Tracey. 2011. “Flexible Cerebral Connectivity Patterns Subserve Contextual Modulations of Pain.” *Cerebral Cortex (New York, N.Y.: 1991)* 21 (3): 719–26. https://doi.org/10.1093/cercor/bhq146.

Rahal, Line, Miguel Thibaut, Isabelle Rivals, Julien Claron, Zsolt Lenkei, Jacobo D. Sitt, Mickael Tanter, and Sophie Pezet. 2020. “Ultrafast Ultrasound Imaging Pattern Analysis Reveals Distinctive Dynamic Brain States and Potent Sub-Network Alterations in Arthritic Animals.” *Scientific Reports* 10 (1): 10485. https://doi.org/10.1038/s41598-020-66967-x.

Roy, Mathieu, Mathieu Piché, Jen-I. Chen, Isabelle Peretz, and Pierre Rainville. 2009. “Cerebral and Spinal Modulation of Pain by Emotions.” *Proceedings of the National Academy of Sciences of the United States of America* 106 (49): 20900–905. https://doi.org/10.1073/pnas.0904706106.

Saper, Clifford B. 1982. “Convergence of Autonomic and Limbic Connections in the Insular Cortex of the Rat.” *Journal of Comparative Neurology* 210 (2): 163–73. https://doi.org/10.1002/cne.902100207.

Schaeuble, Derek, and Brent Myers. 2022. “Cortical–Hypothalamic Integration of Autonomic and Endocrine Stress Responses.” *Frontiers in Physiology* 13 (February). https://doi.org/10.3389/fphys.2022.820398.

Scheidegger, Milan, Martin Walter, Mick Lehmann, Coraline Metzger, Simone Grimm, Heinz Boeker, Peter Boesiger, Anke Henning, and Erich Seifritz. 2012. “Ketamine Decreases Resting State Functional Network Connectivity in Healthy Subjects: Implications for Antidepressant Drug Action.” *PloS One* 7 (9): e44799. https://doi.org/10.1371/journal.pone.0044799.

Shoemaker, J. K., and Ruma Goswami. 2015. “Forebrain Neurocircuitry Associated with Human Reflex Cardiovascular Control.” *Frontiers in Physiology* 6 (September). https://doi.org/10.3389/fphys.2015.00240.

Sieu, Lim-Anna, Antoine Bergel, Elodie Tiran, Thomas Deffieux, Mathieu Pernot, Jean-Luc Gennisson, Mickaël Tanter, and Ivan Cohen. 2015. “EEG and Functional Ultrasound Imaging in Mobile Rats.” *Nature Methods* 12 (9): 831–34. https://doi.org/10.1038/nmeth.3506.

Simons, L. E., M. Pielech, N. Erpelding, C. Linnman, E. Moulton, S. Sava, A. Lebel, et al. 2014. “The Responsive Amygdala: Treatment-Induced Alterations in Functional Connectivity in Pediatric Complex Regional Pain Syndrome.” *Pain* 155 (9): 1727–42. https://doi.org/10.1016/j.pain.2014.05.023.

Soloukey, Sadaf, Arnaud J. P. E. Vincent, Djaina D. Satoer, Frits Mastik, Marion Smits, Clemens M. F. Dirven, Christos Strydis, et al. 2020. “Functional Ultrasound (fUS) During Awake Brain Surgery: The Clinical Potential of Intra-Operative Functional and Vascular Brain Mapping.” *Frontiers in Neuroscience* 13 (January):1384. https://doi.org/10.3389/fnins.2019.01384.

Tan, Linette Liqi, Patric Pelzer, Céline Heinl, Wannan Tang, Vijayan Gangadharan, Herta Flor, Rolf Sprengel, Thomas Kuner, and Rohini Kuner. 2017. “A Pathway from Midcingulate Cortex to Posterior Insula Gates Nociceptive Hypersensitivity.” *Nature Neuroscience* 20 (11): 1591–1601. https://doi.org/10.1038/nn.4645.

Thompson, Scott J., and M. Catherine Bushnell. 2012. “Rodent Functional and Anatomical Imaging of Pain.” *Neuroscience Letters* 520 (2): 131–39. https://doi.org/10.1016/j.neulet.2012.03.015.

Urban, Alan, Clara Dussaux, Guillaume Martel, Clément Brunner, Emilie Mace, and Gabriel Montaldo. 2015. “Real-Time Imaging of Brain Activity in Freely Moving Rats Using Functional Ultrasound.” *Nature Methods* 12 (9): 873–78. https://doi.org/10.1038/nmeth.3482.

Valet, Michael, Till Sprenger, Henning Boecker, Frode Willoch, Ernst Rummeny, Bastian Conrad, Peter Erhard, and Thomas R. Tolle. 2004. “Distraction Modulates Connectivity of the Cingulo-Frontal Cortex and the Midbrain during Pain--an fMRI Analysis.” *Pain* 109 (3): 399–408. https://doi.org/10.1016/j.pain.2004.02.033.

Villemure, Chantal, and M. Catherine Bushnell. 2009. “Mood Influences Supraspinal Pain Processing Separately from Attention.” *The Journal of Neuroscience: The Official Journal of the Society for Neuroscience* 29 (3): 705–15. https://doi.org/10.1523/JNEUROSCI.3822-08.2009.

Wang, Zhuo, Marco A. Ocampo, Raina D. Pang, Mihail Bota, Sylvie Bradesi, Emeran A. Mayer, and Daniel P. Holschneider. 2013. “Alterations in Prefrontal-Limbic Functional Activation and Connectivity in Chronic Stress-Induced Visceral Hyperalgesia.” *PLOS ONE* 8 (3): e59138. https://doi.org/10.1371/journal.pone.0059138.

Wood, Miranda, Othman Adil, Tyler Wallace, Sarah Fourman, Steven P. Wilson, James P. Herman, and Brent Myers. 2019. “Infralimbic Prefrontal Cortex Structural and Functional Connectivity with the Limbic Forebrain: A Combined Viral Genetic and Optogenetic Analysis.” *Brain Structure & Function* 224 (1): 73–97. https://doi.org/10.1007/s00429-018-1762-6.

Yalcin, Ipek, Salim Megat, Florent Barthas, Elisabeth Waltisperger, Mélanie Kremer, Eric Salvat, and Michel Barrot. 2014. “The Sciatic Nerve Cuffing Model of Neuropathic Pain in Mice.” *Journal of Visualized Experiments*, no. 89 (July), 51608. https://doi.org/10.3791/51608.

Zhuo, Min. 2008. “Cortical Excitation and Chronic Pain.” *Trends in Neurosciences* 31 (4): 199–207. https://doi.org/10.1016/j.tins.2008.01.003.

CHAPTER 6

GENERAL DISCUSSION

The main objective of this thesis was to decipher the temporal link between alterations in cerebral Functional Connectivity and the development of neuropathic pain and/or associated comorbidities in a mouse model of neuropathic pain using functional ultrasound imaging (fUS). We addressed the same scientific question using two distinct experimental approaches to overcome their respective limitations. These different approaches were possible thanks to the technological and engineering development in fUS imaging conducted in the laboratory, in close collaboration with Iconeus, who co-funded my PhD.

The four articles presented in this manuscript followed a linear progression of fUS technological advancement and the consequent application to the neurobiological question. Starting by the validation of the experimental protocol and data acquisition in a 2D motor-translated configuration, enabled the investigation of the altered brain circuity in awake conditions. It followed the validation of data acquisition in a 3D-configuration that enabled the investigation of altered functional connectivity in a broader network and finally, made a longitudinal follow-up of the disease possible.

Similar effects found in both studies

Despite the differences in the experimental approaches in both studies, we observed significant changes in connectivity patterns, mostly in the regions involved in the affective-emotional aspect of pain, particularly between the frontal area and regions involved in stress-related responses (Figure 61D).

For example, in the second article, at the 2W time point, we found changes in the connections between the frontal area and the Hypothalamus. Some nuclei of the Hypothalamus are involved in stress integration functions. In particular, the PH receives inputs from various forebrain regions and projecting to stress-related nuclei like the paraventricular nucleus (PVN) (Ulrich-Lai et al. 2011). The increased FC observed in neuropathic animals suggests active reinforcement of the hypothalamic-pituitary-adrenal (HPA) axis in response to ongoing spontaneous pain.

In the fourth article, we found changes in the connections between the frontal area and the Amygdala. Considering previous clinical observations of enhanced FC between the amygdala and multiple cortical and subcortical regions in CRPS patients compared to controls (Simons et al. 2014), and alteration of the FC between the PrL and the amygdala in stress-induced visceral pain in rats (Figure 61C) (Wang et al. 2013), we hypothesize that the changes observed in our study are due to adaptation of pain and fear processing mechanisms, leading to chronification of pain and the development of comorbidities (anxiety and depression).

Moreover, in the fourth article, changes between the frontal area and the insular cortex were evidenced. The Prelimbic cortex and the insula have a common role in stress-regulation. Human imaging studies have

revealed that the insular shifts cardiac autonomic activity, possibly leading to arrhythmias (Oppenheimer and Cechetto 2016). Furthermore, both human and rodent studies include the insula in the central autonomic network (Saper 1982; Shoemaker and Goswami 2015). Our results are consistent with other studies suggesting that IL-insula communication during chronic stress modulates long-term excitatory/inhibitory balance of the insular cortices, which may have significant implications for visceral regulation (De Pace et al. 2020).

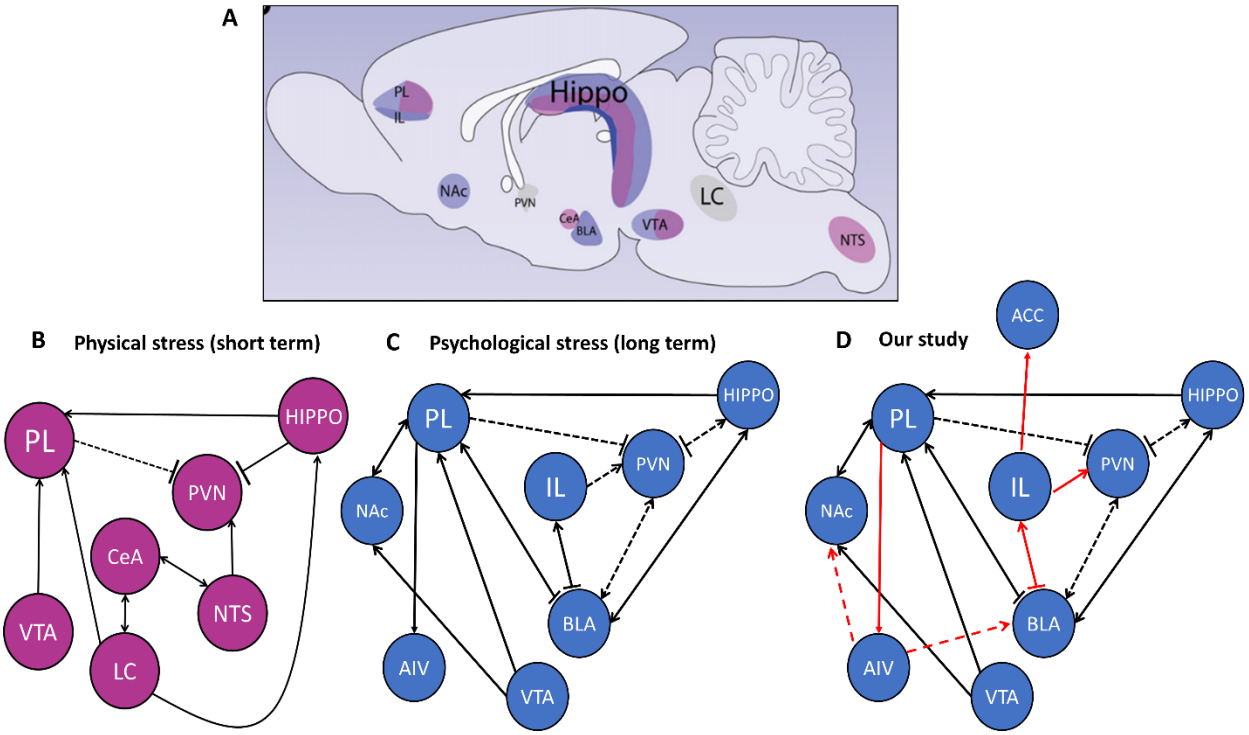

Figure 61: Regions involved in stress-related responses and our study contribution. (A-B-C) (Adapted from Godoy et al. 2018) Schematic representation of primarily neuroanatomical substrates responsible for physical (B) and psychological (C) stressors processing. (D) Readaptation of the figure from Godoy et al. 2018 to illustrate the contribution of our study (red lines). (dotted red lines represents the results ANOVA ns, see article n° 4 chapter5). Prelimbic area (PL), Ventral Tegmental area (VTA), central nucleus of the amygdala (CeA), locus coeruleus (LC), paraventricular nucleus of hypothalamus (PVN), nucleus of the solitary tract (NTS), Hippocampus (HIPPO), Nucleus Accumbens (NAc), Infralimbic (IL), basolateral amygdala (BLA), Anterior Cingulate Cortex (ACC).

Furthermore, in both studies, at the 2W time point, we identified some specific changes in the connectivity in both sham and neuropathic group. The changes involved mostly the frontal area, specifically, in the second article between IL and ACC, and also some changes within the insular cortex. In the fourth article between IL and Amygdala. As the changes are common to both groups of animals who undergo post-

surgical pain, our hypothesis is that is due to post-surgical pain. Interestingly, in the later time points, these changes disappear in sham animals but persist in neuropathic pain animals, suggesting long-lasting pain-related mechanisms. Although more specific experiments are required to confirm these observations, these results suggest that surgical intervention induces early and short-lasting changes in the pain matrix.

Study-specific observations

Both studies brought forward different results: in the second article, we found a specific disconnection within the somatomotor network. These adaptive changes of brain network involved in sensitivity and pain are observed in our study at 8 weeks post lesion (and not earlier at 2 weeks). We hypothesize that these long-lasting rearrangements of the somatomotor network may require several weeks of altered electrophysiological changes to take place, as observed in neuropathic pain by Leblanc et al., (LeBlanc et al. 2016). In anesthetized experiments, we did not confirm such changes.

On the other hand, in awake experiments, we found more differences in the connection with subcortical regions, such as thalamus and hypothalamus. Several studies have demonstrated that the connectivity strength between cortical and sub-cortical regions are reduced under anesthesia. Considering that anesthetics directly affect several neurotransmitter systems, which may lead to alterations in brain baseline function and responsiveness that would potentially explain the changes in the functional connectivity at rest (Paasonen et al. 2017).

Experimental approaches

To overcome the potential bias induced by anesthesia, we performed the first study in awake head-fixed conditions. However, despite intensive habituation, head-fixed conditions can induce stress, which was mitigated by using an alternative head-fixation apparatus called Mobile HomeCage. This apparatus minimizes disruption to normal behavior while ensuring head fixation (Neurotar, https://www.neurotar.com/the-mobile-homecage/). Nonetheless, head-restrained configuration presented major limitations. For example, we encountered difficulties in performing longitudinal studies, due to the invasiveness of the surgery required to implant the head-plate, exposing the skull permanently and causing infections. Several attempts were made to circumvent these problems, but we finally chose not to perform longitudinal studies and to compare different batches of animals, imaged at different time points.

Another important limitation of the awake experiments is the motion artifacts caused by the animal's movements in the mobile home cage. This is even more pronounced in the most lateral para-sagittal sections due to the close vicinity with temporal muscles, producing strong doppler artifacts at the whole-frame level (Tiran et al. 2017). Hence, the signals from lateral brain regions (such as the insular cortex) were very noisy and required extensive signal processing and strict epochs exclusion. Artifacts frequently led to the exclusion of acquisitions, reducing drastically the number of animals included in the final analysis. Secondly, the multislice approach using linear 1D transducers (as described in the first article) introduces a tradeoff between the number of imaged slices and the final volume rate. In order to keep a volume rate compatible with the sampling of spontaneous brain oscillations (i.e. > 0.4 Hz), we restricted the field of view to the contralateral (left) brain hemisphere. While we expected most plastic changes to occur in contralateral brain regions, our study didn't allow for the capture of the entirety of the pain neuromatrix and overlooked any potential changes that occurred in the regions ipsilateral to the nerve lesion.

To overcome the limitation encountered in awake conditions for longitudinal study we conducted the second study under anesthetized conditions. This approach allowed for a longer follow-up of neuropathic pain conditions, at 4 time points. The anesthetized configuration usually allows transcranial imaging through the shaved skin. However, this procedure could not be repeated multiple times due to hair regrowth, particularly ingrown hair. This would have resulted in a thicker skin layer that could affect the quality of the image. Therefore, the skin was cut and sutured during each imaging session.

Limitations in assessing anxio-depressive like behavior in both neuropathic pain studies.

Alongside the Von Frey test, for a comprehensive analysis of the emotional state linked with chronic pain, along with the changes in functional connectivity, it was essential for this study to accurately evaluate the anxio-depressive behaviors in the cohorts of animals. Therefore, we conducted two additional behavioral tests to assess the emergence of comorbidities during the time points investigated. The Novelty suppressed feeding (NSF) test assesses the anxiodepressive-like behavior at 8W and the Splash test assesses the development of depressive-like symptoms overtime. The NSF test was performed once at 8W time point. The Splash test was performed before the cuff surgery to assess the normal grooming behavior and then repeated at each time point.

We performed these tests for both neuropathic studies described in this manuscript. The results obtained (data not shown) for both tests did not show significative differences between the neuropathic groups

and the controls. The results were not consistent within each group, highlighting major variability in the individual behavior of the animals.

The variability in the outcome of the responses to those tests suggests a disruption in the normal behavior. We hypothesized that the perturbation could be due:

- in the awake study: to the head-post implantation
- in the anesthetized study: to the repeated scalp incisions and anesthesia.

Although locomotor activity, nest-building ability, and body weight remained unaffected before and after head-post implantation or scalp suture, both interventions might still influence responses to behavioral assessments such as the splash and NSF tests. It is plausible that head-post implantation procedures potentially impacted grooming behavior due to the general physical discomfort that might cause.

Focus on Insular cortex

We focused our investigations on specific regions known to be involved in the sensory, emotional and cognitive aspects of pain. As we describe already in the introduction of the manuscript (section 5.3.3.5) the insular cortex is known to be involved in sensory-discriminative and affective-motivational aspect of pain (C. Lu et al. 2016). In the process of chronification, it is known to have a role in the shift of brain activation from sensory to affective-emotional circuitry. Due for this important role on the chronification of pain we were particularly interested in investigating the functional connectivity alterations in this region.

Due our interest in these brain areas, we chose carefully the planes of imaging of the first study. Para-sagittal planes allowed us to image the maximum number of regions of interest within the shortest number of translations. In this first study, to capture the insula, we chose a plane at the lateral coordinate L=3.5mm from the midline. However, unfortunately, due to the fact that this plane includes the eye and due to the proximity with temporal muscles, it was consistently contaminated by artifacts coming from muscular movements that are disrupting the doppler signal. As we can see from the picture below, which represents the tissue velocity signal for the three planes. The blue signal represents the most lateral plane imaged, (i.e. the plane at L=3.5mm where we imaged the insula). As shown in Figure 62, the averaged signal from this frame contained a high level of noise compared to the other two planes.

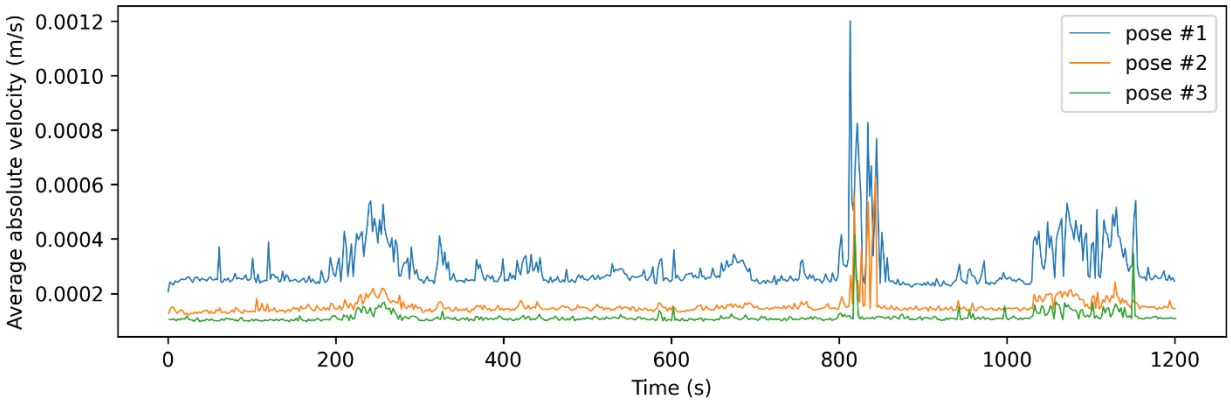

Figure 62: Typical example of motion artifacts observed in fUS signals in awake conditions. Axial tissue velocity (in m/s) was computed from raw ultrasonic frames and represents the average tissue displacement over time.

This in-depth signal analysis raised questions about the reliability of the fUS measure for FC study of lateral brain structures. Consequently, we opted to replicate this study under anesthesia to mitigate motion artefacts and gain deeper insights into the role of the insular cortex in neuropathic pain development and maintenance. Interestingly, leveraging the larger field of view enabled by the multiarray probe, our second study revealed that most alterations were exclusively located in the right insula (ipsilateral to the never lesion). This observation highlights the importance of whole-brain imaging for a more comprehensive and holistic understanding of the cerebral alterations in functional connectivity studies.

In conclusion, our findings contribute to a deeper understanding of the complex neural mechanisms underlying neuropathic pain. With this work, we provide novel perspectives on the pathophysiology of neuropathic pain and demonstrate the capabilities and potential of fUS imaging technique in the field of neuroscience.

BIBLIOGRAPHY

Abaei, Maryam, Devi R Sagar, Elizabeth G Stockley, Clare H Spicer, Malcolm Prior, Victoria Chapman, and Dorothee P Auer. 2016. "Neural Correlates of Hyperalgesia in the Monosodium Iodoacetate Model of Osteoarthritis Pain." *Molecular Pain* 12 (January):174480691664244. https://doi.org/10.1177/1744806916642445.

Aksenov, Daniil P, Limin Li, Michael J Miller, Gheorghe Iordanescu, and Alice M Wyrwicz. 2015. "Effects of Anesthesia on BOLD Signal and Neuronal Activity in the Somatosensory Cortex." *Journal of Cerebral Blood Flow & Metabolism* 35 (11): 1819–26. https://doi.org/10.1038/jcbfm.2015.130.

Amir, Ron, Jeffery D. Kocsis, and Marshall Devor. 2005. "Multiple Interacting Sites of Ectopic Spike Electrogenesis in Primary Sensory Neurons." *The Journal of Neuroscience* 25 (10): 2576–85. https://doi.org/10.1523/JNEUROSCI.4118-04.2005.

Andersson SA, Rydenhag B (1985) Cortical nociceptive systems. Philos Trans R Soc Lond B Biol Sci 308:347–359

Apkarian, A. Vania, Marwan N. Baliki, and Melissa A. Farmer. 2013. "Predicting Transition to Chronic Pain:" *Current Opinion in Neurology* 26 (4): 360–67. https://doi.org/10.1097/WCO.0b013e32836336ad.

Apkarian, A. Vania, Marwan N Baliki, and Paul Y. Geha. 2009a. "Towards a Theory of Chronic Pain." *Progress in Neurobiology* 87 (2): 81–97. https://doi.org/10.1016/j.pneurobio.2008.09.018.

Apkarian, A. Vania, Marwan N. Baliki, and Paul Y. Geha. 2009b. "Towards a Theory of Chronic Pain." *Progress in Neurobiology* 87 (2): 81–97. https://doi.org/10.1016/j.pneurobio.2008.09.018.

Apkarian, A Vania, M Catherine Bushnell, Rolf-Detlef Treede, and Jon-Kar Zubieta. 2005. "Human Brain Mechanisms of Pain Perception and Regulation in Health and Disease." *European Journal of Pain (London, England)* 9 (4): 463–84. https://doi.org/10.1016/j.ejpain.2004.11.001.

Apkarian, A. Vania, Yamaya Sosa, Sreepadma Sonty, Robert M. Levy, R. Norman Harden, Todd B. Parrish, and Darren R. Gitelman. 2004. "Chronic Back Pain Is Associated with Decreased Prefrontal and Thalamic Gray Matter Density." *The Journal of Neuroscience* 24 (46): 10410–15. https://doi.org/10.1523/JNEUROSCI.2541-04.2004.

Apkarian, A.Vania, Richard A. Stea, Stephen H. Manglos, Nikolaus M. Szeverenyi, Robert B. King, and F.Deaver Thomas. 1992. "Persistent Pain Inhibits Contralateral Somatosensory Cortical Activity in Humans." *Neuroscience Letters* 140 (2): 141–47. https://doi.org/10.1016/0304-3940(92)90088-O.

Apkarian, Vania A., Javeria A. Hashmi, and Marwan N. Baliki. 2011. "Pain and the Brain: Specificity and Plasticity of the Brain in Clinical Chronic Pain." *Pain* 152 (3): S49–64. https://doi.org/10.1016/j.pain.2010.11.010.

Atkinson JH, Ancoli-Israel S, Slater MA, Garfin SR, Gillin JC. Subjective sleep disturbance in chronic back pain. Clin J Pain 1988;4:225–32.

Attwell, David, and Costantino Iadecola. 2002. "The Neural Basis of Functional Brain Imaging Signals." *Trends in Neurosciences* 25 (12): 621–25. https://doi.org/10.1016/S0166-2236(02)02264-6.

Baliki, M. N., A. T. Baria, and A. V. Apkarian. 2011. "The Cortical Rhythms of Chronic Back Pain." *Journal of Neuroscience* 31 (39): 13981–90. https://doi.org/10.1523/JNEUROSCI.1984-11.2011.

Baliki, M. N., P. C. Chang, A. T. Baria, M. V. Centeno, and A. V. Apkarian. 2014. “Resting-State Functional Reorganization of the Rat Limbic System Following Neuropathic Injury.” *Scientific Reports* 4 (1): 6186. https://doi.org/10.1038/srep06186.

Baliki, M. N., D. R. Chialvo, P. Y. Geha, R. M. Levy, R. N. Harden, T. B. Parrish, and A. V. Apkarian. 2006. “Chronic Pain and the Emotional Brain: Specific Brain Activity Associated with Spontaneous Fluctuations of Intensity of Chronic Back Pain.” *Journal of Neuroscience* 26 (47): 12165–73. https://doi.org/10.1523/JNEUROSCI.3576-06.2006.

Baliki, M. N., P. Y. Geha, A. V. Apkarian, and D. R. Chialvo. 2008. “Beyond Feeling: Chronic Pain Hurts the Brain, Disrupting the Default-Mode Network Dynamics.” *Journal of Neuroscience* 28 (6): 1398–1403. https://doi.org/10.1523/JNEUROSCI.4123-07.2008.

Baliki, Marwan N, Dante R Chialvo, Paul Y Geha, Robert M Levy, R Norman Harden, Todd B Parrish, and A Vania Apkarian. 2006. “Chronic Pain and the Emotional Brain: Specific Brain Activity Associated with Spontaneous Fluctuations of Intensity of Chronic Back Pain.” *The Journal of Neuroscience : The Official Journal of the Society for Neuroscience* 26 (47): 12165–73. https://doi.org/10.1523/JNEUROSCI.3576-06.2006.

Baliki, Marwan N, Ali R. Mansour, Alex T. Baria, and A. Vania Apkarian. 2014. “Functional Reorganization of the Default Mode Network across Chronic Pain Conditions.” *PLoS ONE* 9 (9). https://doi.org/10.1371/journal.pone.0106133.

Baliki, Marwan N., Thomas J. Schnitzer, William R. Bauer, and A. Vania Apkarian. 2011. “Brain Morphological Signatures for Chronic Pain.” Edited by Raul M. Luque. *PLoS ONE* 6 (10): e26010. https://doi.org/10.1371/journal.pone.0026010.

Baliki, Marwan N, Thomas J. Schnitzer, William R. Bauer, and A. Vania Apkarian. 2011. “Brain Morphological Signatures for Chronic Pain.” *PLoS ONE* 6 (10). https://doi.org/10.1371/journal.pone.0026010.

Baliki, Marwan N., and A. Vania Apkarian. 2015. “Nociception, Pain, Negative Moods, and Behavior Selection.” *Neuron* 87 (3): 474–91. https://doi.org/10.1016/j.neuron.2015.06.005.

Banks SM, Kerns RD. Explaining high rates of depression in chronic pain: A diathesis-stress framework. Psychol Bull 1996;119:95–110.

Baranger, Jerome, Charlie Demene, Alice Frerot, Flora Faure, Catherine Delanoë, Hicham Serroune, Alexandre Houdouin, et al. 2021. “Bedside Functional Monitoring of the Dynamic Brain Connectivity in Human Neonates.” *Nature Communications* 12 (1): 1080. https://doi.org/10.1038/s41467-021-21387-x.

Baron, Ralf, Andreas Binder, and Gunnar Wasner. 2010. “Neuropathic Pain: Diagnosis, Pathophysiological Mechanisms, and Treatment.” *The Lancet Neurology* 9 (8): 807–19. https://doi.org/10.1016/S1474-4422(10)70143-5.

Becerra, L., E. Navratilova, F. Porreca, and D. Borsook. 2013. “Analogous Responses in the Nucleus Accumbens and Cingulate Cortex to Pain Onset (Aversion) and Offset (Relief) in Rats and Humans.” *Journal of Neurophysiology* 110 (5): 1221–26. https://doi.org/10.1152/jn.00284.2013.

Becerra, Lino, Gautam Pendse, Pei-Ching Chang, James Bishop, and David Borsook. 2011. “Robust Reproducible Resting State Networks in the Awake Rodent Brain.” Edited by Yong He. *PLoS ONE* 6 (10): e25701. https://doi.org/10.1371/journal.pone.0025701.

Benbouzid, Malika, Viviane Pallage, Mathieu Rajalu, Elisabeth Waltisperger, Stéphane Doridot, Pierrick Poisbeau, Marie José Freund-Mercier, and Michel Barrot. 2008. "Sciatic Nerve Cuffing in Mice: A Model of Sustained Neuropathic Pain." *European Journal of Pain* 12 (5): 591–99. https://doi.org/10.1016/j.ejpain.2007.10.002.

Bennett, Gary J., and Y.-K. Xie. 1988. "A Peripheral Mononeuropathy in Rat That Produces Disorders of Pain Sensation like Those Seen in Man." *Pain* 33 (1): 87–107. https://doi.org/10.1016/0304-3959(88)90209-6.

Bercoff, J, G Montaldo, T Loupas, D Savery, Fabien Mézière, M Fink, and M Tanter. 2011. "Ultrafast Compound Doppler Imaging: Providing Full Blood Flow Characterization." *IEEE Transactions on Ultrasonics, Ferroelectrics and Frequency Control* 58 (1): 134–47. https://doi.org/10.1109/TUFFC.2011.1780.

Bergel, Antoine, Thomas Deffieux, Charlie Demené, Mickaël Tanter, and Ivan Cohen. 2018. "Local Hippocampal Fast Gamma Rhythms Precede Brain-Wide Hyperemic Patterns during Spontaneous Rodent REM Sleep." *Nature Communications* 9 (1): 5364. https://doi.org/10.1038/s41467-018-07752-3.

Bertolo, Adrien, Mohamed Nouhoum, Silvia Cazzanelli, Jeremy Ferrier, Jean-Charles Mariani, Andrea Kliewer, Benoit Belliard, et al. 2021. "Whole-Brain 3D Activation and Functional Connectivity Mapping in Mice Using Transcranial Functional Ultrasound Imaging." *Journal of Visualized Experiments*, no. 168 (February), 62267. https://doi.org/10.3791/62267.

Bhatia, Anuj, David Flamer, and Prakesh S. Shah. 2015. "Perineural Steroids for Trauma and Compression-Related Peripheral Neuropathic Pain: A Systematic Review and Meta-Analysis." *Canadian Journal of Anesthesia/Journal Canadien d'anesthésie* 62 (6): 650–62. https://doi.org/10.1007/s12630-015-0356-5.

Bimbard, Célian, Charlie Demene, Constantin Girard, Susanne Radtke-Schuller, Shihab Shamma, Mickael Tanter, and Yves Boubenec. 2018. "Multi-Scale Mapping along the Auditory Hierarchy Using High-Resolution Functional UltraSound in the Awake Ferret." *eLife* 7 (June):e35028. https://doi.org/10.7554/eLife.35028.

Bingel, U., M. Quante, R. Knab, B. Bromm, C. Weiller, and C. Büchel. 2003. "Single Trial fMRI Reveals Significant Contralateral Bias in Responses to Laser Pain within Thalamus and Somatosensory Cortices." *NeuroImage* 18 (3): 740–48. https://doi.org/10.1016/S1053-8119(02)00033-2.

Blaize, Kévin, Fabrice Arcizet, Marc Gesnik, Harry Ahnine, Ulisse Ferrari, Thomas Deffieux, Pierre Pouget, et al. 2020. "Functional Ultrasound Imaging of Deep Visual Cortex in Awake Nonhuman Primates." *Proceedings of the National Academy of Sciences* 117 (25): 14453–63. https://doi.org/10.1073/pnas.1916787117.

Bliss, Tim V. P., Graham L. Collingridge, Bong-Kiun Kaang, and Min Zhuo. 2016. "Synaptic Plasticity in the Anterior Cingulate Cortex in Acute and Chronic Pain." *Nature Reviews Neuroscience* 17 (8): 485–96. https://doi.org/10.1038/nrn.2016.68.

Bock, Davi D., Wei-Chung Allen Lee, Aaron M. Kerlin, Mark L. Andermann, Greg Hood, Arthur W. Wetzel, Sergey Yurgenson, Edward R. Soucy, Hyon Suk Kim, and R. Clay Reid. 2011. "Network Anatomy and in Vivo Physiology of Visual Cortical Neurons." *Nature* 471 (7337): 177–82. https://doi.org/10.1038/nature09802.

Boido, Davide, Ravi L. Rungta, Bruno-Félix Osmanski, Morgane Roche, Tomokazu Tsurugizawa, Denis Le Bihan, Luisa Ciobanu, and Serge Charpak. 2019. “Mesoscopic and Microscopic Imaging of Sensory Responses in the Same Animal.” *Nature Communications* 10 (1): 1110. https://doi.org/10.1038/s41467-019-09082-4.

Bornhövd, K., M. Quante, V. Glauche, B. Bromm, C. Weiller, and C. Büchel. 2002. “Painful Stimuli Evoke Different Stimulus–Response Functions in the Amygdala, Prefrontal, Insula and Somatosensory Cortex: A Single-trial fMRI Study.” *Brain* 125 (6): 1326–36. https://doi.org/10.1093/brain/awf137.

Borsook, David, and Lino Becerra. 2011. “CNS Animal fMRI in Pain and Analgesia.” *Neuroscience & Biobehavioral Reviews* 35 (5): 1125–43. https://doi.org/10.1016/j.neubiorev.2010.11.005.

Bourquin, Anne-Frédérique, Maria Süveges, Marie Pertin, Nicolas Gilliard, Sylvain Sardy, Anthony C. Davison, Donat R. Spahn, and Isabelle Decosterd. 2006. “Assessment and Analysis of Mechanical Allodynia-like Behavior Induced by Spared Nerve Injury (SNI) in the Mouse.” *Pain* 122 (1): 14e1–14. https://doi.org/10.1016/j.pain.2005.10.036.

Brooks, Jonathan C.W., Turo J. Nurmikko, William E. Bimson, Krish D. Singh, and Neil Roberts. 2002. “fMRI of Thermal Pain: Effects of Stimulus Laterality and Attention.” *NeuroImage* 15 (2): 293–301. https://doi.org/10.1006/nimg.2001.0974.

Brooks, Jonathan, and Irene Tracey. 2005. “REVIEW: From Nociception to Pain Perception: Imaging the Spinal and Supraspinal Pathways: Imaging the Spinal and Supraspinal Pathways, J. Brooks and I. Tracey.” *Journal of Anatomy* 207 (1): 19–33. https://doi.org/10.1111/j.1469-7580.2005.00428.x.

Brunner, Clément, Micheline Grillet, Arnau Sans-Dublanc, Karl Farrow, Théo Lambert, Emilie Macé, Gabriel Montaldo, and Alan Urban. 2020. “A Platform for Brain-Wide Volumetric Functional Ultrasound Imaging and Analysis of Circuit Dynamics in Awake Mice.” *Neuron* 108 (5): 861-875.e7. https://doi.org/10.1016/j.neuron.2020.09.020.

Büchel, Christian, Karin Bornhövd, Markus Quante, Volkmar Glauche, Burkhard Bromm, and Cornelius Weiller. 2002. “Dissociable Neural Responses Related to Pain Intensity, Stimulus Intensity, and Stimulus Awareness within the Anterior Cingulate Cortex: A Parametric Single-Trial Laser Functional Magnetic Resonance Imaging Study.” *The Journal of Neuroscience* 22 (3): 970–76. https://doi.org/10.1523/JNEUROSCI.22-03-00970.2002.

(Bud) Craig, A. 2003. “A New View of Pain as a Homeostatic Emotion.” *Trends in Neurosciences* 26 (6): 303–7. https://doi.org/10.1016/S0166-2236(03)00123-1.

Bushnell, M. C., G. H. Duncan, R. K. Hofbauer, B. Ha, J.-I. Chen, and B. Carrier. 1999. “Pain Perception: Is There a Role for Primary Somatosensory Cortex?” *Proceedings of the National Academy of Sciences* 96 (14): 7705–9. https://doi.org/10.1073/pnas.96.14.7705.

Bushnell, M. Catherine, Marta Čeko, and Lucie A. Low. 2013. “Cognitive and Emotional Control of Pain and Its Disruption in Chronic Pain.” *Nature Reviews Neuroscience* 14 (7): 502–11. https://doi.org/10.1038/nrn3516.

Cabral, Joana, Morten Kringelbach, and Gustavo Deco. n.d. “Time-Scales over Static Structural Connectivity: Models And.”

Cauda, Franco, Tommaso Costa, Matteo Diano, Katiuscia Sacco, Sergio Duca, Giuliano Geminiani, and Diana M.E. Torta. 2014. “Massive Modulation of Brain Areas After Mechanical Pain Stimulation: A Time-Resolved fMRI Study.” *Cerebral Cortex* 24 (11): 2991–3005. https://doi.org/10.1093/cercor/bht153.

Chang, Catie, and Gary H. Glover. 2010. “Time–Frequency Dynamics of Resting-State Brain Connectivity Measured with fMRI.” *NeuroImage* 50 (1): 81–98. https://doi.org/10.1016/j.neuroimage.2009.12.011.

Chang, Pei-Ching, Maria Virginia Centeno, Daniel Procissi, Alex Baria, and A. Vania Apkarian. 2017. “Brain Activity for Tactile Allodynia: A Longitudinal Awake Rat Functional Magnetic Resonance Imaging Study Tracking Emergence of Neuropathic Pain.” *Pain* 158 (3): 488–97. https://doi.org/10.1097/j.pain.0000000000000788.

Chang, Pei-Ching, Sarah Lynn Pollema-Mays, Maria Virginia Centeno, Daniel Procissi, Massimo Contini, Alex Tomas Baria, Marco Martina, and Apkar Vania Apkarian. 2014. “Role of Nucleus Accumbens in Neuropathic Pain: Linked Multi-Scale Evidence in the Rat Transitioning to Neuropathic Pain.” *PAIN* 155 (6): 1128. https://doi.org/10.1016/j.pain.2014.02.019.

Chapman, C. Richard, Andrew C. N. Chen, Yoko M. Colpitts, and Roy W. Martin. 1981. “Sensory Decision Theory Describes Evoked Potentials in Pain Discrimination.” *Psychophysiology* 18 (2): 114–20. https://doi.org/10.1111/j.1469-8986.1981.tb02923.x.

Chuang, Kai-Hsiang, and Fatima A. Nasrallah. 2017. “Functional Networks and Network Perturbations in Rodents.” *NeuroImage* 163 (December):419–36. https://doi.org/10.1016/j.neuroimage.2017.09.038.

Clark, Jennifer A., Christopher A. Brown, Anthony K.P. Jones, and Wael El-Deredy. 2008. “Dissociating Nociceptive Modulation by the Duration of Pain Anticipation from Unpredictability in the Timing of Pain.” *Clinical Neurophysiology* 119 (12): 2870–78. https://doi.org/10.1016/j.clinph.2008.09.022.

Claron, Julien, Vincent Hingot, Isabelle Rivals, Line Rahal, Olivier Couture, Thomas Deffieux, Mickael Tanter, and Sophie Pezet. 2021. “Large-Scale Functional Ultrasound Imaging of the Spinal Cord Reveals in-Depth Spatiotemporal Responses of Spinal Nociceptive Circuits in Both Normal and Inflammatory States.” *Pain* 162 (4): 1047–59. https://doi.org/10.1097/j.pain.0000000000002078.

Coghill, Robert C., Christine N. Sang, Jose Ma. Maisog, and Michael J. Iadarola. 1999. “Pain Intensity Processing Within the Human Brain: A Bilateral, Distributed Mechanism.” *Journal of Neurophysiology* 82 (4): 1934–43. https://doi.org/10.1152/jn.1999.82.4.1934.

Colloca, Luana, Taylor Ludman, Didier Bouhassira, Ralf Baron, Anthony H. Dickenson, David Yarnitsky, Roy Freeman, et al. 2017. “Neuropathic Pain.” *Nature Reviews Disease Primers* 3 (1): 17002. https://doi.org/10.1038/nrdp.2017.2.

“Cortical and Subcortical Localization of Response to Pain in Man Using Positron Emission Tomography.” 1991. *Proceedings of the Royal Society of London. Series B: Biological Sciences* 244 (1309): 39–44. https://doi.org/10.1098/rspb.1991.0048.

Costigan, Michael, Joachim Scholz, and Clifford J. Woolf. 2009. “Neuropathic Pain: A Maladaptive Response of the Nervous System to Damage.” *Annual Review of Neuroscience* 32 (1): 1–32. https://doi.org/10.1146/annurev.neuro.051508.135531.

Coull, Jeffrey A. M., Dominic Boudreau, Karine Bachand, Steven A. Prescott, Francine Nault, Attila Sík, Paul De Koninck, and Yves De Koninck. 2003. “Trans-Synaptic Shift in Anion Gradient in Spinal Lamina I Neurons as a Mechanism of Neuropathic Pain.” *Nature* 424 (6951): 938–42. https://doi.org/10.1038/nature01868.

Craig, A. D., K. Chen, D. Bandy, and E. M. Reiman. 2000. “Thermosensory Activation of Insular Cortex.” *Nature Neuroscience* 3 (2): 184–90. https://doi.org/10.1038/72131.

Critchley, Hugo D, Stefan Wiens, Pia Rotshtein, Arne Öhman, and Raymond J Dolan. 2004. "Neural Systems Supporting Interoceptive Awareness." *Nature Neuroscience* 7 (2): 189–95. https://doi.org/10.1038/nn1176.

Da Silva, Joyce T., and David A. Seminowicz. 2019. "Neuroimaging of Pain in Animal Models: A Review of Recent Literature." *PAIN Reports* 4 (4): e732. https://doi.org/10.1097/PR9.0000000000000732.

Damoiseaux, J. S., S. A. R. B. Rombouts, F. Barkhof, P. Scheltens, C. J. Stam, S. M. Smith, and C. F. Beckmann. 2006. "Consistent Resting-State Networks across Healthy Subjects." *Proceedings of the National Academy of Sciences* 103 (37): 13848–53. https://doi.org/10.1073/pnas.0601417103.

Davidson, Richard J. 2002. "Anxiety and Affective Style: Role of Prefrontal Cortex and Amygdala." *Biological Psychiatry* 51 (1): 68–80. https://doi.org/10.1016/S0006-3223(01)01328-2.

De Courcy, Jonathan, Hiltrud Liedgens, Marko Obradovic, Tim Holbrook, and Rafal Jakubanis. 2016. "A Burden of Illness Study for Neuropathic Pain in Europe." *ClinicoEconomics and Outcomes Research*, April, 113. https://doi.org/10.2147/CEOR.S81396.

De Pace, Raffaella, Dylan J. Britt, Jeffrey Mercurio, Arianne M. Foster, Lucas Djavaherian, Victoria Hoffmann, Daniel Abebe, and Juan S. Bonifacino. 2020. "Synaptic Vesicle Precursors and Lysosomes Are Transported by Different Mechanisms in the Axon of Mammalian Neurons." *Cell Reports* 31 (11): 107775. https://doi.org/10.1016/j.celrep.2020.107775.

De Simone, R., A. Ranieri, S. Montella, and V. Bonavita. 2013. "Cortical Spreading Depression and Central Pain Networks in Trigeminal Nuclei Modulation: Time for an Integrated Migraine Pathogenesis Perspective." *Neurological Sciences* 34 (S1): 51–55. https://doi.org/10.1007/s10072-013-1392-y.

Decosterd, Isabelle, and Clifford J. Woolf. 2000. "Spared Nerve Injury: An Animal Model of Persistent Peripheral Neuropathic Pain." *Pain* 87 (2): 149–58. https://doi.org/10.1016/S0304-3959(00)00276-1.

Deer, Timothy R., Robert Levy, Joshua Prager, Eric Buchser, Allen Burton, David Caraway, Michael Cousins, et al. 2012. "Polyanalgesic Consensus Conference—2012: Recommendations to Reduce Morbidity and Mortality in Intrathecal Drug Delivery in the Treatment of Chronic Pain." *Neuromodulation: Technology at the Neural Interface* 15 (5): 467–82. https://doi.org/10.1111/j.1525-1403.2012.00486.x.

Deffieux, Thomas, Charlie Demene, Mathieu Pernot, and Mickael Tanter. 2018. "Functional Ultrasound Neuroimaging: A Review of the Preclinical and Clinical State of the Art." *Current Opinion in Neurobiology* 50 (June):128–35. https://doi.org/10.1016/j.conb.2018.02.001.

Deffieux, Thomas, Charlie Demené, and Mickael Tanter. 2021. "Functional Ultrasound Imaging: A New Imaging Modality for Neuroscience." *Neuroscience* 474 (October):110–21. https://doi.org/10.1016/j.neuroscience.2021.03.005.

Demene, Charlie, Jérome Baranger, Miguel Bernal, Catherine Delanoe, Stéphane Auvin, Valérie Biran, Marianne Alison, et al. 2017. "Functional Ultrasound Imaging of Brain Activity in Human Newborns." *Science Translational Medicine* 9 (411): eaah6756. https://doi.org/10.1126/scitranslmed.aah6756.

Demené, Charlie, Elodie Tiran, Lim-Anna Sieu, Antoine Bergel, Jean Luc Gennisson, Mathieu Pernot, Thomas Deffieux, Ivan Cohen, and Mickael Tanter. 2016. "4D Microvascular Imaging Based on Ultrafast Doppler Tomography." *NeuroImage* 127 (February):472–83. https://doi.org/10.1016/j.neuroimage.2015.11.014.

Derbyshire, Stuart W.G, Anthony K.P Jones, Ferenc Gyulai, Stuart Clark, David Townsend, and Leonard L Firestone. 1997. “Pain Processing during Three Levels of Noxious Stimulation Produces Differential Patterns of Central Activity.” *Pain* 73 (3): 431–45. https://doi.org/10.1016/S0304-3959(97)00138-3.

Dillmann, Jennifer, Wolfgang H R Miltner, and Thomas Weiss. 2000. “The In¯uence of Semantic Priming on Event-Related Potentials to Painful Laser-Heat Stimuli in Humans.” *Neuroscience Letters*.

Dizeux, Alexandre, Marc Gesnik, Harry Ahnine, Kevin Blaize, Fabrice Arcizet, Serge Picaud, José-Alain Sahel, Thomas Deffieux, Pierre Pouget, and Mickael Tanter. 2019. “Functional Ultrasound Imaging of the Brain Reveals Propagation of Task-Related Brain Activity in Behaving Primates.” *Nature Communications* 10 (1): 1400. https://doi.org/10.1038/s41467-019-09349-w.

Dolan, R J. 2002. “Emotion, Cognition, and Behavior” 298.

Dosenbach, Nico U. F., Damien A. Fair, Francis M. Miezin, Alexander L. Cohen, Kristin K. Wenger, Ronny A. T. Dosenbach, Michael D. Fox, et al. 2007. “Distinct Brain Networks for Adaptive and Stable Task Control in Humans.” *Proceedings of the National Academy of Sciences* 104 (26): 11073–78. https://doi.org/10.1073/pnas.0704320104.

Dubin, Adrienne E., and Ardem Patapoutian. 2010. “Nociceptors: The Sensors of the Pain Pathway.” *Journal of Clinical Investigation* 120 (11): 3760–72. https://doi.org/10.1172/JCI42843.

Dworkin, Robert H., Miroslav Backonja, Michael C. Rowbotham, Robert R. Allen, Charles R. Argoff, Gary J. Bennett, M. Catherine Bushnell, et al. 2003. “Advances in Neuropathic Pain: Diagnosis, Mechanisms, and Treatment Recommendations.” *Archives of Neurology* 60 (11): 1524. https://doi.org/10.1001/archneur.60.11.1524.

Dworkin, Robert H., Alec B. O’Connor, Miroslav Backonja, John T. Farrar, Nanna B. Finnerup, Troels S. Jensen, Eija A. Kalso, et al. 2007. “Pharmacologic Management of Neuropathic Pain: Evidence-Based Recommendations.” *Pain* 132 (3): 237–51. https://doi.org/10.1016/j.pain.2007.08.033.

Edwards, Robert R., Jon Giles, Clifton O. Bingham, Claudia Campbell, Jennifer A. Haythornthwaite, and Joan Bathon. 2010. “Moderators of the Negative Effects of Catastrophizing in Arthritis.” *Pain Medicine* 11 (4): 591–99. https://doi.org/10.1111/j.1526-4637.2010.00804.x.

Eickhoff, S.B., and V.I. Müller. 2015. “Functional Connectivity.” In *Brain Mapping*, 187–201. Elsevier. https://doi.org/10.1016/B978-0-12-397025-1.00212-8.

Eto, Kei, Hiroaki Wake, Miho Watanabe, Hitoshi Ishibashi, Mami Noda, Yuchio Yanagawa, and Junichi Nabekura. 2011. “Inter-Regional Contribution of Enhanced Activity of the Primary Somatosensory Cortex to the Anterior Cingulate Cortex Accelerates Chronic Pain Behavior.” *The Journal of Neuroscience* 31 (21): 7631–36. https://doi.org/10.1523/JNEUROSCI.0946-11.2011.

Farmer, Melissa A., Marwan N. Baliki, and A. Vania Apkarian. 2012. “A Dynamic Network Perspective of Chronic Pain.” *Neuroscience Letters* 520 (2): 197–203. https://doi.org/10.1016/j.neulet.2012.05.001.

Ferrier, Jeremy, Elodie Tiran, Thomas Deffieux, Mickael Tanter, and Zsolt Lenkei. 2020. “Functional Imaging Evidence for Task-Induced Deactivation and Disconnection of a Major Default Mode Network Hub in the Mouse Brain.” *Proceedings of the National Academy of Sciences* 117 (26): 15270–80. https://doi.org/10.1073/pnas.1920475117.

Finnerup, Nanna B, Nadine Attal, Simon Haroutounian, Ewan McNicol, Ralf Baron, Robert H Dworkin, Ian Gilron, et al. 2015. “Pharmacotherapy for Neuropathic Pain in Adults: A Systematic Review and Meta-Analysis.” *The Lancet Neurology* 14 (2): 162–73. https://doi.org/10.1016/S1474-4422(14)70251-0.

Floresco, Stan B. 2015. “The Nucleus Accumbens: An Interface Between Cognition, Emotion, and Action.” *Annual Review of Psychology* 66 (1): 25–52. https://doi.org/10.1146/annurev-psych-010213-115159.

Fox, Michael D., Maurizio Corbetta, Abraham Z. Snyder, Justin L. Vincent, and Marcus E. Raichle. 2006. “Spontaneous Neuronal Activity Distinguishes Human Dorsal and Ventral Attention Systems.” *Proceedings of the National Academy of Sciences* 103 (26): 10046–51. https://doi.org/10.1073/pnas.0604187103.

Fox, Michael D, and Michael Greicius. 2010. “Clinical Applications of Resting State Functional Connectivity.” *Frontiers in Systems Neuroscience* 4 (19). https://doi.org/10.3389/fnsys.2010.00019.

Fox, Michael D., and Marcus E. Raichle. 2007. “Spontaneous Fluctuations in Brain Activity Observed with Functional Magnetic Resonance Imaging.” *Nature Reviews Neuroscience* 8 (9): 700–711. https://doi.org/10.1038/nrn2201.

Fox, Michael D., Abraham Z. Snyder, Justin L. Vincent, Maurizio Corbetta, David C. Van Essen, and Marcus E. Raichle. 2005. “The Human Brain Is Intrinsically Organized into Dynamic, Anticorrelated Functional Networks.” *Proceedings of the National Academy of Sciences* 102 (27): 9673–78. https://doi.org/10.1073/pnas.0504136102.

Frot, M. 2003. “Dual Representation of Pain in the Operculo-Insular Cortex in Humans.” *Brain* 126 (2): 438–50. https://doi.org/10.1093/brain/awg032.

Frot, Maud, Michel Magnin, François Mauguière, and Luis Garcia-Larrea. 2013. “Cortical Representation of Pain in Primary Sensory-Motor Areas (S1/M1)-a Study Using Intracortical Recordings in Humans: Pain Processing in S1 and M1 Cortex.” *Human Brain Mapping* 34 (10): 2655–68. https://doi.org/10.1002/hbm.22097.

Frot, Maud, Loïc Rambaud, Marc Guénot, and François Mauguière. 1999. “Intracortical Recordings of Early Pain-Related CO2-Laser Evoked Potentials in the Human Second Somatosensory (SII) Area.” *Clinical Neurophysiology* 110 (1): 133–45. https://doi.org/10.1016/S0168-5597(98)00054-9.

Fulham 2004. Neuroimaging M J Fulham, Royal Prince Alfred Hospital, Camperdown, NSW, Australia ã 2004 Elsevier Ltd. All rights reserved. This article is reproduced from the previous edition ã 2004, Elsevier B.V.

Gao, Yu-Rong, Yuncong Ma, Qingguang Zhang, Aaron T. Winder, Zhifeng Liang, Lilith Antinori, Patrick J. Drew, and Nanyin Zhang. 2017. “Time to Wake up: Studying Neurovascular Coupling and Brain-Wide Circuit Function in the Un-Anesthetized Animal.” *NeuroImage* 153 (June):382–98. https://doi.org/10.1016/j.neuroimage.2016.11.069.

Garcia-Larrea, Luis, and Roland Peyron. 2013. “Pain Matrices and Neuropathic Pain Matrices: A Review.” *Pain* 154 (Supplement 1): S29–43. https://doi.org/10.1016/j.pain.2013.09.001.

Gesnik, Marc, Kevin Blaize, Thomas Deffieux, Jean-Luc Gennisson, José-Alain Sahel, Mathias Fink, Serge Picaud, and Mickaël Tanter. 2017. “3D Functional Ultrasound Imaging of the Cerebral Visual System in Rodents.” *NeuroImage* 149 (April):267–74. https://doi.org/10.1016/j.neuroimage.2017.01.071.

Gillebert, Céline R., and Dante Mantini. 2013. “Functional Connectivity in the Normal and Injured Brain.” *The Neuroscientist* 19 (5): 509–22. https://doi.org/10.1177/1073858412463168.

Godoy, Lívea Dornela, Matheus Teixeira Rossignoli, Polianna Delfino-Pereira, Norberto Garcia-Cairasco, and Eduardo Henrique De Lima Umeoka. 2018. “A Comprehensive Overview on Stress Neurobiology: Basic Concepts and Clinical Implications.” *Frontiers in Behavioral Neuroscience* 12 (July):127. https://doi.org/10.3389/fnbeh.2018.00127.

Gottschalk, Allan, and David S Smith. 2001. “New Concepts in Acute Pain Therapy: Preemptive Analgesia” 63 (10).

Gram, Mikkel, Joachim Erlenwein, Frank Petzke, Deborah Falla, Michael Przemeck, Miriam I. Emons, Michael Reuster, Søren S. Olesen, and Asbjørn M. Drewes. 2017. “The Cortical Responses to Evoked Clinical Pain in Patients with Hip Osteoarthritis.” Edited by Philip Allen. *PLOS ONE* 12 (10): e0186400. https://doi.org/10.1371/journal.pone.0186400.

Grandjean, Joanes, Aileen Schroeter, Imene Batata, and Markus Rudin. 2014. “Optimization of Anesthesia Protocol for Resting-State fMRI in Mice Based on Differential Effects of Anesthetics on Functional Connectivity Patterns.” *NeuroImage* 102 (November):838–47. https://doi.org/10.1016/j.neuroimage.2014.08.043.

Greicius, Michael D., Benjamin H. Flores, Vinod Menon, Gary H. Glover, Hugh B. Solvason, Heather Kenna, Allan L. Reiss, and Alan F. Schatzberg. 2007. “Resting-State Functional Connectivity in Major Depression: Abnormally Increased Contributions from Subgenual Cingulate Cortex and Thalamus.” *Biological Psychiatry* 62 (5): 429–37. https://doi.org/10.1016/j.biopsych.2006.09.020.

Greicius, Michael D., Ben Krasnow, Allan L. Reiss, and Vinod Menon. 2003. “Functional Connectivity in the Resting Brain: A Network Analysis of the Default Mode Hypothesis.” *Proceedings of the National Academy of Sciences* 100 (1): 253–58. https://doi.org/10.1073/pnas.0135058100.

Greicius, Michael D, Gaurav Srivastava, Allan L Reiss, and Vinod Menon. 2004. “Default-Mode Network Activity Distinguishes Alzheimer’s Disease from Healthy Aging: Evidence from Functional MRI.” *Proceedings of the National Academy of Sciences of the United States of America* 101 (13): 4637–42. https://doi.org/10.1073/pnas.0308627101.

Guilbaud, G., J. M. Benoist, F. Jazat, and M. Gautron. 1990. “Neuronal Responsiveness in the Ventrobasal Thalamic Complex of Rats with an Experimental Peripheral Mononeuropathy.” *Journal of Neurophysiology* 64 (5): 1537–54. https://doi.org/10.1152/jn.1990.64.5.1537.

Hagmann, Patric, Leila Cammoun, Xavier Gigandet, Reto Meuli, Christopher J Honey, Van J Wedeen, and Olaf Sporns. 2008. “Mapping the Structural Core of Human Cerebral Cortex.” Edited by Karl J Friston. *PLoS Biology* 6 (7): e159. https://doi.org/10.1371/journal.pbio.0060159.

Hampson, Michelle, Bradley S. Peterson, Pawel Skudlarski, James C. Gatenby, and John C. Gore. 2002. “Detection of Functional Connectivity Using Temporal Correlations in MR Images.” *Human Brain Mapping* 15 (4): 247–62. https://doi.org/10.1002/hbm.10022.

Hashmi, Javeria A., Marwan N Baliki, Lejian Huang, Alex T. Baria, Souraya Torbey, Kristina M. Hermann, Thomas J. Schnitzer, and A. Vania Apkarian. 2013a. “Shape Shifting Pain: Chronification of Back Pain Shifts Brain Representation from Nociceptive to Emotional Circuits.” *Brain* 136 (9): 2751–68. https://doi.org/10.1093/brain/awt211.

Hashmi, Javeria A., Marwan N. Baliki, Lejian Huang, Alex T. Baria, Souraya Torbey, Kristina M. Hermann, Thomas J. Schnitzer, and A. Vania Apkarian. 2013b. "Shape Shifting Pain: Chronification of Back Pain Shifts Brain Representation from Nociceptive to Emotional Circuits." *Brain* 136 (9): 2751–68. https://doi.org/10.1093/brain/awt211.

He, Biyu J., Abraham Z. Snyder, Justin L. Vincent, Adrian Epstein, Gordon L. Shulman, and Maurizio Corbetta. 2007. "Breakdown of Functional Connectivity in Frontoparietal Networks Underlies Behavioral Deficits in Spatial Neglect." *Neuron* 53 (6): 905–18. https://doi.org/10.1016/j.neuron.2007.02.013.

Head, H. and Holmes, G., Sensory disturbances from cerebral lesions, Brain, 34 (1911) 102–254.

Ho Kim, Sun, and Jin Mo Chung. 1992. "An Experimental Model for Peripheral Neuropathy Produced by Segmental Spinal Nerve Ligation in the Rat." *Pain* 50 (3): 355–63. https://doi.org/10.1016/0304-3959(92)90041-9.

Hotta, Jaakko, Jukka Saari, Hanna Harno, Eija Kalso, Nina Forss, and Riitta Hari. 2023. "Somatotopic Disruption of the Functional Connectivity of the Primary Sensorimotor Cortex in Complex Regional Pain Syndrome Type 1." *Human Brain Mapping* 44 (17): 6258–74. https://doi.org/10.1002/hbm.26513.

Huang, Shishi, Kenta Wakaizumi, Binbin Wu, Bangli Shen, Bo Wu, Linyu Fan, Marwan N. Baliki, Gonghao Zhan, A. Vania Apkarian, and Lejian Huang. 2019. "Whole-Brain Functional Network Disruption in Chronic Pain with Disk Herniation." *Pain* 160 (12): 2829–40. https://doi.org/10.1097/j.pain.0000000000001674.

Hudetz, Anthony G. 2012. "General Anesthesia and Human Brain Connectivity." *Brain Connectivity* 2 (6): 291–302. https://doi.org/10.1089/brain.2012.0107.

Iadecola, Costantino. 2004. "Neurovascular Regulation in the Normal Brain and in Alzheimer's Disease." *Nature Reviews Neuroscience* 5 (5): 347–60. https://doi.org/10.1038/nrn1387.

Iadecola, Costantino. 2017. "The Neurovascular Unit Coming of Age: A Journey through Neurovascular Coupling in Health and Disease." *Neuron* 96 (1): 17–42. https://doi.org/10.1016/j.neuron.2017.07.030.

Iannetti, G. D., N. P. Hughes, M. C. Lee, and A. Mouraux. 2008. "Determinants of Laser-Evoked EEG Responses: Pain Perception or Stimulus Saliency?" *Journal of Neurophysiology* 100 (2): 815–28. https://doi.org/10.1152/jn.00097.2008.

Iannetti, G. D., and A. Mouraux. 2010. "From the Neuromatrix to the Pain Matrix (and Back)." *Experimental Brain Research* 205 (1): 1–12. https://doi.org/10.1007/s00221-010-2340-1.

Ikeda, Ryo, Yukari Takahashi, Kazuhide Inoue, and Fusao Kato. 2007. "NMDA Receptor-Independent Synaptic Plasticity in the Central Amygdala in the Rat Model of Neuropathic Pain." *Pain* 127 (1): 161–72. https://doi.org/10.1016/j.pain.2006.09.003.

Ito, Rutsuko, and Anja Hayen. 2011. "Opposing Roles of Nucleus Accumbens Core and Shell Dopamine in the Modulation of Limbic Information Processing." *The Journal of Neuroscience* 31 (16): 6001–7. https://doi.org/10.1523/JNEUROSCI.6588-10.2011.

Jaggi, Amteshwar Singh, Vivek Jain, and Nirmal Singh. 2011. "Animal Models of Neuropathic Pain: Animal Models of Neuropathic Pain." *Fundamental & Clinical Pharmacology* 25 (1): 1–28. https://doi.org/10.1111/j.1472-8206.2009.00801.x.

Jasmin, Luc, Alberto Granato, and Peter T. Ohara. 2004. “Rostral Agranular Insular Cortex and Pain Areas of the Central Nervous System: A Tract-tracing Study in the Rat.” *Journal of Comparative Neurology* 468 (3): 425–40. https://doi.org/10.1002/cne.10978.

Jeong, Keun-Yeong, and Ji-Hyuk Kang. 2018. “Investigation of Spinal Nerve Ligation-Mediated Functional Activation of the Rat Brain Using Manganese-Enhanced MRI.” *Experimental Animals* 67 (1): 23–29. https://doi.org/10.1538/expanim.17-0033.

Ji, Guangchen, and Volker Neugebauer. 2014. “CB 1 Augments m G Lu R 5 Function in Medial Prefrontal Cortical Neurons to Inhibit Amygdala Hyperactivity in an Arthritis Pain Model.” *European Journal of Neuroscience* 39 (3): 455–66. https://doi.org/10.1111/ejn.12432.

Ji, Guangchen, Hao Sun, Yu Fu, Zhen Li, Miguel Pais-Vieira, Vasco Galhardo, and Volker Neugebauer. 2010. “Cognitive Impairment in Pain through Amygdala-Driven Prefrontal Cortical Deactivation.” *The Journal of Neuroscience* 30 (15): 5451–64. https://doi.org/10.1523/JNEUROSCI.0225-10.2010.

Jones AK, Brown WD, Friston KJ, Qi LY, Frackowiak RS. Cortical and subcortical localization of response to pain in man using positron emission tomography. Proc R Soc Lond B 1991;244:39–44.

Kanda, Masutaro, Takashi Nagamine, Akio Ikeda, Shinji Ohara, Takeharu Kunieda, Naohito Fujiwara, Shogo Yazawa, et al. 2000. “Primary Somatosensory Cortex Is Actively Involved in Pain Processing in Human.” *Brain Research* 853 (2): 282–89. https://doi.org/10.1016/S0006-8993(99)02274-X.

Kandel E.R., & Schwartz J.H., & Jessell T.M., & Siegelbaum S.A., & Hudspeth A.J., & Mack S(Eds.), [publicationyear2] Principles of Neural Science, Fifth Edition. McGraw-Hill Education. https://neurology.mhmedical.com/content.aspx?bookid=1049&sectionid=59138139

Kang, David, James H. McAuley, Mustafa S. Kassem, Justine M. Gatt, and Sylvia M. Gustin. 2019. “What Does the Grey Matter Decrease in the Medial Prefrontal Cortex Reflect in People with Chronic Pain?” *European Journal of Pain* 23 (2): 203–19. https://doi.org/10.1002/ejp.1304.

Komaki, Yuji, Keigo Hikishima, Shinsuke Shibata, Tsunehiko Konomi, Fumiko Seki, Masayuki Yamada, Naoyuki Miyasaka, et al. 2016. “Functional Brain Mapping Using Specific Sensory-Circuit Stimulation and a Theoretical Graph Network Analysis in Mice with Neuropathic Allodynia.” *Scientific Reports* 6 (1): 37802. https://doi.org/10.1038/srep37802.

Krames, Elliot S. 2014. “The Role of the Dorsal Root Ganglion in the Development of Neuropathic Pain.” *Pain Medicine* 15 (10): 1669–85. https://doi.org/10.1111/pme.12413.

Kuner, Rohini, and Herta Flor. 2017. “Structural Plasticity and Reorganisation in Chronic Pain.” *Nature Reviews Neuroscience* 18 (1): 20–30. https://doi.org/10.1038/nrn.2016.162.

LeBlanc, Brian W., Paul M. Bowary, Yu Chieh Chao, Theresa R. Lii, and Carl Y. Saab. 2016. “Electroencephalographic Signatures of Pain and Analgesia in Rats.” *Pain* 157 (10): 2330–40. https://doi.org/10.1097/j.pain.0000000000000652.

Lee, M. C., A. Mouraux, and G. D. Iannetti. 2009. “Characterizing the Cortical Activity through Which Pain Emerges from Nociception.” *Journal of Neuroscience* 29 (24): 7909–16. https://doi.org/10.1523/JNEUROSCI.0014-09.2009.

Lelic, Dina, Søren Schou Olesen, Massimiliano Valeriani, and Asbjørn Mohr Drewes. 2012. “Brain Source Connectivity Reveals the Visceral Pain Network.” *NeuroImage* 60 (1): 37–46. https://doi.org/10.1016/j.neuroimage.2011.12.002.

Lenartowicz, A., & Poldrack, R. A. (2010). Brain Imaging. Encyclopedia of Behavioral Neuroscience, 187–193. doi:10.1016/b978-0-08-045396-5.00052-x

Lenz, F. A., M. Rios, D. Chau, G. L. Krauss, T. A. Zirh, and R. P. Lesser. 1998. “Painful Stimuli Evoke Potentials Recorded From the Parasylvian Cortex in Humans.” *Journal of Neurophysiology* 80 (4): 2077–88. https://doi.org/10.1152/jn.1998.80.4.2077.

Lenz FA, Gracely RH, Romanoski AJ, Hope EJ, Rowaland LH, Dougherty PM. Stimulation in the human somatosensory thalamus can reproduce both the affective and sensory dimensions of previously experienced pain. Nat Med 1995;1:910–3.

Liang, Z., J. King, and N. Zhang. 2012. “Intrinsic Organization of the Anesthetized Brain.” *Journal of Neuroscience* 32 (30): 10183–91. https://doi.org/10.1523/JNEUROSCI.1020-12.2012.

Lin, Chia Shu. 2014. “Brain Signature of Chronic Orofacial Pain: A Systematic Review and Meta-Analysis on Neuroimaging Research of Trigeminal Neuropathic Pain and Temporomandibular Joint Disorders.” *PLoS ONE*. https://doi.org/10.1371/journal.pone.0094300.

Liu, Ming-Gang, SukJae Joshua Kang, Tian-Yao Shi, Kohei Koga, Ming-Ming Zhang, Graham L. Collingridge, Bong-Kiun Kaang, and Min Zhuo. 2013. “Long-Term Potentiation of Synaptic Transmission in the Adult Mouse Insular Cortex: Multielectrode Array Recordings.” *Journal of Neurophysiology* 110 (2): 505–21. https://doi.org/10.1152/jn.01104.2012.

Loggia, Marco L, Chantal Berna, Jieun Kim, M Christine, Randy L Gollub, Ajay D Wasan, Richard E Harris, Robert R Edwards, and Vitaly Napadow. 2014. “Disrupted Brain Circuitry for Pain-Related Reward/Punishment in Fibromyalgia.” *Arthritis Rheumatol.* 66 (1): 203–12. https://doi.org/10.1002/art.38191.Disrupted.

Logothetis, Nikos K. 2008. “What We Can Do and What We Cannot Do with fMRI.” *Nature* 453 (7197): 869–78. https://doi.org/10.1038/nature06976.

Longo, Matthew R., Gian Domenico Iannetti, Flavia Mancini, Jon Driver, and Patrick Haggard. 2012. “Linking Pain and the Body: Neural Correlates of Visually Induced Analgesia.” *The Journal of Neuroscience* 32 (8): 2601–7. https://doi.org/10.1523/JNEUROSCI.4031-11.2012.

Lowe, Mark J, Micheal D Phillips, Joseph T Lurito, David Mattson, Mario Dzemidzic, and Vincent P Mathews. 2002. “Multiple Sclerosis: Low-Frequency Temporal Blood Oxygen Level-Dependent Fluctuations Indicate Reduced Functional Connectivity Initial Results.” *Radiology* 224 (9): 184–92. https://doi.org/10.1148/radiol.2241011005.

Lu, Changbo, Tao Yang, Huan Zhao, Ming Zhang, Fancheng Meng, Hao Fu, Yingli Xie, and Hui Xu. 2016. “Insular Cortex Is Critical for the Perception, Modulation, and Chronification of Pain.” *Neuroscience Bulletin* 32 (2): 191–201. https://doi.org/10.1007/s12264-016-0016-y.

Lu, Hanbing, Qihong Zou, Hong Gu, Marcus E. Raichle, Elliot A. Stein, and Yihong Yang. 2012a. “Rat Brains Also Have a Default Mode Network.” *Proceedings of the National Academy of Sciences* 109 (10): 3979–84. https://doi.org/10.1073/pnas.1200506109.

Luppino, Giuseppe, Massimo Matelli, Rosolino Camarda, and Giacomo Rizzolatti. 1993. “Corticocortical Connections of Area F3 (SMA-proper) and Area F6 (pre-SMA) in the Macaque Monkey.” *Journal of Comparative Neurology* 338 (1): 114–40. https://doi.org/10.1002/cne.903380109.

Macé, Emilie, Gabriel Montaldo, Ivan Cohen, Michel Baulac, Mathias Fink, and Mickael Tanter. 2011. "Functional Ultrasound Imaging of the Brain." *Nature Methods* 8 (8): 662–64. https://doi.org/10.1038/nmeth.1641.

Mace, Emilie, Gabriel Montaldo, Bruno-Felix Osmanski, Ivan Cohen, Mathias Fink, and Mickael Tanter. 2013. "Functional Ultrasound Imaging of the Brain: Theory and Basic Principles." *IEEE Transactions on Ultrasonics, Ferroelectrics and Frequency Control* 60 (3): 492–506. https://doi.org/10.1109/TUFFC.2013.2592.

Macé, Émilie, Gabriel Montaldo, Stuart Trenholm, Cameron Cowan, Alexandra Brignall, Alan Urban, and Botond Roska. 2018. "Whole-Brain Functional Ultrasound Imaging Reveals Brain Modules for Visuomotor Integration." *Neuron* 100 (5): 1241-1251.e7. https://doi.org/10.1016/j.neuron.2018.11.031.

Magni, Guido, Cesare Caldieron, Silio Rigatti-Luchini, and Harold Merskey. 1990. "Chronic Musculoskeletal Pain and Depressive Symptoms in the General Population. An Analysis of the 1st National Health and Nutrition Examination Survey Data." *Pain* 43 (3): 299–307. https://doi.org/10.1016/0304-3959(90)90027-B.

Mairesse J, Zinni M, Pansiot J, Hassan-Abdi R, Demene C, Colella M, Charriaut-Marlangue C, Rideau Batista Novais A, Tanter M, Maccari S, Gressens P, Vaiman D, Soussi-Yanicostas N, Baud O (2019) Oxytocin receptor agonist reduces perinatal brain damage by targeting microglia. Glia 67:345–359. https://doi.org/10.1002/ glia.v67.210.1002/glia.23546.

Majeed, Waqas, Matthew Magnuson, and Shella D. Keilholz. 2009. "Spatiotemporal Dynamics of Low Frequency Fluctuations in BOLD fMRI of the Rat." *Journal of Magnetic Resonance Imaging* 30 (2): 384–93. https://doi.org/10.1002/jmri.21848.

Mantini, D., M. G. Perrucci, C. Del Gratta, G. L. Romani, and M. Corbetta. 2007. "Electrophysiological Signatures of Resting State Networks in the Human Brain." *Proceedings of the National Academy of Sciences* 104 (32): 13170–75. https://doi.org/10.1073/pnas.0700668104.

Martikainen, Ilkka K, Emily B Nuechterlein, Marta Peciña, Tiffany M Love, Chelsea M Cummiford, Carmen R Green, Christian S Stohler, and Jon-Kar Zubieta. 2015. "Chronic Back Pain Is Associated with Alterations in Dopamine Neurotransmission in the Ventral Striatum." *The Journal of Neuroscience : The Official Journal of the Society for Neuroscience* 35 (27): 9957–65. https://doi.org/10.1523/JNEUROSCI.4605-14.2015.

Mayhew, Stephen D., Nicholas Hylands-White, Camillo Porcaro, Stuart W.G. Derbyshire, and Andrew P. Bagshaw. 2013. "Intrinsic Variability in the Human Response to Pain Is Assembled from Multiple, Dynamic Brain Processes." *NeuroImage* 75 (July):68–78. https://doi.org/10.1016/j.neuroimage.2013.02.028.

Melzack R, Casey KL. Sensory, motivational, and central control determinants of pain. In: Kenshalo DR, Ed. The skin senses. Springfield, IL: CC Thomas; 1968. p. 423-39.

Melzack R. Phantom limbs, the self and the brain (The D.O. Hebb Memorial Lecture). Can Psychol. 1989;30:114.

Melzack, Ronald. 2005. "Evolution of the Neuromatrix Theory of Pain. The Prithvi Raj Lecture: Presented at the Third World Congress of World Institute of Pain, Barcelona 2004." *Pain Practice* 5 (2): 85–94. https://doi.org/10.1111/j.1533-2500.2005.05203.x.

Menon, Sreevalsan S., and K. Krishnamurthy. 2019. “A Comparison of Static and Dynamic Functional Connectivities for Identifying Subjects and Biological Sex Using Intrinsic Individual Brain Connectivity.” *Scientific Reports* 9 (1): 5729. https://doi.org/10.1038/s41598-019-42090-4.

Metz, Alexia E., Hau-Jie Yau, Maria Virginia Centeno, A. Vania Apkarian, and Marco Martina. 2009. “Morphological and Functional Reorganization of Rat Medial Prefrontal Cortex in Neuropathic Pain.” *Proceedings of the National Academy of Sciences* 106 (7): 2423–28. https://doi.org/10.1073/pnas.0809897106.

Moisset, Xavier, and Didier Bouhassira. 2007. “Brain Imaging of Neuropathic Pain.” *NeuroImage* 37 (SUPPL. 1): 80–88. https://doi.org/10.1016/j.neuroimage.2007.03.054.

Montaldo, G., M. Tanter, J. Bercoff, N. Benech, and M. Fink. 2009. “Coherent Plane-Wave Compounding for Very High Frame Rate Ultrasonography and Transient Elastography.” *IEEE Transactions on Ultrasonics, Ferroelectrics and Frequency Control* 56 (3): 489–506. https://doi.org/10.1109/TUFFC.2009.1067.

Moraga-Amaro, Rodrigo, and Jimmy Stehberg. 2012. “The Insular Cortex and the Amygdala: Shared Functions and Interactions.” In *The Amygdala - A Discrete Multitasking Manager*, edited by Barbara Ferry. InTech. https://doi.org/10.5772/48495.

Moriarty, Orla, Brian E. McGuire, and David P. Finn. 2011. “The Effect of Pain on Cognitive Function: A Review of Clinical and Preclinical Research.” *Progress in Neurobiology* 93 (3): 385–404. https://doi.org/10.1016/j.pneurobio.2011.01.002.

Morris, Laurel S., Christian Sprenger, Ken Koda, Daniela M. de la Mora, Tomomi Yamada, Hiroaki Mano, Yuto Kashiwagi, Yoshichika Yoshioka, Yasuhide Morioka, and Ben Seymour. 2018. “Anterior Cingulate Cortex Connectivity Is Associated with Suppression of Behaviour in a Rat Model of Chronic Pain.” *Brain and Neuroscience Advances* 2 (January):239821281877964. https://doi.org/10.1177/2398212818779646.

Mosconi, Tony, and Lawrence Kruger. 1996. “Fixed-Diameter Polyethylene Cuffs Applied to the Rat Sciatic Nerve Induce a Painful Neuropathy: Ultrastructural Morphometric Analysis of Axonal Alterations.” *Pain* 64 (1): 37–57. https://doi.org/10.1016/0304-3959(95)00077-1.

Moulton, Eric A., Gautam Pendse, Lino R. Becerra, and David Borsook. 2012. “BOLD Responses in Somatosensory Cortices Better Reflect Heat Sensation than Pain.” *The Journal of Neuroscience* 32 (17): 6024–31. https://doi.org/10.1523/JNEUROSCI.0006-12.2012.

Mouraux, A., J. M. Guérit, and L. Plaghki. 2004. “Refractoriness Cannot Explain Why C-Fiber Laser-Evoked Brain Potentials Are Recorded Only If Concomitant Aδ-Fiber Activation Is Avoided.” *Pain* 112 (1): 16–26. https://doi.org/10.1016/j.pain.2004.05.024.

Mouraux, A., and L. Plaghki. 2007. “Cortical Interactions and Integration of Nociceptive and Non-Nociceptive Somatosensory Inputs in Humans.” *Neuroscience* 150 (1): 72–81. https://doi.org/10.1016/j.neuroscience.2007.08.035.

Mouraux, André, and Gian Domenico Iannetti. 2018. “The Search for Pain Biomarkers in the Human Brain.” *Brain* 141 (12): 3290–3307. https://doi.org/10.1093/brain/awy281.

Mutso, Amelia A., Bogdan Petre, Lejian Huang, Marwan N. Baliki, Souraya Torbey, Kristina M. Herrmann, Thomas J. Schnitzer, and A. Vania Apkarian. 2014. “Reorganization of Hippocampal Functional

Connectivity with Transition to Chronic Back Pain." *Journal of Neurophysiology* 111 (5): 1065–76. https://doi.org/10.1152/jn.00611.2013.

Navratilova, Edita, Christopher W. Atcherley, and Frank Porreca. 2015. "Brain Circuits Encoding Reward from Pain Relief." *Trends in Neurosciences* 38 (11): 741–50. https://doi.org/10.1016/j.tins.2015.09.003.

Neugebauer, Volker. 2015. "Amygdala Pain Mechanisms." In *Pain Control*, edited by Hans-Georg Schaible, 227:261–84. Handbook of Experimental Pharmacology. Berlin, Heidelberg: Springer Berlin Heidelberg. https://doi.org/10.1007/978-3-662-46450-2_13.

Neugebauer, Volker, Vasco Galhardo, Sabatino Maione, and Sean C. Mackey. 2009. "Forebrain Pain Mechanisms." *Brain Research Reviews*, A Decade of Pain Research: New Approaches, New Targets, 60 (1): 226–42. https://doi.org/10.1016/j.brainresrev.2008.12.014.

Nicholson, Bruce, and Sunil Verma. 2004. "Comorbidities in Chronic Neuropathic Pain." *Pain Medicine* 5 (suppl 1): S9–27. https://doi.org/10.1111/j.1526-4637.2004.04019.x.

Oh, Seung Wook, Julie A. Harris, Lydia Ng, Brent Winslow, Nicholas Cain, Stefan Mihalas, Quanxin Wang, et al. 2014. "A Mesoscale Connectome of the Mouse Brain." *Nature* 508 (7495): 207–14. https://doi.org/10.1038/nature13186.

Oppenheimer, Stephen, and David Cechetto. 2016. "The Insular Cortex and the Regulation of Cardiac Function." In *Comprehensive Physiology*, edited by Y. S. Prakash, 1st ed., 1081–1133. Wiley. https://doi.org/10.1002/cphy.c140076.

Osmanski, Bruno-Félix, Sophie Pezet, Ana Ricobaraza, Zsolt Lenkei, and Mickael Tanter. 2014. "Functional Ultrasound Imaging of Intrinsic Connectivity in the Living Rat Brain with High Spatiotemporal Resolution." *Nature Communications* 5 (1): 5023. https://doi.org/10.1038/ncomms6023.

Paasonen, Jaakko, Raimo A. Salo, Joanna K. Huttunen, and Olli Gröhn. 2017. "Resting-state Functional MRI as a Tool for Evaluating Brain Hemodynamic Responsiveness to External Stimuli in Rats." *Magnetic Resonance in Medicine* 78 (3): 1136–46. https://doi.org/10.1002/mrm.26496.

Paasonen, Jaakko, Petteri Stenroos, Raimo A. Salo, Vesa Kiviniemi, and Olli Gröhn. 2018. "Functional Connectivity under Six Anesthesia Protocols and the Awake Condition in Rat Brain." *NeuroImage* 172 (May):9–20. https://doi.org/10.1016/j.neuroimage.2018.01.014.

Patel, Ryan, and Anthony H. Dickenson. 2016. "Neuronal Hyperexcitability in the Ventral Posterior Thalamus of Neuropathic Rats: Modality Selective Effects of Pregabalin." *Journal of Neurophysiology* 116 (1): 159–70. https://doi.org/10.1152/jn.00237.2016.

Pawela, Christopher P., Bharat B. Biswal, Younghoon R. Cho, Dennis S. Kao, Rupeng Li, Seth R. Jones, Marie L. Schulte, Hani S. Matloub, Anthony G. Hudetz, and James S. Hyde. 2008. "Resting-state Functional Connectivity of the Rat Brain." *Magnetic Resonance in Medicine* 59 (5): 1021–29. https://doi.org/10.1002/mrm.21524.

Perl, Edward R. 2007. "Ideas about Pain, a Historical View." *Nature Reviews Neuroscience* 8 (1): 71–80. https://doi.org/10.1038/nrn2042.

Petersen, Erika A., and Konstantin V. Slavin. 2014. "Peripheral Nerve/Field Stimulation for Chronic Pain." *Neurosurgery Clinics of North America* 25 (4): 789–97. https://doi.org/10.1016/j.nec.2014.07.003.

Peyron, R., B. Laurent, and L. García-Larrea. 2000. “Functional Imaging of Brain Responses to Pain. A Review and Meta-Analysis.” *Clinical Neurophysiology* 30 (5): 263–88.

Peyron, R. Functional brain imaging: what has it brought to our understanding of neuropathic pain? A special focus on allodynic pain mechanisms. Pain 157, S67–S71 (2016).

Peyron, Roland, Luis García-Larrea, Marie-Claude Grégoire, Nicolas Costes, Philippe Convers, F. Lavenne, Francıois Mauguière, Daniel Michel, and Bernard Laurent. 1999. “Haemodynamic Brain Responses to Acute Pain in Humans.” *Brain* 122 (9): 1765–80. https://doi.org/10.1093/brain/122.9.1765.

Phelps, Elizabeth A, Mauricio R Delgado, Katherine I Nearing, and Joseph E LeDoux. n.d. “Extinction Learning in Humans: Role of the Amygdala and vmPFC.”

Pitcher, Graham M., Jennifer Ritchie, and James L. Henry. 1999. “Nerve Constriction in the Rat: Model of Neuropathic, Surgical and Central Pain:” *Pain* 83 (1): 37–46. https://doi.org/10.1016/S0304-3959(99)00085-8.

Porro, Carlo A. 2003. “Functional Imaging and Pain: Behavior, Perception, and Modulation.” *The Neuroscientist* 9 (5): 354–69. https://doi.org/10.1177/1073858403253660.

Porro, Carlo A., Valentina Cettolo, Maria Pia Francescato, and Patrizia Baraldi. 1998. “Temporal and Intensity Coding of Pain in Human Cortex.” *Journal of Neurophysiology* 80 (6): 3312–20. https://doi.org/10.1152/jn.1998.80.6.3312.

Rabut, Claire, Jérémy Ferrier, Adrien Bertolo, Bruno Osmanski, Xavier Mousset, Sophie Pezet, Thomas Deffieux, Zsolt Lenkei, and Mickaël Tanter. 2020. “Pharmaco-fUS: Quantification of Pharmacologically-Induced Dynamic Changes in Brain Perfusion and Connectivity by Functional Ultrasound Imaging in Awake Mice.” *NeuroImage* 222 (November):117231. https://doi.org/10.1016/j.neuroimage.2020.117231.

Radat, F., A. Margot-Duclot, and N. Attal. 2013. “Psychiatric Co-morbidities in Patients with Chronic Peripheral Neuropathic Pain: A Multicentre Cohort Study.” *European Journal of Pain* 17 (10): 1547–57. https://doi.org/10.1002/j.1532-2149.2013.00334.x.

Rahal, Line, Miguel Thibaut, Isabelle Rivals, Julien Claron, Zsolt Lenkei, Jacobo D. Sitt, Mickael Tanter, and Sophie Pezet. 2020. “Ultrafast Ultrasound Imaging Pattern Analysis Reveals Distinctive Dynamic Brain States and Potent Sub-Network Alterations in Arthritic Animals.” *Scientific Reports* 10 (1): 10485. https://doi.org/10.1038/s41598-020-66967-x.

Raichle, Marcus E. 2015. “The Brain’s Default Mode Network.” *Annual Review of Neuroscience* 38 (1): 433–47. https://doi.org/10.1146/annurev-neuro-071013-014030.

Rainville, Pierre. 2002. “Brain Mechanisms of Pain Affect and Pain Modulation.” *Current Opinion in Neurobiology* 12 (2): 195–204. https://doi.org/10.1016/S0959-4388(02)00313-6.

Rainville, Pierre, Gary H. Duncan, Donald D. Price, Benoît Carrier, and M. Catherine Bushnell. 1997. “Pain Affect Encoded in Human Anterior Cingulate But Not Somatosensory Cortex.” *Science* 277 (5328): 968–71. https://doi.org/10.1126/science.277.5328.968.

Rau, Richard, Pieter Kruizinga, Frits Mastik, Markus Belau, Nico de Jong, Wolfgang Scheffer, and Georg Maret. n.d. “3D Functional Ultrasound Imaging of Pigeons.”

Réaux-Le-Goazigo, Annabelle, Benoit Beliard, Lauriane Delay, Line Rahal, Julien Claron, Noémi Renaudin, Isabelle Rivals, et al. 2022. “Ultrasound Localization Microscopy and Functional Ultrasound Imaging Reveal Atypical Features of the Trigeminal Ganglion Vasculature.” *Communications Biology* 5 (1): 330. https://doi.org/10.1038/s42003-022-03273-4.

Rungta, Ravi L, Bruno-Félix Osmanski, Davide Boido, Mickael Tanter, and Serge Charpak. 2017. “Light Controls Cerebral Blood Flow in Naive Animals.” *Nature Communications* 8 (1): 14191. https://doi.org/10.1038/ncomms14191.

Ruscheweyh, Ruth, Oliver Wilder-Smith, Ruth Drdla, Xian-Guo Liu, and Jürgen Sandkühler. 2011. “Long-Term Potentiation in Spinal Nociceptive Pathways as a Novel Target for Pain Therapy.” *Molecular Pain* 7 (January):1744-8069-7–20. https://doi.org/10.1186/1744-8069-7-20.

Salgado, Sanjay, and Michael G. Kaplitt. 2015. “The Nucleus Accumbens: A Comprehensive Review.” *Stereotactic and Functional Neurosurgery* 93 (2): 75–93. https://doi.org/10.1159/000368279.

Salomons, Tim V., Gian Domenico Iannetti, Meng Liang, and John N. Wood. 2016. “The ‘Pain Matrix’ in Pain-Free Individuals.” *JAMA Neurology* 73 (6): 755. https://doi.org/10.1001/jamaneurol.2016.0653.

Salvador, R., A. Martínez, E. Pomarol-Clotet, S. Sarró, J. Suckling, and E. Bullmore. 2007. “Frequency Based Mutual Information Measures between Clusters of Brain Regions in Functional Magnetic Resonance Imaging.” *NeuroImage* 35 (1): 83–88. https://doi.org/10.1016/j.neuroimage.2006.12.001.

Sandkühler, Jürgen, and Xianguo Liu. 1998. “Induction of Long-term Potentiation at Spinal Synapses by Noxious Stimulation or Nerve Injury.” *European Journal of Neuroscience* 10 (7): 2476–80. https://doi.org/10.1046/j.1460-9568.1998.00278.x.

Sandrin, L, S. Catheline, M. Tanter, X. Hennequin, and M. Fink. 1999. “Time-Resolved Pulsed Elastography with Ultrafast Ultrasonic Imaging.” *Ultrasonic Imaging* 21 (4): 259–72. https://doi.org/10.1177/016173469902100402.

Saper, Clifford B. 1982. “Convergence of Autonomic and Limbic Connections in the Insular Cortex of the Rat.” *Journal of Comparative Neurology* 210 (2): 163–73. https://doi.org/10.1002/cne.902100207.

Sawamoto, Nobukatsu, Manabu Honda, Tomohisa Okada, Takashi Hanakawa, Masutaro Kanda, Hidenao Fukuyama, Junji Konishi, and Hiroshi Shibasaki. 2000. “Expectation of Pain Enhances Responses to Nonpainful Somatosensory Stimulation in the Anterior Cingulate Cortex and Parietal Operculum/Posterior Insula: An Event-Related Functional Magnetic Resonance Imaging Study.” *The Journal of Neuroscience* 20 (19): 7438–45. https://doi.org/10.1523/JNEUROSCI.20-19-07438.2000.

Scholz, Joachim, Nanna B. Finnerup, Nadine Attal, Qasim Aziz, Ralf Baron, Michael I. Bennett, Rafael Benoliel, et al. 2019. “The IASP Classification of Chronic Pain for ICD-11: Chronic Neuropathic Pain.” *Pain* 160 (1): 53–59. https://doi.org/10.1097/j.pain.0000000000001365.

Schweinhardt, P., A. Kuchinad, C. F. Pukall, and M. C. Bushnell. 2008. “Increased Gray Matter Density in Young Women with Chronic Vulvar Pain.” *Pain* 140 (3): 411–19. https://doi.org/10.1016/j.pain.2008.09.014.

Schweinhardt, Petra, and M. Catherine Bushnell. 2010. “Pain Imaging in Health and Disease — How Far Have We Come?” *Journal of Clinical Investigation* 120 (11): 3788–97. https://doi.org/10.1172/JCI43498.

Seminowicz, David A., Timothy H. Wideman, Lina Naso, Zeinab Hatami-Khoroushahi, Summaya Fallatah, Mark A. Ware, Peter Jarzem, et al. 2011. “Effective Treatment of Chronic Low Back Pain in Humans Reverses Abnormal Brain Anatomy and Function.” *The Journal of Neuroscience* 31 (20): 7540–50. https://doi.org/10.1523/JNEUROSCI.5280-10.2011.

Seymour, Ben, John P O’Doherty, Peter Dayan, Martin Koltzenburg, Anthony K Jones, Raymond J Dolan, Karl J Friston, and Richard S Frackowiak. 2004. “Higher-Order Learning in Humans” 429.

Sforazzini, Francesco, Adam J. Schwarz, Alberto Galbusera, Angelo Bifone, and Alessandro Gozzi. 2014. “Distributed BOLD and CBV-Weighted Resting-State Networks in the Mouse Brain.” *NeuroImage* 87 (February):403–15. https://doi.org/10.1016/j.neuroimage.2013.09.050.

Shoemaker, J. K., and Ruma Goswami. 2015. “Forebrain Neurocircuitry Associated with Human Reflex Cardiovascular Control.” *Frontiers in Physiology* 6 (September). https://doi.org/10.3389/fphys.2015.00240.

Shuler, Marshall G., David J. Krupa, and Miguel A. L. Nicolelis. 2001. “Bilateral Integration of Whisker Information in the Primary Somatosensory Cortex of Rats.” *The Journal of Neuroscience* 21 (14): 5251–61. https://doi.org/10.1523/JNEUROSCI.21-14-05251.2001.

Sieu, Lim-Anna, Antoine Bergel, Elodie Tiran, Thomas Deffieux, Mathieu Pernot, Jean-Luc Gennisson, Mickaël Tanter, and Ivan Cohen. 2015. “EEG and Functional Ultrasound Imaging in Mobile Rats.” *Nature Methods* 12 (9): 831–34. https://doi.org/10.1038/nmeth.3506.

Simons, L. E., M. Pielech, N. Erpelding, C. Linnman, E. Moulton, S. Sava, A. Lebel, et al. 2014. “The Responsive Amygdala: Treatment-Induced Alterations in Functional Connectivity in Pediatric Complex Regional Pain Syndrome.” *Pain* 155 (9): 1727–42. https://doi.org/10.1016/j.pain.2014.05.023.

Singer, Tania, Ben Seymour, John O’Doherty, Holger Kaube, Raymond J. Dolan, and Chris D. Frith. 2004. “Empathy for Pain Involves the Affective but Not Sensory Components of Pain.” *Science* 303 (5661): 1157–62. https://doi.org/10.1126/science.1093535.

Smith, M T, M L Perlis, M S Smith, D E Giles, and T P Carmody. n.d. “Sleep Quality and Presleep Arousal in Chronic Pain.”

Spisák, Tamás, Zsófia Pozsgay, Csaba Aranyi, Szabolcs Dávid, Pál Kocsis, Gabriella Nyitrai, Dávid Gajári, Miklós Emri, András Czurkó, and Zsigmond Tamás Kincses. 2017. “Central Sensitization-Related Changes of Effective and Functional Connectivity in the Rat Inflammatory Trigeminal Pain Model.” *Neuroscience* 344 (March):133–47. https://doi.org/10.1016/j.neuroscience.2016.12.018.

Sukul, Vishad V., and Konstantin V. Slavin. 2014. “Deep Brain and Motor Cortex Stimulation.” *Current Pain and Headache Reports* 18 (7): 427. https://doi.org/10.1007/s11916-014-0427-2.

Talbot, Jeanne D., Sean Marrett, Alan C. Evans, Ernst Meyer, M. Catherine Bushnell, and Gary H. Duncan. 1991. “Multiple Representations of Pain in Human Cerebral Cortex.” *Science* 251 (4999): 1355–58. https://doi.org/10.1126/science.2003220.

Tan, T., P. Barry, S. Reken, M. Baker, and On behalf of the Guideline Development Group. 2010. “Pharmacological Management of Neuropathic Pain in Non-Specialist Settings: Summary of NICE Guidance.” *BMJ* 340 (mar24 1): c1079–c1079. https://doi.org/10.1136/bmj.c1079.

Tanter, M., J. Bercoff, L. Sandrin, and M. Fink. 2002. “Ultrafast Compound Imaging for 2-D Motion Vector Estimation: Application to Transient Elastography.” *IEEE Transactions on Ultrasonics, Ferroelectrics and Frequency Control* 49 (10): 1363–74. https://doi.org/10.1109/TUFFC.2002.1041078.

Tanter, Mickael, and Mathias Fink. 2014. “Ultrafast Imaging in Biomedical Ultrasound.” *IEEE Transactions on Ultrasonics, Ferroelectrics, and Frequency Control* 61 (1): 102–19. https://doi.org/10.1109/TUFFC.2014.2882.

“The Structure of the Nervous System of the Nematode *Caenorhabditis Elegans*.” 1986. *Philosophical Transactions of the Royal Society of London. B, Biological Sciences* 314 (1165): 1–340. https://doi.org/10.1098/rstb.1986.0056.

Thompson, Jeremy M., and Volker Neugebauer. 2017. “Amygdala Plasticity and Pain.” *Pain Research and Management* 2017:1–12. https://doi.org/10.1155/2017/8296501.

Thompson, Jeremy M., and Volker Neugebauer. 2019. “Cortico-Limbic Pain Mechanisms.” *Neuroscience Letters* 702 (May):15–23. https://doi.org/10.1016/j.neulet.2018.11.037.

Thompson, Scott J., and M. Catherine Bushnell. 2012. “Rodent Functional and Anatomical Imaging of Pain.” *Neuroscience Letters* 520 (2): 131–39. https://doi.org/10.1016/j.neulet.2012.03.015.

Tiran, Elodie, Jérémy Ferrier, Thomas Deffieux, Jean-Luc Gennisson, Sophie Pezet, Zsolt Lenkei, and Mickaël Tanter. 2017. “Transcranial Functional Ultrasound Imaging in Freely Moving Awake Mice and Anesthetized Young Rats without Contrast Agent.” *Ultrasound in Medicine & Biology* 43 (8): 1679–89. https://doi.org/10.1016/j.ultrasmedbio.2017.03.011.

Tracey, Irene, and Patrick W. Mantyh. 2007. “The Cerebral Signature for Pain Perception and Its Modulation.” *Neuron* 55 (3): 377–91. https://doi.org/10.1016/j.neuron.2007.07.012.

Treede, Rolf-Detlef, Daniel R Kenshalo, Richard H Gracely, and Anthony K.P Jones. 1999. “The Cortical Representation of Pain.” *Pain* 79 (2): 105–11. https://doi.org/10.1016/S0304-3959(98)00184-5.

Tolle, Thomas R., Tanja Kaufmann, Thomas Siessmeier, Stefan Lautenbacher, Achim Berthele, Frank Munz, Walter Zieglgänsberger, et al. 1999. “Region-Specific Encoding of Sensory and Affective Components of Pain in the Human Brain: A Positron Emission Tomography Correlation Analysis.” *Annals of Neurology* 45 (1): 40–47. https://doi.org/10.1002/1531-8249(199901)45:1<40::AID-ART8>3.0.CO;2-L.

Ulrich-Lai, Yvonne M., Kenneth R. Jones, Dana R. Ziegler, William E. Cullinan, and James P. Herman. 2011. “Forebrain Origins of Glutamatergic Innervation to the Rat Paraventricular Nucleus of the Hypothalamus: Differential Inputs to the Anterior versus Posterior Subregions.” *The Journal of Comparative Neurology* 519 (7): 1301–19. https://doi.org/10.1002/cne.22571.

Upadhyay, Jaymin, Scott J. Baker, Prasant Chandran, Loan Miller, Younglim Lee, Gerard J. Marek, Unal Sakoglu, et al. 2011. “Default-Mode-Like Network Activation in Awake Rodents.” Edited by Pedro Antonio Valdes-Sosa. *PLoS ONE* 6 (11): e27839. https://doi.org/10.1371/journal.pone.0027839.

Urban, Alan, Clara Dussaux, Guillaume Martel, Clément Brunner, Emilie Mace, and Gabriel Montaldo. 2015. “Real-Time Imaging of Brain Activity in Freely Moving Rats Using Functional Ultrasound.” *Nature Methods* 12 (9): 873–78. https://doi.org/10.1038/nmeth.3482.

Vachon-Presseau, Etienne, Pascal Tétreault, Bogdan Petre, Lejian Huang, Sara E. Berger, Souraya Torbey, Alexis T. Baria, et al. 2016. “Corticolimbic Anatomical Characteristics Predetermine Risk for Chronic Pain.” *Brain* 139 (7): 1958–70. https://doi.org/10.1093/brain/aww100.

Van Essen, David C., Stephen M. Smith, Deanna M. Barch, Timothy E.J. Behrens, Essa Yacoub, and Kamil Ugurbil. 2013. "The WU-Minn Human Connectome Project: An Overview." *NeuroImage* 80 (October):62–79. https://doi.org/10.1016/j.neuroimage.2013.05.041.

Vidal, Benjamin, Marine Droguerre, Marco Valdebenito, Luc Zimmer, Michel Hamon, Franck Mouthon, and Mathieu Charvériat. 2020. "Pharmaco-fUS for Characterizing Drugs for Alzheimer's Disease – The Case of THN201, a Drug Combination of Donepezil Plus Mefloquine." *Frontiers in Neuroscience* 14 (August):835. https://doi.org/10.3389/fnins.2020.00835.

Vidal, Benjamin, Marine Droguerre, Ludovic Venet, Luc Zimmer, Marco Valdebenito, Franck Mouthon, and Mathieu Charvériat. 2020. "Functional Ultrasound Imaging to Study Brain Dynamics: Application of Pharmaco-fUS to Atomoxetine." *Neuropharmacology* 179 (November):108273. https://doi.org/10.1016/j.neuropharm.2020.108273.

Vincent, Justin L., Itamar Kahn, Abraham Z. Snyder, Marcus E. Raichle, and Randy L. Buckner. 2008. "Evidence for a Frontoparietal Control System Revealed by Intrinsic Functional Connectivity." *Journal of Neurophysiology* 100 (6): 3328–42. https://doi.org/10.1152/jn.90355.2008.

Vogt, Brent A., Gail R. Berger, and Stuart W. G. Derbyshire. 2003. "Structural and Functional Dichotomy of Human Midcingulate Cortex." *European Journal of Neuroscience* 18 (11): 3134–44. https://doi.org/10.1111/j.1460-9568.2003.03034.x.

Von Korff, Michael, Paul Crane, Michael Lane, Diana L. Miglioretti, Greg Simon, Kathleen Saunders, Paul Stang, Nancy Brandenburg, and Ronald Kessler. 2005. "Chronic Spinal Pain and Physical–Mental Comorbidity in the United States: Results from the National Comorbidity Survey Replication." *Pain* 113 (3): 331–39. https://doi.org/10.1016/j.pain.2004.11.010.

Wager, Tor D., Lauren Y. Atlas, Martin A. Lindquist, Mathieu Roy, Choong-Wan Woo, and Ethan Kross. 2013. "An fMRI-Based Neurologic Signature of Physical Pain." *New England Journal of Medicine* 368 (15): 1388–97. https://doi.org/10.1056/NEJMoa1204471.

Wall, Patrick D. 1965. "A Gate Control System Modulates Sensory Input from the Skin before It Evokes Pain Perception and Response." 150.

Wang, Zhuo, Marco A. Ocampo, Raina D. Pang, Mihail Bota, Sylvie Bradesi, Emeran A. Mayer, and Daniel P. Holschneider. 2013. "Alterations in Prefrontal-Limbic Functional Activation and Connectivity in Chronic Stress-Induced Visceral Hyperalgesia." *PLOS ONE* 8 (3): e59138. https://doi.org/10.1371/journal.pone.0059138.

Wells, Jack A., Sayaka Shibata, Akihiko Fujikawa, Masayasu Takahashi, Tsuneo Saga, and Ichio Aoki. 2017. "Functional MRI of the Reserpine-Induced Putative Rat Model of Fibromyalgia Reveals Discriminatory Patterns of Functional Augmentation to Acute Nociceptive Stimuli." *Scientific Reports* 7 (1): 38325. https://doi.org/10.1038/srep38325.

Weng, Xiechuan, Trevor Smith, Jean Sathish, and Laiche Djouhri. 2012. "Chronic Inflammatory Pain Is Associated with Increased Excitability and Hyperpolarization-Activated Current (I h) in C- but Not Aδ-Nociceptors." *Pain* 153 (4): 900–914. https://doi.org/10.1016/j.pain.2012.01.019.

White, Tonya, and Vince D. Calhoun. 2019. "Dissecting Static and Dynamic Functional Connectivity: Example From the Autism Spectrum." *Journal of Experimental Neuroscience* 13 (January):117906951985180. https://doi.org/10.1177/1179069519851809.

Whitfield-Gabrieli, S, and J M Ford. 2012. “Default Mode Network Activity and Connectivity in Psychopathology.” *Annual Review of Clinical Psychology* 8:49–76. https://doi.org/10.1146/annurev-clinpsy-032511-143049.

Williams, D. J., A. R. Crossman, and P. Slater. 1977. “The Efferent Projections of the Nucleus Accumbens in the Rat.” *Brain Research* 130 (2): 217–27. https://doi.org/10.1016/0006-8993(77)90271-2.

Woolf, Clifford J, and Richard J Mannion. 1999. “Neuropathic Pain: Aetiology, Symptoms, Mechanisms, and Management.” *The Lancet* 353 (9168): 1959–64. https://doi.org/10.1016/S0140-6736(99)01307-0.

Wu, Gang, Matthias Ringkamp, Beth B. Murinson, Esther M. Pogatzki, Timothy V. Hartke, Himali M. Weerahandi, James N. Campbell, John W. Griffin, and Richard A. Meyer. 2002. “Degeneration of Myelinated Efferent Fibers Induces Spontaneous Activity in Uninjured C-Fiber Afferents.” *The Journal of Neuroscience* 22 (17): 7746–53. https://doi.org/10.1523/JNEUROSCI.22-17-07746.2002.

Wurtz, R H. 1969. “Visual Receptive Fields of Striate Cortex Neurons in Awake Monkeys.” *Journal of Neurophysiology* 32 (5): 727–42. https://doi.org/10.1152/jn.1969.32.5.727.

Yalcin, Ipek, Yohann Bohren, Elisabeth Waltisperger, Dominique Sage-Ciocca, Jerry C. Yin, Marie-José Freund-Mercier, and Michel Barrot. 2011. “A Time-Dependent History of Mood Disorders in a Murine Model of Neuropathic Pain.” *Biological Psychiatry* 70 (10): 946–53. https://doi.org/10.1016/j.biopsych.2011.07.017.

Zhao, Peng, Stephen G Waxman, and Bryan C Hains. 2006. “Sodium Channel Expression in the Ventral Posterolateral Nucleus of the Thalamus after Peripheral Nerve Injury.” *Molecular Pain* 2 (January):1744-8069-2–27. https://doi.org/10.1186/1744-8069-2-27.

Zhuo, Min. 2008. “Cortical Excitation and Chronic Pain.” *Trends in Neurosciences* 31 (4): 199–207. https://doi.org/10.1016/j.tins.2008.01.003.

Zhuo, Min. “Long-Term Potentiation in the Anterior Cingulate Cortex and Chronic Pain,” n.d., 11. 2014.

LIST OF FIGURES

LIST OF ABBREVIATIONS

ACC= Anterior Cingulate Cortex

Acs= Adenylyl cyclases

AI= anterior insular cortex

AID= Agranular insular area, dorsal part

AIP= Agranular insular area, posterior part

AIV= Agranular insular area, ventral part

ALPFC= Anterolateral Prefrontal Cortex

AMPA= α-amino-3-hydroxy-5-methyl-4-isoxazolepropionic acid

AMYG= Amygdala

ASIC= Acid-Sensing Ion Channels

BG= Basal Ganglia

BLA= basolateral amygdala

BOLD= Blood Oxygen Level Dependent

CaM= Calmodulin

CBF= cerebral blood flow

CBP= Chronic Back Pain

CBV= cerebral blood volume

CC = Cingulate Cortex

CCI= Chronic Constriction Injury

CeA= Central nucleus of the Amygdala

CFA= chronic pain model

CGRP= Calcitonin gene–related peptide

CL= Centrolateral nucleus

CNS= Central Nervous System

CPu= Caudoputamen

CRPS= complex regional pain syndrome

CT= computed tomography

dFC= dynamic Functional Connectivity

DLPFC= Dorsolateral Prefrontal Cortex

DMN= Default Mode Network

DRG= Dorsal Root Ganglion

DTI= Diffusion Tensor Imaging

ECMS= Epidural Motor Cortex Stimulation

ECT= Emission Computed Tomography ()

EEG= Electroencephalographic

ET= Emission Tomography

FC= Functional Connectivity

fMRI= functional Magnetic Resonance Imaging

FRP= Frontal pole, cerebral cortex

fUS= functional ultrasound imaging

GABA= γ-amino butyric acid

GluRs= post-synaptic glutamate receptors

HIP= hippocampal region

HIPPO= Hippocampus

HRF= hemodynamic response function

HT= Hypothalamus

HYP= Hypothalamus

IASP= International Association for the Study of Pain

IC= Insular cortex

IL= infralimbic

LA= lateral amygdala

LC= locus coeruleus

LO= Lateral Orbital cortex

LS= Lateral septal complex

LTD= Long-term Depression

LTP= Long-Term Potentiation

L-VGCCs= L-type voltage-gated calcium channels

M1= primary Motor area

M1= primary Motor cortex

M2= secondary Motor area

MDvc= ventrocaudal part of Medial Dorsal nucleus

MEG= Magnetoencephalography

mPFC= medial Prefrontal Cortex

NAc= Nucleus accumbens

NeuPSIG= Neuropathic Pain Special Interest Group

NICE= UK National Institute for Health and Care Excellence

NMDA= N-methyl-d-aspartic acid or N-methyl-d-aspartate

NMR= nuclear magnetic resonance

NTS= nucleus of the solitary tract

OA= Orbital area

OA= osteoarthritis

PAG= Periaqueductal gray

PB= Parabrachial nuclei

PCC= Posterior Cingulate Cortex

PET= Positron Emission Tomography

Pf= Parafascicular nucleus

PFC= Prefrontal Cortex

PI= Posterior Insular cortex

PL= prelimbic area

PMC= premotor cortex

PNS= Peripheral Nervous System

PNS= Peripheral nervous system

PPC= Posterior Parietal Cortex

PSNL= Partial Sciatic Nerve Ligation

PVN= Paraventricular Nucleus of hypothalamus

ROIs= Regions of Interest

RSA= Retrosplenial area

RSN= Resting State Networks

rTMS= repetitive Transcranial Magnetic Stimulation

S1= primary Somatosensory cortex

S1HL= Primary somatosensory area, hind-limb

S1TR= Primary somatosensory area, trunk

S2= secondary Somatosensory cortex

sAMY= striatum-like amygdalar nuclei

SC= Structural Connectivity

SM1= primary sensorimotor cortex

SMA= supplementary motor area

SMA= Supplementary Motor cortices

SMN= Sensory Motor Network

SNI= Spared Nerve Injury

SNL= Spinal Nerve Ligation

SPECT= Single-Photon Emission Computed Tomography

SQUID= superconducting quantum interference device

TCD= Transcranial Doppler

tDCS= trans-cranial Direct Current Stimulation

TG= Trigeminal Ganglion

THAL= Thalamus

TMS= Transcranial Magnetic Stimulation

TRP= Transient Receptor Potential

VMpo= posterior part of ventromedial nucleus

VPI= Ventral Posterior Inferior nucleus

VPL= Ventral Posterior Lateral nucleus

VPM= Ventral Posterior Medial nucleus

VPM= ventral posterior medial nucleus

VTA= Ventral Tegmental Area

µDoppler= ultrafast doppler

SCIENTIFIC OUTPUT

Publication in peer-reviewd journals

Bertolo, Adrien*, Mohamed Nouhoum*, **Silvia Cazzanelli***, Jeremy Ferrier*, Jean-Charles Mariani, Andrea Kliewer, Benoit Belliard, et al. 'Whole-Brain 3D Activation and Functional Connectivity Mapping in Mice Using Transcranial Functional Ultrasound Imaging'. Journal of Visualized Experiments, no. 168 (24 February 2021): 62267. https://doi.org/10.3791/62267.

Koorliyil Haritha, Jacobo Sitt, Isabelle Rivals, Yushan Liu, Adrien Bertolo, **Silvia Cazzanelli**, Alexandre Dizeux, Thomas Deffieux, Mickael Tanter, and Sophie Pezet. "Specific and Non-Uniform Brain States during Cold Perception in Mice." The Journal of Neuroscience, January 5, 2024, e0909232023. https://doi.org/10.1523/JNEUROSCI.0909-23.2023.

Bertolo, Adrien, Jeremy Ferrier, **Silvia Cazzanelli**, Samuel Diebolt, Mickael Tanter, Sophie Pezet, Mathieu Pernot, Bruno Osmanski, Thomas Deffieux. 'High sensitivity mapping of brain-wide functional networks in awake mice using simultaneous multi-slice fUS imaging'. Imaging Neuroscience https://doi.org/10.1162/imag_a_00030

Publication in preparation

Cazzanelli, Silvia, Samuel Le Meur Diebolt, Youenn Travert-Jouanneau, Luc Eglin, Adrien Bertolo, Thomas Deffieux, Mickael Tanter, Bruno-Felix Osmanski, Jeremy Ferrier and Sophie Pezet. 'Resting state-fUS imaging of functional connectivity in awake mice with neuropathic pain: insights into pain and stress networks'.

Cazzanelli, Silvia, Youenn Travert-Jouanneau, Samuel Diebolt, Luc Eglin, Adrien Bertolo, Thomas Deffieux, Mickael Tanter, Bruno-Felix Osmanski, Jeremy Ferrier and Sophie Pezet. 'Longitudinal fUS imaging of functional connectivity during neuropathic pain development in mice revealed long lasting alterations of pain and stress networks'.

Peer-reviewed abstracts

Silvia Cazzanelli, Samuel Diebolt, Adrien Bertolo, Jérémy Ferrier, Mathis Vert, Thomas Deffieux, Bruno-Félix Osmanski, Mickaël Tanter, Sophie Pezet. 'Functional alterations of intrinsic networks at various stages of neuropathic pain and comorbidity development'. *International Headache and Pain Symposium 2022. Oral presentation.*

Silvia Cazzanelli, Samuel Diebolt, Adrien Bertolo, Jérémy Ferrier, Mathis Vert, Thomas Deffieux, Bruno-Félix Osmanski, Mickaël Tanter, Sophie Pezet. 'Functional alterations of intrinsic networks in the various stages of neuropathic pain and comorbidity development'. *FENS Forum 2022. Poster presentation.*

Silvia Cazzanelli, Samuel Diebolt, Adrien Bertolo, Jérémy Ferrier, Mathis Vert, Thomas Deffieux, Bruno-Félix Osmanski, Mickaël Tanter, Sophie Pezet. 'Functional alterations of intrinsic networks at various stages of neuropathic pain and comorbidity development'. *fUSbrain 2022. Poster presentation.*

Silvia Cazzanelli, Samuel Diebolt, Adrien Bertolo, Jérémy Ferrier, Mathis Vert, Lauriane Delay, Thomas Deffieux, Bruno-Félix Osmanski, Mickael Tanter, Sophie Pezet. 'Functional alterations of intrinsic networks at various stages of neuropathic pain and its comorbidity'. *SFN 2022. Poster presentation.*

Silvia Cazzanelli, Luc Eglin, Samuel Diebolt, Youenn Travert-Jouanneau, Adrien Bertolo, Jérémy Ferrier, Thomas Deffieux, Bruno-Félix Osmanski, Mickael Tanter, Sophie Pezet. 'Functional alterations of intrinsic networks at various stages of neuropathic pain in a mouse model of neuropathic pain'. *NeuPSIG2023. Poster presentation.*

RÉSUMÉ

La douleur neuropathique est une sensation de douleur anormale qui persiste au-delà du cours temporel de la guérison naturelle. Elle interfère avec la qualité de vie du patient et est associée à plusieurs comorbidités telles que l'anxiété et la dépression. Des études antérieures ont suggéré que la douleur chronique pourrait résulter d'une plasticité neuronale anormale et inadaptée dans les structures connues pour être impliquées dans la perception de la douleur (Bliss et al. 2016). Cela signifie qu'une lésion nerveuse déclencherait une potentialisation à long terme de la transmission synaptique dans les aires cérébrales liées à la douleur (Zhuo et al. 2014). Comme ces régions sont également impliquées dans les aspects émotionnels de la douleur, notre hypothèse est que la plasticité inadaptée susmentionnée dans ces zones cérébrales pourrait constituer un mécanisme clé pour le développement de comorbidités, telles que l'anxiété et la dépression.

Au cours de ma thèse, nous avons choisi de tester cette hypothèse de travail par l'étude des altérations de la connectivité fonctionnelle (CF) intrinsèque des réseaux cérébraux par imagerie fonctionnelle ultrasonore (fUS) dans un modèle murin de douleur neuropathique. Cette technique de neuro-imagerie relativement récente a permis de nombreuses avancées en neurosciences, grâce à sa haute résolution spatio-temporelle, à sa sensibilité, mais aussi son adaptabilité, permettant des études chez l'animal anesthésié ou éveillé.

Dans une première étude, j'ai mis au point un protocole expérimental permettant d'imager le cerveau des souris éveillées de façon reproductible et avec un minimum de stress et d artefacts de mouvements et ai également été impliquée dans le développement d'un nouvel algorithme d'analyse des signaux générées par ces acquisitions. Cette première approche étant réalisée avec une sonde linéaire en mouvement qui ne permet pas de visualiser l'entièreté du cerveau, dans une seconde étude, j'ai participe au développement d'une nouvelle technologie de sonde compilées et motorisée.

Fort de ces développements technologiques, j'ai alors utilisé ces nouvelles approches pour tester mon hypothèse neurobiologique. J'ai entrepris deux études en parallèle chez des animaux anesthésiés pour l'une et éveillés pour la seconde, chez lesquelles nous avons étudié le lien temporel entre les altérations de la CF cérébrale et le développement de la douleur neuropathique et/ou des comorbidités associées. Pour cela, nous avons mesuré la CF (en période de repos) chez des souris atteintes de douleur neuropathique, à trois moments différents : I) 2 semaines après l'induction de la douleur neuropathique (manchon autour du nerf sciatique) II) à 8 semaines post-induction, lorsque l'anxiété émerge et III) à 12 semaines post-induction, lorsque la dépression apparait (12W). Ce suivi longitudinal a également été réalisé en parallèle sur un groupe d'animaux contrôles.

Nos résultats indiquent des changements significatifs de la CF dans les principales régions cérébrales impliquées dans la transmission ou la modulation de la sensibilité ou de la douleur, suggérant la mise en place d'une plasticité inadaptée du réseau de la douleur, suite à la lésion nerveuse. De plus, nous observons une évolution temporelle de ces altérations, potentiellement corrélée à l'apparition des comorbidités associées. Ainsi, ces mécanismes pourraient participer à la chronicisation de la douleur.

MOTS CLÉS

Imagerie fUS, connectivité fonctionnelle, réseau de la douleur, douleur neuropathique, comorbidités.

ABSTRACT

Neuropathic pain is an abnormal pain sensation that persists longer than the temporal course of natural healing. It interferes with the patient's quality of life and leads to several comorbidities, such as anxiety and depression. It has been suggested that chronic pain may result from abnormal and maladaptive neuronal plasticity in the structures known to be involved in pain perception (Bliss et al. 2016). This means that nerve injury would trigger long-term potentiation of synaptic transmission in pain-related areas (Zhuo et al. 2014). Since these regions are also involved in the emotional aspects of pain, our hypothesis is that the aforementioned maladaptive plasticity in these brain areas could constitute a key mechanism for the development of comorbidities such as anxiety and depression.

My PhD aimed at testing this working hypothesis, through the study of brain resting state functional connectivity (FC) using functional ultrasound imaging (fUS) in a mouse model of neuropathic pain. FUS is a relatively recent neuroimaging technique that enabled numerous advances in neuroscience, thanks to its high spatio-temporal resolution, its sensitivity, but also its adaptability, allowing studies in anesthetized or awake animals.

In a first study, I developed an experimental protocol allowing the brains of awake mice to be imaged in a reproducible manner and with minimal stress and movement artifacts and was also involved in the development of a new algorithm for the analysis of the signals generated by these acquisitions. As this first approach was carried out with a moving linear probe which does not allow the entire brain to be visualized, in a second study, I participated in the development of a new compiled and motorized probe technology.

Building on these technological developments, I then used these new approaches to test my neurobiological hypothesis. I undertook two parallel studies in animals anesthetized for one and awake for the second, in which we studied the temporal link between alterations in cerebral FC and the development of neuropathic pain and/or associated comorbidities. To do this, we measured the resting-state functional connectivity (FC) in anesthetized and in awake head-fixed mice, at three time points: I) 2 weeks after induction of neuropathic pain (cuff around the sciatic nerve), II) at 8 weeks post-induction during the emergence of anxiety (8W) and III) at 12 weeks post-induction during the emergence of depression. This longitudinal follow-up has been conducted concurrently on a control group.

Our results show significant changes in FC in major pain-related brain regions in accordance with the development of neuropathic pain symptoms. These findings suggest that the pain network undergoes maladaptive plasticity following nerve injury which could contribute to pain chronification. Moreover, the time course of these connectivity alterations between regions of the pain network could be correlated with the subsequent apparition of associated comorbidities.

KEYWORDS

fUS imaging, functional connectivity, pain network, neuropathic pain, comorbidities.